



UNIVERSITAT_{DE}
BARCELONA

Cellular and animal models of antibody-mediated encephalitis: from pathogenesis to novel therapeutics

Estibaliz Maudes

ADVERTIMENT. La consulta d'aquesta tesi queda condicionada a l'acceptació de les següents condicions d'ús: La difusió d'aquesta tesi per mitjà del servei TDX (www.tdx.cat) i a través del Dipòsit Digital de la UB (diposit.ub.edu) ha estat autoritzada pels titulars dels drets de propietat intel·lectual únicament per a usos privats emmarcats en activitats d'investigació i docència. No s'autoritza la seva reproducció amb finalitats de lucre ni la seva difusió i posada a disposició des d'un lloc aliè al servei TDX ni al Dipòsit Digital de la UB. No s'autoritza la presentació del seu contingut en una finestra o marc aliè a TDX o al Dipòsit Digital de la UB (framing). Aquesta reserva de drets afecta tant al resum de presentació de la tesi com als seus continguts. En la utilització o cita de parts de la tesi és obligat indicar el nom de la persona autora.

ADVERTENCIA. La consulta de esta tesis queda condicionada a la aceptación de las siguientes condiciones de uso: La difusión de esta tesis por medio del servicio TDR (www.tdx.cat) y a través del Repositorio Digital de la UB (diposit.ub.edu) ha sido autorizada por los titulares de los derechos de propiedad intelectual únicamente para usos privados enmarcados en actividades de investigación y docencia. No se autoriza su reproducción con finalidades de lucro ni su difusión y puesta a disposición desde un sitio ajeno al servicio TDR o al Repositorio Digital de la UB. No se autoriza la presentación de su contenido en una ventana o marco ajeno a TDR o al Repositorio Digital de la UB (framing). Esta reserva de derechos afecta tanto al resumen de presentación de la tesis como a sus contenidos. En la utilización o cita de partes de la tesis es obligado indicar el nombre de la persona autora.

WARNING. On having consulted this thesis you're accepting the following use conditions: Spreading this thesis by the TDX (www.tdx.cat) service and by the UB Digital Repository (diposit.ub.edu) has been authorized by the titular of the intellectual property rights only for private uses placed in investigation and teaching activities. Reproduction with lucrative aims is not authorized nor its spreading and availability from a site foreign to the TDX service or to the UB Digital Repository. Introducing its content in a window or frame foreign to the TDX service or to the UB Digital Repository is not authorized (framing). Those rights affect to the presentation summary of the thesis as well as to its contents. In the using or citation of parts of the thesis it's obliged to indicate the name of the author.

Cellular and animal models of antibody-mediated encephalitis: from pathogenesis to novel therapeutics

Doctoral thesis presented by

Estibaliz Maudes



Doctoral program in Biomedicine, area of Neuroscience

Fundació Clínic per la Recerca Biomèdica

Institut d'Investigacions Biomèdiques August Pi i Sunyer

Universitat de Barcelona

Barcelona, June 2024

Thesis director and tutor



Josep Dalmau, MD, PhD

Thesis co-director



Carlos Matute, PhD



UNIVERSITAT DE
BARCELONA

Cover and back cover design by Lucia Prellezo @lucia.prellezo.art

All rights reserved. No part of this publication may be reproduced by any means including electronic, mechanical, photocopying, recording or otherwise, without permission of the author, or when appropriate, of the scientific journal in which parts of this thesis have been published.

A los pacientes y a las familias

Zuretzat, ama

Abbreviations

AMPAR	α -amino-3-hydroxy-5-methyl-4-isoxazolepropionic acid receptor
ATD	Amino terminal domain
CASPR	Contactin-associated protein 2
CBA	Cell-based assay
CD	Cluster of differentiation
CNS	Central nervous system
CSF	Cerebrospinal fluid
DPPX	Dipeptidyl-peptidase-like protein 6
EAE	Experimental autoimmune encephalomyelitis
FCA	Freund's complete adjuvant
FLAIR	Fluid-attenuated inversion recovery
GABA _A R	γ -aminobutyric acid type A receptor
GABA _B R	γ -aminobutyric acid type B receptor
GluK2	Glutamate ionotropic receptor kainate type subunit 2
GLUT1	Glucose transporter 1
HEK	Human embryonic kidney
IgG	Immunoglobulin class G
LEMS	Lambert-Eaton myasthenic syndrome
LGI1	Leucine-rich glioma inactivated 1
mGluR	Metabotropic glutamate receptor
MOG	Myelin oligodendrocyte glycoprotein
MRI	Magnetic resonance imaging
MS	Multiple sclerosis
NMDAR	N-methyl-D-aspartate receptor
PAM	Positive allosteric modulator
PNS	Paraneoplastic cerebellar degeneration
SCLC	Small cell lung cancer
SEZ6L2	Seizure 6-like protein 2
VGCC	Voltage-gated calcium channel

Table of contents

I. Abstract	9
II. General introduction.....	17
Antibody-associated diseases of the nervous system.....	19
Encephalitis – definition and etiological characterization	19
Encephalitis as paraneoplastic manifestations of cancer	20
Autoimmune disorders of the neuromuscular junction and peripheral nerves – discovery of antibodies altering neurological function.....	24
A paradigm shift: from antibody-associated brain diseases to antibody-mediated brain diseases	27
Antibody-mediated encephalitis	29
Anti-NMDAR encephalitis	36
Anti-mGluR5 encephalitis.....	46
Mechanisms underlying antibody-mediated encephalitis: cellular and animal models	50
Effects of patients’ antibodies in cultured neurons	52
Passive cerebroventricular transfer of antibodies to mice	60
Active immunization.....	66
III. Hypotheses	71
IV. Objectives	77
V. General methods	81
VI. Publications	91
Contribution report.	93
Paper I. Human metabotropic glutamate receptor 5 antibodies alter receptor levels and behavior in mice.....	99

Paper II. NMDA receptor antibodies in autoimmune encephalopathy alter oligodendrocyte levels and behavior in mice	107
Paper III. Allosteric modulation of NMDARs reverses patients' autoantibody effects in mice.....	117
Paper IV. Allosteric modulation of NMDARs reverses patients' autoantibody effects in mice.....	151
Paper V. Positive allosteric modulation of NMDARs prevents the altered surface dynamics caused by patients' antibodies.	163
Paper VI. Neuro-immunobiology in a mouse model of anti-NMDAR encephalitis and assessment of treatment approaches.	171
VII. Discussion	241
VIII. Conclusions.....	257
IX. Bibliography	261
X. Annex.....	281
Resumen científico	283
Resumen divulgativo.....	289
Other publications	291
Acknowledgements / Agradecimientos.....	293

Chapter I

Abstract

Background

Antibody-mediated encephalitides represent a novel category of brain inflammatory disorders mediated by antibodies targeting neural cell-surface proteins. The most prevalent form is anti-N-methyl-D-aspartate receptor (NMDAR) encephalitis, characterized by autoantibodies against the GluN1 subunit of NMDAR, leading to severe neuropsychiatric symptoms that often improve with immunotherapy. Unlike conventional brain imaging, diffusion tensor imaging studies have demonstrated extensive white matter changes in patients, as oligodendrocytes are responsible for myelin synthesis and express NMDAR. Most patients experience a slow recovery, with lingering memory and cognitive deficits, and the optimal treatment approach remains unclear. New therapeutic approaches, such as the NMDAR positive allosteric modulator (PAM) SGE-301, should be tested as complementary treatment to immunotherapy. There is a critical need for models that provide a comprehensive neuro-immunobiological understanding of the disease and offer a clinical course long enough to facilitate the assessment of potential new treatments.

Another less common form of antibody-mediated encephalitis is anti-metabotropic glutamate receptor 5 (mGluR5) encephalitis. This disorder is less well-characterized, and the effect of patients' antibodies has not yet been assessed *in vivo*.

Objectives

- 1) To determine the pathogenicity of the antibodies of patients with anti-mGluR5 encephalitis in a mouse model of cerebroventricular antibody transfer.
- 2) To investigate the effect of the antibodies of patients with anti-NMDAR encephalitis on cultures of oligodendrocytes.
- 3) To assess whether SGE-301 prevents and restores the pathological effect of patients' anti-NMDAR antibodies in a mouse model.
- 4) To elucidate whether SGE-301 modifies the cell surface dynamics of NMDARs.
- 5) To develop an animal model of anti-NMDAR encephalitis by active immunization in order to characterize the neuro-immunobiology of the disease and test different treatments, including immunotherapy and SGE-301.

Methods

To develop a mouse model of anti-mGluR5 encephalitis, patients' antibodies were continuously infused for 14 days into the cerebroventricular system of ten-week-old C57BL/6J male mice. Memory and anxiety were assessed, and the antibody effects on hippocampal mGluR5 clusters were determined. To study the effect of antibodies from patients with anti-NMDAR encephalitis on oligodendrocytes, cultures of oligodendrocytes were exposed to patients' CSF, and the activity of NMDARs was assessed with calcium imaging. To assess the potential therapeutic effect of SGE-301, adult mice receiving cerebroventricular infusion of CSF from patients with anti-NMDAR encephalitis for 14 days were treated daily with this NMDAR PAM, either from the start of antibody infusion or upon symptom onset. Mice were evaluated for memory, density of hippocampal NMDAR clusters and synaptic plasticity (long-

term potentiation, LTP). To investigate how SGE-301 affects the surface dynamics of NMDARs, cultured hippocampal neurons were treated with SGE-301 alone or with antibodies from patients with anti-NMDAR encephalitis, and NMDAR membrane dynamics were assessed with single-molecule imaging. To develop a novel mouse model of anti-NMDAR encephalitis, eight-week-old female mice (C5BL/6J) were immunized with a 30 amino acid GluN1 peptide and AddaVax adjuvant. The model was thoroughly characterized, including the development of NMDAR antibodies (class, subclass, epitope spreading), changes in memory and behavior, effects of antibodies on NMDAR density and function, hippocampal plasticity, and analysis of brain immunological infiltrates and synthesis of antibodies in deep cervical lymph nodes. Using this model, anti-CD20 immunotherapy and SGE-301 were assessed.

Results

- 1) Mice infused with antibodies from patients with anti-mGluR5 encephalitis showed memory impairment, increased anxiety and decreased neuronal surface mGluR5. After antibody clearance, both behavioral and molecular changes reversed to normal conditions.
- 2) In oligodendrocytes incubated with CSF antibodies from patients with anti-NMDAR encephalitis, the NMDAR-mediated calcium currents were significantly reduced.
- 3) In mice infused with CSF antibodies from patients with anti-NMDAR encephalitis, daily subcutaneous administration of SGE-301 prevented and recovered the memory impairment and hippocampal synaptic alterations caused by the antibodies.

- 4) NMDAR surface trajectories in neurons treated with SGE-301 were upregulated, mainly in the synapse. Treatment with antibodies from patients with anti-NMDAR encephalitis reduced NMDAR membrane dynamics and increased their confinement. SGE-301 antagonized these antibody effects in the synaptic and extrasynaptic membrane compartments, restoring normal NMDAR membrane dynamics.
- 5) Mice immunized with the GluN1 peptide developed serum and CSF polyclonal (mainly IgG1) NMDAR antibodies resulting in a decrease of surface NMDAR clusters in the brain and reduction of hippocampal plasticity. These findings were associated with brain inflammatory infiltrates (predominantly B cells and plasma cells), activation of microglia, microglial phagocytosis of NMDAR bound to IgG, synthesis of antibodies in deep cervical lymph nodes, psychotic-like behavior, memory deficit, depressive-like behavior, abnormal movements, and lower threshold to develop seizures. Most symptoms and neurobiological alterations were reversed by treatment with anti-CD20 immunotherapy and SGE-301.

Conclusions

My studies have contributed to gain insight into the pathophysiology of anti-mGluR5 and anti-NMDAR encephalitis. The first study provides robust evidence of the pathogenicity of patient's mGluR5 antibodies, leading to mGluR5 brain density reduction and subsequent neuropsychiatric symptoms. The second study suggests a link between antibody-mediated dysfunction of NMDARs in oligodendrocytes and the white matter alterations reported in patients with anti-NMDAR encephalitis. The third and fourth studies offer evidence in a well-established mouse model of cerebroventricular transfer of patient's NMDAR antibodies that SGE-301 antagonizes and reverses the synaptic

and pathogenic effects of the antibodies. The fifth study sheds light on the molecular mechanism of this PAM at the surface dynamics. The sixth study offers a novel mouse model of anti-NMDAR encephalitis by active immunization that mirrors most of the neuro-immunobiological alterations of anti-NMDAR encephalitis. The study also provides a novel treatment strategy that combines immunotherapy to eliminate the antibody-producing cells, and a NMDAR PAM, resulting in recovery of all clinical and neurobiological paradigms. Finally, this model suggests a novel immunological paradigm which includes epitope spreading in the brain and a polyclonal immune response probably fine-tuned in the deep cervical lymph nodes.



Chapter II

General introduction

Antibody-associated diseases of the nervous system

Encephalitis – definition and etiological characterization

Encephalitis is an inflammatory brain disorder usually caused by infectious or immune-mediated mechanisms. It typically leads to altered level of consciousness, seizures, memory deficits, and behavioral or psychiatric symptoms.¹ Although the annual incidence of acute encephalitis seems low, ranging from 0.07 to 12.6 cases per 100,000 people,²⁻⁴ its high mortality rate (5-15%)⁵ and substantial morbidity (e.g., cognitive deficits, epilepsy) underscores the social and economic impact of this medical condition.

It has been estimated that 40-50% of encephalitis cases arise from infectious agents that can be viral, bacterial or fungal,⁶ with herpes simplex viral encephalitis being the most frequent infectious encephalitis in high-income countries.⁷ Another 20-30% of cases are believed to have an autoimmune origin, where patients develop an immune response against antigens that are expressed by neurons or glial cells. Some of these patients develop antibodies that can be detected in serum and cerebrospinal fluid (CSF). The remaining 20-40% of encephalitis cases have an unclear etiology (idiopathic).

Identifying the etiology of encephalitis is crucial since it influences patient treatment and outcomes. The discovery of antibodies targeting the N-methyl-D-aspartate receptor (NMDAR) in a group of patients exhibiting a specific syndrome, known today as anti-NMDAR encephalitis, laid the foundation for defining the category of antibody-mediated autoimmune encephalitis. This discovery transformed the

diagnosis and treatment of several neurological and psychiatric syndromes previously thought to be idiopathic or of unknown origin. The discovery of anti-NMDAR encephalitis and related disorders was profoundly influenced by the pioneering studies done with paraneoplastic neurological syndromes, which led to the discovery of anti-neuronal antibodies, and with the antibody-mediated diseases of the peripheral nervous system.

Encephalitis as paraneoplastic manifestations of cancer

In the 1960s, early theories suggested that paraneoplastic diseases of the central nervous system (CNS) might be immune-mediated, though evidence was then inconclusive. In 1985, Graus et al., made an important discovery involving two patients with paraneoplastic sensory neuronopathy and small cell lung cancer (SCLC), in whom he found serum antibodies that reacted with proteins expressed by the nuclei of neurons.⁸ Subsequent studies showed that the antibodies also recognized proteins expressed by the tumor,⁹ providing robust evidence that ectopic expression by the tumor of a neuronal protein could trigger an immune response that cross-reacted with the same protein in neurons of the dorsal root ganglia and brain.

Currently, these disorders, known as paraneoplastic neurological syndromes (PNS), are understood to be rare disorders driven by cancer-induced immune responses against neuronal proteins, also known as onconeural antigens. These responses result in a variety of clinical manifestations (Table 1). PNS occurs in less than 1% of cancer patients and typically presents with a subacute onset, with symptoms developing over days to weeks.¹⁰ The neurological symptoms often progress rapidly, over weeks or a few months, leading to severe disability and sometimes death.¹¹ Notably, neurological symptoms usually precede the discovery

of the underlying cancer, which is often microscopic or not yet detectable. Thus, detecting and treating the associated tumor is crucial for managing PNS. Whole-body positron emission tomography – computed tomography scans (FDG-PET/CT) are the most effective tests for detecting these cancers based on their hypermetabolic activity.¹²

The discovery of onconeural antibodies substantially advanced the diagnosis of PNS as they are reliable disease biomarkers. In PNS associated with antibodies against intracellular proteins, these antibodies recognize linear epitopes, facilitating their detection in assays that use fixed cells transfected with the target onconeural antigens, or immunoblots of recombinant proteins or neuronal protein lysates. However, research indicates that these antibodies do not drive the pathogenicity of the disease. Studies using cultured neurons have shown that these antibodies cannot access the intracellular compartment where the corresponding onconeural antigens are expressed.¹³ Additionally, animal models involving passive transfer of patients' antibodies failed to reproduce the disease symptoms,^{14,15} suggesting that these antibodies are likely not pathogenic.

The pathogenicity of PNS appears to be primarily mediated by T cells. Autopsy findings reveal inflammatory infiltrates in the brain, consisting mainly of CD3+ and CD8+ lymphocytes, with fewer CD4+ cells, indicating a predominance of T-cytotoxic lymphocytes over T-helper cells. Furthermore, cytotoxicity has been demonstrated by PNS patients' T cells specifically reacting to tumor cells expressing neuronal antigens.¹⁶ Several neuropathological studies have shown T-cytotoxic cells surrounding neurons undergoing degeneration through perforin and granzyme B-mediated neurotoxicity.¹⁷

These data suggest a model where dendritic cells phagocytose apoptotic tumor cells that ectopically express neuronal proteins. After processing the antigens, they are presented to the immune system in the local tumor-draining lymph nodes. This activates specific T-cell responses, predominantly T-cytotoxic cells, that mediate the pathogenicity in PNS.

Moreover, in PNS associated with antibodies against intracellular proteins, treatments like plasma exchange or intravenous immunoglobulins are generally ineffective. Since the antibodies themselves are not pathogenic, strategies to deplete antibodies or antibody producing cells rarely result in substantial clinical improvement. Therefore, treatment strategies should primarily focus on tumor removal and inhibition of the T-cell mediated mechanisms.¹⁸

The hypothesis that T cytotoxic cells being the pathogenic agent in PNS has recently been reinforced by the use of immune checkpoint inhibitors as treatments for cancer. The main targets of immune checkpoint inhibitors are programmed cell death 1 (PD1), programmed death ligand 1 (PD-L1), and cytotoxic T-lymphocyte-associated protein 4 (CTLA4), which are negative regulators of T cell immune function.¹⁹ By blocking these downregulators of immunity, immune checkpoint inhibitors enhance the immune attack against cancer cells, resulting in effective anti-tumor responses. In rare cases, activation of the immune system by immune checkpoint inhibitors leads to autoimmune adverse events that can affect almost any organ, including the nervous system.²⁰ In this context, approximately 1% of patients develop PNS and other inflammatory CNS disorders after subclinical immune responses against cancer proteins are amplified by the checkpoint inhibitors.²¹ These findings support the theory of T cells are the pathogenic drivers of PNS associated with antibodies against intracellular antigens.

Table 1. Clinical features of onconeural antibodies.

Antibody or antigen	Main antigen function	Main paraneoplastic neurological syndrome	Associated cancer types (%)	Antibody positive cancer patients without PNS (%)
Hu (ANNA1)	Regulation of mRNAs related to neuronal development and plasticity	Encephalomyelitis; sensory neuronopathy	SCLC (75), NSCLC (10), and extrathoracic cancers (15)	SCLC (16)
CV2 (CRMP5)	Axon guidance and neurite outgrowth signaling	Encephalomyelitis; sensorimotor neuropathy	SCLC (77), NSCLC (5), thymoma (8), or extra-thoracic cancers (10)	SCLC (5-6), thymomas (12)
SOX1	Transcription factor that regulates CNS development	LEMS and PCD in the context of SCLC	SCLC (93), NSCLC (4), and extra-thoracic cancers (3)	SCLC (16)
Yo (PCA1)	Unknown	PCD	Ovarian (62), breast (26), and fallopian tube (12) cancers	2
Ri (ANNA2)	Regulation of mRNAs related to neuronal development and plasticity	Brainstem encephalitis; opsoclonus	Breast (51), lung (30), and others (19)	Ovarian cancer (4), SCLC (1.5)
Amphiphysin*	Recruitment of dynamin to clathrin-mediated endocytosis in synaptic vesicles	Stiff-person syndrome; encephalomyelitis; sensory neuropathy	SCLC (59), breast (35), and others (6)	Breast cancer (0.8), SCLC (1)
Tr (DNER)*	Mediation in neuron-glia interaction	PCD	Hodgkin lymphoma (100)	2
Ma1/Ma2	Unknown	Limbic, diencephalic and brainstem encephalitis	Testicular (42), lung (17), and other (36) cancers	0
KLHL11	Member of the E3 ubiquitin-protein ligase complex	Cerebellar ataxia and brainstem encephalitis	Testicular cancers and teratomas ^a	Teratoma (5)
PCA2	Microtubule-associated protein involved in neuronal differentiation	Encephalomyelitis	SCLC (40), NSCLC (24)	2

^aFrequency differs in two reported series: Maudes et al.: teratoma (61%), testicular cancer (30%); Dubey et al.: testicular cancer (92%). SCLC: small cell lung cancer, NSCLC: non-SCLC, LEMS: Lambert-Eaton Myasthenic Syndrome, SPS: stiff-person syndrome, PCD: paraneoplastic cerebellar degeneration, KLHL11: Kelch-like 1. *These antigens are not intracellular, but are included in this table because they are strongly associated with cancer. From²²

Autoimmune disorders of the neuromuscular junction and peripheral nerves – discovery of antibodies altering neurological function

Unlike classical PNS of the central nervous system where the initial findings pointing to an autoimmune etiology stemmed from neuropathological observations, the discovery of the immune etiology of disorders of the neuromuscular junction (e.g., myasthenia gravis, Lambert-Eaton myasthenic syndrome [LEMS]) and neuromyotonia, came from different observations.

For myasthenia gravis, researchers in the 1960s noted that these patients were predominantly young women, frequently having other autoimmune diseases and thymic abnormalities. Observations of symptom transmission from pregnant women to neonates led to the hypothesis of an antibody-mediated mechanism targeting an “endplate” protein.²³ This was confirmed through a rabbit immunization model against acetylcholine receptors (AChR), which replicated the symptoms of the human disease.²⁴ These findings were supported by experiments of passive IgG transfer to rats, revealing symptom development and electrophysiologic features characteristic of myasthenia gravis.^{25,26} Additionally, the disproportionate reduction of AChRs relative to the amount of injected antibodies suggested complement-related pathogenic mechanisms. In 1978, researchers discovered that the reduction of AChR in myasthenic patients resulted in part, from the cross-linking and internalization of receptors by patients’ antibodies.²⁷

LEMS, another neuromuscular junction disorder, was suspected to be autoimmune due to clinical observations; approximately 50% of LEMS patients had an underlying tumor, often SCLC. In 1982, researchers identified one or more organ-specific autoantibodies in 29 of 64 LEMS patients, reinforcing the autoimmune theory.²⁸ Further confirmation of an immune-mediated etiology came from the observations that plasma exchange led to improvement of patients' clinical and electrophysiologic alterations, and that passive transfer of patients' IgG to mice induced the same neurophysiological alterations as those seen in patients.²⁹ These findings culminated in identifying that patients' antibodies targeted P/Q-type voltage-gated calcium channels (VGCC).^{30,31}

In the case of neuromyotonia (also called Isaacs' syndrome or peripheral nerve hyperexcitability), the frequent presence of thymoma and other tumors, along with AChR antibodies in some patients, supported an immune-mediated etiology.³²⁻³⁴ Passive transfer of patient's IgG to mice increased resistance to d-tubocurarine (a neuromuscular blocker).³⁵ This finding suggested that neuromyotonia was associated with an antibody-mediated alteration of voltage-gated potassium channels (VGKC) that normally regulate nerve excitability. In 2002, a series of 60 patients with neuromyotonia showed that 35% had VGKC antibodies.³⁶ Later studies showed that the antibodies of patients with neuromyotonia actually targeted a protein interacting with VGKC, known as contactin-associated protein-like 2 (CASPR2).⁶

Today, myasthenia gravis, LEMS, and neuromyotonia are recognized as autoimmune disorders of the peripheral nervous system. The first two share some symptoms including fatigable skeletal muscle weakness that can involve breathing, swallowing, and speaking, whereas patients with neuromyotonia develop cramps, muscle twitching (fasciculations or myokymia), stiffness, delayed muscle relaxation (pseudomyotonia), and spontaneous or evoked carpal or pedal spasms.

Clinical observations suggest an association between these disorders and altered mechanisms in the development of self-tolerant T-cells. Normally, AChR are expressed in the thymus.³⁷ Dysregulation of regulatory T cells may lead to self-reactive T and B cells directed against muscle antigens.^{38,39} Thymic abnormalities, like hyperplasia or thymoma, are frequent causes of this immunological dysregulation. Notably, 10-20% of myasthenia gravis patients have thymoma, and about 30% of thymoma patients develop myasthenia gravis.⁴⁰ Thymus removal often benefits these patients, highlighting the key role of the thymus in the context of the disease.⁴¹ Unlike myasthenia gravis, 60% of patients with LEMS have an underlying SCLC, strongly indicating a search for this type of tumor in these patients.⁴²

In autoimmune neuromuscular junction disorders, antibodies are pathogenic and directly alter the function of the neuromuscular synapse. The main alterations include: 1) crosslinking and internalization of the target antigen, as occurs in myasthenia gravis with antibodies against AChR and LEMS with antibodies against VGCC; 2) blocking protein-protein interactions, as occurs in the

variant of myasthenia gravis associated with anti-MuSK antibodies; and 3) postsynaptic muscle membrane lysis via complement activation, as also occurs in myasthenia gravis.

Due to the antibody-mediated etiology, immunotherapies targeting autoantibodies or antibody-producing cells effectively treat these diseases. Moreover, a better understanding of the physiopathology of the neuromuscular transmission and how it is affected by patients' antibodies, led to new treatment approaches focused on compensating or antagonizing the antibody effects, such as acetylcholinesterase inhibitors in myasthenia gravis, or potassium channel blockers (3-4 diaminopyridine) in LEMS.⁴³

A paradigm shift: from antibody-associated brain diseases to antibody-mediated brain diseases

Clinical, pathological and immunological studies in PNS of the CNS and disorders of the neuromuscular junction laid the groundwork that culminated with the discovery of encephalitis directly mediated by autoantibodies. By the mid-2000s, most currently known PNS had been reported. At that time, the only two CNS disorders associated with antibodies against neuronal cell-surface proteins were a subtype of paraneoplastic cerebellar degeneration linked to antibodies against the metabotropic glutamate receptor 1 (mGluR1),⁴⁴ and limbic encephalitis attributed to VGKC antibodies. Subsequent research revealed that VGKC antibodies were in fact directed, not against the VGKC, but against leucine-rich glioma-inactivated protein 1 (LGI1) or CASPR2.⁴⁵ Nonetheless, the conceptual impact of the initial study of VGKC antibodies was

important, leading to the classification of limbic encephalitis into two categories: paraneoplastic (related to antibodies against intracellular proteins) and non-paraneoplastic (related to VGKC antibodies).

This classification was soon challenged by two pivotal studies. A 2005 study described 7 patients with suspected immune-mediated encephalitis; 6 patients had antibodies against neuronal cell-surface proteins, exhibiting distinct immunostaining patterns in the neuropil of rat brain.⁴⁶ Remarkably, despite severe symptoms and the presence of tumors in four patients, all experienced substantial neurological improvement following immunotherapy. This study demonstrated a more extensive repertoire of neuronal cell-surface antibodies than previously thought and highlighted the efficacy of treatment, emphasizing the importance of a prompt and correct diagnosis.

The second study focused on four young women presenting with encephalitis characterized by prominent psychiatric symptoms and rapid neurological deterioration, including decreased level of consciousness, and central hypoventilation.⁴⁷ All four patients had an ovarian teratoma. The clinical similarity among these patients pointed to a common autoimmune disorder, which was confirmed with the identification of CSF and serum antibodies that produced an identical pattern of immunostaining of the neuropil of rat brain and the cell surface of neurons. The target antigen was characterized as NMDAR in 2007, leading to naming the disorder as anti-NMDAR encephalitis.⁴⁸ The techniques employed for the discovery of this disease were later applied to larger cohorts of patients with

suspected autoimmune encephalitis, resulting in the identification of multiple antibodies linked to distinct syndromes.

The realization that some CNS diseases are mediated by neuronal autoantibodies was groundbreaking, significantly impacting clinical practice over the past 20 years. Neurological syndromes previously classified as idiopathic or atypical are now recognized as immune-mediated and treatable. Different autoantibodies associated with distinct clinical syndromes have become invaluable biomarkers in guiding diagnostic evaluations. Detection of these antibodies in serum or CSF confirms the diagnosis of distinct autoimmune encephalitis and for some antibodies supports the need to search for an associated tumor.

Antibody-mediated encephalitis

This novel category of CNS inflammatory disorders mediated by antibodies against neural cell-surface proteins, ion channels or receptors is known as antibody-mediated encephalitis. These disorders are different from the previously known PNS as the associated antibodies are directed against extracellular antigens (Figure 1), they can occur with or without tumors, the pathogenic mechanisms are predominantly B cell-mediated (rather than cytotoxic T-cell mediated), and the disorders are more responsive to immunotherapy (Table 2)

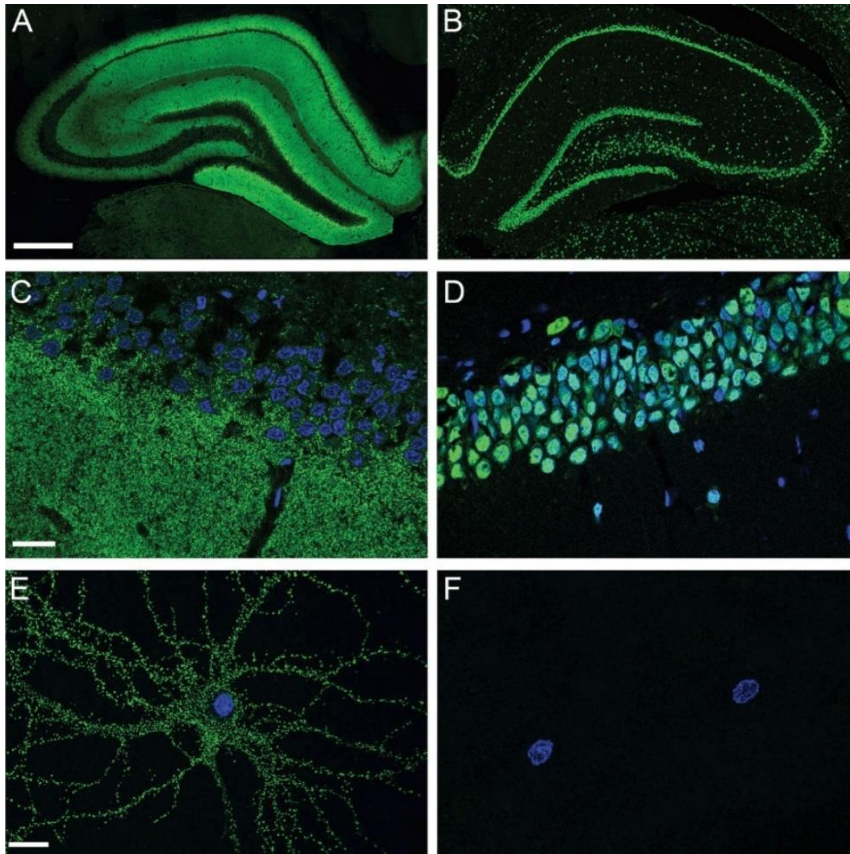


Figure 1. Comparison of brain and neuronal reactivity of antibodies against a cell surface and an intracellular antigen. Coronal section of rat hippocampus immunolabeled with an antibody against a cell surface receptor (NMDAR) from a patient with anti-NMDAR encephalitis (A), compared with an antibody against an intracellular protein (Hu) from a patient with SCLC (B). A high magnification of the reactivity is shown in C and D. Compared with the NMDAR antibody that shows intense reactivity with the neuropil of the hippocampus, the Hu antibody does not react with the neuropil, and only shows intracellular staining after tissue permeabilization. In cultures of neurons, only the NMDAR antibody reacts with the cell surface antigen in live neurons (E). The Hu antibody does not reach the target antigen in live neurons (F). Scale bars in A and B, 500 μm ; C and D, 20 μm ; E and F, 10 μm . From²²

Table 2. Clinical features of autoimmune encephalitis related to intracellular versus cell surface antigens.

Intracellular and onconeural antigens	Cell surface or synaptic antigens
Mediated by cytotoxic T cell mechanisms	Mediated by B cell and antibody-related mechanisms
Frequently paraneoplastic, except for GAD65 and other less common antibodies (e.g., AK5)	Variably paraneoplastic (0-70%), depending on the type of antibody
Patients usually older than 50 years	Patients of all ages; some diseases preferentially occur in specific age groups
Tumors almost always malignant	Tumors can be benign
Monophasic neurologic disease	Relapses in ~10-35% of cases, depending on the antibody
Outcome dependent on tumor control	Outcome not totally dependent on tumor control
Limited response to treatment	70-80% substantial recovery

From²²

There are currently 19 known disorders that fall within the category of antibody-mediated encephalitis. The clinical features, main symptoms, and antibody effects associated to each antibody are summarized in Table 3.

Antibody-mediated encephalitis can be challenging to diagnose, as symptoms may mimic those of other neurological or psychiatric diseases. Moreover, most types of encephalitis share several symptoms regardless of their etiology (e.g., bacterial, viral or autoimmune), emphasizing the importance to recognize the cause in order to treat the patient appropriately. To facilitate the diagnosis of autoimmune encephalitis, Graus et al (2016) proposed a clinical diagnostic algorithm with criteria of probable and definite

autoimmune encephalitis.⁴⁹ Minimal requirements to initially consider a potential autoimmune encephalitis included the subacute onset of working memory deficits, altered mental status or psychiatric symptoms, and at least one of the following: new focal CNS findings, seizures not explained by a previous disorder, CSF pleocytosis, and MRI features suggestive of encephalitis.

Serum and CSF samples from patients who meet these requirements are tested with rat brain immunohistochemistry for determination of neuronal or glial cell surface antibodies. Each of these autoantibodies gives a distinct pattern of brain immunoreactivity, thus allowing the association of the immunoreactive pattern with a specific syndrome (Figure 2). The identity of the antibody target is identified by cell-based assays, which consists in immunocytochemistry with cells that recombinantly express different neuronal or glial proteins. If the target antigen is different from all that are currently known, the patient's serum or CSF is assessed with immunocytochemistry using live cultured neurons to determine if the antigen is on the cell surface.



Figure 2. Rat brain immunostaining with patients' autoantibodies against neuronal cell-surface and synaptic proteins (neuropil immunostaining). Sagittal and coronal sections of rat brain immunostained with 13 representative autoantibodies against neuronal cell-surface and synaptic proteins. For DNER and mGluR1, which predominantly react with cerebellum, the coronal section has been replaced by a sagittal section of cerebellum. All tissue sections have been mildly counterstained with hematoxylin. Scale bars, 2 mm. From⁵⁰

Table 3. Extracellular neuronal antigens in autoimmune encephalitis.

Target antigen	Clinical features	Main presenting symptoms and tumor	Main IgG subclass
NMDAR	80% female, median age 21 years (2 months – 85 years)	Psychiatric symptoms, cognitive impairment, seizures, abnormal movements, and coma. Ovarian teratoma (58% in women 18 – 45 years)	IgG ₁
AMPA	70% female, median age 56 years (23 – 81)	LE with memory loss, psychiatric features. SCLC, thymoma, and breast cancer	IgG ₁
GABA _B R	60% male, median age 61 years (16 – 77)	LE with severe seizures, memory loss. SCLC	IgG ₁
LGI1	65% male, median age 60 years (30 – 80)	LE, memory loss, faciobrachial dystonic seizures. No tumor associated	IgG ₄
CASPR2	85% male, median age 60 years (46 – 77)	Neuromyotonia, muscle spasms, fasciculations, LE, memory loss, Morvan syndrome. Thymoma	IgG ₄
GABA _A R	50% female, median age 40 (2.5 months – 88 years)	Status epilepticus. Infrequently, thymoma	IgG ₁
DPPX	70% male, median age 57 years (35 – 69)	Confusion, diarrhea, hyperekplexia No tumor associated	IgG ₁ / IgG ₄
D2R	50% female, median age 5.5 years (1.6 months – 15 years)	Dystonia, chorea. No tumor associated	Unknown
mGluR5	60% male, median age 29 years (6 – 75)	Non-focal encephalitis, memory loss, confusion. Hodgkin's lymphoma	IgG ₁

Neurexin-3α	80% female, median age 44 years (23 – 50)	Confusion, seizures, and decreased level of consciousness No tumor associated	IgG ₁
IgLON5	50% male, median age 64 years (46 – 83)	REM and NREM parasomnia with sleep breathing problems, brainstem dysfunction, and gait instability. No tumor associated	IgG ₄
Amphiphysin	100% female, median age 58 years (39 – 73)	Stiff-person syndrome, encephalomyelitis. SCLC, breast cancer	IgG ₁
DNER (Tr)	78% male, median age 61 years (14 – 75)	PCD. Hodgkin's lymphoma	IgG ₁
mGluR1	50% male, median age 58 years (33 – 81)	Severe cerebellar syndrome, cerebellar atrophy. Hodgkin's lymphoma	IgG ₁
P/Q-type VGCC	52% female, median age 57 years (9 – 87)	LEMS, PCA. SCLC, Hodgkin's lymphoma	Unknown
GlyR	60% male, median age 47 years (1 – 75)	Progressive encephalomyelitis with rigidity and myoclonus (PERM), stiff-person syndrome. No tumor associated	IgG ₁
SEZ6L2	78% female, median age 62 years (54 – 73)	Subacute cerebellar syndrome with frequent extrapyramidal symptoms. No tumor associated	IgG ₄
mGluR2	2 reported cases; both female, 78 and 3 years	PCA. Various tumors	IgG ₁
GluK2R	62.5% male, median age 32 years (14 – 75)	Encephalitis with prominent cerebellar involvement. No tumor associated	IgG ₁

LE: limbic encephalitis, SCLC: small cell lung cancer, REM: rapid eye movement, NREM: non-REM, PCD: paraneoplastic cerebellar degeneration, LEMS: Lambert-Eaton Myasthenic Syndrome, PCA: paraneoplastic cerebellar ataxia. From ²²

Anti-NMDAR encephalitis

Anti-NMDAR encephalitis is the most common form of antibody-mediated encephalitis, with an estimated annual incidence of 1.5 persons per million.⁵¹ Patients develop antibodies against a restricted antigenic region of the extracellular domain of the GluN1 subunit of NMDAR, specifically around residues N368/G369.⁵²

NMDAR structure and function

The NMDAR is an ionotropic glutamate receptor comprised of two GluN1 and two GluN2 or GluN3 subunits (Figure 3).^{53–56} There are eight alternatively spliced GluN1 isoforms, four GluN2 subunits (A-D) each coded by a different gene, and two GluN3 subunits (A-B), also coded by separate genes.⁵⁷ GluN1, which is the obligatory subunit of the receptor, and GluN3 bind glycine, whereas GluN2 binds glutamate. Each GluN subunit features three large extracellular domains (the amino-terminal domain subdivided into two lobes, and the S1 and S2 domains that contain the agonist binding site), three transmembrane domains (TM1, TM3, and TM4), a membrane-associated loop (TM2), and an intracellular C-terminal domain that connects the receptor to scaffolding proteins and signaling systems.⁵⁴

In mature neurons, many GluN1/GluN2B receptors are predominantly found outside the synapse, while GluN1/GluN2A/GluN2B complexes become the principal synaptic receptors in the hippocampus and forebrain.⁵⁸

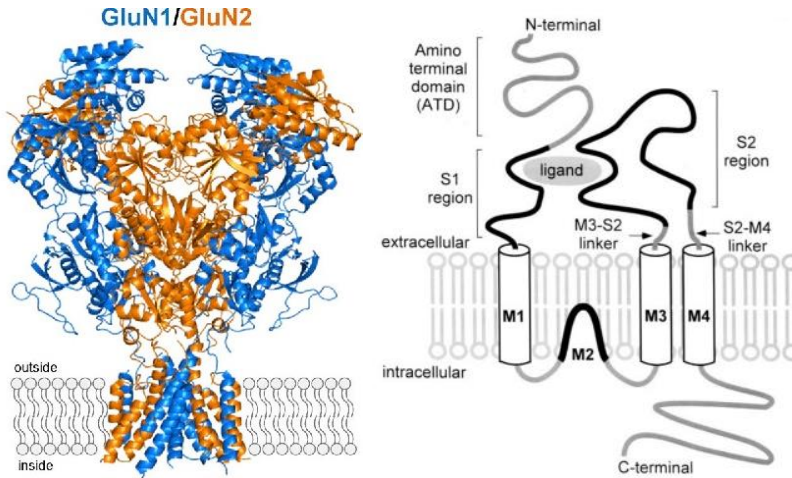


Figure 3: NMDAR structure and subunits. (A) 3D structure of NMDAR. Most NMDARs are composed of two GluN1 and two GluN2 subunits, which can be GluN2A-D. GluN1 subunits are the obligatory subunits in all NMDARs. (B) Representation of the domains of a GluN. All GluNs have three extracellular domains: the amino terminal domain (ATD), and the S1 and S2 domains that contain the ligand binding site. In addition, all subunits have three membrane-spanning domains (M1, 3, 4), a membrane loop (M2), and an intracellular C-terminal domain that connects the receptor to scaffolding proteins and messenger systems. The antibodies of patients with anti-NMDAR encephalitis react with a conformational epitope region in the ATD of GluN1. From^{53,54}

NMDARs exhibit a voltage-dependent block by Mg^{2+} , and function as a coincidence detector.^{59,60} Binding by the agonist glutamate alone is insufficient for channel activation, as Mg^{2+} remains bound to the channel pore effectively blocking ion transport. Membrane depolarization is required to dislodge the Mg^{2+} from the receptor's channel. Therefore, the coincidence of presynaptic glutamate release, a co-agonist (typically glycine or D-serine), and strong depolarization of the post-synaptic neuron (removing Mg^{2+} from the channel) are required for the opening of NMDAR channels. This process allows the influx of Na^+ and Ca^{2+} and efflux of K^+ ions. The high Ca^{2+} permeability of NMDARs triggers the activation of Ca^{2+} -dependent enzymes, facilitating long-term alterations in synaptic structure and connectivity.

NMDARs play critical roles in synaptic transmission and remodeling, dendritic sprouting, and hippocampal long-term potentiation (LTP), a mechanism crucial for memory formation and learning. Mice lacking GluN1 die from hypoventilation within hours after birth.⁶¹ Hippocampal CA1 region-specific GluN1 knockout mice show severe deficits in spatial and temporal learning and a significant reduction in LTP in the Schaffer collateral-CA1 synapse, demonstrating the role of the NMDAR in establishing synaptic plasticity and memory formation.⁶²

Clinical features of anti-NMDAR encephalitis

Anti-NMDAR encephalitis affects individuals of all ages (reported cases range from 8 months to 85 years), but patients are usually children and young adults. About 37% of patients are younger than 18, and 58% are between 18 and 44 years old. The median age at disease onset is 21 years, with a notable predominance of females (~4:1). Although the disease can occur without a tumor association, up to 50% of young female patients have an ovarian teratoma.

Distinct symptoms often develop sequentially, starting with a viral-like prodrome, followed by prominent psychiatric symptoms accompanied or followed by neurological alterations. Two to three weeks after onset, most patients have memory deficits, seizures, dyskinesias, decreased level of consciousness, dysautonomia or central hypoventilation, often requiring intensive care. Recovery generally mirrors the progression of the disease, with cognitive and psychiatric symptoms being the last to improve (Figure 4). There is a slight variation in symptom manifestation according to age: children frequently present with seizures and movement disorders, whereas

adults more commonly experience psychotic-like behavior and other behavioral alterations. Relapses occur in about 20% of cases, even many years after the first episode. Early relapses are frequently associated to a reduction or discontinuation of immunotherapy or tumor recurrence for paraneoplastic cases.

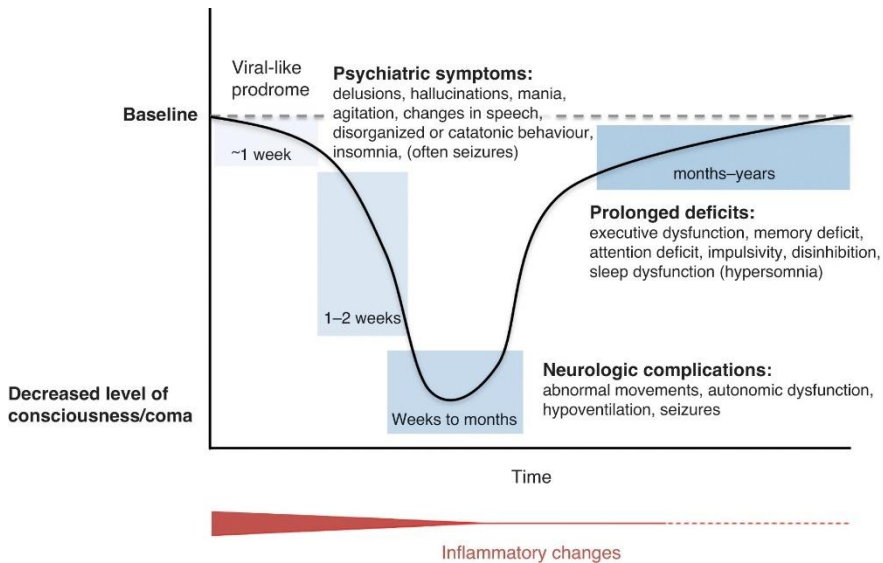


Figure 4. Stages and clinical course of anti-NMDAR encephalitis. This graphic representation of the full-fledged syndrome of anti-NMDAR encephalitis in teenagers and young adults shows the predominance of psychiatric symptoms at the initial phase of the disease. These symptoms are usually accompanied or followed by neurologic alterations (e.g., abnormal movements, seizures, dysautonomia, coma) that eventually improve or resolve, and lead to a prolonged phase of recovery with prominent involvement of executive functions, memory, and attention. Inflammatory changes in CSF or brain MRI predominate in the early stage of the disease. From

Triggers of the disease

Like other autoimmune diseases, anti-NMDAR encephalitis involves a breakdown in immunologic self-tolerance. Two primary triggers have been identified. First, as noted up to 50% of young female patients have an ovarian teratoma that contains nervous system expressing NMDAR, which is hypothesized to initiate the immune

response. This is supported by histological studies showing extensive inflammatory infiltrates in teratomas from patients with anti-NMDAR encephalitis, compared with teratomas from individuals not affected by the disease.⁶³ Recent studies that prospectively followed patients from the time of diagnosis of HSE showed that about 25% developed neurological relapses caused by autoimmune mechanisms. These relapses, frequently preceded by the development of NMDAR and other neuronal antibodies, almost always occurred within three months after successful treatment of the viral infection.⁶⁴

Neuropathological findings

Pathological studies on autoimmune encephalitis are scarce, mainly due to the partial or complete recovery of most patients; however, when available the findings are remarkably different from those reported in patients with cytotoxic T cell-mediated mechanisms, including paraneoplastic syndromes with onconeural antibodies and non-cancer-related encephalitis with GAD65 or AK5 antibodies.

In these latter disorders biopsy and autopsy studies usually show frequent and extensive infiltrates of T cells, often in close apposition to neurons or forming neuronophagic clusters of T cells that lead to irreversible neuronal loss accompanied by astrogliosis.^{17,65}

In contrast, brain biopsy studies of patients with anti-NMDAR encephalitis are often normal or show only mild inflammatory changes.⁶⁶ Autopsy studies show inflammatory infiltrates predominantly composed of B cells and plasma cells, with infrequent perivascular and parenchymal CD3+/CD8- T cells in basal ganglia, amygdala, and hippocampus (Figure 5A-M).⁶⁷ In contrast with T cell-

mediated disorders, these infiltrates are almost never in close apposition to neurons or forming neuronophagic clusters. Moreover, these autopsy studies show microglial activation and a significant decrease of NMDAR immunoreactivity in the areas of the brain examined, mainly hippocampus (Figure 5N-P).⁶⁷

White matter alteration in anti-NMDAR encephalitis

Conventional magnetic resonance imaging (MRI) scans show non-specific changes in only 40% of patients, such as increased intensity in cortical/subcortical regions in T2 and fluid-attenuated inversion recovery (FLAIR) sequences, or transient contrast enhancement in these regions and the meninges.^{48,68} The MRI may also reveal myelin changes that do not correspond well with the clinical presentation.⁶⁸

Previous studies have attempted to explain this clinical-radiological discrepancy (severe protracted symptoms but mild or transient MRI changes) using more complex multimodal MRI techniques. In particular, diffusion tensor imaging (DTI) studies demonstrate that patients have extensive white matter changes in deep white matter tracts and superficial intracortical white matter that appear to correlate with disease severity.^{69,70} In fact, oligodendrocytes, which are responsible for axonal myelin sheath's synthesis in the white matter of the central nervous system, have been shown to express NMDAR.⁷¹

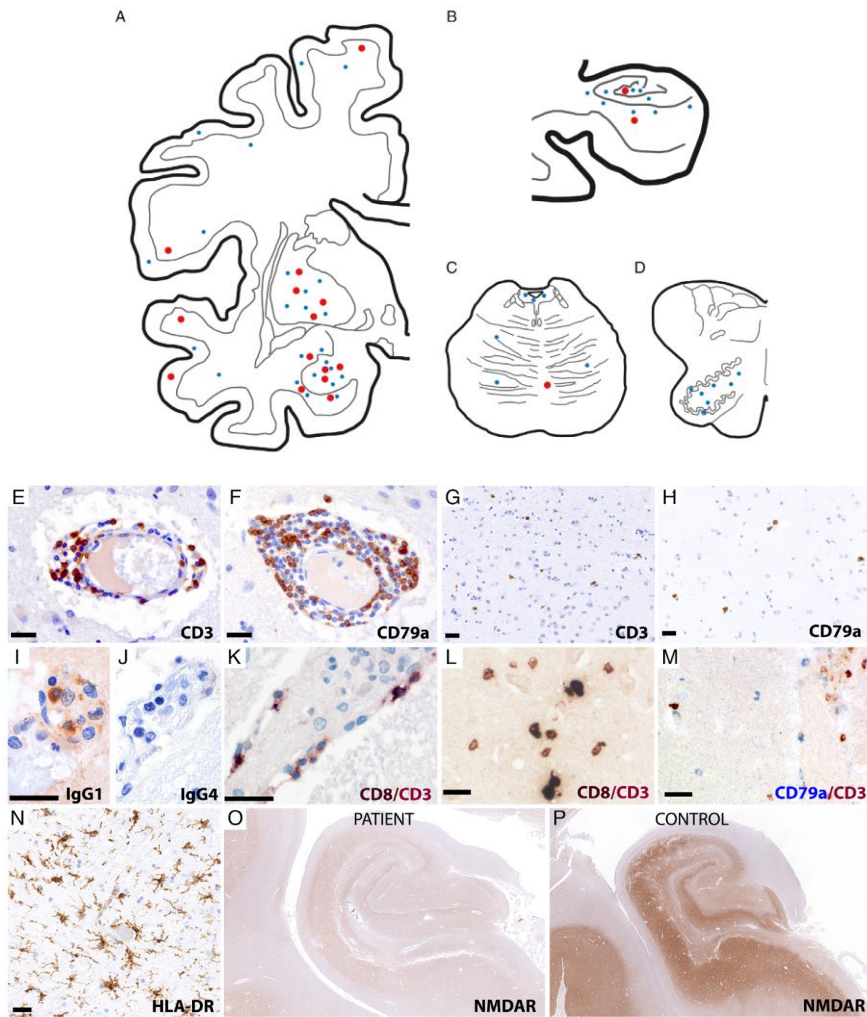


Figure 5. Neuropathology of untreated NMDAR-encephalitis. Topographic distribution of inflammation in the brain shows a prominent involvement of basal ganglia and amygdala (A), and hippocampus (B) while pons and medulla oblongata (C, D) display only scattered T cells and plasma cells (A–D; red: CD79a+plasma cells; blue: CD3+T cells). The inflammatory infiltrates were characterized by perivascular CD3+T cells (E) and CD79a+plasmablasts/plasma cells (F). Parenchymal lymphocytes were dominantly composed of CD3+T cells and CD79+plasmablasts/plasma cells (G, H). Plasma cells were IgG1 positive (I) and IgG4 negative (J). Double immunostaining revealed that perivascular T cell inflammation was composed of equal CD3+CD8-(red) and CD3+CD8+(brown) cells (K). Parenchymal lymphocytes were dominantly composed of CD3+CD8-T cells (red) (L) and CD79+plasmablasts/plasma cells (blue) (M). HLA-DR staining revealed pronounced microglial activation (N). Immunohistochemical staining of the hippocampus showed a significant decrease of NMDAR-expression compared to an age-matched control (O, P). Scale bars: 25 μ m. From⁶⁷

These receptors are activated following glutamate release in spiking axons. This activation induces oligodendroglial surface expression of glucose transporter GLUT1 in myelin compartments, resulting in increased cytosolic glucose and subsequent lactate release to provide axons metabolic support (Figure 6). Conditional knock out of NMDARs in oligodendrocytes have also been shown to alter the rate of myelin growth due to reduced expression of GLUT1.⁷¹

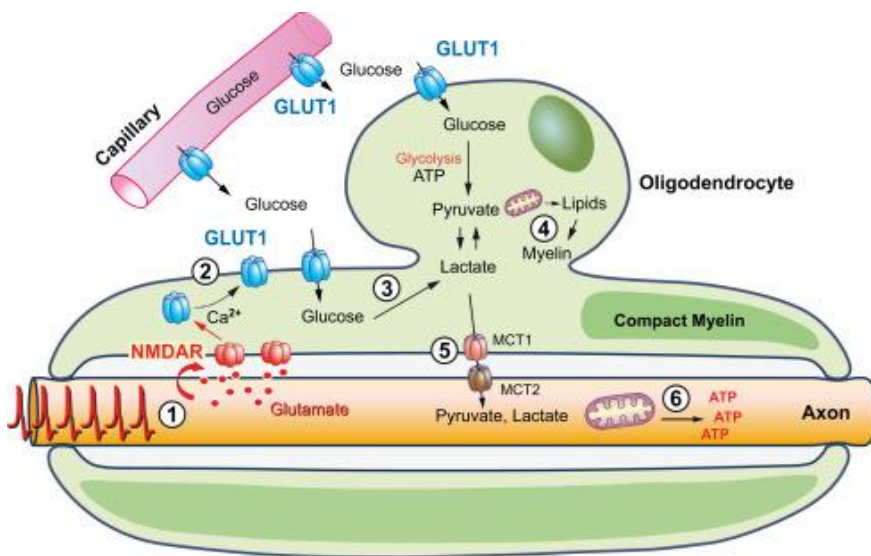


Figure 6. Schematic depiction of oligodendroglial NMDAR signaling. Model in which axonal electrical activity in developing white matter tracts constitutes a glutamatergic signal for the surrounding oligodendrocytes (1). After myelination, NMDARs associated with the internodal/paranodal membrane respond to axonal glutamate release as a surrogate marker for increased axonal electrical activity and energy needs, causing (2) the incorporation of additional glucose transporters into oligodendrocytes and the adaptation of glucose uptake (feed-forward regulation). Glycolysis products (3) are initially used for ATP and lipid synthesis (4). Later, mature oligodendrocytes release lactate (or pyruvate) to fuel the axonal compartment (5) for mitochondrial ATP production (6). Regulation of oligodendroglial glucose uptake by axonal energy needs could help prevent abnormal accumulation of lactate. From

Treatment and long recovery process

Anti-NMDAR encephalitis, while severe and potentially lethal, has become more effectively treatable due to advances in recent years. The primary treatment strategy involves immunotherapy and, when applicable, the removal of an associated tumor. First-line treatments aim to decrease inflammation with corticosteroids, and remove the autoantibodies using intravenous immunoglobulins (IVIg), plasma exchange, or a combination of both. If these fail, second-line treatments that target the antibody-producing B cells such as rituximab or cyclophosphamide are useful.⁵¹

Despite the severity of the disease, most patients respond to immunotherapy. In a study of 577 patients with anti-NMDAR encephalitis, 53% showed clinical improvement within four weeks of diagnosis, and 81% experienced substantial recovery by the last follow-up.⁷² However, after recovery from the acute phase patients often endure a prolonged recovery process, dominated by residual behavioral and cognitive deficits that can persist for many months, or become irreversible. A systematic review of 54 patients highlighted that the most significant challenges were in memory, particularly delayed verbal memory, and executive functioning.⁷³ These lingering symptoms are often under-recognized, likely because they are overshadowed by the dramatic recovery from more acute symptoms such as seizures, abnormal movements, or decreased level of consciousness. A recent study demonstrated that the cognitive and psychiatric symptoms in the post-acute stage of the disease often resemble those of schizophrenia,⁷⁴ but it remains unclear the best approach to treatment.

This slow clinical recovery could be due to persistent immune activation against NMDAR within the CNS, severe impairment of synaptic function and long-term plasticity, limited penetration of current immunotherapies through the blood-brain barrier (BBB), or a combination of these factors. In this sense, anti-NMDAR encephalitis is similar to antibody-mediated neuromuscular junction diseases (myasthenia gravis or LEMS) in which despite the effectiveness of immunotherapy, patients often require additional treatments.³⁸ These adjuvant therapies aim to counteract or compensate for the disruptions caused by autoantibodies, such as using acetylcholinesterase inhibitors in myasthenia gravis.

In anti-NMDAR encephalitis emerging research also suggests potential adjuvant treatments. For instance, in studies with cultured neurons and passive transfer models using patients' CSF NMDAR antibodies in mice, the administration of a soluble form of ephrin-B2, an agonist of the ephrin-B2 receptor that clusters and retains NMDARs at the synapse, antagonized and reversed all antibody-mediated effects.⁷⁵ While promising, this treatment was administered intraventricularly, and currently, no ephrin-B2 agonists can cross the BBB. Another important development involves 24(S)-hydroxycholesterol, a brain-derived cholesterol metabolite that acts as a potent and selective positive allosteric modulator (PAM) of NMDARs.⁷⁶ In hippocampal slices, 24S-HC enhanced the induction of long-term potentiation (LTP) and reversed LTP deficits caused by ketamine (a non-competitive antagonist of NMDARs). Synthetic analogues of 24S-HC, like SGE-301, have shown similar mechanisms of action.⁷⁶ In rats, the administration of SGE-301 reverted memory

deficits caused by phencyclidine, another non-competitive antagonist of NMDARs. Moreover, application of SGE-301 to cultures of neurons exposed to CSF of patients with anti-NMDAR encephalitis prevented the antibody-mediated dysfunction of NMDARs.⁷⁷ An advantage of this compound is that it is optimized for systemic delivery, offering potential as a complementary treatment for anti-NMDAR encephalitis in the post-acute stage of the disease.

Anti-mGluR5 encephalitis

The clinical syndrome, currently known to be associated with mGluR5 antibodies, was initially described by Ian Carr in 1982, who gave it the name of Ophelia syndrome.⁷⁸ The patient was a young woman with Hodgkin's lymphoma who developed prominent neuropsychiatric symptoms with severe memory loss. Dr. Carr, father of the patient, considered that the disease was humorally mediated, probably by a "tumor-secreted neurotransmitter-like molecule".

It was not until the antibodies and target antigen were identified that the disorder was properly characterized. This was first demonstrated with the study of two patients with features similar to those reported by Dr. Carr (neuropsychiatric symptoms, memory impairment, and Hodgkin's lymphoma), along with antibodies in serum and CSF that reacted with rat brain and cultured hippocampal neurons. Subsequent immunoprecipitation studies with neuronal proteins and mass spectrometry revealed that the antigen was mGluR5.⁷⁹ Results from this study led to the development of a diagnostic test consisting in a cell-based assay that expresses mGluR5 receptors.

mGluR5 structure and function

mGluR5, one of the various metabotropic G protein-coupled receptors (GPCR) for the neurotransmitter glutamate (Figure 7), is involved in several neuronal processes and, consequently, in multiple CNS disorders. There are eight types of glutamate metabotropic receptors: group I, consisting of mGluR1 and mGluR5, mainly activates phospholipase C; group II, with mGluR2 and mGluR3 and group III, comprising mGluR6, mGluR7 and mGluR8, typically inhibit adenylate cyclase.⁸⁰ These receptors are obligatory dimers, each monomer possesses a large extracellular domain that mediates dimerization by forming an intermolecular disulfide bridge. The extracellular domain is composed of the venus flytrap domain (VFT), which contains the binding site for glutamate, and a cysteine-rich domain (CRD) that links the VFT to the 7-transmembrane domain (7TM), which activates G proteins.⁸¹

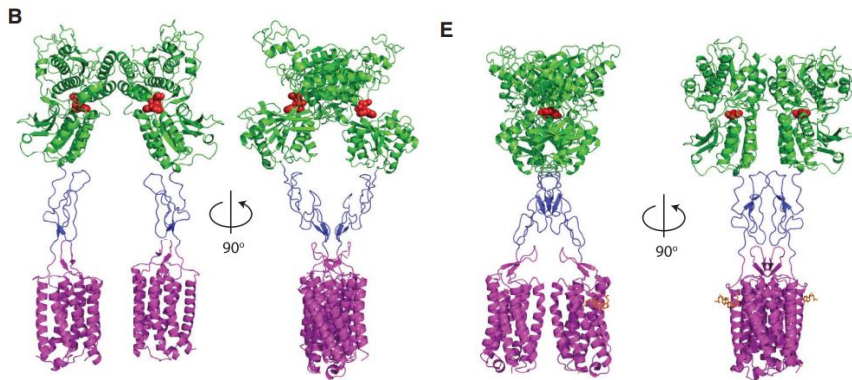


Figure 7. mGluR5 structure. 3D structures of the closed (A) or open (B) conformations of mGluR5. Orthosteric ligands are represented in red. VFTs are colored in green, CRDs in blue, and 7TMs in magenta. From⁸¹

The mGluR5 receptor, which is predominantly expressed post-synaptically in the cortex, striatum, hippocampus, caudate, nucleus accumbens, astrocytes, glia and peripheral sensory neurons,⁸² plays an important role in synaptic plasticity and neurodevelopment, and is involved in mechanisms of pain and memory formation. It has been linked to disorders such as psychosis, schizophrenia, anxiety, depression, addiction, and pain disorders. Regarding signal transduction, mGluR5 couples to Gαq/11, activating phospholipase C, which then generates inositol-1,4,5-triphosphate (IP3) and diacylglycerol (DAG), leading to intracellular calcium (iCa^{2+}) mobilization. Downstream effects involve the phosphorylation of ERK1/2 and p38 MAPK, activating transcription factors implicated in long-term depression (LTD).⁸²

It is known that activation of mGluR5 modulates the function of other glutamate receptors, in particular the ionotropic NMDA and AMPA receptors. For instance, mGluR5 activation increases NMDAR open channel probability while inhibiting NMDAR-mediated adenylate cyclase activation.⁸² Moreover, mGluR5 partners with mGluR1 in the hippocampus, contributing to LTD. GluR5 also co-localizes in the synapse with several different GPCRs and anchoring proteins like Homer.⁸²

Clinical features

Anti-mGluR5 encephalitis is a very rare disease, with less than 20 patients reported worldwide to date.⁸³ The largest cohort published comprised eleven patients with a median age of 29 years, ranging from 6 to 75.⁸⁴ Six patients had tumor associations: five with Hodgkin's lymphoma and one with SCLC. Common prodromal

symptoms included headache, upper respiratory tract infection and fever. Main clinical features were psychiatric manifestations including behavioral or personality/mood changes, irritability, agitation, anxiety, depression or psychosis. Almost all (91%) the patients exhibited altered cognition, with deficits in memory, visuospatial, and executive functions. Some patients presented with movement disorders, including tremor, orofacial dyskinesias or dystonia. All patients had CSF pleocytosis, and in those with paired serum/CSF samples, mGluR5 antibodies were identified in both samples.

Eight patients received first line immunotherapy (corticosteroids, plasma exchange, or IVIg) or second line immunotherapy (rituximab). At the last follow-up, all patients had complete or partial improvement of the neurologic symptoms, similar to the responses seen in other antibody-mediated encephalitis like anti – NMDAR encephalitis.

Mechanisms underlying antibody-mediated encephalitis: cellular and animal models

Until anti-NMDAR encephalitis was first described in 2007, most neuronal autoantibodies identified had been primarily associated with PNS and were directed against intracellular antigens. Initial investigations using cellular, or animal models did not demonstrate the pathogenicity of these autoantibodies; thus, their detection was regarded as a biomarker of PNS or the associated tumor. However, the discovery of anti-NMDAR encephalitis shifted this paradigm. A distinctive feature of this encephalitis was that the antibodies reacted with live neurons (therefore, with accessible surface epitopes), and the associated symptoms, despite being severe, substantially improved with immunotherapy. These observations, coupled with the resemblance of the clinical features with those caused by genetic or pharmacologically mediated reduction of NMDAR function, led to the hypothesis that these antibodies were directly pathogenic.

As indicated, there are currently 19 disorders of the CNS in which the associated antibodies target neuronal cell-surface proteins, including excitatory receptors, inhibitory receptors, and other proteins involved in synaptic function. In all these disorders the pathogenic antibodies are of IgG class, whereas the role and significance of variably present IgA and IgM antibodies are unclear. In addition to the immunoglobulin class, it is important to consider the IgG subclass. Many of the antibodies associated with autoimmune

encephalitis are IgG1 (with or without IgG3 or IgG2) and less frequently IgG4.⁵⁰ Each disorder typically associates with specific IgG subclasses, reflecting distinct disease mechanisms (Figure 8). For example, IgG1 and IgG3 have two arms with the same epitope specificity,⁸⁵ which facilitates crosslinking and internalization of antigens, as seen for instance in the encephalitis associated with NMDAR, AMPAR, GABA_AR, and GluK2R antibodies.^{86–89} Another mechanism that has been identified for IgG1 antibodies is the functional blocking of the target antigen, as in the case of GABA_BR antibodies.⁹⁰ Although IgG1 antibodies can activate complement, this mechanism is rarely observed in autoimmune encephalitis.⁶⁷ In contrast, IgG4 antibodies cannot induce crosslinking and internalization of the antigen; instead, they cause inhibition of protein-protein interactions, as seen for example in the case of LGI1, CASPR2 and IgLON5 antibodies.^{91–93} IgG4 antibodies are unable to activate complement.

The potential role of complement-mediated neuronal injury in antibody-mediated encephalitis is unclear. Although experiments with cultured neurons suggest a pathogenic role for complement in the presence of IgG1 antibodies, tissue samples from patients do not show deposits of complement, except for a few cases with anti-LGI1 encephalitis. This paradigm is different from anti-aquaporin 4 neuromyelitis optica, in which patients often develop irreversible deficits and autopsy studies show evidence of complement-mediated astrocytic injury.^{94,95}

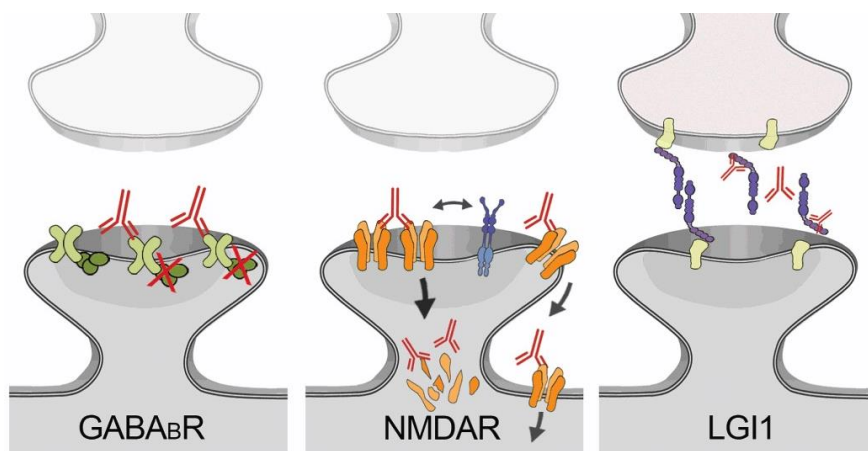


Figure 8. Proposed mechanisms of functional interaction of autoantibodies with neuronal cell-surface proteins. Based on experimental models, the presence of antibodies in the brain may lead to neuronal dysfunction by different mechanisms, including functional blocking of the target antigen (GABA_BR antibodies), receptor crosslinking and internalization (NMDAR antibodies), and disruption of protein–protein interactions (LGI1 leading to a decrease of Kv1.1 and AMPAR). These mechanisms depend on the type of antigen and subclass of IgG; whereas IgG1 antibodies frequently crosslink and internalize the target antigen, IgG4 antibodies alter protein–protein interactions. From²²

Effects of patients' antibodies in cultured neurons

The initial step to confirm the pathogenic effects of patients' autoantibodies involved assessing whether they can induce alterations in cultured neurons. To this end, the hippocampi of rat embryos are dissected, and the dissociated neurons are cultured and exposed to patients' antibodies. These primary cultures of rat hippocampal neurons, capable of establishing functional synapses, have proven to be exceptionally useful for identifying both functional and structural synaptic changes mediated by the autoantibodies associated to various forms of autoimmune encephalitis. Typically, these experiments are conducted when the cultures are 2-3 weeks old and involve exposing them to patients' serum (diluted ~1:100) or CSF (diluted 1:2) for several hours or days. This experimental model

is also employed to evaluate monoclonal antibodies derived from patients' B cells or plasma cells. The assessment may include measuring antibody binding to extracellular epitopes of neuronal receptors or cell surface proteins, quantifying the antibody-mediated changes in the levels of these receptors or proteins at synaptic and extrasynaptic sites, visualizing the internalized antigen-antibody complexes, and performing electrophysiological assessments of the effects of the antibodies on synaptic function and excitability using whole-cell patch clamp studies. A summary of all known antibody effects in vitro can be found in Table 4.

Among all antibody-mediated encephalitis, the pathogenicity of NMDAR antibodies was the first to be demonstrated in cellular models. Early studies incubating rat hippocampal neurons with patients' antibodies showed a selective and reversible reduction in the surface content of NMDAR clusters, correlating with patients' antibody titers.⁸⁶ This reduction occurred through antibody-mediated internalization of surface NMDARs, a mechanism specific to patient antibodies, as Fab fragments (one-arm or monovalent antibody fragments) were able to bind to NMDARs but did not reduce their surface levels.⁸⁶ However, subsequent crosslinking with anti-Fab antibodies replicated the effect observed with intact patient antibodies (Figure 9).

Table 4. Target antigens, epitope regions, and antibody effects in vitro.

Antigen	Structural properties	Epitope targets	Antibody effects on neurons ^a
NMDAR	Ionotropic receptor, heterotetramer composed of two GluN1 subunits (obligatory) and two GluN2 (α-d), or GluN3	GluN1	Alter surface dynamics and crosslink and internalize NMDAR. ^{86,98} Disrupt the interaction of NMDAR with ephrin B2 and dopamine receptors. ^{75,99} Decreased synaptic NMDAR-mediated currents. ⁹⁶ Reduced NMDAR currents and GLUT1 expression in oligodendrocytes. ¹⁰⁰ *
AMPA	Ionotropic receptor. Most are heterotetramers composed on GluA1-4 subunits	Mostly GluA2, but also GluA1	Induce receptor internalization and a reduction of synaptic GluA2-containing AMPAR followed by compensatory ryanodine receptor-dependent incorporation of synaptic non-GluA2 AMPAR. ¹⁰¹
GluK2R	Ionotropic receptor. Hetero- or homotetramer, resulting from the combination of GluK1-5	GluK2	Induce internalization of GluK2. ⁸⁹
GABA _A R	Ionotropic receptor. Heteropentamer resulting from combination of 19 different subunits	Main targets α1, and β3, but also γ subunit	Alter surface diffusion and induce internalization of GABA _A R. ¹⁰²
GABA _B R	Metabotropic receptor. Heterodimer composed of two subunits (GABA _{B1} and GABA _{B2})	GABA _{B2}	Do not induce receptor internalization. Preliminary data suggests antibodies directly block the function of receptor. ⁹⁰
mGluR1	Metabotropic receptor. Homodimer and intragroup heterodimer (mGluR1 and mGluR5)	mGluR1	Induce internalization of mGluR1. ¹⁰³ In cultures rodent Purkinje cells, prevent induction of long-term depression. ¹⁰⁴
mGluR2	Metabotropic receptor. Homodimer and intra- and intergroup heterodimer (mGluR2 and mGluR4)	mGluR2	Antibodies do not modify the levels of receptors, other potential pathogenic mechanisms are unknown. ¹⁰⁵
mGluR5	Metabotropic receptor. Homodimer and intragroup heterodimer (mGluR1 and mGluR5)	mGluR5	Induce internalization of mGluR5. ⁸⁴
D2R	Metabotropic receptor. Homo- and heterodimers (D2/D2 and D1/D2)	N-terminus; residues 20-29 and 23-37	In HEK transfected cells, patients' antibodies decrease the intensity of fluorescent immunolabelling, suggesting a decrease of receptors. ¹⁰⁶
GlyR	Ionotropic receptor. Heteropentameric composed of 3 or 4 α1 subunits and 2 or 1 β subunits	N-terminus; residues 29-62	In spinal motor neurons, antibodies decrease glycinergic synaptic currents after 15 min, suggesting a direct antagonistic effect. ¹⁰⁷ On HEK, antibodies influenced glycine's potency, suggesting that antibodies affect transitions between open/closed/desensitized stages of the channel. ¹⁰⁸
LGI1	Synaptic linker protein that interacts with presynaptic ADAM23 and postsynaptic ADAM22. Organizes a trans-synaptic complex that includes presynaptic Kv1.1 potassium channel and postsynaptic AMPAR.	EPTP and LRR domains	Patients' antibodies cause a decrease of Kv potassium channels and AMPAR, ⁹² leading to presynaptic effects (increase excitability with reduced pair pulse facilitation), and postsynaptic effects (impairment of LTP). ¹⁰⁹

CASPR2	Transmembrane axonal protein. In myelinated nerves, interacts with TAG-1. Organizes and concentrates VGKC at juxtaparanodes. In the CNS expressed at the axon initial segment. Found mainly in inhibitory presynaptic, but also excitatory postsynaptic compartment.	Multiple-target epitopes in the extracellular domain including one in the discoidin domain	Antibodies interfere in the binding of CASPR2 to contactin-2 (or TAG-1). ¹¹⁰ In one study, antibodies did not affect the surface expression levels of CASPR2, ¹¹⁰ whereas in another study they did, along with a decrease of AMPAR clusters and mEPSC amplitudes. ¹¹¹
DPPX	Membrane glycoprotein that tunes up the voltage-gated A-type Kv4.2 channels by remodeling channel gating.	DPPX, antibodies do not recognize Kv4.2	Antibodies cause a decrease of DPPX clusters and Kv4.2 protein. ¹¹² Antibodies increased neuronal excitability in preparation of myenteric neurons. ¹¹³
Neurexin-3α	Synaptic cell-adhesion protein located at the presynaptic region that interacts with the postsynaptic ligand LRRTM2.	Neurexin-3α, antibodies do not react with LRRTM2	Antibodies cause a decrease of Neurexin-3α and the total number of synapses. ¹¹⁴
IgLON5	Synaptic glycosylated protein attached to the plasma membrane through a GPI anchor. Belongs to the immunoglobulin superfamily of cell-adhesion molecules.	Immunoglobulin-like domain 2 of IgLON5	Antibodies cause an irreversible reduction of IgLON5 clusters, ¹¹⁵ disrupt the cytoskeletal organizations resulting in dystrophic neurites and axonal swelling, ¹¹⁶ and interfere with protein interactions. ¹¹⁷
SEZ6L2	Named brain-specific receptor-like protein A. Type 1 transmembrane protein; interacts with AMPAR.	SEZ6L2	Antibodies did not alter total or synaptic SEZ6L2 or AMPAR clusters (unknown mechanism). ¹¹⁸
DNER (or Tr)	Glycosylated protein highly expressed in Purkinje cells. Mediates neuron-glia interactions through Notch signaling.	Amino acids 128 and 308; and 302-675. Glycosylation is needed	Unknown mechanism.
P/Q-type VGCC	Composed of 5 subunits (α1, α2, β, γ, δ). Converts the electrical signal of the action potential to an increase of intracellular Ca ²⁺ to initiate neurotransmitter release. Expressed in Purkinje cells and at presynaptic neuromuscular junction.	α1 subunit	In a small-cell cancer line, antibodies decreased K ⁺ -induced Ca ²⁺ influx. In HEK-expressing VGCC, antibodies caused a reduction of Ca ²⁺ currents. ¹¹⁹ In cultures of rat cerebellar neurons, antibodies caused a significant downregulation of P/Q-type VGCC. ¹²⁰
Amphiphysin	N-BAR domain protein enriched in presynaptic ending. Involved in clathrin-mediated endocytosis.	SH3 domain	In cultured neurons and brain slices antibodies altered the function of inhibitory synapses by disturbing vesicular endocytosis. ¹²¹

^aUnless indicated, all studies were done with cultured neurons and quantified the cell surface and synaptic density of the antigen (actual number of clusters of receptor or protein). *Description forms part of this thesis.

Given the role of NMDARs as ionotropic channels, significant attention has focused on changes in NMDAR-mediated currents following autoantibody exposure. Interestingly, prolonged (~12-24 hour) exposure of cultured hippocampal neurons to patients' CSF resulted in reduced NMDAR-mediated currents,^{86,96} though short (minutes) exposure did not show significant effects on individual channel function.⁹⁷ Collectively, these findings suggest that patients' antibodies cause hypofunction of NMDARs primarily through depletion of their surface expression rather than directly modifying the functional properties of the channels. Patients' antibodies did not affect other synaptic proteins, the number of synapses, dendritic spines, dendritic complexity, or neuronal survival.

The dynamics of antibody-mediated internalization of receptors were explored in cultured neurons exposed to patients' IgG for durations ranging from 15 minutes to 48 hours. A noticeable decrease in NMDAR density was observed as early as 2 hours post-exposure, with the most significant effects noted at 12 hours and no further reduction with longer exposures.⁹⁷ Additionally, when neurons were pre-treated with a functional blocker of NMDAR (AP5), the pathogenic effect of patients' antibodies was unchanged, overall indicating that the internalization induced by the antibodies was independent of receptor functionality.⁹⁷

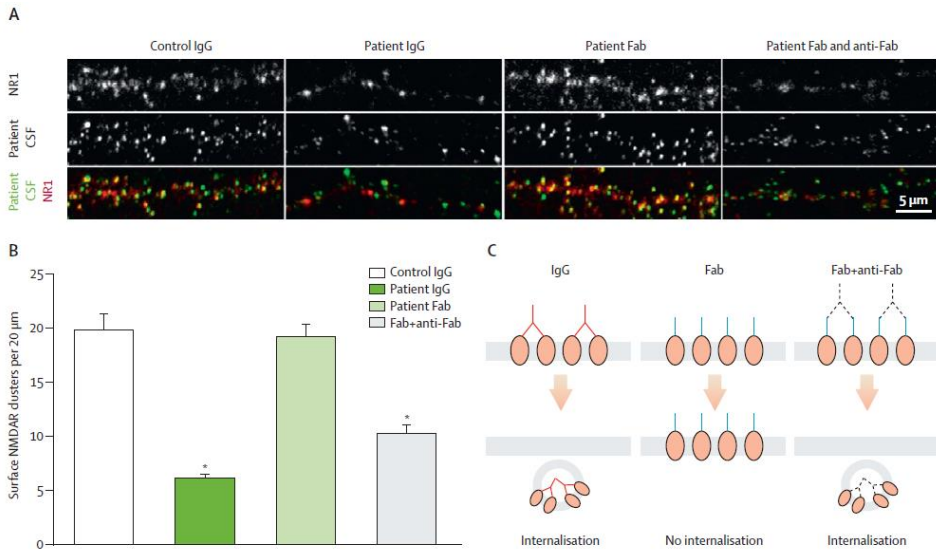


Figure 9. Mechanism of antibody-mediated NMDAR internalization. (A) Hippocampal neurons immunostained for surface and internal (total) N-methyl-D-aspartate receptor (NMDAR) clusters (top row, stained with commercial NR1 subunit antibody), surface NMDAR clusters only (middle row, stained with patients' cerebrospinal fluid [CSF]) and their co-localization (bottom row, surface NMDAR clusters in yellow). Treatment with patients' IgG for 1 day decreases surface and total NMDAR cluster density compared with control IgG. Treatment with patient Fab fragments does not affect surface or total NMDAR cluster density, whereas treatment with divalent patient Fab fragments (Fab fragments and anti-Fab secondary antibodies) decreases surface and total NMDAR cluster density to an extent similar to patients' IgG. (B) Effects of patients' IgG, Fab fragments, and divalent Fab fragments on surface and total NMDAR cluster density. ($n=30$ cells, four independent experiments; two samples from patients, two samples from control patients with unrelated neurological disorders with no immune system involvement). All values are mean \pm SE. * = significant difference (one-way ANOVA test followed by Bonferroni's multiple comparison test, $p < 0.00071$). (C) Graphic representation of the effect of each treatment on surface receptor clusters. From¹²²

The lateral mobility of NMDARs is a critical regulator of their function at the neuronal surface.^{123–125} Since the redistribution of receptors at the subcellular level is implicated in the pathology of NMDAR encephalitis, extensive research has been conducted to precisely characterize the effect of autoantibodies on NMDAR surface trafficking. These studies have shown that the antibodies cause changes in NMDAR surface diffusion.^{98,126} Notably, single-particle

tracking experiments have revealed that short exposure to patients' NMDAR antibodies increases the mobility of synaptic NMDARs, indicated by an increase in both mean square displacement and diffusion coefficients of GluN2A-containing NMDARs.⁹⁸ It is believed that this increase in receptor mobility is, at least partially, induced by antibody-mediated disruption of GluN1 interaction with EphrinB2 receptors in the postsynaptic compartment.⁹⁸ This hypothesis is supported by the finding that autoantibody application reduces the association of NMDAR with EphrinB2 receptors, and that activation of EphrinB2 receptors, which strengthens its interaction with GluN1, impedes antibody-mediated synaptic displacement.⁹⁸ However, continuous autoantibody exposure promotes a converse immobilization of extrasynaptically localized GluN2B-containing receptors, consistent with other studies demonstrating antibody-mediated crosslinking of NMDARs at extrasynaptic sites.¹²⁷ These findings, combined with previous results, support a molecular model of the disease in which NMDAR antibodies disrupt synaptically anchored protein-protein interactions, leading to receptor displacement from postsynaptic compartments.^{86,98,127} Subsequently, the enrichment of NMDARs in extrasynaptic areas results in the formation of immobilized macro-clusters of crosslinked receptors, which are then internalized from the neuronal surface.¹²⁷ This process ultimately drives a functional reduction in NMDAR-mediated currents at synaptic compartments, despite a lack of direct antibody-mediated modification of channel function.

These pioneering studies served as a model to assess the pathogenicity of antibodies in other antibody-mediated encephalitis. In the case of anti-mGluR5 encephalitis, patients' antibodies have shown pathogenicity in hippocampal cultured neurons. Neurons exposed to patients' IgG had a reduction of total and synaptic cell-surface mGluR5 (Figure 10).⁸⁴ Removal of autoantibodies from the culture medium led to full receptor density recovery within seven days, suggesting that the antibodies might cross-link and internalize the receptors, similar to what it is observed in anti-NMDAR encephalitis.

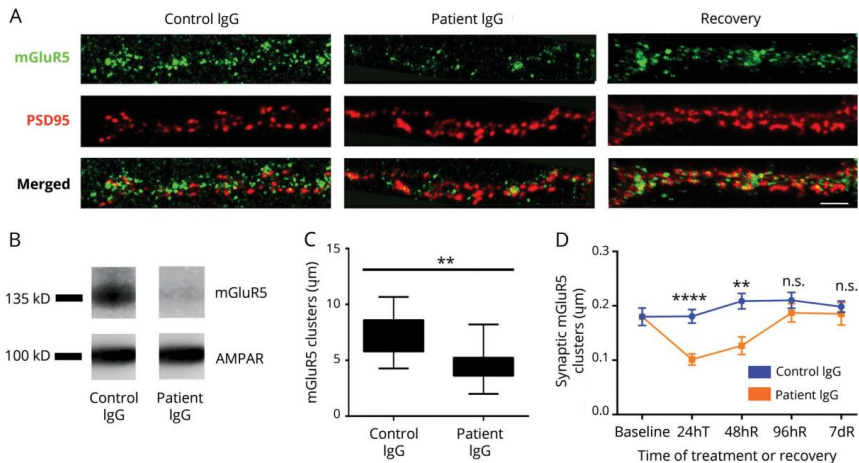


Figure 10: Patient's antibodies cause a specific decrease of density of cell-surface mGluR5 clusters in cultured neurons. Representative confocal images (from 40 dendrites per condition) showing a decrease of density of cell-surface metabotropic glutamate receptor 5 (mGluR5) clusters in neurons treated for 24 hours with patient's immunoglobulin G (IgG) compared with neurons treated with control IgG (A). Quantification analysis of total mGluR5 clusters after 24 hours of treatment is shown in panel (C). Specific decrease of mGluR5 protein, but not α -amino-3-hydroxy-5-methyl-4-isoxazolepropionic acid receptor (AMPA) protein, is also demonstrated using immunoblot of biotinylated neuronal membrane fractions from neurons treated for 24 hours with patient's IgG compared to control IgG (B). These effects were reversible, and baseline levels of total (A, right column, 7 days recovery) and synaptic (D) neuronal cell-surface mGluR5 clusters (from analysis of 20 dendrites per condition per time point) were progressively restored over 96 hours to 7 days. Statistical analyses by 2-way analysis of variance; mean and SEM are plotted. Scale bar = 10 μ m. $**p < 0.05$, $****p < 0.0001$. PSD95 = postsynaptic density protein 95; R = recovery; T = treatment. From⁸⁴

Passive cerebroventricular transfer of antibodies to mice

In our experience, the demonstration of antigen-specific antibody effects in cultured neurons usually indicates similar pathogenic effects in animal models of passive transfer of patients' antibodies, typically accompanied by impairments in memory and behavior. To confirm that an autoimmune encephalitis is antibody-mediated, the following criteria must be demonstrated in an animal model: (1) infusion of patients' antibodies, but not controls, causes neurological symptoms in animals, (2) the infused antibodies specifically react with the target neural antigen, (3) the antibodies alter the structure or function of the target antigen, leading to synaptic or neural dysfunction, (4) the induced neurological symptoms correlate with the structural and functional effects of the antibodies.¹²⁸

The most common approach for testing whether antibodies from patients with autoimmune encephalitis cause symptoms involves infusing the antibodies into the cerebroventricular system of mice.²² In this passive transfer model, patients' antibodies or human-derived monoclonal antibodies are infused into the ventricular system. During this period, animals are evaluated for memory impairment, behavioral changes, or signs of seizures, and assessments are made to determine the reversibility of any alterations after the infusion has stopped. Mice are euthanized at various time points to assess the binding of antibodies to brain tissue and to identify antibody-mediated functional and molecular alterations. This method has been applied in several models of antibody-mediated encephalitis, and a summary of the findings is presented in Table 5.

The first and most extensively studied model of passive transfer focuses on anti-NMDAR encephalitis. Planagumà et al. developed this model using bilateral catheters implanted in the lateral ventricles of mice and connected to subcutaneous osmotic pumps, which continuously infused either patients' or controls' undiluted CSF into the mice for 14 days (Figure 11).¹²⁹

During and after the infusion, several behavioral tasks were conducted to evaluate memory (novel object recognition), anhedonia (sucrose preference test), depressive-like behaviors (tail suspension and forced swimming tests), anxiety (black and white and elevated plus maze tests), aggressive behavior (resident-intruder test) and locomotor activity, along with examining potential associations with brain antibody binding and NMDAR levels.

The infusion of patients' CSF, but not control CSF, induced progressive memory deficits, along with anhedonic and depressive-like behaviors, without affecting locomotor activity. The most prominent effects were observed in the novel object recognition task, which was severely impaired on day 18 (4 days after the infusion ceased) but began to recover over the following week.¹²⁹ Brain tissue studies revealed a progressive accumulation of human IgG, peaking on day 18 and primarily located in the hippocampus. Further analysis confirmed these antibodies as anti-NMDAR. Additionally, analysis of NMDAR clusters in the hippocampus showed a progressive reduction in the density of cell-surface and synaptic NMDAR, without affecting the density of AMPAR or PSD95.¹²⁹ These changes occurred in parallel with the aforementioned memory and behavioral alterations and gradually improved after day 18, with reversion of symptoms,

reduction of brain-bound antibodies, and restoration of normal levels of cell-surface and synaptic NMDAR.¹²⁹ Pathological examinations found no evidence of inflammatory infiltrates or complement deposits, providing strong evidence that antibodies from patients with anti-NMDAR encephalitis alter memory and behavior through the reduction of cell-surface NMDAR.

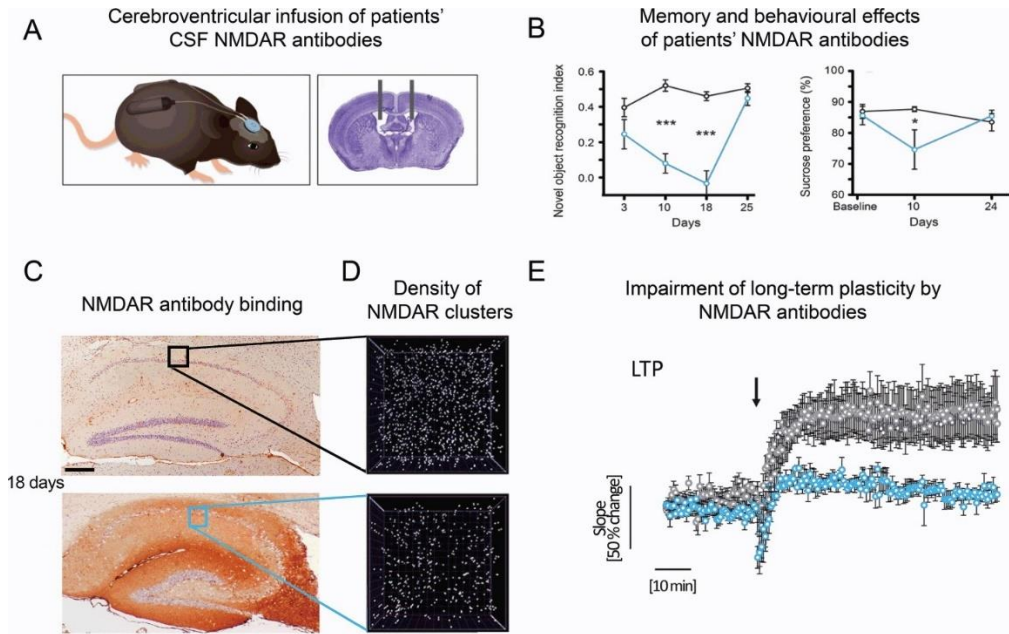


Figure 11. Patients' NMDAR antibodies decrease the levels of NMDAR resulting in impairment of memory, behavior, and hippocampal plasticity. (A) Subcutaneously placed osmotic pumps filled with patients' CSF are connected to cannulas inserted in the lateral ventricles. The osmotic pumps deliver a continuous infusion of patients' CSF antibodies for 14 days. During the infusion period and until day 25, animals undergo regular memory and behavioral tests (B), and subgroups of representative animals are sacrificed at different time points to determine the presence of antibodies in the brain (C) and the effect of the antibodies on the levels of NMDARs (D) and hippocampal LTP (E). Note that compared with control CSF (grey line in B), patients' CSF (blue line in B) caused a progressive and robust decrease of memory (novel object location) and anhedonia (sucrose preference) until day 18 (four days after the pumps stopped the infusion of patients' antibodies), followed by recovery of deficits. Panel C demonstrates the presence of human IgG in the hippocampus of a representative animal infused with control CSF (top) and patients' CSF (bottom); in both examples, the hippocampus corresponds to day 18. Panel D shows the density of NMDARs in the corresponding hippocampal areas (small squares) of (C). Note that the presence of patients' antibodies in hippocampus (C, bottom) is accompanied by a substantial reduction of clusters of NMDARs (D, bottom). Panel E shows that the reduction of NMDAR clusters is accompanied by a severe impairment of hippocampal LTP (the blue line corresponds to an animal infused with patients' CSF, and the grey line to an animal infused with control CSF). As occurred with memory and behavior, the changes in the levels of NMDARs and plasticity progressively reversed after the infusion of antibodies was stopped (not shown). One or more asterisks indicate that the findings are statistically significant. Scale bar in C, 200 μ m. From²²

Table 5. Animal models using transfer of human antibodies against neuronal cell surface proteins.

Antigen	Approach	Results: behavioral, molecular and/or electrophysiological	Comments
NMDAR	Cerebroventricular infusion/injection of patients' antibodies or human monoclonal antibodies to mice	Infusion of patients' CSF antibodies caused memory loss, anhedonia, depressive-like behavior, psychotic-like behavior along with decreased levels of NMDAR clusters and interacting protein (ephrin B2 receptor, dopamine receptors). Antibodies impaired long-term synaptic potentiation (LTP). All effects were reversible. ^{75,99,129}	Findings in animal tissue were similar to those obtained with cultured neurons. A model using human monoclonal antibody showed the same results. ¹³⁰
AMPA	Cerebroventricular infusion/injection of patients' antibodies to mice	Infusion of patients' GluA2 IgG antibodies caused a reduction of memory and learning along with internalization and reduction of GluA2-containing AMPARs followed by a compensatory incorporation of non-GluA2 AMPARs. Antibodies impaired LTP. Effects were reversible. ¹³¹	Findings in animal tissue were similar to those obtained with cultured neurons.
mGluR1	Injection of patients' antibodies into the subarachnoid space of mice	Antibodies caused progressive ataxia with wide gait and severe difficulty walking. The effect was reversible. ⁴⁴ In another study, in-vivo application to the flocculus evoked disturbances in the performance of compensatory eye movements. ¹⁰⁴	Reversibility of the antibody-induced ataxia was confirmed by other authors. ¹³²
mGluR5*	Cerebroventricular infusion of patients' antibodies to mice	Infusion of patients' mGluR5 antibodies caused a reduction of memory and increased anxiety along with a reduction of mGluR5 in the hippocampus. Effects were reversible. ¹³³	Findings in animal tissue were similar to those obtained with cultured neurons.
GlyR	Exposure of zebrafish larvae to patients' antibodies	A lesion of the skin covering the fourth ventricle of the larvae permitted diffusion of antibodies into the ventricular space. Larvae exposed to patients' antibodies showed severely impaired escape responses, decreased GlyR in the lateral region of the spinal cord. ¹⁰⁸	Reversibility of effects was not determined

LGI1	Cerebroventricular infusion of patients' antibodies to mice	Antibodies caused severe memory loss along with a decrease of synaptic Kv1.1 and AMPAR, and LTP impairment. Patch-clamp of DG granule cells and CA1 pyramidal neurons showed neuronal hyperexcitability with increased glutamatergic transmission. All effects were reversible. ¹³⁴	Memory and LTP impairment were confirmed in another study using patient-derived monoclonal antibodies. ¹³⁵
CASPR2	Systemic or intracerebral infusion/injections of patients' antibodies to mice	Cerebroventricular infusion of patients' antibodies caused memory impairment along with hippocampal reduction of surface CASPR2 clusters and decreased CASPR2/TAG1 colocalization, and decreased levels of Kv1.1 and GluA1. All effects were reversible. ¹³⁶	Other authors using systemic injections in mice reported delayed-onset of mechanical hypersensitivity. ¹³⁷ Another study injecting patients' antibodies to the visual cortex of mice reported reduction of mEPSC amplitudes. ¹¹¹
P/Q-type VGCC	Injection of patients' antibodies into the subarachnoid space of mice	Mice injected with IgG from patients with LEMS and PCD and VGCC antibodies developed reversible ataxia and memory loss. Mice injected with IgG from patients with LEMS without ataxia did not develop cerebellar symptoms. ¹³⁸	In another study, rabbit polyclonal VGCC antibodies against the DIII domain of the mouse $\alpha 1$ channel caused cerebellar symptoms in mice. ¹³⁹
Amphiphysin	Systemic or intracerebral injections of patients' antibodies to rodents	Intraperitoneal injections of patients' antibodies to a rat model of EAE caused muscle stiffness and spasms. ¹⁴⁰ Intrathecal injection of human IgG antibodies produced anxiety behavior, and stiffness and muscle spasms in rats. ¹⁴¹ Antibodies were internalized into neurons and colocalized with presynaptic vesicular proteins. ¹²¹	Neurons from amphiphysin deficient mice did not internalize patients' IgG. GABAergic synapses were more vulnerable than glutamatergic synapses to antibody-mediated vesicular endocytosis. ¹²¹

* Model developed as a consequence of this thesis.

Active immunization models

While passive transfer models established the pathogenicity of human antibodies in antibody-mediated encephalitis, they do not fully represent the complexity of these diseases, lacking deeper insights into their immunopathology. This limitation highlights the need for active immunization models that more accurately replicate the human disease.

The first animal model of a CNS disease developed by active immunization was the Experimental Autoimmune Encephalomyelitis (EAE) model, which tried to reproduce Multiple Sclerosis (MS). Initiated in the 1930s, Thomas Rivers and colleagues provided the first evidence that immune cells can attack the brain. Their simple experiments established what is now known as the EAE model. These experiments involved intramuscular injections of brain extracts from rabbits into Rhesus macaques, causing in most animals paralysis in association with CNS immune infiltration and demyelinating lesions.¹⁴² The researchers also noted that the disease-inducing capacity of the brain extracts was proportionate to their myelin content, providing the first hint that myelin was involved in disease induction.

The success of these experiments required multiple injections (up to 85 per animal) over a period of a year. However, when the process was modified by Elvin Kabat combining brain extracts with a new adjuvant developed by Jules Freund, the model could be induced by just a single injection.¹⁴³ It took another decade before researchers recognized some of the similarities between EAE and MS.¹⁴⁴

Currently, EAE is the most commonly used model for the study of demyelinating disorders and other types of inflammatory demyelination. Rather than using brain extracts, EAE is now typically induced by the subcutaneous injection of Myelin Oligodendrocyte Glycoprotein (MOG) protein or peptides mixed with Freund's adjuvant in rodents.¹⁴⁵ It is argued that pathophysiologically EAE more closely resembles MOG-antibody associated disease (MOGAD) than MS, due to its non-relapsing remitting course and the use of MOG as the autoimmune trigger. The typical clinical course of EAE involves ascending flaccid paralysis, characterized by widespread neuroinflammation, demyelination plaques, and neuronal damage in the spinal cord. Advances in research have led to various types of the EAE model, each reflecting aspects of the human disease pathology and informing the development of potential therapeutic interventions. Interestingly, the mechanism involved varies depending on the type of immunization. For example, the use of MOG peptides primes an immune response mediated by CD4 T cells (B cell independent) whereas the use of MOG protein results in an EAE that requires the participation of B cells.¹⁴⁶

For autoimmune encephalitis, the models of passive transfer of patients' antibodies have been extremely useful to demonstrate that the antibodies have direct pathogenic effects on the structure and function of the target antigen, but these models have limitations related to the absence of immune activation and inflammatory changes, as well as the preferential diffusion of the infused antibodies to structures surrounding the ventricular system. In contrast, active immunization models facilitate the assessment of the effects of antibodies synthesized by the animal, alongside the mechanisms mediated by effects inflammatory and T cell responses.

These models should aim to replicate all symptoms of the human disease, ensuring that antibodies target the same antigenic regions, belong to the same IgG subclass, and cause molecular and electrophysiological alterations similar to those mediated by patients' antibodies. Furthermore, the participation of the T-cell immune response should be similar to that of the human disease (characterized in autopsy studies as mild), and the main clinical and immunopathological alterations should be potentially reversible with treatment.

Active immunization models also offer the possibility to obtain a more prolonged follow-up (weeks or months) of the clinical and biological alterations when compared with passive transfer models, in which antibody effects only last for a few days (~14 days), therefore, facilitating the testing of potential new therapies.

In the past five years, some researchers have attempted to develop models of anti-NMDAR encephalitis through active immunization. However, these models only partially met the required criteria (Table 6). One of these models, employing NMDAR proteo-liposomes, elicited a fulminant encephalitis (with frequent mortality) that manifested with some of the acute phase symptoms of NMDAR encephalitis, but lacked a comprehensive exploration of antibody-mediated molecular mechanisms.¹⁴⁷ A subsequent study used a peptide from the GluN1 amino terminal domain (ATD) combined with Freund's complete adjuvant (FCA), showing that animals developed anxiety and memory impairment along with B and plasma cell infiltration in leptomeningeal and circumventricular regions.¹⁴⁸ However, the study did not address the molecular effects of the

antibodies. A similar study expanded this approach with a longer GluN1₃₅₆₋₃₈₅ peptide and FCA, replicating memory deficits and synaptic changes, but without examining inflammatory brain infiltrates.¹⁴⁹ In contrast, another study used immunization with a mix of peptides that resulted in antibody synthesis but failed to induce memory and other behavioural alterations.¹⁵⁰ In another study, the authors compared different immunization protocols, including two previously reported,^{148,149} revealing major differences in the phenotype of mice immunized with different protocols, but not addressing key features related to the pathogenicity of mouse antibodies or alterations in synaptic plasticity.¹⁵¹ Another recent study immunized juvenile mice with the GluN1₃₅₆₋₃₈₅ peptide and FCA, which produced only memory alterations and antibodies in serum, but did not explore antibodies in CSF, molecular antibody effects, or immune brain infiltrates.¹⁵² Lastly, a recently published model immunized wild-type and ApoE^{-/-} mice with a long fragment of the GluN1 ATD and FCA.¹⁵³ This study examined antibodies only in serum, noted memory alterations and anxiety, reduced NMDAR levels, but did not examine the immunobiology.

A common finding across these models is that the immune responses are predominantly driven by B cells, with absent to moderate brain infiltration by T cells. All models showed the development of NMDAR antibodies supporting the concept that NMDAR autoimmunity is sufficient to cause the multiple symptoms of the disease. However, none of the models provided a comprehensive assessment of animal behavior, explored the neurobiology and immunobiology, or examined the prolonged clinical course.

Table 6: Animal models of anti-NMDAR encephalitis developed by active immunization.

Features		Pan et al. 2019 ¹⁵⁰	Jones et al. 2019 ¹⁴⁷	Wagnon et al. 2020 ¹⁴⁸	Ding et al. 2021 ¹⁴⁹	Linnoila et al. 2023 ¹⁵⁴	He et al. 2023 ¹⁵²	Yu et al. 2023 ¹⁵³	Maudes et al. 2024*
Immunization	GluN1 immunogen	mix of peptides	proteo-liposomes	15aa peptide	30aa peptide	15 and 30aa peptides	30aa peptide	extracellular segment	30aa peptide
	Adjuvant	FCA	none	FCA	FCA	FCA	FCA	FCA	AddaVax
Neuro-biology	Reduced NMDAR density in brain	n/a	n/a	n/a	✓	✓	n/a	✓	✓
	GluN1 bound to brain antibodies	n/a	n/a	n/a	n/a	n/a	n/a	n/a	✓
	Changes in brain plasticity	n/a	n/a	n/a	n/a	n/a	✓	n/a	✓
Immunology	Antibody presence	serum	serum	serum and CSF	serum and CSF	serum and CSF	serum	serum	serum and CSF
	Pathogenicity of antibodies in vitro	n/a	NMDAR density ↓	Ca ²⁺ currents ↓	NMDAR density ↓	n/a	n/a	NMDAR density ↓	NMDAR density and Ca ²⁺ currents ↓
	B and plasma cell infiltrates in brain	n/a	✓	✓	n/a	✓	n/a	n/a	✓
	T cell infiltrates in brain	n/a	✓	x	n/a	✓	n/a	n/a	rare
Clinical and behavioral assessment	Memory	n/a	✓	✓	✓	✓	✓	✓	✓
	Psychosis	predisposition	n/a	n/a	n/a	n/a	n/a	n/a	✓
	Abnormal movements	n/a	✓	x	x	x	x	x	✓
	Hyperactivity	n/a	✓	x	x	x	x	x	x
	Depression	n/a	n/a	✓	✓	✓	n/a	x	✓
	Anxiety	n/a	✓	✓	✓	✓	x	✓	predisposition
	Seizures	n/a	spontaneous	threshold ↓	threshold ↓	n/a	threshold ↓	n/a	threshold ↓
	Reversibility	n/a	high mortality	n/a	n/a	n/a	n/a	n/a	✓
	Clinical staged evolution	x	x	x	x	x	x	x	✓

* Model developed as a consequence of this thesis

Chapter III

Hypotheses

Based on the concepts previously described, antibody-mediated encephalitis represents a rapidly expanding group of neurologic disorders whose cause and treatment were unknown until recently. Understanding the pathogenic mechanisms of patients' antibodies provides insight into how autoimmunity can affect brain function, leading to reversible symptoms that range from minor alterations to psychotic behavior and severe neurological symptoms.

Anti-mGluR5 encephalitis is a very rare disease. The pathogenic role of antibodies from anti-mGluR5 encephalitis patients has been suggested by the response of patients' symptoms to immunotherapy and further supported by studies showing that the antibodies bind to the cell surface of cultured neurons, causing a depletion of mGluR5 levels. However, these antibody-mediated alterations and their potential effect on behavior have not been explored in animals. This thesis addresses these questions using a mouse model of cerebroventricular transfer of patients' IgG.

Anti-NMDAR encephalitis is considered the most common antibody mediated autoimmune encephalitis. An intriguing feature of this disease is the dissociation between the severity of the symptoms in most patients and the low frequency of MRI abnormalities using standard clinical imaging sequences. However, studies with advanced imaging show extensive changes in white matter integrity in most patients. Given that oligodendrocytes also express NMDAR, we postulated that the function of NMDAR in oligodendrocytes might also be impaired in patients' with anti-NMDAR encephalitis.

Although anti-NMDAR encephalitis is a treatable disease, it often takes several months or more than one year for patients to return to most of their normal activities. Therefore, novel therapeutic strategies aimed to speed improvement are of great interest. Given that most symptoms in anti-NMDAR encephalitis are associated with NMDAR hypofunction, it is reasonable to hypothesize that a potent and selective PAM (i.e., SGE-301) of this receptor could potentially prevent and reverse the pathogenic effects of patients' antibodies. However, the mechanisms of action of this PAM remain unclear. Since patients' antibodies cause alterations in the surface dynamics of NMDAR, we hypothesized that SGE-301 could modulate NMDAR membrane dynamics.

Finally, even though passive transfer models with patients' antibodies have been instrumental in establishing the pathogenicity of the antibodies, they do not provide further insights into the immunopathology of the disease. Recently, additional approaches to model the disease based on active immunization of mice with NMDAR have resulted in different phenotypes, ranging from fulminant encephalitis to milder symptoms depending on the model. However, there is an unmet need for models that can offer a more comprehensive assessment of the neurobiology and immunobiology of the disease, alongside a clinical course long enough to facilitate the evaluation of potential therapies on all these paradigms.

Therefore, we postulated that immunization with a GluN1 peptide would develop a model of anti-NMDAR encephalitis allowing the assessment of clinical, neurobiological and immunobiological alterations over an extended period of time. Moreover, this novel mouse model of anti-NMDAR encephalitis would provide the opportunity to assess the efficacy of novel treatments such as SGE-301, and to compare these treatments with the currently used B-cell depleting immunotherapy (anti-CD20).

Therefore, considering all the above, I hypothesized that:

1. Cerebroventricular infusion of patients' mGluR5 antibodies to mice should model the alterations observed in patients with anti-mGluR5 encephalitis.
2. Oligodendrocyte function is likely to be impaired by exposure to antibodies from patients with anti-NMDAR encephalitis.
3. Treatment with a positive allosteric modulator of NMDAR, such as the oxysterol derivative SGE-301, is likely to prevent and restore the antibody-mediated alterations observed in mouse models of passive transfer of patients' NMDAR antibodies.
4. Positive allosteric modulators of NMDARs, like SGE-301, probably modifies the surface dynamics of NMDARs.
5. Active immunization of mice with a peptide from the main immunogenic region of GluN1 adapted to prime B cell responses, should result in the clinical, neurobiological and immunobiological manifestations of anti-NMDAR encephalitis.
6. Treatment with anti-CD20 immunotherapy and SGE-301 should reverse the clinical and underlying biological alterations associated to the anti-NMDAR encephalitis caused by active immunization of mice.

Chapter IV

Objectives

The indicated hypotheses will be tested in the following objectives:

- 1.** Determine the pathogenicity of anti-mGluR5 patients' antibodies in a mouse model of cerebroventricular infusion.
- 2.** Investigate the effect of antibodies from patients with anti-NMDAR encephalitis on cultures of oligodendrocytes, evaluating the activity of oligodendrocyte NMDARs and the expression of glucose transporter GLUT1.
- 3.** Assess whether SGE-301, a positive allosteric modulator of NMDAR, prevents and restores the pathological effect of antibodies from patients with anti-NMDAR encephalitis in a passive cerebroventricular transfer mouse model.
- 4.** Elucidate the effects of SGE-301 on the cell surface dynamics of NMDAR.
- 5.** Develop an animal model of anti-NMDAR encephalitis in order to characterize the neurobiology, immunobiology, clinical phenotype, and reversibility of the disease with two types of treatments, an anti-CD20 (frequently used to treat the human disease), and a novel therapeutic approach with a positive allosteric modulator of the NMDAR (SGE301).

Chapter V

General methods

The general methods used in this thesis are briefly summarized below and can be found in more detail in the enclosed publications. Additional methods of particular interest for each individual project are described in the corresponding manuscript.

Determination of the presence of autoantibodies in serum and CSF samples

Serum and CSF samples from patients with anti-NMDAR and anti-mGluR5 encephalitis, and from healthy participants (controls), were used in these projects. Patients were clinically identified in our Institution (FCRB-IDIBAPS, Hospital Clinic de Barcelona) according to criteria developed by Dr. Graus and Dr. Dalmau (Graus et al. Lancet, 2016). The presence of autoantibodies was determined with rat brain immunohistochemistry and cell-based assays. These tests together with immunocytochemistry with live neurons were commonly used in all projects of this thesis.

Immunohistochemistry on rat brain tissue

Immunohistochemistry on rat brain tissue with human serum or CSF samples represents our first level of antibody screening for patients with suspicion of autoimmune encephalitis. This technique, adapted to cell surface proteins, is highly sensitive to detect antibodies in serum and CSF, providing distinct patterns of immunostaining characteristic of each autoantibody.

Immunohistochemistry is performed with non-perfused rat brain. In brief, animals are sacrificed, and the brain removed, split sagittally, fixed by immersion in 4% paraformaldehyde for 1 hour at 4°C, and cryoprotected with 40% sucrose for 48 hours. The tissue is then

embedded in freezing compound, snap-frozen in isopentane chilled with liquid nitrogen, and cut into 7 μm sections using a cryostat. Sections of tissue are then sequentially incubated with patients' or controls serum (dilution range, 1:100 to 1:500) or CSF (1:2 to 1:5), the appropriate secondary antibody (mouse anti-human), and the reactivity developed with a standard method of avidin-biotin peroxidase and diaminobenzidine.

Cell-based assay

To confirm the specificity of the reactivity of patients' antibodies (e.g., NMDAR or mGluR5), we use cell-based assays (CBA). Briefly, HEK293 cells are seeded in plates containing poly-D-lysine coated coverslips, and 24 hours later, when the confluency is approximately 80%, cells are transfected using lipofectamine 2000 with the desired plasmid (e.g., GluN1/GluN2b or mGluR5). One day after transfection, cells are incubated with patients' serum or CSF either before (live CBA) or after fixation with 4% paraformaldehyde (fixed CBA). A commercial antibody specific for the antigen is used as control for the transfection. Reactivity is developed with anti-human Alexa Fluor 488 and the appropriate fluorescent secondary antibody for the commercial antibody and observed under a fluorescent microscope.

Immunohistochemistry of cultured live hippocampal neurons

To determine whether any reactivity identified with tissue immunostaining is directed against neuronal surface antigens, we use immunolabeling of cultured live hippocampal neurons. Briefly, hippocampi are isolated from rat embryos at embryonic day 18,

dissociated with trypsin and seeded in plates with poly-L-lysine coated coverslips. Neurons are cultured in neurobasal medium for 15-21 days at 37°C, 5% CO₂, and 95% humidity. For immunocytochemistry, neurons in coverslips are incubated with serum or CSF for 1 hour, fixed with 4% paraformaldehyde, developed with an anti-human Alexa Fluor 488 secondary antibody, and observed under a fluorescent microscope.

Determination of antibody effects in cultured neurons

Confocal microscopy

The potential effect of patients' antibodies on cultured neurons is assessed measuring the alteration of the target antigen at the synaptic and extrasynaptic sites, using confocal microscopy. In brief, hippocampal neurons are isolated and cultured as described above. Neurons at 14-17 days in vitro are exposed to patients' CSF or serum for 12 hours. The effect of patients' antibodies on specific receptors or synaptic proteins is then assessed with a specific commercial antibody against the receptor of interest (e.g., anti-GluN1 or anti-mGluR5) and a synaptic marker, typically PSD95. Then, clusters of total cell-surface and synaptic receptor (determined as co-localizing with PSD95) are quantified with confocal microscopy (Zeiss LSM710) using the software Imaris (Bitplane).

Single-particle tracking by Photoactivated Localization Microscopy (PALM)

The effect of the NMDAR PAM SGE-301 on the surface dynamics of NMDAR was assessed by PALM. For PALM experiments neurons are transfected at 10 days in vitro with Homer-GFP and GluN1-mEos3.2 using calcium phosphate transfection. Afterwards, neurons are

treated with SGE-301 or vehicle for 12 hours. Live neurons are imaged in an open chamber (Ludin chamber, Life Imaging Services) at 37°C. Transfected cells are detected with Homer-GFP signal, and GluN1-mEos3.2 is photoactivated using a 405nm laser. The resulting single-molecule fluorescence is excited with a 561nm laser. Surface GluN1-mEos is tracked for 200 frames using Metamorph software. Detection and reconnection of trajectories is done with PALM Tracer plugin for Metamorph. Homer-GFP is utilized as a synaptic marker to discriminate synaptic and extrasynaptic NMDAR trajectories.

Studies with mice

For all our animal experiments we use C57BL6/J mice (Charles River) housed in our animal facility (Unitat d'Experimentació Animal de Medicina, Centres Científics i Tecnològics, Universidad de Barcelona) at a controlled temperature ($21 \pm 1^\circ\text{C}$) and humidity ($55 \pm 10\%$) with illumination at 12-h cycles, and food and water *ad libitum*. Experiments are performed during the light phase, and animals are habituated to the room for 30 min before each experiment. All procedures are performed following standard ethical guidelines (European Communities Directive 2010/63/EU), approved by the local ethical committee (CEEA-316/22), and reported in accordance with the ARRIVE guidelines.

Cerebroventricular infusion of patients' antibodies to mice

To develop a mouse model for anti-mGluR5 encephalitis and study a potential treatment for the behavioral and synaptic effects of anti-NMDAR encephalitis patients' antibodies, we have used cerebroventricular infusion of patients' antibodies in mice.

In brief, bilateral intraventricular catheters connected to two osmotic minipumps subcutaneously placed on the back of male C57BL6/J ten-week-old mice. Each pump contains 100 µl of patients' CSF or purified IgG and infuse patients' antibodies for 14 days at a constant flow rate of 0.25 ml/h.

Development of a mouse model of anti-NMDAR encephalitis by active immunization

To immunize mice against NMDAR, female C57BL6/J, eight-week-old mice were subcutaneously injected with 200 µg of the GluN1^{356 – 386} peptide or saline and AddaVax adjuvant on days 1 and 28. All animals received 100 ng of Bordetella pertussis toxin intraperitoneally at the time of immunization and 48 hours later. To assess different treatments, a subset of mice received 250 µg of anti-CD20 intravenously on day 35. Another subset of mice received from day 47 until end of the study, 10 mg/kg of SGE-301 or vehicle intraperitoneally.

Characterization of animal models

The models and effect of different treatments in mice were assessed using a battery of behavioral tests, hippocampal electrophysiological studies, and confocal microscopy. The effect of active immunization and immunotherapy were also studied by flow cytometry studies of spleen and immune cell brain infiltrates.

Memory and behavior

Test	Assessment	Basis
Novel Object Location (NOL) test	Visuospatial memory	Animals with good memory tend to spend more time exploring an object in a novel rather than in a familiar location
Locomotor Activity (LA)	Horizontal and vertical activity	Ability to move in all planes
Prepulse Inhibition of the acoustic startle response (PPI)	Psychotic-like behaviour	Healthy animals do not startle when an intense acoustic stimulus is preceded by a less intense one
Black and White (BW) test	Anxiety-like behaviour	This test measures the conflict between the innate exploratory behaviour and natural aversion to brightly illuminated areas, animals with higher anxiety will explore less
Tail Suspension Test (TST)	Depressive-like behaviour	Healthy animals will try to escape from an aversive stimulus such as being hung from the tail

Table 7: Behavioral tests used for the study of the animal models in this thesis.

Hippocampal electrophysiological studies

In all animal models, the assessment of functional effects on long-term plasticity was performed in acute hippocampal slices obtained from mice at different time points by recording field excitatory postsynaptic potentials after proper stimulation of the Schaffer collateral-CA1 pathway.

Immunohistochemistry and confocal microscopy

To study the effects of patients' antibodies, immunization or treatments on the brain, mice were sacrificed, and the brain was extracted and processed as described for rat brain tissue immunohistochemistry. The presence of antibodies bound to tissue and specific target binding was assessed by human or mouse IgG immunolabelling and immunoprecipitation with A/G agarose beads from fresh brain tissue. In addition, the effects of antibodies were assessed with confocal microscopy including quantification of the clusters of the target antigens using primary antibodies against the specific receptor of interest (e.g., mGluR5, NMDAR) and PSD95 as a synaptic marker.

Flow cytometry studies

The effectiveness of the immunization and immunotherapy were assessed by flow cytometry studies of spleen and immune cell brain infiltrates. Briefly, brain and spleen were homogenized, filtered and separated by Ficoll or Percoll gradients.

Cells were collected and stained with fluorophore-conjugated antibodies to mark for different immune phenotypes (Table 8). Data was acquired in a Cytex Aurora cytometer.

Marker	Fluorophore	Cell type
CD11b	eFluor 450	Macrophages and microglia
CD45	APC	Leukocyte
CD3	Alexa Fluor 488	T cell
CD4	PE-Cyanine 5.5	T-helper
CD8	Brilliant Ultra Violet 737	T-cytotoxic
CD19	PE-Cyanine 5	B cell
CD27	Super Bright 702	Memory B cell
IgD	Super Bright 600	Naïve B cells
CD138	PE	Plasma cell

Table 8: Cell markers used for flow cytometry studies in this thesis.

Chapter VI

Publications



Contribution report

Below please find my comments on the publications of Estibaliz Maudes as part of the group of reports that comprise her doctoral thesis entitled “Cellular and animal models of antibody-mediated encephalitis: from pathogenesis to novel therapeutics”. The comments include my assessment on her participation as well as the journal impact factor.

Paper I. Human metabotropic glutamate receptor 5 antibodies alter receptor levels and behavior in mice.

Estibaliz Maudes, Francesco Mannara, Anna García-Serra, Marija Radosevic, Araceli Mellado, Ana Beatriz Serafim, Jesús Planagumà, Lidia Sabater, Josep Dalmau, Marianna Spatola.

Annals of Neurology. 2022; 92: 81-86.

Impact factor according to Journal of Citation Reports (JCR) in 2021: 11.274 (D1).

PhD candidate contribution: The PhD candidate participated in animal surgery and behavior tests. She performed mice sacrifices and the removal of mouse brains. She did all tissue processing for immunohistochemistry and confocal analysis of mGluR5 clusters. She participated in statistical analysis. She prepared the figures and wrote the original and revised versions of the manuscript.

This article is not expected to be included in any other doctoral thesis.

Paper II. NMDA receptor antibodies in autoimmune encephalopathy alter oligodendrocyte function.

Carlos Matute, Alicia Palma, Maria Pilar Serrano-Regal, **Estibaliz Maudes**, Saikat Barman, Maria Victoria Sánchez-Gómez, Maria Domercq, Niels Goebels, Josep Dalmau.

Annals of Neurology. 2020, 87(5), 670-676.

Impact factor JCR 2020: 10.422 (D1).

PhD candidate contribution: The PhD candidate participated in the conceptual and experimental design of the study. She selected and tested for antibodies all human samples used in the study. She performed the immunoabsorption of patients' samples. She participated in the statistical analysis and initial drafting of the manuscript and revised the final manuscript for intellectual content.

This article is not expected to be included in any other thesis.

Paper III. Allosteric modulation of NMDA receptors prevents the antibody effects of patients with anti-NMDAR encephalitis.

Francesco Mannara, Marija Radosevic, Jesús Planagumà, David Soto, Esther Aguilar, Anna García-Serra, **Estibaliz Maudes**, Marta Pedreño, Steven Paul, James Doherty, Michael Quirk, Jing Dai, Xavier Gasull, Mike Lewis, Josep Dalmau.

Brain. 2020, 143(9), 2709-2720.

Impact Factor JCR 2020: 13.501 (D1).

PhD candidate contribution: The PhD candidate participated in the following experiments: animal behavior tests, administration of treatment, removal of mouse brain and tissue processing for immunohistochemistry. She performed the immunoabsorption of patients' CSF. She revised the manuscript for intellectual content.

This article was included in the PhD thesis of Anna García-Serra.

Paper IV. Allosteric modulation of NMDARs reverses patients' autoantibody effects in mice.

Marija Radosevic, Jesús Planagumà, Francesco Mannara, Araceli Mellado, Esther Aguilar, Lidia Sabater, Jon Landa, Anna García-Serra, **Estibaliz Maudes**, Xavier Gasull, Mike Lewis, Josep Dalmau.

Neurology: Neuroimmunology & Neuroinflammation. 2022, 9(1), e1122.

Impact factor JCR 2022: 8.8 (D1).

PhD candidate contribution: The PhD candidate participated in the following experiments: animal behavior tests, administration of treatment, removal of mouse brain and tissue processing for immunohistochemistry. She revised the manuscript for intellectual content.

This article is not expected to be included in any other doctoral thesis.

Paper V. Positive allosteric modulation of NMDARs prevents the altered surface dynamics caused by patients' antibodies.

Estibaliz Maudes, Zoë Jamet, Laura Marmolejo, Josep Dalmau, Laurent Groc.

Neurology: Neuroimmunology & Neuroinflammation. 2024, 11(4), e200261.

Impact factor JCR 2022: 8.8 (D1).

PhD candidate contribution: The PhD candidate participated in the experimental design of the study. She performed all hippocampal neuron treatments with patients' samples and/or drug and all single-particle tracking experiments. She analyzed the data, performed the statistics, drafted the manuscript, including figures, and wrote the original and revised version of the manuscript.

This article is not expected to be included in any other thesis.

Paper VI. Neuro-immunobiology in a mouse model of anti-NMDAR encephalitis and assessment of treatment approaches.

Estibaliz Maudes, Jesús Planagumà, Laura Marmolejo, Marija Radosevic, Ana Beatriz Serafim, Esther Aguilar, Carlos Sindreu, Jon Landa, Anna García-Serra, Francesco Mannara, Marina Cunqueiro, Anna Smith, Chiara Milano, Paula Peixoto-Moledo, Mar Guasp, Raquel Ruiz-Garcia, Sarah M. Gray, Marianna Spatola, Pablo Loza-Alvarez, Lidia Sabater, Carlos Matute, Josep Dalmau.

Submitted to Brain. 2024.

Impact factor JCR 2022: 14.5 (D1).

PhD candidate contribution: The PhD candidate participated in the conceptual and experimental design of the study and performed most of the experiments including the development of the model, behavioral assessment, treatment administration, obtaining and processing all tissue samples, immunohistochemical studies, immuno-precipitation, and flow cytometry studies. She performed the statistical analyses, drafted the manuscript, and supplemental material, and wrote the original and revised versions of the manuscript.

This article is expected to be included in the thesis of Laura Marmolejo and Ana Beatriz Serafim.

Thesis director and tutor

A handwritten signature in black ink, appearing to read 'Josep Dalmau', with a long horizontal stroke extending to the right.

Josep Dalmau, MD, PhD

Thesis co-director

A handwritten signature in blue ink, appearing to read 'Carlos Matute', with a stylized 'C' and 'M'.

Carlos Matute, PhD

Paper I

*Human metabotropic glutamate receptor 5 antibodies alter
receptor levels and behaviors in mice*

Estibaliz Maudes, Francesco Mannara, Anna García-Serra, Marija
Radosevic, Araceli Mellado, Ana Beatriz Serafim, Jesús Planagumà,
Lidia Sabater, Josep Dalmau,[†] Marianna Spatola[†]

[†] These authors share seniority

Annals of Neurology 2022; 92: 81–86

IF JCR 2021: 11.27 (D1)

Human Metabotropic Glutamate Receptor 5 Antibodies Alter Receptor Levels and Behavior in Mice

Estibaliz Maudes, MSc ¹,
 Francesco Mannara, PhD ¹,
 Anna García-Serra, PhD ¹,
 Marija Radosevic, PhD ¹,
 Araceli Mellado, BS ¹,
 Ana Beatriz Serafim, BS ¹,
 Jesús Planagumà, PhD ¹,
 Lidia Sabater, PhD ¹,
 Josep Dalmau, MD, PhD ^{1,2,3,4†} and
 Marianna Spatola, MD, PhD ^{1,5†}

Ophelia syndrome or encephalitis with antibodies against the metabotropic glutamate receptor 5 (mGluR5) manifests with behavioral changes, memory deficits, and anxiety. To study the antibody pathogenicity, mice received continuous cerebroventricular infusion of patients' or controls' immunoglobulin G (IgG) for 14 days, followed by a 15-day washout. The effects on hippocampal mGluR5 clusters were determined by confocal microscopy. Animals infused with patients' IgG, but not controls' IgG, showed memory impairment, increased anxiety, and decreased neuronal surface mGluR5 clusters. After antibody clearance, both behavioral and molecular changes reversed to baseline conditions. These findings support the pathogenicity of these antibodies in anti-mGluR5 encephalitis.

ANN NEUROL 2022;92:81–86

Antibodies targeting the metabotropic glutamate receptor 5 (mGluR5) have been identified in patients with autoimmune encephalitis.¹ Anti-mGluR5 encephalitis manifests with memory deficits, anxiety, seizures, and behavioral changes, and is often associated with Hodgkin lymphoma (Ophelia syndrome).^{1–3}

A pathogenic role of these antibodies has been suggested by the response of patients' symptoms to immunotherapy^{1–3} and further supported by studies showing that the antibodies bind to the cell surface of cultured neurons and cause a depletion of the levels of mGluR5.^{1,3} However, these antibody-mediated alterations and their potential effect on behavior have not been explored in animals. Here, we addressed these

questions in a mouse model of cerebroventricular transfer of patients' immunoglobulin G (IgG).

Materials and Methods

Purification of IgG from Serum of Patients or Controls

IgG was purified from pooled serum of 2 reported patients with anti-mGluR5 encephalitis (Cases #1 and #6 in Spatola et al³) or healthy blood donors (controls) using protein A/G agarose beads columns (#20423; Pierce, Rockford, IL), normalized to a concentration of 2 µg/µl, and kept at –80 °C until use.³ The reactivity of purified IgG with mGluR5 was confirmed by rat brain tissue showing a characteristic pattern of immunostaining^{1,3} and by cell-based assay with human embryonic kidney 293 cells transfected with mGluR5.³

Animal Surgery

Cerebroventricular infusion (14 days duration) of purified IgG (from patients or controls) was performed as reported.⁴ Briefly, male C57BL/6J mice (Charles River, Wilmington, MA), aged 8 to 10 weeks, had bilateral catheters (#3280PD-2.0/SP; Plastics One, Roanoke, VA) inserted into the lateral ventricles. Catheters were then connected through a polyethylene tube (#C314CT, Plastics One) to subcutaneously implanted osmotic pumps filled with purified IgG (#1002; Alzet, Cupertino, CA; volume = 100 µl, flow rate = 0.25 µl/h).

Behavioral Testing

To assess whether patients' IgG altered behavior in mice, a panel of standardized behavioral tests was applied by investigators blinded to the experimental conditions, as reported.^{4,5} These tests assessed memory (Novel Object Location), anxiety (Black&White, Open Field), locomotor activity, weight, and food/water intake. The timing of the studies (explained below) in relation to IgG infusion is shown in Figure 1A.

From the ¹Neuroimmunology Program, August Pi i Sunyer Biomedical Research Institute (IDIBAPS), Hospital Clinic, University of Barcelona, Barcelona, Spain; ²Department of Neurology, University of Pennsylvania, Philadelphia, PA; ³Center for Biomedical Research Network, Rare Diseases (CIBERER), Madrid, Spain; ⁴Catalan Institution for Research and Advanced Studies (ICREA), Barcelona, Spain; and ⁵Ragon Institute of Massachusetts General Hospital, Massachusetts Institute of Technology, and Harvard Medical School, Cambridge, MA

Address correspondence to Dr Spatola, Institut d'Investigacions Biomèdiques August Pi i Sunyer (IDIBAPS), University of Barcelona, Casanova, 143; Floor 3^o, Barcelona 08036, Spain. E-mail: marianna.spatola@gmail.com

Received Jan 21, 2022, and in revised form Mar 24, 2022. Accepted for publication Mar 26, 2022.

View this article online at wileyonlinelibrary.com. DOI: 10.1002/ana.26362.

†J.D. and M.S. share senior authorship.

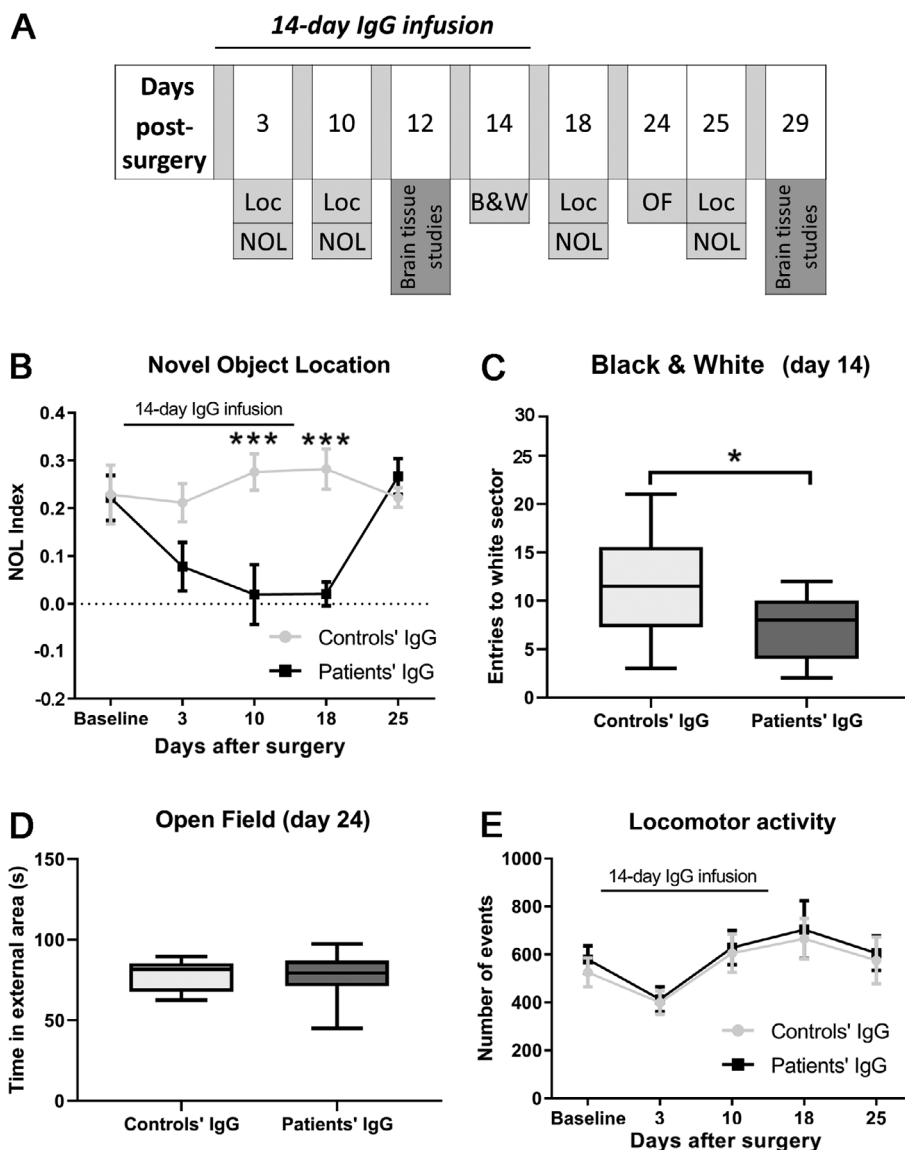


FIGURE 1: Infusion of patients' immunoglobulin G (IgG) with metabotropic glutamate receptor 5 antibodies causes reversible memory impairment and increased anxiety in mice. (A) Schedule of behavioral tests and brain tissue studies in relation to IgG infusion. At day 0, catheters and osmotic pumps were placed and infusion of patients' or controls' IgG was started. Infusion lasted for 14 days. Memory (Novel Object Location [NOL]), anxiety (Black&White [B&W] and Open Field [OF]), and locomotor activity (Loc) were assessed at the indicated days postsurgery. (B) Memory assessment by NOL index in mice treated with patients' (black squares and line) or controls' IgG (gray dots and line). A higher NOL index indicates better object recognition memory. *** $p < 0.001$. (C) Anxiety assessment by B&W test performed 14 days after surgery. The number of entries into the bright/white compartment of the arena during a 5-minute period in mice treated with patients' (dark gray box plot) or controls' (white box plot) IgG is shown. Fewer entries to the white sector indicate more anxiety. Box plots represent the median, 25th percentile, and 75th percentile; whiskers represent minimum to maximum values. * $p < 0.05$. (D) On day 24, 10 days after IgG infusion had stopped, anxiety was assessed using the OF test, to reduce learning effects. Time spent in the external section of the arena over a 10-minute period in mice treated with patients' (dark gray box plot) or controls' (white box plot) IgG is shown. Greater time spent in the external section indicates increased anxiety. Box plots represent the median, 25th percentile, and 75th percentile; whiskers represent minimum to maximum values. No statistically significant difference was observed between the groups. (E) Locomotor activity assessment by movement counts over a 10-minute period in mice treated with patients' (black squares and line) or controls' (gray dots and line) IgG. Values indicate mean values across animals at each time point, and error bars represent standard error of the mean. For each behavioral test, 12 animals were assessed per treatment group (patients' IgG and controls' IgG). Statistical analysis was assessed by 2-way analysis of variance (B, E) and unpaired t test (C, D), with an α error of 0.05.

Brain Tissue Immunohistochemistry and Immunofluorescence

On day 12 or 29, subsets of mice were euthanized, and the brains removed, fixed in 4% paraformaldehyde, cryoprotected with 40%

sucrose, embedded with freezing media (#4583; Tissue-Tek, Torrance, CA), and snap-frozen with methyl butane cooled in liquid nitrogen.⁴ To determine whether the infused mGluR5 antibodies were able to bind to mice brain tissue, 5 μ m-thick brain

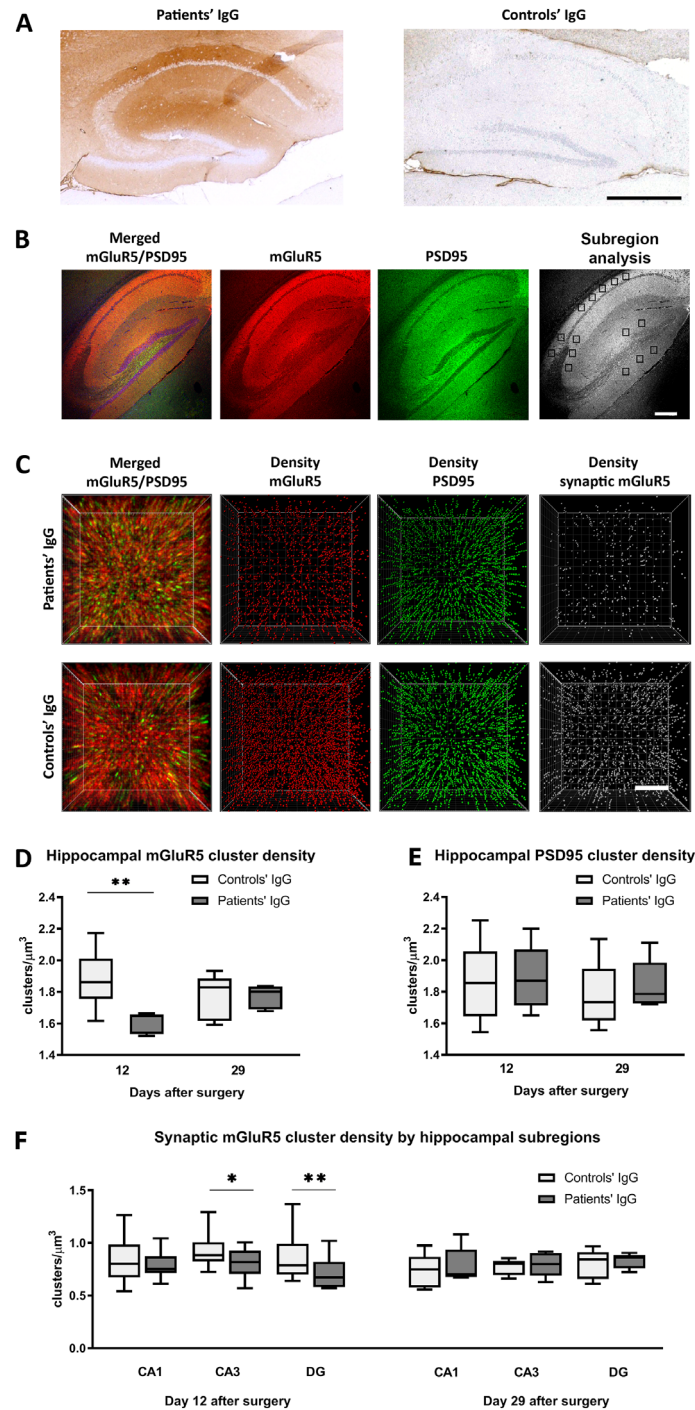


FIGURE 2: Patients' immunoglobulin G (IgG) bind to mice brain and associate with a reversible decrease in total cell surface and synaptic metabotropic glutamate receptor 5 (mGluR5) clusters. (A) Human IgG immunolabeling of representative hippocampal sections, showing strong immunostaining in the brain of a mouse treated with patients' IgG (left panel) and absence of staining in the brain of a mouse treated with controls' IgG (right panel) on day 12. Scale bar = 400 μm . (B) Hippocampal section from a representative mouse infused with patients' IgG demonstrating the immunostaining of mGluR5 (red), PSD95 (green), and the merged reactivities (orange). Squares in the panel labeled "Subregion analysis" indicate the hippocampal subregions (CA1, CA3, and dentate gyrus [DG]) that were used for confocal microscopy quantification of PSD95, and total and synaptic mGluR5 clusters in each animal. Scale bar = 200 μm . (C) Three-dimensional projections of a hippocampal area (DG subregion) showing a representative analysis of total mGluR5 (red) and PSD95 (green) clusters and merged projections (orange). Synaptic mGluR5 clusters (gray) are defined as mGluR5 clusters that colocalize with PSD95. Scale bar = 2 μm . (D–F) Quantification analyses of hippocampal cell surface mGluR5 (total surface, D; synaptic, F) and PSD95 (E) cluster density (clusters/ μm^3) in mice treated with patients' or controls' IgG. Analyses were performed in the whole hippocampus (D, E) and in the CA1, CA3, and DG hippocampal subregions (F). Box plots represent the median, 25th percentile, and 75th percentile; whiskers indicate minimum and maximum values. For each time point (12 and 29 days), 5 mice infused with patients' IgG and 5 with controls' IgG were examined. Statistical analysis was assessed by linear model of mixed effects with an α error of 0.05. * $p < 0.05$, ** $p < 0.01$.

sections were immunostained with biotinylated goat anti-human IgG (#109–035-088; Jackson ImmunoResearch, West Grove, PA), as reported.⁴

On day 12 or 29, the effects of patients' antibodies on hippocampal mGluR5 clusters (total cell surface and synaptic) were examined using immunofluorescence and confocal microscopy. Synaptic mGluR5 was defined by the colocalization of mGluR5 with the synaptic marker PSD95. Quantification of surface mGluR5 clusters was performed in the entire hippocampus and several hippocampal subregions (CA1, CA3, and dentate gyrus [DG]). Primary antibodies included human serum anti-mGluR5 and rabbit polyclonal antibody against PSD95 (#18258; Abcam, Cambridge, MA), and secondary antibodies included Alexa Fluor 594 goat anti-human IgG and Alexa Fluor 488 goat anti-rabbit IgG (#A11014, #A11008; Molecular Probes, Eugene, OR).^{3,4}

Statistical Analyses

Differences in mGluR5 cluster densities between mice treated with patients' or controls' IgG were analyzed using a linear model of mixed effects. Behavioral tests were analyzed using independent *t* tests or 2-way analysis of variance with Bonferroni correction, as appropriate. The alpha level used to determine significance was $p < 0.05$. Statistical tests and graphs were performed using Prism (v7; GraphPad Software, San Diego, CA) and R studio (v4.0.0).

Ethical Approval

The use of patients' samples for research purposes and animal procedures (which complied with European 2010/63/UE and Spanish RD 53/2013 regulations) were approved by the local ethical committee of the University of Barcelona, Spain.

Results

Patients' IgG Caused Severe Memory Loss and Increased Anxiety

Mice infused with patients' IgG, but not controls' IgG, developed visuospatial memory impairment, as indicated by a decrease of the Novel Object Location index (see Fig 1B). The memory impairment became significant on day 10 (during IgG infusion), and reversed to values similar to those of controls by day 25 (11 days after the infusion was stopped; see Fig 1B).

On day 14, mice infused with patients' IgG, compared to those infused with controls' IgG, showed significantly fewer entries into the white sector of the arena in the Black&White paradigm (see Fig 1C), indicating increased levels of anxiety. To avoid learning effects, we used a different anxiety test (Open Field) on day 24, which showed anxiety levels similar to those of control mice (see Fig 1D). No significant differences between experimental groups were noted in measures of locomotor activity (see Fig 1E), weight, and food/water intake (not shown).

Patients' IgG Bound to Mouse Brain and Caused a Decrease of mGluR5 Cluster Density

On day 12, brains of mice infused with patients' IgG, but not controls' IgG, showed intense antihuman IgG immunostaining in the hippocampus (Fig 2A), reflecting the presence of patients' antibodies bound to brain tissue. This staining was no longer seen in the subset of mice sacrificed 15 days after the IgG infusion had stopped (day 29, data not shown). Moreover, on day 12, hippocampi from animals infused with patients' IgG had a significant decrease of total and synaptic mGluR5 clusters, mainly in the subregions CA3 and DG, without affecting PSD95 cluster density (see Fig 2B–F). These effects were reversible, and on day 29 (15 days after the IgG infusion had stopped) the total and synaptic mGluR5 cluster densities had recovered to levels similar to those of controls (see Fig 2D–F).

Discussion

Our study demonstrates that the infusion of IgG from patients with anti-mGluR5 encephalitis into the cerebroventricular system of mice caused memory loss and increased anxiety in association with a significant reduction of the levels of mGluR5 in the hippocampus. These effects were reversible upon removal of the antibodies, in keeping with the improvement of patients after antibody-depleting treatments.^{1–3} Thus, together with results from our previous study showing that patients' antibodies caused a reduction of mGluR5 clusters in cultured neurons,³ the current findings provide robust evidence of the antibody pathogenicity linking memory and anxiety alterations with a reduction of mGluR5 levels.

The current animal model has been widely validated for the study of antibody pathogenicity in other disorders such as N-methyl-D-aspartate receptor (NMDAR), leucine-rich glioma-inactivated 1 (LGI1), α -amino-3-hydroxy-5-methyl-4-isoxazolepropionic acid receptor (AMPA receptor), or contactin-associated protein 2 (CASPR2) antibody-associated encephalitis.^{4,6,7} Thus, it has the advantage of providing the direct effects of the antibodies on the corresponding target in the brain, without requiring opening the blood–brain barrier with lipopolysaccharide, which by itself causes inflammation and behavioral alterations. Limitations include that the antibody effects predominate around the areas of infusion (hippocampus, frontal regions), and are not accompanied by inflammatory infiltrates.⁴ Because mGluR5 antibodies associate with a characteristic syndrome across different patients, but antibodies in all autoimmune encephalitis are polyclonal, the use of pooled IgG, instead of IgG from a single case or patient-derived monoclonal antibodies, has the advantage of better representing the repertoire of

pathogenic antibodies of the disease, allowing generalization of the findings.

mGluR5 is involved in various neuronal processes, including memory formation⁸ and anxiety responses.⁹ In rodents, pharmacological potentiation of mGluR5 with positive allosteric modulators (PAMs) is associated with better learning and memory,^{10,11} whereas genetic deletion of mGluR5 results in impaired spatial learning.¹² These findings are in line with the immune-depletion of mGluR5 of the current model resulting in memory impairment, whereas restoration of mGluR5 levels upon clearance of patients' antibodies led to memory recovery.

The role of mGluR5 in memory acquisition is thought to be largely mediated by the potentiation of NMDAR responses.^{13,14} Whether the effects of mGluR5 antibodies on memory are also dependent on NMDAR modulation is unknown. Future in vitro and animal studies should address whether mGluR5 antibodies also affect NMDAR responses and whether pharmacologic modulation of mGluR5 (or NMDAR) by PAMs is able to rescue the molecular effects and memory impairment, as recently reported in a model of NMDAR antibody effects.¹⁵

Here, in addition to memory impairment, mice intrathecally exposed to patients' IgG showed increased anxiety, which is in agreement with the clinical phenotype of anti-mGluR5 encephalitis.¹⁻³ The role of mGluR5 in anxiety responses is not completely understood. For example, pharmacological modulation of mGluR5 by negative allosteric modulators results in reduced levels of anxiety in mice.¹⁶ However, genetic deletion of mGluR5 in older mice, but not in young ones, is associated with increased anxiety.¹⁷ These contrasting results might be at least partially explained by the remarkable variability in the effects of mGluR5 on anxiety circuits based on receptor location, cell type, and age.¹⁷⁻¹⁹ In our model, we focused on the antibody effects on the hippocampus, which is involved in both memory and stress response, and is clinically and radiologically involved in anti-mGluR5 encephalitis.

Future studies including mGluR5 positron emission tomography in humans⁹ should explore whether other brain regions relevant to anxiety, such as the amygdala or the ventromedial prefrontal cortex, are also altered. Moreover, experimental models will help to determine whether the effect of patients' antibodies on mGluR5 differ depending on brain regions (eg, hippocampus vs amygdala)¹⁹ and how the antibody-mediated changes in mGluR5 contribute to generate anxiety.

Acknowledgments

E.M. is a recipient of the Basque Government Doctoral Fellowship Program (PRE_2021_2_0138). A.G.-S.

received the FI-AGAUR grant from La Generalitat de Catalunya (2020 FI_B2 00208). J.P. received research funding from Fondo de Investigación Sanitaria-Instituto de Salud Carlos III (FIS PI20/00280). M.S. received personal research funding from the University of Lausanne and University Hospital of Lausanne Joint Foundation, the American Academy of Neurology, and the Swiss National Research Foundation. This work was conducted with support from the Cellex Foundation, Edmond Safra Foundation, and Harvard Catalyst, Harvard Clinical and Translational Science Center (National Center for Advancing Translational Sciences, NIH Award UL1 TR002541) and financial contributions from Harvard University and its affiliated academic health care centers. The content is solely the responsibility of the authors and does not necessarily represent the official views of Harvard Catalyst, Harvard University and its affiliated academic health care centers, or the NIH.

We thank E. Aguilar and M. Alba for their excellent technical support and Dr T. Thaweethai for his help with statistical analyses.

Author Contributions

E.M., J.D., and M.S. contributed to the conception and design of the study; E.M., F.M., A.G.-S., A.M., A.B.S., M.R., J.P., L.S., and M.S. contributed to the acquisition and analysis of data; E.M., M.S., and J.D. contributed to drafting the text and preparing the figures. All authors revised the final draft of the manuscript.

Potential Conflicts of Interest

Nothing to report.

References

1. Lancaster E, Martinez-Hernandez E, Titulaer MJ, et al. Antibodies to metabotropic glutamate receptor 5 in the Ophelia syndrome. *Neurology* 2011;77:1698-1701.
2. Mat A, Adler H, Merwick A, et al. Ophelia syndrome with metabotropic glutamate receptor 5 antibodies in CSF. *Neurology* 2013; 42:7-8.
3. Spatola M, Sabater L, Planagumà J, et al. Encephalitis with mGluR5 antibodies: symptoms and antibody effects. *Neurology* 2018;90: e1964-e1972.
4. Planagumà J, Leypoldt F, Mannara F, et al. Human N-methyl D-aspartate receptor antibodies alter memory and behaviour in mice. *Brain* 2015;138:94-109.
5. Seibenhener ML, Wooten MC. Use of the open field maze to measure locomotor and anxiety-like behavior in mice. *J Vis Exp* 2015;96: e52434.
6. Dalmau J, Graus F. Pathogenesis and disease mechanisms in neuronal antibody-mediated encephalitis. In: *Autoimmune encephalitis and related disorders of the central nervous system*. Cambridge, UK: Cambridge University Press, 2022.

7. Joubert B, Petit-Pedrol M, Planagumà J, et al. Human CASPR2 antibodies reversibly alter memory and CASPR2 protein complex. *Ann Neurol* 2022;91:801–813.
8. Bikbaev A, Neyman S, Ngomba R, et al. mGluR5 mediates the interaction between late-LTP, network activity, and learning. *PLoS One* 2008;3:e2155.
9. Terbeck S, Akkus F, Chesterman LP, et al. The role of metabotropic glutamate receptor 5 in the pathogenesis of mood disorders and addiction: combining preclinical evidence with human positron emission tomography (PET) studies. *Front Neurosci* 2015;9:86.
10. Ayala JE, Chen Y, Banko JL, et al. mGluR5 positive allosteric modulators facilitate both hippocampal LTP and LTD and enhance spatial learning. *Neuropsychopharmacology* 2009;34:2057–2071.
11. Doria JG, de Souza JM, Silva FR, et al. The mGluR5 positive allosteric modulator VU0409551 improves synaptic plasticity and memory of a mouse model of Huntington's disease. *J Neurochem* 2018;147:222–239.
12. Lu YM, Jia Z, Janus C, et al. Mice lacking metabotropic glutamate receptor 5 show impaired learning and reduced CA1 long-term potentiation (LTP) but normal CA3 LTP. *J Neurosci* 1997;17:5196–5205.
13. Matta JA, Ashby MC, Sanz-Clemente A, et al. mGluR5 and NMDA receptors drive the experience- and activity-dependent NMDA receptor NR2B to NR2A subunit switch. *Neuron* 2011;70:339–351.
14. Le Aloisi E, Corf K, Dupuis J, et al. Altered surface mGluR5 dynamics provoke synaptic NMDAR dysfunction and cognitive defects in Fmr1 knockout mice. *Nat Commun* 2017;8:1103.
15. Mannara F, Radosevic M, Planagumà J, et al. Allosteric modulation of NMDA receptors prevents the antibody effects of patients with anti-NMDAR encephalitis. *Brain* 2020;143:2709–2720.
16. Cai G, Wang X, Che Y, et al. Basimglurant, an mGluR5-selective negative allosteric modulator, does not reduce pain but alleviates pain related anxiety-like behavior. *Neurology* 2016;86:P4.065.
17. Inta D, Vogt MA, Luoni A, et al. Significant increase in anxiety during aging in mGlu5 receptor knockout mice. *Behav Brain Res* 2013;241:27–31.
18. Jong YJ, Harmon SK, O'Malley KL. Location and cell-type-specific bias of metabotropic glutamate receptor, mGlu5, negative allosteric modulators. *ACS Chem Neurosci* 2019;10:4558–4570.
19. Rahman MM, Kedia S, Fernandes G, et al. Activation of the same mGluR5 receptors in the amygdala causes divergent effects on specific versus indiscriminate fear. *Elife* 2017;6:e25665.

Paper II



*NMDA receptor antibodies in autoimmune encephalopathy
alter oligodendrocyte function.*

Carlos Matute, Alicia Palma, Maria Pilar Serrano-Regal, **Estibaliz
Maudes**, Saikat Barman, Maria Victoria Sánchez-Gómez, Maria
Domercq, Niels Goebels, Josep Dalmau.

Annals of Neurology. 2020, 87(5), 670-676.

IF JCR 2020: 10.422 (D1).

N-Methyl-D-Aspartate Receptor Antibodies in Autoimmune Encephalopathy Alter Oligodendrocyte Function

Carlos Matute, PhD ¹, Ana Palma, MSc,¹ María Paz Serrano-Regal, MSc,¹ Estibaliz Maudes, MSc,² Sumanta Barman, MSc,³ María Victoria Sánchez-Gómez, PhD,¹ María Domercq, PhD,¹ Norbert Goebels, MD,³ and Josep Dalmau, MD, PhD ^{2,4,5}

Objective: Antibodies against neuronal N-methyl-D-aspartate receptors (NMDARs) in patients with anti-NMDAR encephalitis alter neuronal synaptic function and plasticity, but the effects on other cells of the nervous system are unknown.

Methods: Cerebrospinal fluid (CSF) of patients with anti-NMDAR encephalitis (preabsorbed or not with GluN1) and a human NMDAR-specific monoclonal antibody (SSM5) derived from plasma cells of a patient, along the corresponding controls, were used in the studies. To evaluate the activity of oligodendrocyte NMDARs and α -amino-3-hydroxy-5-methyl-4-isoxazolepropionic acid (AMPA) receptors in vitro after exposure to patients' CSF antibodies or SSM5, we used a functional assay based on cytosolic Ca^{2+} imaging. Expression of the glucose transporter (GLUT1) in oligodendrocytes was assessed by immunocytochemistry.

Results: NMDAR agonist responses were robustly reduced after preincubation of oligodendrocytes with patients' CSF or SSM5 but remained largely unaltered with the corresponding controls. These effects were NMDAR specific, as patients' CSF did not alter responses to AMPA receptor agonists and was abrogated by preabsorption of CSF with HEK cells expressing GluN1 subunit. Patients' CSF also reduced oligodendrocyte expression of glucose transporter GLUT1 induced by NMDAR activity.

Interpretation: Antibodies from patients with anti-NMDAR encephalitis specifically alter the function of NMDARs in oligodendrocytes, causing a decrease of expression of GLUT1. Considering that normal GLUT1 expression in oligodendrocytes and myelin is needed to metabolically support axonal function, the findings suggest a link between antibody-mediated dysfunction of NMDARs in oligodendrocytes and the white matter alterations reported in patients with this disorder.

ANN NEUROL 2020;87:670–676

Recent studies have identified a group of human disorders in which synaptic receptors are directly targeted by autoantibodies.¹ In particular, autoantibodies to the GluN1 subunit of the N-methyl-D-aspartate receptor (NMDAR) cause receptor internalization and reduced surface expression in neurons, leading to encephalitis

symptoms that include psychosis, cognitive decline, seizures, and coma.² An intriguing feature of this disease is the dissociation between the severity of symptoms of most patients and the low frequency (~32%) of magnetic resonance imaging (MRI) abnormalities using standard clinical sequences.³ Yet studies with diffusion tensor imaging

View this article online at [wileyonlinelibrary.com](https://onlinelibrary.wiley.com/doi/10.1002/ana.25699). DOI: 10.1002/ana.25699

Received Apr 9, 2019, and in revised form Jan 15, 2020. Accepted for publication Feb 6, 2020.

Address correspondence to Dr Matute, Achucarro Basque Center for Neuroscience, E-48940 Leioa, Spain, E-mail: carlos.matute@ehu.es; and Dr Dalmau, Institut d'Investigacions Biomèdiques August Pi i Sunyer, Hospital Clínic, Universitat de Barcelona, Barcelona, Spain. E-mail: jdalmau@clinic.cat

From the ¹Achucarro Basque Center for Neuroscience, Biomedical Research Networking Center on Neurodegenerative Diseases and Department of Neurosciences, University of the Basque Country, Leioa, Spain; ²August Pi i Sunyer Biomedical Research Institute, Hospital Clínic, University of Barcelona, Barcelona, Spain; ³Department of Neurology, Medical Faculty, Heinrich Heine University Düsseldorf, Düsseldorf, Germany; ⁴Department of Neurology, University of Pennsylvania, Philadelphia, PA; and ⁵Catalan Institution for Research and Advanced Studies (ICREA), Barcelona, Spain

(DTI) and superficial white matter mean diffusivity show extensive changes in white matter integrity in most patients.^{4,5}

Oligodendrocytes make myelin and support axons metabolically with lactate.⁶ Like neurons, oligodendrocytes express NMDARs, which plays a critical role in supplying lactate to axons to sustain proper propagation of action potentials.⁷ Thus, stimulation of NMDARs by glutamate released from axons results in a translocation of the glucose transporter GLUT1 into the oligodendrocyte plasma membrane and myelin compartment, enhancing glucose uptake and glycolytic support of fast spiking axons.⁷

Here, we tested the hypothesis that the function of NMDARs in oligodendrocytes may also be impaired in patients with anti-NMDAR encephalitis. We provide proof-of-principle evidence that the activity of those receptors is robustly reduced in patients with anti-NMDAR encephalitis and that these changes affect the expression of GLUT1.

Patients and Methods

Patients, Control Cerebrospinal Fluid Samples, and Monoclonal Antibodies

The 7 patients included in the study were selected from a previously reported cohort of cases with anti-NMDAR encephalitis.³ All 7 patients fulfilled criteria of anti-NMDAR encephalitis,⁸ and their random selection was based on the amount of cerebrospinal fluid (CSF) available for the current studies. The median age was 16 years (range = 10–25 years), and 4 were female. In all cases, the CSF was obtained during the acute stage of the disease, and all were negative for glial autoantibodies such as aquaporin-4, myelin oligodendrocyte glycoprotein, and glial fibrillary acidic protein. By the time of diagnosis (in all cases within 4 weeks of disease onset), 6 patients had normal clinical MRI studies, and 1 had a 0.2mm abnormality on fluid-attenuated inversion-recovery (FLAIR)/T2 sequences in the right temporal lobe. NMDAR antibody titers were determined by serial dilutions of CSF using a cell-based assay (median = 1/160, range = 1/20–1/640). For controls, we used the CSF of 3 patients with noninflammatory mild cognitive decline and 4 patients with normal pressure hydrocephalus who were negative for NMDAR antibodies. The effect of the same patients' CSF antibodies (and lack of effect of control CSF) had been previously reported in investigations using cultured neurons and cerebroventricular transfer of CSF antibodies to mice, resulting in robust NMDAR internalization, impairment of hippocampal long-term potentiation, and memory deficits.⁹ In all instances, the

CSF samples had been dialyzed against phosphate-buffered saline and the exclusion of other antibodies confirmed with tissue immunohistochemistry and NMDAR immunoabsorption experiments.⁹

Pooled CSF from the 3 patients with the highest NMDAR antibody titers (all >1:80) was immunoabsorbed with HEK293T cells expressing the GluN1 subunit of the NMDAR or cells not expressing this subunit, as previously reported.¹⁰ A recombinant monoclonal human antibody (SSM5) derived from intrathecal plasma cells of a patient with anti-NMDAR encephalitis and a control isotype against an irrelevant antigen (12D7) were used in some assays. The high specificity of SSM5 and its effects on mice behavior and synaptic NMDARs (which were similar to those caused by pooled CSF from patients) and the lack of effect of 12D7 have been previously reported.¹¹

Animal Ethics Statement

This study was carried out in accordance with the recommendations and approval of the internal animal ethics committee of the University of the Basque Country (UPV/EHU), in accordance with the European Communities Council Directive. Rats of both sexes were used for all experiments.

Oligodendrocyte Culture

Highly enriched cultures of oligodendrocytes were prepared from mixed glial cultures obtained from newborn Sprague–Dawley rat forebrain cortices as previously described.¹² Briefly, after detaching from mixed cultures, oligodendrocyte progenitor cells were seeded onto poly-D-lysine-coated coverslips and cultured at 37°C and 5% CO₂ in SATO differentiation medium containing the following: 1mg/ml bovine serum albumin, 100µg/ml transferrin, 16µg/ml putrescine, 40ng/ml thyroxine, 30ng/ml tri-iodothyronine, 60ng/ml progesterone, 40ng/ml sodium selenite, 63µg/ml N-acetyl-cysteine, 5µg/ml insulin (all from Sigma-Aldrich, St Louis, MO); and 2mM L-glutamine plus 10ng/ml CNTF and 1ng/ml NT3 (both from PeproTech, Rocky Hill, NJ) to induce oligodendrocyte maturation for 6 days. At this stage, the majority of cells expressed myelin basic protein, a marker of mature oligodendrocytes (Fig 1A).

Cytosolic Ca²⁺ Imaging

Oligodendrocytes were incubated with each individual patient or control CSF sample (diluted 1:50) at 37°C for 4 hours, and the effect on NMDA-mediated cytosolic [Ca²⁺] was measured as reported.¹³ In brief, after incubation with patient or control CSF, oligodendrocytes were loaded with Fluo-4 AM (1mM; Molecular Probes;

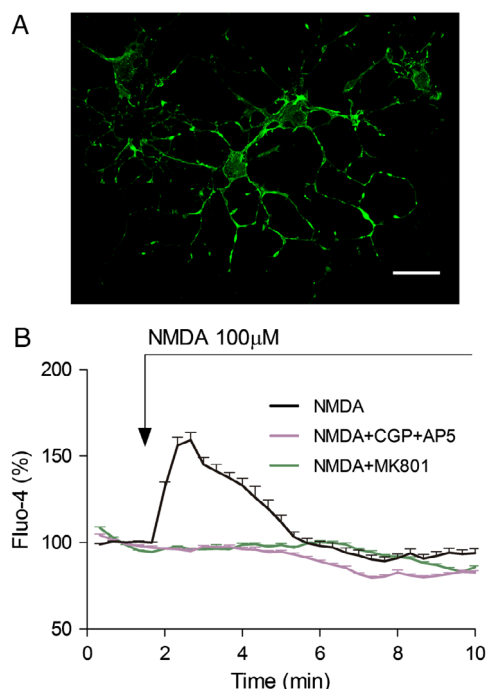


FIGURE 1: Functional assay of N-methyl-D-aspartate (NMDA) receptor (NMDAR) responses in oligodendrocyte cultures derived from the rat forebrain. (A) Myelin basic protein staining showing the typical branched appearance of oligodendrocytes in these cultures. Bar = 30 μm. **(B)** Recordings of Ca^{2+} responses following application of NMDA plus glycine (both at 100 μM; arrow) using Fluo-4. Responses are blocked in the presence of NMDAR antagonists CGP39551 (1 μM) and AP5 (100 μM; NMDA + CGP + AP5) and MK801 (50 μM; NMDA + MK801). In all instances, data represent the average \pm standard error of the mean of values obtained from at least 2 to 3 different cultures and analyzed using one-way analysis of variance with Tukey post-test (NMDA alone vs NMDA plus antagonists, $p < 0.001$).

Invitrogen, Barcelona, Spain) in incubation buffer for 30 minutes at 37°C followed by 20 minutes wash to allow de-esterification. Oligodendrocytes were then exposed to NMDA applied together with glycine (both at 100 μM), and the Ca^{2+} images were acquired through a 40X objective by an inverted LCS SP8 confocal microscope (Leica, Wetzlar, Germany) at an acquisition rate of 1 frame/10 seconds during 5 minutes. For data analysis, a homogeneous population of 15 to 25 cells per coverslip was selected in the field of view, and oligodendrocyte somata were selected as region of interest. Background values were always subtracted and data expressed as $F/F_0 \pm$ standard error of the mean (SEM; %), in which F represents the fluorescence value for a given time point and F_0 represents the mean of the resting fluorescence level. For each individual patients' CSF or control CSF, this experiment was repeated 3 times in oligodendrocyte cultures grown in identical conditions.

To confirm that the effects were related to NMDAR-specific antibodies, we ran similar experiments where oligodendrocytes were incubated with the indicated pooled patients' CSF preabsorbed with HEK293 cells expressing or not expressing GluN1 or with the monoclonal human anti-GluN1 (SSM5) or the corresponding isotype control (12D7) as reported.¹¹

Immunofluorescence Staining

Cultured oligodendrocytes were processed for immunostaining as described previously.¹⁴ Briefly, cells were fixed in 4% paraformaldehyde in phosphate-buffered saline and incubated with mouse antimyelin basic protein antibodies (1:500; BioLegend, San Diego, CA) or anti-GLUT 1 (1:250; Santa Cruz Biotechnology, Dallas, TX) followed by goat antimouse IgG Alexa Fluor-488 (1:400; Invitrogen) secondary antibody. Both 4',6-diamidino-2-phenylindole (DAPI) and calcein-AM (Molecular Probes) staining were used to identify nuclei and cells, respectively. Cells were visualized with a laser scanning confocal microscope (LCS SP8) at the Analytic and High-Resolution Microscopy Facility in the Achucarro Basque Center for Neuroscience.

Statistical Analysis

CSF samples from each of the patients and controls ($n = 7$ each) were used to treat 3 different cultures at identical conditions. To analyze NMDA responses, calcium recordings were obtained from 15 to 25 cells for each sample and culture, and the mean of the responses for each sample was used for analysis. Data obtained with α -amino-3-hydroxy-5-methyl-4-isoxazolepropionic acid (AMPA) responses and with human monoclonal antibodies and isotype control were analyzed in a similar way. Statistical analysis for comparisons between multiple experimental groups was made using 1-way analysis of variance (ANOVA) with Tukey post hoc test. For comparisons among individual control and patients' CSF samples ($n = 7$ each), we normalized by the naive response to minimize the potential variability on NMDA response between cultures and analyzed the data using 2-tailed Student t test. To analyze GLUT1 expression, fluorescence intensity was recorded from 15 to 20 cells for each sample and culture. The mean of 3 different cultures was obtained for each condition. Statistical analysis was made using one-way ANOVA with Tukey post hoc test. All data are shown as mean \pm SEM. In all cases, statistical analyses were performed using Prism version 5.0 (GraphPad Software, San Diego, CA). Differences were considered statistically significant where $p < 0.05$.

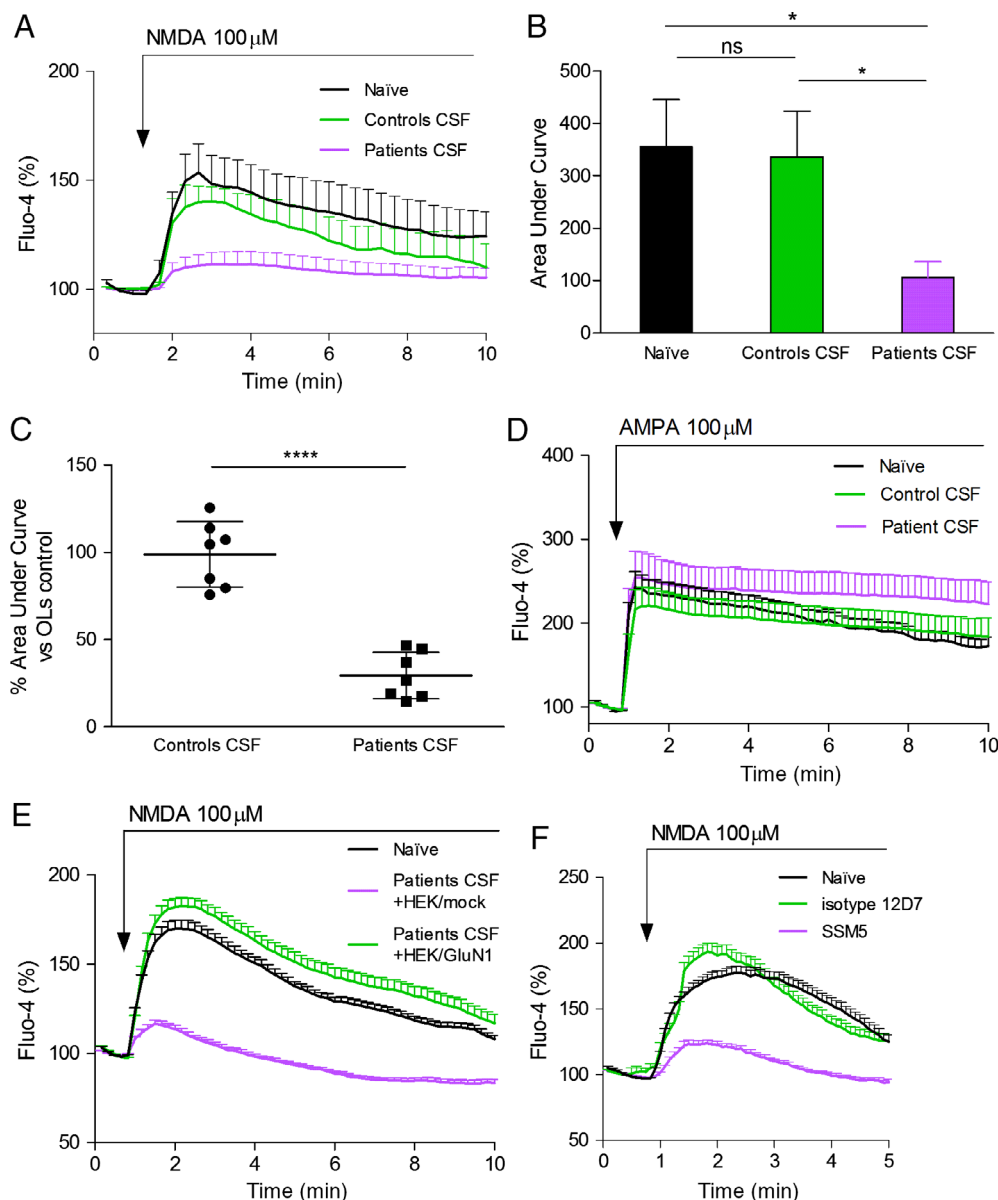


FIGURE 2: Specific N-methyl-D-aspartate (NMDA) receptor (NMDAR) responses in oligodendrocytes (OLs) in response to agonist application after incubation with patient and control cerebrospinal fluid (CSF). (A) Recordings of the basal Ca^{2+} responses in naïve OLs (black trace, naïve) were not significantly modified after incubation with CSF from control subjects (green trace, mean value of 7 control CSF samples in 3 different experiments) but were significantly reduced following exposure to patients' CSF (magenta trace, mean value of 7 patients' CSF samples in 3 different experiments); $p < 0.001$, one-way analysis of variance (ANOVA) with Tukey post-test. (B) Histogram depicting the area under the curve displayed by the recordings in (A). Note that the values after preincubation with CSFs from patients are lower than in control naïve OLs or after preincubation with control CSF; $*p < 0.05$, one-way ANOVA with Tukey post-test. (C) Graph showing the effects of each individual CSF from controls or patients on the NMDAR responses in naïve OLs (100%); $****p < 0.001$, unpaired 2-tailed Student t test. (D) The α -amino-3-hydroxy-5-methyl-4-isoxazolepropionic acid (AMPA) receptor responses are similar in OLs not preincubated with CSF (naïve, black) and those preincubated with control CSF (green) or patients' CSF (magenta). (E) Preabsorption of pooled patients' CSF in HEK cells transfected with GluN1 (green), but not with HEK cells mock transfected (magenta), results in NMDA responses similar to those of naïve (black) OLs (naïve vs patients' CSF + HEK/mock, $p < 0.001$; patients' CSF + HEK/GluN1 vs patients' CSF + HEK/mock, $p < 0.001$; one-way ANOVA with Tukey post-test). (F) Pretreatment of OLs with the human monoclonal NMDAR antibody SSM5, but not isotype control 12D7, abolishes the NMDA response (naïve vs SSM5, $p < 0.001$; 12D7 isotype vs SSM5, $p < 0.001$; one-way ANOVA with Tukey post-test). In all graphs, data of each sample represent the average \pm standard error of the mean of values obtained from 3 different cultures. n.s. = not significant.

Results

NMDARs are highly permeable to Ca^{2+} upon activation by their endogenous ligands. Because of that, we set an assay to evaluate whether patients' antibodies were able to alter NMDAR function using Fluo-4, a calcium indicator that exhibits an increased fluorescence upon binding Ca^{2+} , and time-lapse fluorescence microscopy. Cultured oligodendrocytes exposed to NMDA applied together with glycine induced a robust and fast increase in cytosolic Ca^{2+} with a peak amplitude of $159 \pm 4\%$ compared with resting levels (100%) that progressively decreased to baseline by around 5 to 10 minutes of stimulation (see Fig 1B). To assess the specificity of the responses triggered by NMDA and glycine, we used CGP39551 (1 μM) and AP5 (100 μM), 2 potent, selective and competitive NMDAR antagonists, as well as MK801 (50 μM), a noncompetitive antagonist that binds to a site located within the NMDAR-associated ion channel and thus prevents Ca^{2+} flux. In all instances, the responses to NMDA and glycine were abolished in the presence of these antagonists (see Fig 1B).

The profile and amplitude of agonist responses were not significantly altered by preincubation of oligodendrocytes for 4 hours with CSF obtained from controls (peak response = $140 \pm 7\%$ vs $154 \pm 13\%$ for naive oligodendrocytes; Fig 2A). Instead, after preincubation with CSF from patients with anti-NMDAR encephalitis, the cytosolic Ca^{2+} responses to NMDA plus glycine exhibited a sharp reduction (maximal amplitude = $111 \pm 5\%$), indicative of a strong reduction in the number of receptors being available to the agonists in the oligodendrocyte plasma membrane (see Fig 2A).

To further analyze the changes in the responses during the whole period of recording, we calculated the area under the curve to compare the levels of Ca^{2+} accumulated over the time window examined. This analysis revealed that CSF from healthy donors on average did not significantly alter Ca^{2+} cytosolic load over time after incubation with the agonists ($336 \pm 87\%$ vs $355 \pm 91\%$ in naive cells). In contrast, CSF from patients with anti-NMDAR encephalitis nearly abolished the response ($106 \pm 30\%$ vs agonists alone or control CSF, $p < 0.05$, in both instances; see Fig 2B). An individual analysis of the effects of CSF from patients showed different levels of NMDAR remaining functionality ranging from 15 to 47% (see Fig 2C), whereas CSF from controls had little or no effect ($>76\%$ or higher functionality preserved). The intensity of effects of patients' CSF antibodies correlated with CSF antibody titers in 6 of 7 patients (data not shown).

As AMPA receptors (AMPA) are highly expressed in oligodendrocytes,¹⁵ we tested whether activation of these receptors with AMPA applied together with

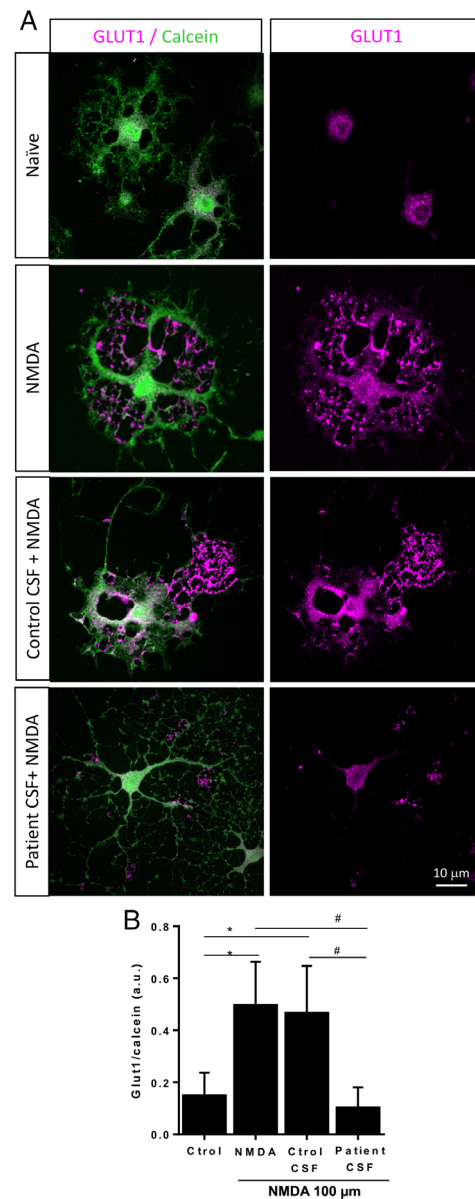


FIGURE 3: Effects of patients' cerebrospinal fluid (CSF) on the GLUT1 expression (magenta) in oligodendrocytes (green) after N-methyl-D-aspartate receptor (NMDA) receptor (NMDAR) activation. (A) First row (naive) shows minimal expression of GLUT1 (magenta) by oligodendrocytes (green) without NMDAR activation. Second row shows that the application of NMDA induces extensive expression of GLUT1. This NMDA-induced expression of GLUT1 is not affected if oligodendrocytes are preincubated with controls' CSF (third row) but is dramatically reduced if oligodendrocytes are preincubated with patients' CSF (fourth row). **(B)** Quantitation of results described in (A); * $p < 0.05$; # $p < 0.05$ using one-way analysis of variance with Tukey post-test. Oligodendrocytes are counterstained with calcein (green). Data represent the average \pm standard error of the mean of values obtained from oligodendrocytes in 2 coverslips from 3 different cultures.

cyclothiazide (both at 100 μM) was affected by patients' CSF. Contrary to the robust effect of patients' CSF on the

NMDAR-mediated responses, no effects were observed on the profile of AMPAR-mediated responses (see Fig 2D), strongly suggesting the specific blockade of NMDARs by patients' CSF.

The specificity of the changes in NMDAR-mediated responses caused by patients' CSF antibodies was further assessed with 2 different approaches. First, we used pooled patients' CSF samples preabsorbed with HEK293 cells expressing GluN1 or with cells not expressing this subunit (mock transfected cells). These experiments showed that the effect of patients' CSF antibodies were abrogated when CSF samples were preabsorbed with HEK293 cells expressing GluN1 but not with samples preabsorbed with HEK293 mock transfected cells (see Fig 2E). Second, we assessed the changes in oligodendrocyte NMDAR-mediated responses using a previously reported monoclonal human GluN1 antibody (SSM5) and the corresponding isotype control (12D7).¹¹ We found that pretreatment of oligodendrocytes with SSM5, but not 12D7, efficiently blocked the NMDAR-mediated responses (see Fig 2F). Taken together, these 2 sets of experiments provide robust evidence that the reduction of NMDAR-mediated responses in oligodendrocytes is mediated by patients' GluN1 antibodies.

NMDAR activity in oligodendrocytes mediates the translocation of GLUT1 to the membrane and myelin compartment, a feature that has structural consequences for the white matter.⁷ Therefore, having shown that patients' CSF antibodies impaired NMDAR activation, we next determined whether they affected the NMDAR-dependent peripheral expression of GLUT1. These studies showed that the levels of GLUT1 were substantially reduced in secondary and tertiary processes of oligodendrocytes pretreated with patients' CSF antibodies but not controls' CSF (Fig 3). Overall, these findings provide a potential link between anti-NMDAR encephalitis and white matter alterations described in patients with this disorder.

Discussion

In this study, we show that treatment of oligodendrocytes with CSF from patients with anti-NMDAR encephalitis or a recombinant monoclonal antibody derived from plasma cells of a patient, but not the corresponding controls, decreased receptor activation by NMDA. These pathogenic effects were abrogated when patients' CSF was preabsorbed in NMDAR-expressing HEK293 cells, confirming the pathogenic role of the antibodies. Moreover, patients' CSF antibodies did not alter AMPAR function, suggesting a specific impairment in NMDAR activation. These antibody-mediated effects were associated with a reduced expression of GLUT1 in the distal processes of

oligodendrocytes. Because expression of GLUT1 is important for axonal function, the findings suggest a novel pathogenic mechanism beyond the reported antibody effects on neuronal synaptic receptors and plasticity.

In oligodendrocytes, NMDARs control the supply of energy substrates to support the proper function of axons via GLUT1 translocation to the oligodendrocyte membrane.⁷ Studies have shown that the amplitude of the action potentials in axons during high-frequency stimulation decreases in the absence of NMDAR in oligodendrocytes and recovers more slowly when returning at low frequency stimuli.⁷ Prolonged loss of NMDAR function in oligodendroglia leads to axonal pathology and neuroinflammation in white matter tracts, resulting in neurological symptoms and motor dysfunction.⁷ Although astrocytes can also support axonal function by releasing lactate in the white matter,¹⁶ the direct oligodendrocyte-axon interaction is needed to adjust energy demands and prevent long-term structural damage.⁷

In a series of 577 patients with anti-NMDAR encephalitis, 67% had normal clinical MRI studies, and for the most part the other patients had mild or transient cortical-subcortical FLAIR abnormalities.³ The high frequency of normal findings using standard MRI sequences was also indicated in a systematic review of the literature that included 1,167 patients, showing that 62% had normal MRI. Moreover, among the 38% of patients with abnormal findings, the subcortical white matter was as frequently involved as the gray matter.¹⁷ In contrast, when a cohort of 24 patients was examined using MRI DTI sequences, all patients had widespread changes in white matter integrity that correlated with disease severity. Interestingly, 17 (71%) of these patients had normal standard clinical MRIs.¹⁸ In another study of 46 patients with anti-NMDAR encephalitis (36 recovered and 10 unrecovered from the disease), the unrecovered patients showed widespread superficial white matter damage compared with the recovered patients and healthy controls who had normal findings.⁴ Thus, anti-NMDAR encephalitis is associated with characteristic alterations of functional connectivity and widespread changes of white matter integrity, despite normal findings in routine clinical MRI.¹⁸

Based on the current findings and previously reported clinical and pathological studies in which cellular inflammatory infiltrates are usually mild without clear involvement of the white matter,¹⁹ we postulate that the indicated MRI white matter changes may be directly mediated by NMDAR antibodies. The white matter effects, along with the previously reported impairment of synaptic function and plasticity,^{9,20} would help explain the dissociation between symptom severity and frequently normal MRI clinical sequences (despite almost constant

DTI changes). A future task is to determine whether patients' antibodies alter white matter integrity in an existing animal model of passive transfer of antibodies,²¹ examining changes in expression of GLUT1, how these changes correlate with white matter abnormalities (using rodent MRI studies), and the degree of reversibility of these alterations. These studies are important because there are currently no biomarkers of the course of the disease²²; therefore, a better understanding of the white matter changes during the disease may lead to a potentially useful biomarker.

Acknowledgment

This study was supported by Biomedical Research Networking Center on Neurodegenerative Diseases (CB06/05/0076; C.M.) and by grants from the Ministry of Economy and Competitiveness (SAF2016-75292-R; C.M.), Basque Government (IT702-13 and PIBA2016; C.M. and M.D., respectively), Forschungskommission of Heinrich Heine University Düsseldorf, Germany (N.G.), Instituto de Salud Carlos III/FEDER (FIS 17/00234 and PIE 16/00014; J.D.), CIBERER CB15/00010 (J.D.), La Caixa Foundation Health Research Award (J.D.), AGAUR Generalitat de Catalunya (J.D.), Safra Foundation, and Fundació CELLEX (J.D.). A.P. and M.P.S.-R. hold fellowships from the University of the Basque Country and the Ministry of Economy and Competitiveness, respectively.

We thank S. Marcos for her expert assistance with tissue culture, Dr L. Escobar for her support with Leica TCS STED SP8 laser scanning confocal microscope, Dr J. Ballesteros, F. Soria, and T. Armangué for advice in statistics analysis, and the Animal Facility (SGIker) of the University of the Basque Country (UPV/EHU).

Author Contributions

C.M. and J.D. contributed to the conception and design of the study. All authors contributed to the acquisition and analysis of data. C.M. and J.D. contributed to drafting the text and preparing the figures.

Potential Conflicts of Interest

J.D.: royalties, Athena Diagnostics, Euroimmun; research project, SAGE Therapeutics.

References

- Dalmau J, Geis C, Graus F. Autoantibodies to synaptic receptors and neuronal cell surface proteins in autoimmune diseases of the central nervous system. *Physiol Rev* 2017;97:839–887.
- Dalmau J, Gleichman AJ, Hughes EG, et al. Anti-NMDA-receptor encephalitis: case series and analysis of the effects of antibodies. *Lancet Neurol* 2008;7:1091–1098.
- Titulaer MJ, McCracken L, Gabilondo I, et al. Late-onset anti-NMDA receptor encephalitis. *Neurology* 2013;81:1058–1063.
- Phillips OR, Joshi SH, Narr KL, et al. Superficial white matter damage in anti-NMDA receptor encephalitis. *J Neurol Neurosurg Psychiatry* 2018;89:518–525.
- Peer M, Prüss H, Ben-Dayana I, et al. Functional connectivity of large-scale brain networks in patients with anti-NMDA receptor encephalitis: an observational study. *Lancet Psychiatry* 2017;4:768–774.
- Nave KA, Werner HB. Myelination of the nervous system: mechanisms and functions. *Annu Rev Cell Dev Biol* 2014;30:503–533.
- Saab AS, Tzvetavona ID, Trevisiol A, et al. Oligodendroglial NMDA receptors regulate glucose import and axonal energy metabolism. *Neuron* 2016;91:119–132.
- Graus F, Titulaer MJ, Balu R, et al. A clinical approach to diagnosis of autoimmune encephalitis. *Lancet Neurol* 2016;15:391–404.
- Planagumà J, Haselmann H, Mannara F, et al. Ephrin-B2 prevents N-methyl-D-aspartate receptor antibody effects on memory and neuroplasticity. *Ann Neurol* 2016;80:388–400.
- Höftberger R, Sepulveda M, Armangué T, et al. Antibodies to MOG and AQP4 in adults with neuromyelitis optica and suspected limited forms of the disease. *Mult Scler* 2015;21:866–874.
- Malviya M, Barman S, Golombek KS, et al. NMDAR encephalitis: passive transfer from man to mouse by a recombinant antibody. *Ann Clin Transl Neurol* 2017;4:768–783.
- Sánchez-Gómez MV, Serrano MP, Alberdi E, et al. Isolation, expansion, and maturation of oligodendrocyte lineage cells obtained from rat neonatal brain and optic nerve. *Methods Mol Biol* 2018;1791:95–113.
- Ruiz A, Alberdi E, Matute C. Cg37157, an inhibitor of the mitochondrial $\text{Na}^+/\text{Ca}^{2+}$ exchanger, protects neurons from excitotoxicity by blocking voltage-gated Ca^{2+} channels. *Cell Death Dis* 2014;5:e1156.
- Arellano RO, Sánchez-Gómez MV, Alberdi E, et al. Axon-to-glia interaction regulates GABAA receptor expression in oligodendrocytes. *Mol Pharmacol* 2016;89:63–74.
- Butt AM, Fern RF, Matute C. Neurotransmitter signaling in white matter. *Glia* 2014;62:1762–1779.
- Brown AM, Ransom BR. Astrocyte glycogen and brain energy metabolism. *Glia* 2007;55:1263–1271.
- Bacchi S, Franke K, Wewegama D, et al. Magnetic resonance imaging and positron emission tomography in anti-NMDA receptor encephalitis: a systematic review. *J Clin Neurosci* 2018;52:54–59.
- Finke C, Kopp UA, Scheel M, et al. Functional and structural brain changes in anti-N-methyl-D-aspartate receptor encephalitis. *Ann Neurol* 2013;74:284–296.
- Dalmau J, Tüzün E, Wu HY, et al. Paraneoplastic anti-N-methyl-D-aspartate receptor encephalitis associated with ovarian teratoma. *Ann Neurol* 2007;61:25–36.
- Moscato EH, Peng X, Jain A, et al. Acute mechanisms underlying antibody effects in anti-N-methyl-D-aspartate receptor encephalitis. *Ann Neurol* 2014;76:108–119.
- Planagumà J, Leypoldt F, Mannara F, et al. Human N-methyl D-aspartate receptor antibodies alter memory and behaviour in mice. *Brain* 2015;138:94–109.
- Dalmau J, Armangué T, Planagumà J, et al. An update on anti-NMDA receptor encephalitis for neurologists and psychiatrists: mechanisms and models. *Lancet Neurol* 2019;18:1045–1057.

Paper III

Allosteric modulation of NMDA receptors prevents the antibody effects of patients with anti-NMDAR encephalitis.

Francesco Mannara, Marija Radosevic, Jesús Planagumà, David Soto, Esther Aguilar, Anna García-Serra, **Estibaliz Maudes**, Marta Pedreño, Steven Paul, James Doherty, Michael Quirk, Jing Dai, Xavier Gasull, Mike Lewis, Josep Dalmau.

Brain. 2020, 143(9), 2709-2720.

IF JCR 2020: 13.501 (D1).

Allosteric modulation of NMDA receptors prevents the antibody effects of patients with anti-NMDAR encephalitis

Francesco Mannara,^{1,*} Marija Radosevic,^{1,*} Jesús Planagumà,^{1,*} David Soto,^{1,2} Esther Aguilar,¹ Anna García-Serra,¹ Estibaliz Maudes,¹ Marta Pedreño,¹ Steven Paul,^{3,4} James Doherty,³ Michael Quirk,³ Jing Dai,³ Xavier Gasull,^{1,2} Mike Lewis^{3,#} and Josep Dalmau^{1,5,6,#}

*,#These authors contributed equally to this work.

Anti-N-methyl-D-aspartate receptor (NMDAR) encephalitis is an immune-mediated disease characterized by a complex neuropsychiatric syndrome in association with an antibody-mediated decrease of NMDAR. About 85% of patients respond to immunotherapy (and removal of an associated tumour if it applies), but it often takes several months or more than 1 year for patients to recover. There are no complementary treatments, beyond immunotherapy, to accelerate this recovery. Previous studies showed that SGE-301, a synthetic analogue of 24(S)-hydroxycholesterol, which is a potent and selective positive allosteric modulator of NMDAR, reverted the memory deficit caused by phencyclidine (a non-competitive antagonist of NMDAR), and prevented the NMDAR dysfunction caused by patients' NMDAR antibodies in cultured neurons. An advantage of SGE-301 is that it is optimized for systemic delivery such that plasma and brain exposures are sufficient to modulate NMDAR activity. Here, we used SGE-301 to confirm that in cultured neurons it prevented the antibody-mediated reduction of receptors, and then we applied it to a previously reported mouse model of passive cerebroventricular transfer of patient's CSF antibodies. Four groups were established: mice receiving continuous (14-day) infusion of patients' or controls' CSF, treated with daily subcutaneous administration of SGE-301 or vehicle (no drug). The effects on memory were examined with the novel object location test at different time points, and the effects on synaptic levels of NMDAR (assessed with confocal microscopy) and plasticity (long-term potentiation) were examined in the hippocampus on Day 18, which in this model corresponds to the last day of maximal clinical and synaptic alterations. As expected, mice infused with patient's CSF antibodies, but not those infused with controls' CSF, and treated with vehicle developed severe memory deficit without locomotor alteration, accompanied by a decrease of NMDAR clusters and impairment of long-term potentiation. All antibody-mediated pathogenic effects (memory, synaptic NMDAR, long-term potentiation) were prevented in the animals treated with SGE-301, despite this compound not antagonizing antibody binding. Additional investigations on the potential mechanisms related to these SGE-301 effects showed that (i) in cultured neurons SGE-301 prolonged the decay time of NMDAR-dependent spontaneous excitatory postsynaptic currents suggesting a prolonged open time of the channel; and (ii) it significantly decreased, without fully preventing, the internalization of antibody-bound receptors suggesting that additional, yet unclear mechanisms, contribute in keeping unchanged the surface NMDAR density. Overall, these findings suggest that SGE-301, or similar NMDAR modulators, could potentially serve as complementary treatment for anti-NMDAR encephalitis and deserve future investigations.

- 1 Institut d'Investigacions Biomèdiques August Pi i Sunyer (IDIBAPS), Hospital Clínic, Universitat de Barcelona, Barcelona, Spain
- 2 Laboratori de Neurofisiologia, Departament de Biomedicina, Facultat de Medicina i Ciències de la Salut, Institut de Neurociències, Universitat de Barcelona, Barcelona, Spain
- 3 Sage Therapeutics, Cambridge, MA, USA

Received December 5, 2019. Revised April 3, 2020. Accepted April 22, 2020. Advance access publication August 24, 2020

© The Author(s) (2020). Published by Oxford University Press on behalf of the Guarantors of Brain. All rights reserved.

For permissions, please email: journals.permissions@oup.com

- 4 Departments of Psychiatry and Neurology, Washington University School of Medicine, St Louis, USA
 5 Department of Neurology, University of Pennsylvania, Philadelphia, USA
 6 Institució Catalana de Recerca i Estudis Avançats (ICREA), Barcelona, Spain

Correspondence to: Josep Dalmau, MD, PhD

IDIBAPS-Hospital Clínic, Universitat de Barcelona, Department of Neurology, c/Villarroel

170, 08036 Barcelona, Spain

E-mail: jdalmau@clinic.cat

Keywords: animal model; anti-NMDAR encephalitis; SGE-301; treatment

Abbreviations: EPSC = excitatory postsynaptic current; fEPSP = field excitatory postsynaptic potential; LTP = long-term potentiation; NMDAR = NMDA receptor; PAM = positive allosteric modulator; SGE-301 = $\Delta^{5,6}$ -3 β -oxy-nor-cholenyl-dimethylcarbinol; TBS = theta-burst stimulation

Introduction

Anti-NMDA receptor (NMDAR) encephalitis is an immune-mediated disease characterized by a complex neuropsychiatric syndrome and the presence of CSF antibodies against the GluN1 subunit of NMDARs (Dalmau *et al.*, 2008). The disorder can be triggered by systemic tumours, usually a teratoma of the ovary, and less frequently by herpes simplex encephalitis (Armangue *et al.*, 2018), but in many cases no trigger is identified. At disease onset patients develop psychosis, insomnia, abnormal movements, seizures, decreased level of consciousness, dysautonomia, or coma, which in about 85% of cases respond to immunotherapy and removal of the tumour when it applies (Titulaer *et al.*, 2013; Viacoz *et al.*, 2014). However, it often takes several months or more than 1 year for patients to return to most of their activities. During the process of recovery the clinical features are different from those of the acute stage, including impairment of attention, memory, executive functions, or behaviour (Dalmau *et al.*, 2011; Finke *et al.*, 2012; Peer *et al.*, 2017). The reasons for this slow clinical recovery are unclear but may include a persisting immune activation against NMDAR within the CNS, a severe impairment of synaptic function and long-term plasticity, a limited blood–brain barrier penetration of current immunotherapies, or a combination of these factors. Studies examining the effects of patients NMDAR antibodies in cultured neurons (Hughes *et al.*, 2010; Mikasova *et al.*, 2012) or mice (Planaguma *et al.*, 2015, 2016) have shown that they mediate a broad loss of surface NMDARs, regardless of synaptic localization or subunit composition (Warikoo *et al.*, 2018), leading to impairment of synaptic plasticity and memory (Planaguma *et al.*, 2015, 2016).

In some respects, the treatment paradigm of anti-NMDAR encephalitis resembles that of antibody-mediated diseases of the neuromuscular junction, such as myasthenia gravis or the Lambert-Eaton myasthenic syndrome (LEMS), where despite evidence that several immunotherapies are effective, most patients need additional treatment for a faster or sustained improvement. These treatments are addressed to compensate or overcome the mechanisms altered by the autoantibodies, for example, acetylcholinesterase inhibitors

(pyridostigmine) in myasthenia gravis, or the presynaptic potassium channel blocker (3,4-diaminopyridine) in LEMS (Newsom-Davis, 2003; Wirtz *et al.*, 2010). In studies using cultured neurons (Mikasova *et al.*, 2012; Planaguma *et al.*, 2016) or passive transfer of patient's CSF NMDAR antibodies to mice (Planaguma *et al.*, 2016), a soluble form of ephrin-B2 (an agonist of the ephrin-B2 receptor that clusters and retains NMDARs at the synapse) was able to antagonize all antibody-mediated effects including NMDAR internalization and impairments of long-term plasticity and visuospatial memory. As a proof-of-principle, this finding showed that interfering with the antibody-mediated mechanisms could potentially be used as a complementary treatment with immunotherapy (Mikasova *et al.*, 2012); however, ephrin-B2 was administered intraventricularly and there are no available ephrin-B2 agonists that cross the blood–brain barrier.

There is evidence that a major brain-derived cholesterol metabolite, 24(S)-hydroxycholesterol [24(S)-HC], is a very potent, direct, and selective positive allosteric modulator (PAM) of NMDARs (Paul *et al.*, 2013). In hippocampal slices, application of 24(S)-HC enhanced the ability of subthreshold stimuli to induce long-term potentiation (LTP), and reversed the LTP deficits caused by the NMDAR channel blocker, ketamine. Several synthetic analogues of 24(S)-HC such as $\Delta^{5,6}$ -3 β -oxy-nor-cholenyl-dimethylcarbinol (SGE-201) or SGE-301 shared similar mechanisms of action (Paul *et al.*, 2013). In rats, the administration of SGE-301 reverted the memory deficit caused by phencyclidine, a non-competitive NMDAR antagonist (Paul *et al.*, 2013). Moreover, application of SGE-301 to cultures of neurons exposed to CSF antibodies from patients with anti-NMDAR encephalitis prevented the antibody-mediated dysfunction of NMDARs (Warikoo *et al.*, 2018). An advantage of this compound is that it is optimized for systemic delivery such that plasma and brain exposures are sufficient to modulate activity in preclinical models of NMDAR hypofunction (Paul *et al.*, 2013). These findings led us to investigate whether SGE-301 was able to prevent the antibody-mediated reduction of NMDAR and memory impairment observed in a previously reported model of cerebroventricular transfer of patient's CSF antibodies.

Materials and methods

Animals, surgery, and patients' CSF

Seventy-six male C57BL/6J mice (Charles River), 8–10 weeks old (25–30 g) were used for the studies including, memory and locomotor activity ($n = 47$ mice), confocal immunohistochemistry assessment of levels of NMDAR and other synaptic proteins, and electrophysiological studies ($n = 29$ mice). Animal care, anaesthesia, insertion of bilateral ventricular catheters (PlasticsOne, model 3280PD-2.0; coordinates: 0.2 mm posterior and ± 1.00 mm lateral from bregma, depth 2.2 mm), and connection of each catheter to a subcutaneous osmotic pump for continuous infusion of CSF (Alzet; volume 100 μ l, flow rate 0.25 μ l/h for 14 days) have been reported (Planaguma *et al.*, 2015). The CSF infused was pooled from samples of 10 patients with high titre IgG GluN1 antibodies (all $> 1:320$), and 10 patients with normal pressure hydrocephalus without NMDAR antibodies (control samples).

The presence of NMDAR antibodies in patient's CSF (and absence in controls' CSF) was examined with three different techniques: brain tissue immunohistochemistry, HEK293T cells expressing NMDAR, and cultured neurons, as reported (Ances *et al.*, 2005; Dalmau *et al.*, 2008). Patients' and controls' CSF were then pooled in two different samples and filtered (Amicon Ultracel 30K, Sigma-Aldrich), dialysed against phosphate-buffered saline (PBS), and normalized to a physiological concentration of 2 mg IgG/dl (Planaguma *et al.*, 2016). The absence of other antibodies in pooled patient's CSF was confirmed using an aliquot immunoabsorbed with HEK293T expressing GluN1, showing: (i) abrogation of reactivity with mouse brain and HEK293T cells expressing NMDARs; and (ii) abrogation of NMDAR internalization (Supplementary Fig. 1).

Written informed consent was obtained from all patients. The study was approved by the local institutional review board (Hospital Clinic, HCB/2018/0192), and animal studies were approved by the Local Ethical Committee of the University of Barcelona following European (2010/63/UE) and Spanish (RD 53/2013) regulations about the use and care of experimental animals.

Preparation and treatment with SGE-301

SGE-301 is a potent allosteric modulator of NMDAR that has been characterized previously (Paul *et al.*, 2013). For the current studies, we adopted a subcutaneous administration paradigm (versus intraperitoneal) to minimize interaction with the centrally fixed osmotic minipumps. Therefore, we ran plasma and brain pharmacokinetic studies to measure exposures of SGE-301 present at the time of *in vivo* testing. The method of determination of plasma and brain concentration of SGE-301 is described in the Supplementary material. At 1 h, we achieved 1954 ± 157 ng/ml plasma and 523 ± 86 ng/g brain exposures. At 4 h, we achieved 985 ± 173 ng/ml plasma and 1350 ± 120 ng/g brain exposures (Supplementary Fig. 2). These exposures are similar to those reported after intraperitoneal administration (Paul *et al.*, 2013).

For studies with cultured neurons, lyophilized SGE-301 was weighed and dissolved in dimethyl sulphoxide (DMSO) to a stock concentration of 10 mM; the solution was then sonicated for 1 h at 40°C and used at a working concentration of 10 μ M. For studies using mice, lyophilized SGE-301 was weighed and

dissolved in a solution of 30% 2-hydroxypropyl- β -cyclodextrin (HPBCD, Sigma-Aldrich) in distilled water. The solution was then vortexed for 5 min, sonicated for 40 min, and stirred for 2 h at 50°C. After adjusting the pH to 5.5–7.0, working aliquots were prepared and kept frozen at -20°C . A similar solution of 30% HPBCD in distilled water, but without drug, served as control (vehicle). Aliquots with or without drug were thawed and vortexed for 2 min before use.

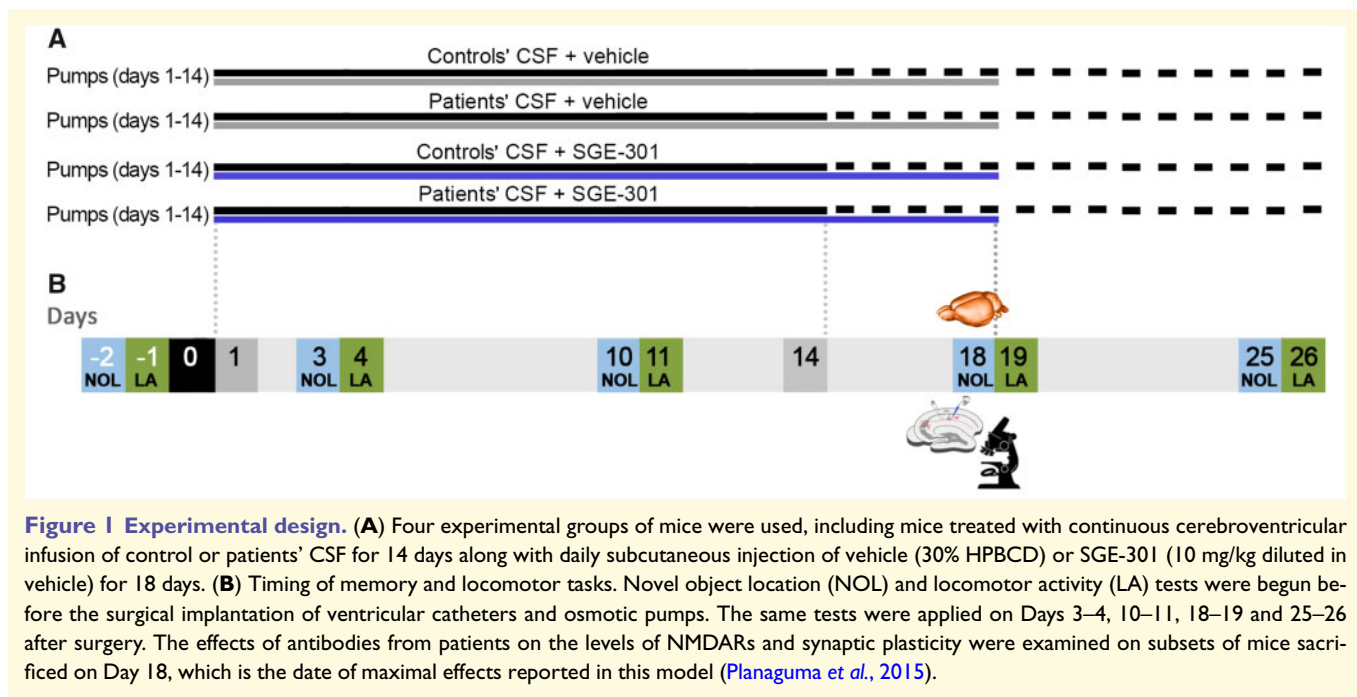
Experimental design

Four experimental groups were established including mice infused with patients' or controls' CSF along with subcutaneous administration of SGE-301 (10 mg/kg) or vehicle (Fig. 1A). The administration of SGE-301 began on Day 1 (coinciding with Day 1 of infusion of CSF) until Day 18 (4 days after the infusion of CSF had stopped), which was the last day with maximal memory deficits and reduction of NMDAR synaptic clusters observed in this model (Planaguma *et al.*, 2015). The selected animal tasks (novel object location; locomotor activity) and the timing of the tasks (Fig. 1B) were based on previous experience with this model, showing that patient's CSF NMDAR antibodies caused a progressive decrease of visuospatial memory until Day 18, subsequently followed by progressive recovery several days after the antibody infusion stopped (Planaguma *et al.*, 2015). In contrast, patient antibodies did not significantly alter the locomotor activity (included here as control, and to ensure that animals did not have motor limitations in exploring the objects). All tasks were performed by researchers blinded to experimental conditions.

Immunohistochemistry and confocal microscopy

Techniques related to immunolabelling of live cultures of dissociated rodent hippocampal neurons, immunoabsorption of patient samples with GluN1-expressing HEK cells, brain tissue processing, and quantitative brain tissue immunoperoxidase staining, have previously been reported (Planaguma *et al.*, 2015). To determine the effects of patient antibodies in cultured rat hippocampal neurons, 17-day *in vitro* cultures were exposed to patient or controls' CSF (diluted 1:100) along with 10 μ M SGE-301 or vehicle for 24 or 48 h, and the cell surface clusters of NMDAR, PSD95, phospho-S295-PSD95, and the co-localization of NMDAR/PSD95 (representing synaptic NMDAR) were quantified with specific biomarkers and confocal microscopy (Supplementary material). Determination of antibody-bound internalized NMDAR was carried out as previously reported (Moscatto *et al.*, 2014) (Supplementary material).

To determine the effects of patient antibodies on the number of clusters of NMDAR and PSD95, non-permeabilized 5- μ m thick brain sections (obtained on Day 18, Fig. 1B) were blocked with 5% goat serum, and serially incubated with a human CSF NMDAR-antibody sample (1:20, used as primary antibody) for 2 h at room temperature and the secondary Alexa Fluor[®] 488 goat anti-human IgG (1:1000, A-11013, ThermoFisher) for 1 h at room temperature. Tissue sections were then permeabilized with 0.3% Triton[™] X-100 for 10 min at room temperature, and serially incubated with rabbit polyclonal anti-PSD95 (1:250, ab18258 Abcam) overnight at 4°C, and the corresponding secondary Alexa Fluor[®] 594 goat anti-rabbit IgG (1:1000, A-11012, ThermoFisher) for 1 h at room temperature. Slides



were then mounted with ProLongTM Gold antifade reagent for 4 min, containing 6-diamidino-2-phenylindole dihydrochloride (DAPI, P36935; ThermoFisher) and results scanned with Zeiss LSM710 confocal microscope (Carl Zeiss) with EC-Plan NEOFLUAR CS 100×/1.3 NA oil objective. For each animal, five identical image stacks in three hippocampal areas (CA1, CA3 and dentate gyrus; total 15 image stacks) were acquired as reported (Planaguma et al., 2015). Each z-stack comprised 50 optical images that were deconvolved with AutoQuantX3 (Bitplane, Oxford Instruments). The mean density of clusters of NMDAR or PSD95 was obtained using a spot detection algorithm from Imaris suite 7.6.4 (Bitplane), and the cluster density expressed as spots/mm³. The clusters of NMDAR that co-localized with PSD95 were defined as synaptic. For each experimental group, the mean cluster densities of NMDAR or PSD95 were normalized with the corresponding values in control animals (infused with controls' CSF and treated with vehicle).

To determine the levels of synaptic phospho-S295-PSD95 in brain tissue, 5-μm thick brain sections permeabilized as above and blocked with 5% goat serum and 1% bovine serum albumin (BSA) were incubated with rabbit anti-phospho-S295-PSD95 (1:200, ab76108, Abcam) and mouse anti-PSD95 (diluted 1:200, 124 011, Synaptic Systems) for 1 h. Slides were then washed and incubated with Alexa Fluor[®] 488 goat anti-rabbit IgG and Alexa Fluor[®] 594 goat anti-mouse IgG (both diluted 1:500, A-11034, A-11032, ThermoFisher). Results were scanned as above, and the cluster density of phospho-S295-PSD95 and PSD95 was determined with Imaris (Bitplane) software.

Electrophysiological studies

Preparation of acute hippocampal slices on Day 18 (Fig. 1B) and field potential recordings and analysis were performed as reported (Planaguma et al., 2016) (Supplementary material).

To determine the effects of chronic exposure to SGE-301 on NMDAR currents we treated 18 days *in vitro* (div) cultures of

hippocampal neurons with controls' CSF (diluted 1:100) or controls' CSF + SGE-301 (10 μM) for 48 h prior to whole-cell patch clamp recordings of spontaneous NMDAR-mediated excitatory postsynaptic currents (sEPSCs) (Supplementary material).

Memory and locomotor activity tasks

Visuospatial memory was assessed with the novel object location discrimination index, and the locomotor activity was automatically determined using locomotor activity boxes (11 × 21 × 18 cm, Imetronic) for 1 h (Planaguma et al., 2015) (Supplementary material).

Statistical analysis

Data from behavioural studies (novel object location and locomotor activity) were analysed using repeated-measures two-way ANOVA. Human IgG intensities from different brain regions and confocal cluster densities of NMDAR and PSD95 on cultured neurons and brain tissue were analysed using one-way ANOVA. Density levels of phospho-S295-PSD95 in cultured neurons and brain tissue were assessed with unpaired *t*-test. The electrophysiological data were assessed by one-way ANOVA (LTP and paired-pulse facilitation: PP2/PP1 ratios) and unpaired *t*-test (paired-pulse facilitation: analysis of increase of PP2 slope compared with PP1 in each of the experimental groups independent of each other). A *P*-value < 0.05 was considered significant. All ANOVA tests included *post hoc* analyses with Bonferroni correction for multiple testing. Analysis of NMDAR-mediated spontaneous EPSCs in cultures of neurons chronically exposed to SGE-301 was performed with Student's *t*-tests. Statistical analyses were performed with GraphPad Prism v.6 (La Jolla, CA, USA).

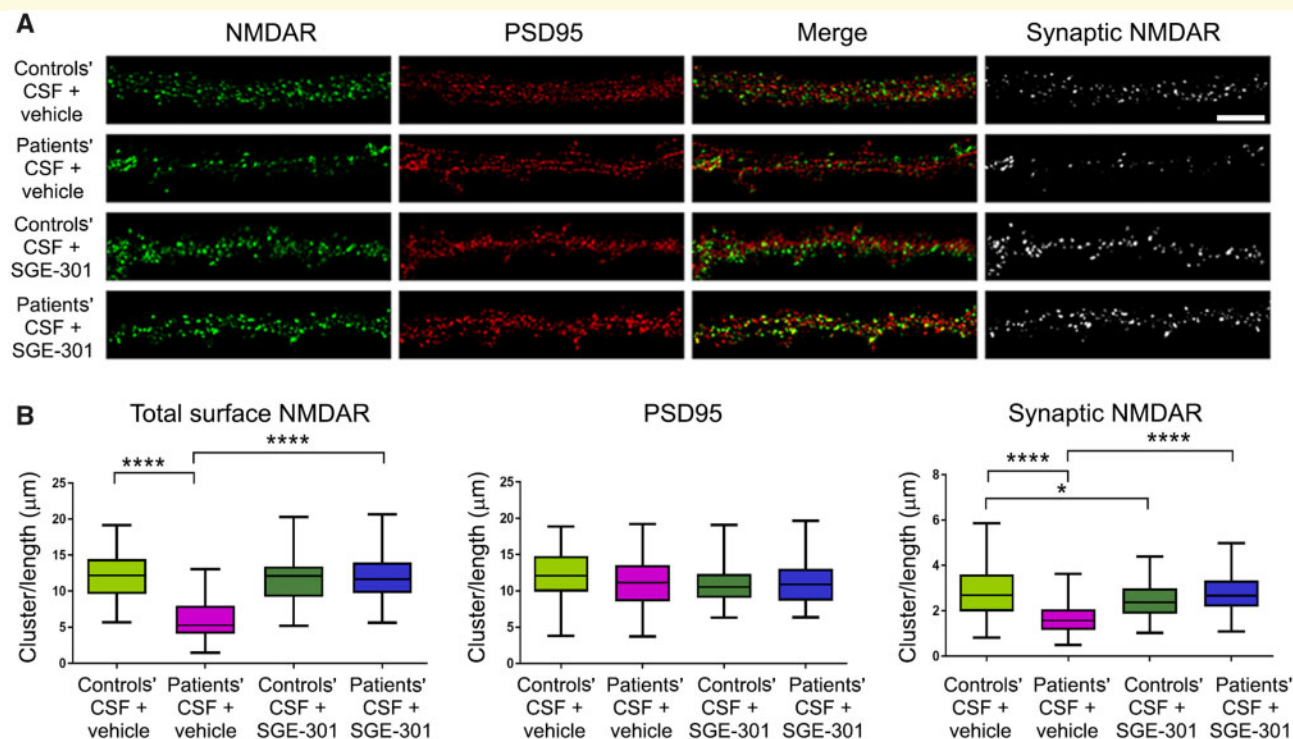


Figure 2 Treatment with SGE-301 prevents the reduction of NMDARs caused by patients' antibodies in cultured neurons.

(A) Representative dendrites of hippocampal neurons immunostained for surface NMDAR (green) and PSD95 (red) after 24 h treatment with patients' CSF or controls' CSF, each with either vehicle or SGE-301. Synaptic NMDARs are defined as those that co-localize with PSD95 (white channel). Scale bars = 10 μm . (B) Quantification of the density of surface and synaptic NMDAR. Cultures co-treated with patients' CSF antibodies and vehicle showed a significant decrease of total cell surface and synaptic NMDARs without affecting the density of PSD95. In contrast, cultures co-treated with the same patients' CSF and SGE-301 did not show reduction of NMDARs. No effects on total cell surface NMDARs were noted in neurons treated with CSF from controls with vehicle or SGE-301, although the presence of SGE-301 was associated with a mild reduction of synaptic NMDARs. The density of PSD95 was not affected by any of these conditions. $n = 15$ dendrites per condition, three independent experiments. Box plots show the median, and 25th and 75th percentiles; whiskers indicate the minimum and maximum values. Significance of treatment effect was assessed by one-way ANOVA ($P < 0.0001$ for NMDAR, synaptic NMDAR) with Bonferroni *post hoc* correction: * $P < 0.05$; *** $P < 0.0001$. Additional information is available in [Supplementary Table 1](#).

Data availability

The authors confirm that the data supporting the findings of this study are available within the article and its [Supplementary material](#).

Results

Treatment with SGE-301 prevents the pathogenic effects of antibodies in cultured neurons

We and others have previously reported that NMDAR antibodies of patients cause a reduction of the clusters of synaptic and extrasynaptic NMDARs in cultured neurons (Hughes *et al.*, 2010; Mikasova *et al.*, 2012), and in an animal model of cerebroventricular infusion of patients' CSF (Planaguma *et al.*, 2015). Here, we first used cultured neurons to determine whether the antibody effects were

prevented by SGE-301. As expected, neurons treated with patients' CSF and vehicle showed a significant decrease of total cell surface and synaptic NMDAR clusters compared with neurons treated with controls' CSF and vehicle. However, neurons treated with the same patients' CSF antibodies along with SGE-301, instead of vehicle, showed no significant change of the levels of total cell surface or synaptic NMDARs (Fig. 2). To determine whether this was due to abrogation of receptor internalization, we quantified the clusters of antibody-bound internalized NMDAR (Moscato *et al.*, 2014) showing that treatment with SGE-301 significantly reduced the levels of internalized antibody-bound receptors, but did not completely abolish the internalization (Supplementary Fig. 3). Overall, these findings show that SGE-301 prevents the antibody-mediated decrease of cell-surface NMDAR, and suggest that this treatment effect is due to a reduction of internalized antibody-bound receptors along with additional, yet unclear mechanisms, which overall keep the clusters of surface receptors similar to control levels.

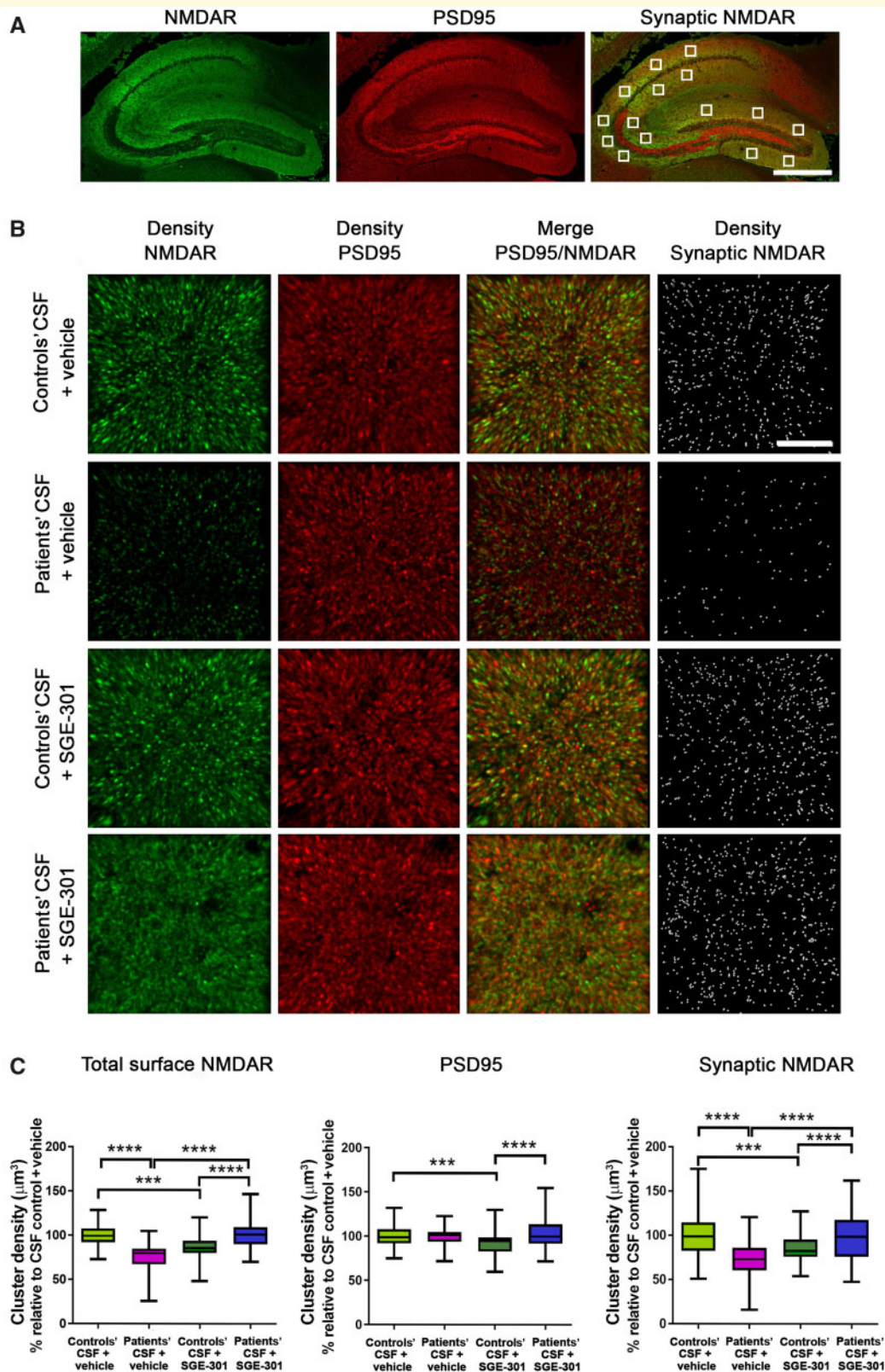


Figure 3 Treatment with SGE-301 prevents the reduction of NMDARs caused by patients' antibodies in hippocampus. (A) Hippocampus of mouse immunolabelled for NMDAR and PSD95. Images were merged (synaptic NMDAR, yellow colour) and post-processed to demonstrate co-localizing clusters. White squares indicate the analysed areas in CA1, CA3, and dentate gyrus. Each square is a 3D stack of 50 sections. Scale bar = 500 μm . (B) 3D projection and analysis of the density of total cell surface NMDAR clusters, PSD95, and synaptic NMDAR clusters (defined as those that co-localized with PSD95). Each 3D projection is a representative CA1 square region (as those shown in A) of an animal representative of each experimental condition infused with control or patients' CSF along with SGE-301 or vehicle. Merged

(continued)

Neurons treated for 24 h with controls' CSF and SGE-301 showed a mild decrease of synaptic NMDAR clusters. To explore the cause of this decrease of synaptic NMDAR we examined the effects of a longer (48 h) neuronal exposure to SGE-301, which demonstrated a decrease of synaptic and extrasynaptic NMDAR clusters (Supplementary Fig. 4A). Considering that phosphorylation of Ser295 enhances the accumulation of PSD95 and that Ser295 phosphorylation is suppressed by chronic NMDAR activation (Kim *et al.*, 2007), we determined whether SGE-301 changed the levels of phospho-S295-PSD95. This experiment showed a reduction of phospho-S295-PSD95 without significant decrease of total PSD95 (Supplementary Fig. 4B). A similar reduction of phospho-S295-PSD95 was obtained when cultured neurons were incubated with bicuculline, as reported (Kim *et al.*, 2007), and used here as control (Supplementary Fig. 4C). These findings indicate that prolonged neuronal exposure to SGE-301 leads to a reduction of NMDARs accompanied by a decrease of phospho-S295-PSD95, suggesting the presence of compensatory changes to the positive modulation of NMDAR.

To determine the effects of chronic exposure to SGE-301 on NMDAR currents we treated hippocampal neuronal cultures with controls' CSF (diluted 1:100) or controls' CSF + SGE-301 (10 μ M) for 48 h prior to whole-cell patch clamp recordings of NMDAR-mediated spontaneous EPSCs. Recordings revealed that SGE-301 did not modify the amplitude or frequency of spontaneous EPSC (Supplementary Fig. 5) but significantly slowed the decay phase of the spontaneous EPSC, as shown by a longer decay time constant (262.0 ± 37.3 ms versus 368.6 ± 49.8 ms; $P < 0.05$; Supplementary Fig. 5B). These findings suggest that SGE-301 enhances NMDAR-mediated EPSCs by slowing their decay phase, most probably by increasing the channel's open time and thus decreasing NMDAR's deactivation time.

Treatment with SGE-301 prevents the antibody-mediated reduction of NMDAR in mice

We next assessed whether SGE-301 antagonized the antibody effects in the hippocampus of mice infused with patients' CSF antibodies. Fifteen hippocampal areas with 50 optical z -sections per area, representing 750 optical sections per animal (five animals per experimental group), were investigated (Fig. 3A). Animals infused with patients' CSF

and treated with vehicle showed a significant decrease of the density of total and synaptic NMDAR clusters compared with animals infused with controls' CSF and treated with vehicle or SGE-301. Similarly, as observed with cultured neurons, the pathogenic effect of patients' CSF antibodies was prevented in the group of animals that received the same patients' CSF but were treated with SGE-301 instead of vehicle (Fig. 3B and C). To assess whether the treatment effect of SGE-301 was due to a direct interference with patient's antibody binding to NMDARs, we determined the intensity of human IgG bound to hippocampus in mice representative of the four experimental groups. This study showed that SGE-301 did not modify the intensity of patients' CSF IgG present in hippocampus suggesting that the drug did not block the binding of the antibody to NMDARs (Supplementary Fig. 6).

An additional finding of these studies was that in control conditions (e.g. animals not infused with antibodies) chronic administration of SGE-301 caused a decrease of total cell surface and synaptic NMDAR clusters as well as a decrease of PSD95, as shown by comparison of the groups of animals treated with controls' CSF with or without SGE-301 (Fig. 3C). Moreover, the hippocampus of mice infused with controls' CSF and chronically treated with SGE-301 had a significant decrease of Ser295 phosphorylated PSD95 and total PSD95 compared with animals not treated with SGE-301 (Supplementary Fig. 7). Overall, these studies showed that subcutaneous administration of SGE-301 prevented the antibody-mediated reduction of synaptic and extrasynaptic clusters of NMDARs, and that in control conditions (animals not infused with NMDAR antibodies) SGE-301 led to a decrease of levels of NMDAR and PSD95 suggesting, as with the experiments with neurons, the presence of compensatory mechanisms to the positive modulatory effect of SGE-301 on NMDARs.

Treatment with SGE-301 prevents the impairment of LTP caused by NMDAR antibodies of patients

Acute brain slices from mice infused with patient or controls' CSF treated with SGE-301 or vehicle, were used to record field excitatory postsynaptic potentials (fEPSPs) in the CA1 region of the hippocampus (Fig. 4A). Animals infused with patients' CSF showed a significant reduction of LTP compared with animals infused with controls' CSF, as shown by

Figure 3 Continued

images [merge: PSD95 (red)/NMDAR (green)] were postprocessed and used to calculate the density of clusters (density = spots/ μ m³). Scale bar = 2 μ m. (C) Quantification of the density of total (left) and synaptic (right) NMDAR clusters, and total PSD95 at Day 18 in a pooled analysis of hippocampal areas (CA1, CA3, and dentate gyrus). Mean density of clusters in animals treated with controls' CSF + vehicle was defined as 100%. For each condition, five animals were examined (15 hippocampal areas per animal). Box plots show the median, and 25th and 75th percentile; whiskers indicate the minimum or maximum values. Significance of treatment effect was assessed by one-way ANOVA ($P = 0.0001$) and *post hoc* analysis with Bonferroni correction; *** $P < 0.001$; **** $P < 0.0001$. Additional information is available in Supplementary Table 1.

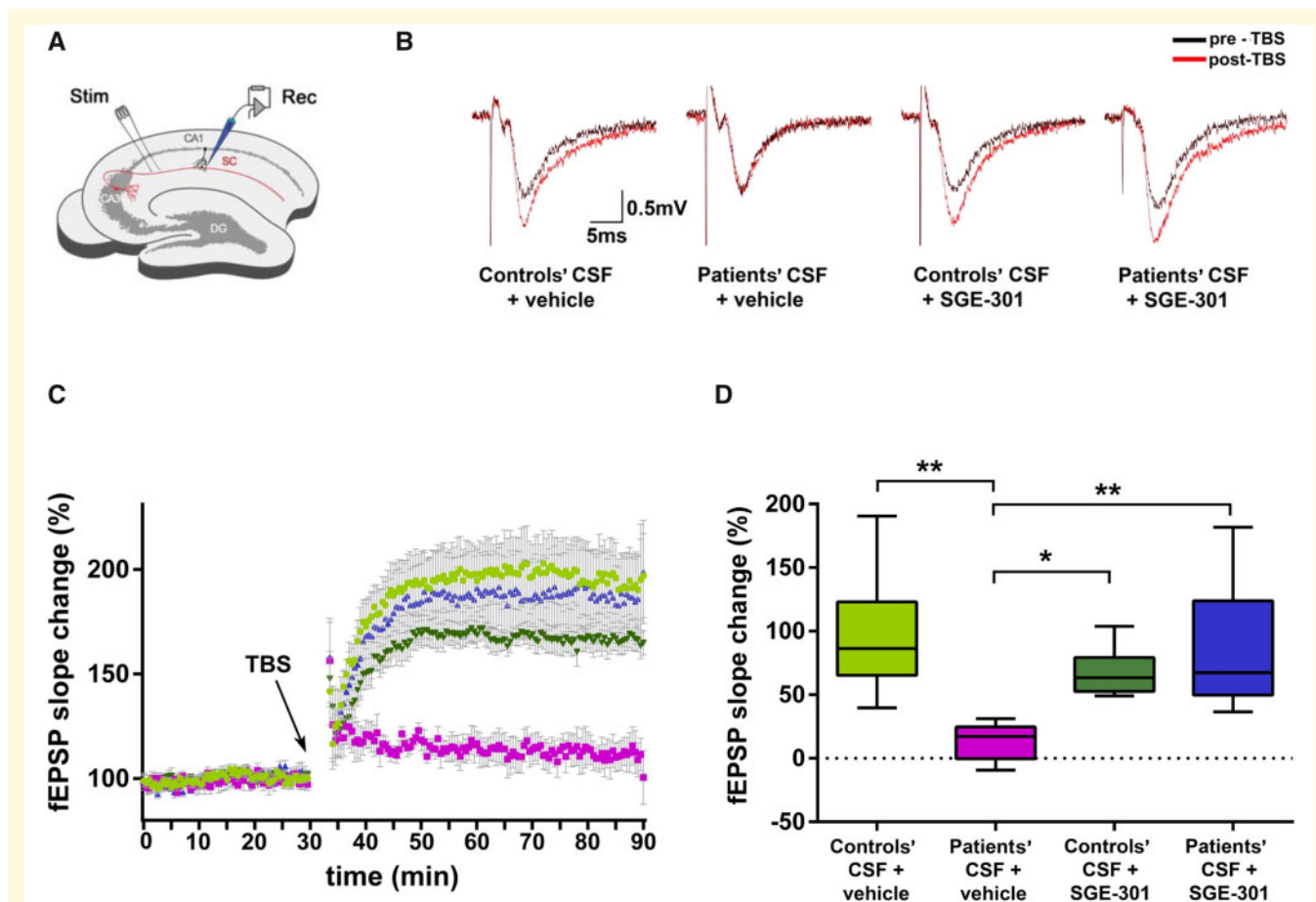


Figure 4 Treatment with SGE-301 prevents the impairment of LTP caused by NMDAR antibodies from patients. (A) The Schaffer collateral pathway (SC, red) was stimulated (Stim) and field potentials were recorded (Rec) in the CA1 region of the hippocampus. LTP was induced by TBS. CA = cornu ammonis; DG = dentate gyrus. (B) Example traces of individual recordings showing baseline fEPSPs before LTP induction (black traces) and after LTP (red traces). Slope and peak amplitude of fEPSPs are increased after TBS in mice infused with controls' CSF and treated with vehicle or SGE-301, and are strongly impaired in animals infused with patients' CSF and treated with vehicle. In mice infused with patients' CSF and treated with SGE-301 the increase of slope is improved. Note that initial peak amplitude of fEPSP may vary within individual recordings. (C) Time course of fEPSP recordings demonstrating robust changes in fEPSP slope in the animals infused with controls' CSF treated with vehicle ($n = 8$ recordings from seven animals, light green), or treated with SGE-301 ($n = 10$ recordings from seven animals, dark green), which was stable throughout the recording period after TBS (arrow). In animals infused with patients' CSF and treated with vehicle ($n = 6$ recordings from five animals, pink) the induction of LTP was markedly impaired. In contrast, animals infused with the same patients' CSF and treated with SGE-301 ($n = 7$ recordings from six animals, blue) show resolved effects on synaptic plasticity after LTP induction. The fEPSP values of all animals for each of the groups are presented as mean \pm standard error of the mean (SEM). (D) Quantification of fEPSP slope change showing a significant reduction of fEPSP slope in animals infused with patients' CSF and treated with vehicle compared with the other groups of animals. Note that animals infused with patients' CSF and treated with SGE-301 did not show reduction of fEPSP slope. The number of recordings and animals used are the same as those indicated in C. Box plots show the median, 25th and 75th percentiles; whiskers indicate minimum and maximum values. Significance was assessed by one-way ANOVA ($P < 0.01$) and Bonferroni *post hoc* correction test was applied: * $P < 0.05$; ** $P < 0.01$. Additional information is available in [Supplementary Table 1](#).

analysis of fEPSP slope change (Fig. 4B and C). Quantitative analysis showing median changes in slope values during the stable period post-theta-burst stimulation (TBS) (from Minutes 15 to 60, of 60 min after TBS) showed a reduced potentiation of fEPSP in mice infused with patients' CSF compared with those infused with controls' CSF (Fig. 4D). Treatment with SGE-301 prevented patients' CSF antibody-mediated impairment of LTP (Fig. 4C and D). Compared with these findings, animals infused with controls' CSF, with

or without treatment with SGE-301, did not show impairment of LTP, although the control group treated with SGE-301 showed a non-significant reduction of fEPSP slope change (Fig. 4C). This finding probably reflects the decreased density of NMDAR clusters noted in the confocal analysis of effects of SGE-301 in animals infused with controls' CSF (Fig. 3C).

In contrast to the severe reduction of hippocampal LTP, short-term plasticity was not affected in animals infused

with patients' CSF antibodies, as expected from the experience with previous studies (Planaguma *et al.*, 2016). Indeed, fEPSP recordings following a standard paired-pulse protocol showed significant facilitation consistent with increased pre-synaptic release probability (Supplementary Fig. 8A and B). This effect was similar in the four experimental groups (Supplementary Fig. 8C). Overall, these studies showed a severe impairment of postsynaptic, but not presynaptic, plasticity after TBS in animals infused with CSF from patients, but not in animals infused with the same patients' CSF and simultaneously treated with SGE-301.

Treatment with SGE-301 prevents memory loss caused by NMDAR antibodies from patients

Mice infused with patients' CSF and treated with daily subcutaneous administration of vehicle developed a progressive decrease of the novel object location index, with maximal deficit on Days 10 and 18 (4 days after stopping the antibody infusion), followed by progressive memory improvement until reaching the baseline pre-infusion level on Day 25 (Fig. 5, pink line) (Planaguma *et al.*, 2015). In contrast, mice infused with the same patients' CSF but treated with daily subcutaneous injections of SGE-301 instead of vehicle, showed no alteration of the novel object location index (Fig. 5, blue line); these findings were similar to those of mice infused with controls' CSF treated with SGE-301 or vehicle (Fig. 5, light and dark green lines). The total time of exploration of the two objects (not moved + novel location) was similar in animals of the four experimental groups (Supplementary Fig. 9A). The locomotor activity was also similar in the four groups of animals (Supplementary Fig. 9B–D). Overall, these findings showed that daily subcutaneous administration of SGE-301 prevented the hippocampal memory impairment caused by NMDAR antibodies from patients in this animal model.

Discussion

In this proof-of-concept study we show that a synthetic analogue (SGE-301) of the brain-derived cholesterol metabolite 24(S)-HC prevented the pathogenic effects of antibodies from patients with anti-NMDAR encephalitis in hippocampal neuronal cultures and in a previously reported model of cerebroventricular transfer of antibodies (Planaguma *et al.*, 2015, 2016). These findings and the good brain concentration after subcutaneous dosing suggest that oxysterol-based NMDAR PAMs could serve as potential treatments for anti-NMDAR encephalitis.

Like steroids, oxysterols are well recognized signalling molecules that interact with membrane-bound as well as soluble intracellular receptors (Radhakrishnan *et al.*, 2007). In particular, 24-hydroxylated oxysterol, such as 24 (S)-HC and the synthetic analogues, SGE-201 and SGE-301, are

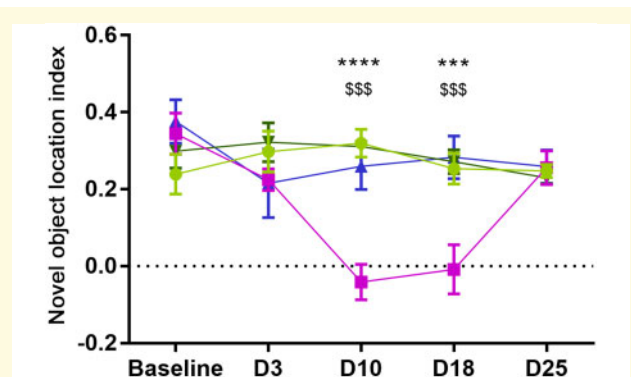


Figure 5 SGE-301 prevented the visuospatial memory deficits caused by NMDAR antibodies from patients. Mice infused with patients' CSF antibodies and treated with vehicle (pink line) showed a significant reduction of the novel object location index. This memory deficit was prevented in the group of mice infused with the same patients' CSF antibodies but treated with SGE-301 (blue line). No significant memory changes were noted in the groups of mice infused with controls' CSF and treated with vehicle (light green line) or SGE-301 (dark green line). Number of animals: controls' CSF + vehicle = 11; patients' CSF + vehicle = 10; controls' CSF + SGE-301 = 12; patients' CSF + SGE-301 = 10. A higher index represents better visuospatial memory. Data are presented as mean \pm SEM. Significance of assessment was performed by repeated-measures two-way ANOVA ($P < 0.0001$) with Bonferroni *post hoc* correction. Patient's CSF + vehicle versus controls' CSF + vehicle: **** $P < 0.0001$, \$\$\$ $P < 0.001$. Patient CSF + vehicle versus patients' CSF + SGE-301: *** $P < 0.001$. Additional information is available in Supplementary Table 1.

known for a striking selectivity for NMDARs (Paul *et al.*, 2013; Linsenbardt *et al.*, 2014). The enzyme involved in synthesis of 24(S)-HC (cholesterol 24-hydroxylase; CYP46A1) is expressed predominantly in the endoplasmic reticulum of neurons and dendrites (Ramirez *et al.*, 2008) and its deficiency causes severe impairment of hippocampal LTP and memory in mice (Kotti *et al.*, 2006). Using slices of hippocampus of rats, previous studies showed that application of 24(S)-HC or synthetic oxysterols (SGE-201 or SGE-301) reversed the LTP inhibition caused by ketamine (a non-competitive antagonist of NMDAR) (Paul *et al.*, 2013). In rats, the impairment of memory and active social interactions caused by phencyclidine (PCP), a non-competitive antagonist of NMDARs, were significantly improved by SGE-301 (Paul *et al.*, 2013). These findings, together with results from our studies, suggest that SGE-301 prevents the NMDAR hypo-function caused by pharmacological antagonists as well as by immune-mediated mechanisms.

Studies with chimeric GluN-GluK subunits suggest that GluN transmembrane domains are critical for oxysterol modulation (Wilding *et al.*, 2016), which would be consistent with the lipophilic nature of these modulators. SGE-301 increases channel open probability, potentiating NMDAR function, and appears to bind to a site independent of other allosteric modulators of NMDAR function (Paul *et al.*,

2013; Wilding *et al.*, 2016). In a previous study in which cultured rat hippocampal neurons were exposed for 48 h to patients' CSF NMDAR antibodies or controls' CSF and during the last 24 h each condition was treated with SGE-301 or vehicle, those that were treated with SGE-301 showed increased NMDAR function compared with those treated with vehicle (Warikoo *et al.*, 2018). Similar to our observed prolonged spontaneous EPSCs duration after SGE-301 (Supplementary Fig. 5), the authors found an increase of NMDAR function in the neurons exposed to controls' CSF and treated with SGE-301, which was attributed to an increase in open probability of NMDAR (Warikoo *et al.*, 2018). These findings led to the suggestion that SGE-301 does not interfere directly with the patient's antibody-mediated internalization of NMDARs (Warikoo *et al.*, 2018). However, the authors did not consider that the maximal antibody-mediated reduction of NMDARs in cultured neurons occurs within the first 12–24 h of incubation (before SGE-301 was applied); afterwards, the clusters of NMDARs remain decreased for as long as the antibodies are present in the media (Moscato *et al.*, 2014; Ladepeche *et al.*, 2018). Our current data show that when CSF antibodies from patients were co-applied with SGE-301 to cultures of neurons, the expected antibody-mediated effects were prevented and the NMDAR clusters were not decreased. Similar findings occurred in the animal model, showing that the density of total cell surface and synaptic NMDAR clusters in mice infused with patients' CSF and treated with SGE-301 was not significantly different from that of control mice (infused with controls' CSF and treated with vehicle). In contrast, animals infused with CSF from patients but not treated with SGE-301 showed the expected significant reduction of NMDARs. This reduction of NMDAR was associated with severe impairment of LTP and visuospatial memory, which were prevented when animals were simultaneously treated with SGE-301.

We noted that mice infused with controls' CSF and treated with SGE-301 compared with mice infused with the same controls' CSF and treated with vehicle, showed a decrease of total cell surface and synaptic NMDAR clusters. A similar effect was noted in neuronal cultures treated for 48 h with controls' CSF and SGE-301. We postulated that this finding represents a compensatory mechanism to the chronic PAM activity of SGE-301. Studies have shown that phosphorylation of Ser295 enhances the accumulation of PSD95 and that phospho-S295-PSD95 is suppressed by chronic NMDAR activation (Kim *et al.*, 2007). In line with these studies, we found that mice infused with controls' CSF and chronically treated with SGE-301 had lower amounts of phospho-S295-PSD95 and PSD95 compared with mice treated with vehicle. Neuronal cultures treated for 48 h with SGE-301 showed an effect in the same direction, including a reduction of phospho-S295-PSD95 that was more intense than that of total PSD95. Similar mechanisms induced by the chronic PAM effect of SGE-301 may be involved in the change, although not significant, in fEPSP slope after

induction of LTP in control animals treated with SGE-301 compared with those treated with vehicle.

Data from this and a previous study (Planaguma *et al.*, 2016) show that antibodies from patients do not affect paired-pulse facilitation, suggesting that presynaptic neurotransmitter release is unaffected in all experimental groups and that postsynaptic mechanisms are responsible for the decrease of LTP in animals treated with patients' CSF. In another report using hippocampal neuronal cultures, antibodies from patients specifically decreased NMDAR-mediated currents (along with a specific reduction of NMDAR clusters) without affecting AMPA receptor-mediated currents (Hughes *et al.*, 2010). These studies, along with the selective SGE-301 PAM effect on NMDAR (Paul *et al.*, 2013), suggest that the impairment of LTP (and its prevention by SGE-301) in animals infused with patients' CSF is via modulation of NMDAR.

The exact molecular mechanisms by which SGE-301 prevents the effects of patient antibodies are unknown. We found that SGE-301 does not block the binding of antibodies from patients to hippocampus, suggesting several alternative mechanisms, such as interference with antibody-induced internalization of receptors, increase of recruitment of NMDARs, or both. In preliminary studies with cultured neurons treated with antibodies from patients, we found that SGE-301 significantly decreased (without fully preventing) antibody-mediated NMDAR internalization, suggesting that in this setting, a recruitment of NMDARs to the cell surface and synapse may be facilitated by the drug.

Our study design does not allow for the assessment of whether SGE-301 reverses the antibody-mediated decrease of NMDAR and associated memory deficit because animals infused with antibodies from patients were simultaneously treated with SGE-301, and they did not develop any of those alterations. Although previous studies showed that application of SGE-301 to neuronal cultures exposed to patient antibodies for 24 h accelerated the recovery from the antibody effects (Warikoo *et al.*, 2018), it is unclear if SGE-301 would fully reverse symptoms already established and if so, how long it would take to recovery. It is also unclear whether SGE-301 would be effective for symptoms other than memory impairment; future animal models reproducing the entire repertoire of symptoms in the acute and chronic stage of the disease would facilitate these studies. Finally, there is evidence that SGE-301 and similar PAMs potentiate the NMDAR responses for many minutes beyond their presence in the media, a feature attributed to their strong lipophilicity or potential intracellular accumulation (Paul *et al.*, 2013; Warikoo *et al.*, 2018). Therefore, a dosing less frequent than that used in our model (e.g. every other day instead of daily dosing) may result in the same beneficial effects.

The experience with current treatment approaches to anti-NMDAR encephalitis and the outcome of most patients emphasizes the importance of our findings. During the acute stage of anti-NMDAR encephalitis,

patients often require intensive immunotherapy, anti-epileptics, psychoactive medications, and intensive care support, along with tumour removal if this applies (Titulaer *et al.*, 2013). This stage is usually followed by a protracted process of recovery in which symptoms of the acute phase (psychosis, seizures, abnormal movements, decreased level of consciousness) are no longer present, and the patient is at home or in a rehabilitation centre showing other symptoms such as deficit of memory, attention, cognition, abnormal behaviour, or executive dysfunction (Finke *et al.*, 2012, 2013; Titulaer *et al.*, 2013). Our model, in which the local transfer of human NMDAR antibodies into the mouse cerebroventricular system predominantly affects hippocampal NMDAR (Planaguma *et al.*, 2015), provides a proof-of-principle that targeting the antibody-related mechanisms as complementary treatment for anti-NMDAR encephalitis may mitigate or shorten the process of recovery. In preliminary studies, SAGE-718 (a PAM closely related to SGE-301 designed for oral bioavailability and once daily dosing) showed a good tolerability profile in healthy volunteers in a double-blind, placebo-controlled phase 1 single ascending dose study (Koenig *et al.*, 2019) and is currently being used in a trial for Huntington's disease (which, at early stages, appears to associate with reduced NMDAR function). The tasks for the future are to better understand the underlying mechanisms by which SGE-301 prevents patient antibody effects, assess the ability of this compound to reverse established symptoms, and determine its optimal dosing and frequency of treatment.

Acknowledgements

We thank Mercedes Alba, Eva Caballero, and Araceli Mellado-Berguillo (IDIBAPS, Hospital Clínic, University of Barcelona) for their technical support.

Funding

This study was funded by Plan Nacional de I + D + I and cofinanced by the Instituto de Salud Carlos III (ISCIII)—Subdirección General de Evaluación y Formento de la Investigación Sanitaria—and the Fondo Europeo de Desarrollo Regional (ISCIII-FEDER; 17/00234 and 17/00296); Project Integrative of Excellence (PIE 16/00014); Centro de Investigación Biomédica en Red de Enfermedades Raras (CIBERER, #CB15/00010); RETICS Oftared RD16/0008/0014 (X.G.); “la Caixa” Foundation (ID 100010434, under the agreement LCF/PR/HR17/52150001); The Safra Foundation (J.D.), and Fundació CELLEX (J.D.); BFU2017-83317-P (D.S.); Pla Estratègic de Recerca i Innovació en Salut (PERIS, SLT002/16/00346, J.P.); and Agència de Gestió d'Ajuts Universitaris i de Recerca (FI-AGAUR) grant program by the Generalitat de Catalunya (2019FI_B1 00212, A.G.-S.), Basque Government Doctoral Fellowship

Program, PRE-2019-1-0255 (E.M.), and Maria de Maeztu MDM-2017-0729 to Institut de Neurociències.

Competing interests

J.D. receives royalties from Athena Diagnostics for the use of Ma2 as an autoantibody test and from Euroimmun for the use of NMDA as an antibody test. He received a licensing fee from Euroimmun for the use of GABA_B receptor, GABA_A receptor, DPPX and IgLON5 as autoantibody tests; he has received a research grant from Sage Therapeutics. S.P., J.D., M.Q., J.D., and M.L. work at Sage Therapeutics.

Supplementary material

Supplementary material is available at *Brain* online.

References

- Ances BM, Vitaliani R, Taylor RA, Liebeskind DS, Voloschin A, Houghton DJ, et al. Treatment-responsive limbic encephalitis identified by neuropil antibodies: MRI and PET correlates. *Brain* 2005; 128: 1764–77.
- Armangue T, Spatola M, Vlagea A, Mattozzi S, Carceles-Cordon M, Martinez-Heras E, et al. Frequency, symptoms, risk factors, and outcomes of autoimmune encephalitis after herpes simplex encephalitis: a prospective observational study and retrospective analysis. *Lancet Neurol* 2018; 17: 760–72.
- Dalmau J, Gleichman AJ, Hughes EG, Rossi JE, Peng X, Lai M, et al. Anti-NMDA-receptor encephalitis: case series and analysis of the effects of antibodies. *Lancet Neurol* 2008; 7: 1091–8.
- Dalmau J, Lancaster E, Martinez-Hernandez E, Rosenfeld MR, Balice-Gordon R. Clinical experience and laboratory investigations in patients with anti-NMDAR encephalitis. *Lancet Neurol* 2011; 10: 63–74.
- Finke C, Kopp UA, Pruss H, Dalmau J, Wandinger KP, Ploner CJ. Cognitive deficits following anti-NMDA receptor encephalitis. *J Neurol Neurosurg Psychiatry* 2012; 83: 195–8.
- Finke C, Kopp UA, Scheel M, Pech LM, Soemmer C, Schlichting J, et al. Functional and structural brain changes in anti-N-methyl-D-aspartate receptor encephalitis. *Ann Neurol* 2013; 74: 284–96.
- Hughes EG, Peng X, Gleichman AJ, Lai M, Zhou L, Tsou R, et al. Cellular and synaptic mechanisms of anti-NMDA receptor encephalitis. *J Neurosci* 2010; 30: 5866–75.
- Kim MJ, Futai K, Jo J, Hayashi Y, Cho K, Sheng M. Synaptic accumulation of PSD-95 and synaptic function regulated by phosphorylation of serine-295 of PSD-95. *Neuron* 2007; 56: 488–502.
- Koenig A, Murck H, Paskavitz J, Hoffmann E, Li S, Silber C, et al. Double-blind, placebo-controlled phase 1 single ascending dose study of SAHE-718. International College of Neuropsychopharmacology (CINP) 2019 Congress. Athens, Greece; 2019.
- Kotti TJ, Ramirez DM, Pfeiffer BE, Huber KM, Russell DW. Brain cholesterol turnover required for geranylgeraniol production and learning in mice. *Proc Natl Acad Sci USA* 2006; 103: 3869–74.
- Ladepeche L, Planaguma J, Thakur S, Suarez I, Hara M, Borbely JS, et al. NMDA receptor autoantibodies in autoimmune encephalitis cause a subunit-specific nanoscale redistribution of NMDA receptors. *Cell Rep* 2018; 23: 3759–68.
- Linsendardt AJ, Taylor A, Emmett CM, Doherty JJ, Krishnan K, Covey DF, et al. Different oxysterols have opposing actions at N-methyl-D-aspartate receptors. *Neuropharmacology* 2014; 85: 232–42.

- Mikasova L, De Rossi PBouchet D, Georges F, Rogemond V, Didelot A, et al. Disrupted surface cross-talk between NMDA and Ephrin-B2 receptors in anti-NMDA encephalitis. *Brain* 2012; 135: 1606–21.
- Moscato EH, Peng X, Jain A, Parsons TD, Dalmau J, Balice-Gordon RJ. Acute mechanisms underlying antibody effects in anti-N-methyl-D-aspartate receptor encephalitis. *Ann Neurol* 2014; 76: 108–19.
- Newsom-Davis J. Therapy in myasthenia gravis and Lambert-Eaton myasthenic syndrome. *Semin Neurol* 2003; 23: 191–8.
- Paul SM, Doherty JJ, Robichaud AJ, Belfort GM, Chow BY, Hammond RS, et al. The major brain cholesterol metabolite 24(S)-hydroxycholesterol is a potent allosteric modulator of N-methyl-D-aspartate receptors. *J Neurosci* 2013; 33: 17290–300.
- Peer M, Pruss H, Ben-Dayana I, Paul F, Arzy S, Finke C. Functional connectivity of large-scale brain networks in patients with anti-NMDA receptor encephalitis: an observational study. *Lancet Psychiatry* 2017; 4: 768–74.
- Planaguma J, Haselmann H, Mannara F, Petit-Pedrol M, Grunewald B, Aguilar E, et al. Ephrin-B2 prevents N-methyl-D-aspartate receptor antibody effects on memory and neuroplasticity. *Ann Neurol* 2016; 80: 388–400.
- Planaguma J, Leyboldt F, Mannara F, Gutierrez-Cuesta J, Martin-Garcia E, Aguilar E, et al. Human N-methyl D-aspartate receptor antibodies alter memory and behaviour in mice. *Brain* 2015; 138: 94–109.
- Radhakrishnan A, Ikeda Y, Kwon HJ, Brown MS, Goldstein JL. Sterol-regulated transport of SREBPs from endoplasmic reticulum to Golgi: oxysterols block transport by binding to Insig. *Proc Natl Acad Sci USA* 2007; 104: 6511–8.
- Ramirez DM, Andersson S, Russell DW. Neuronal expression and subcellular localization of cholesterol 24-hydroxylase in the mouse brain. *J Comp Neurol* 2008; 507: 1676–93.
- Titulaer MJ, McCracken L, Gabilondo I, Armangue T, Glaser C, Iizuka T, et al. Treatment and prognostic factors for long-term outcome in patients with anti-NMDA receptor encephalitis: an observational cohort study. *Lancet Neurol* 2013; 12: 157–65.
- Viaccoz A, Desestret V, Ducray F, Picard G, Cavillon G, Rogemond V, et al. Clinical specificities of adult male patients with NMDA receptor antibodies encephalitis. *Neurology* 2014; 82: 556–63.
- Warikoo N, Brunwasser SJ, Benz A, Shu HJ, Paul SM, Lewis M, et al. Positive allosteric modulation as a potential therapeutic strategy in anti-NMDA receptor encephalitis. *J Neurosci* 2018; 38: 3218–29.
- Wilding TJ, Lopez MN, Huettner JE. Chimeric glutamate receptor subunits reveal the transmembrane domain is sufficient for NMDA receptor pore properties but some positive allosteric modulators require additional domains. *J Neurosci* 2016; 36: 8815–25.
- Wirtz PW, Titulaer MJ, Gerven JM, Verschuuren JJ. 3,4-diaminopyridine for the treatment of Lambert-Eaton myasthenic syndrome. *Expert Rev Clin Immunol* 2010; 6: 867–74.

SUPPLEMENTARY INFORMATION

1. Determination of plasma and brain concentration of SGE-301
2. Immunofluorescence and confocal studies with cultured live neurons
3. Electrophysiological studies
4. Novel object location and locomotor activity
5. Supplementary Fig. 1: Absence of antibodies other than NMDAR in patients' CSF
6. Supplementary Fig. 2: Plasma and brain exposures of SGE-301 after subcutaneous administration
7. Supplementary Fig. 3: SGE-301 decreases the number of antibody-bound internalized NMDAR
8. Supplementary Fig. 4: Cultures of rat hippocampal neurons treated for 48 hours with SGE-301 show a reduction of clusters of NMDAR and phospho-S295-PSD95
9. Supplementary Fig. 5: SGE-301 slows the decay phase of NMDAR-mediated spontaneous excitatory post-synaptic currents (sEPSC) in cultured neurons
10. Supplementary Fig. 6: Administration of SGE-301 does not change the amount of patients' IgG present in mice hippocampus
11. Supplementary Fig. 7: Subcutaneous administration of SGE-301 leads in control mice to a reduction of clusters of phospho-S295-PSD95 and PSD95
12. Supplementary Fig. 8: Paired-pulse facilitation is unaffected in animals infused with patients' CSF and treated with or without SGE-301
13. Supplementary Fig. 9: Total time of exploration and locomotor activity were not affected by treatment with SGE-301
14. Supplementary Table: Values and statistics for figures 2-5

Determination of plasma and brain concentration of SGE-301

SGE-301 was measured using liquid-liquid extraction and quantified by LC-MS/MS. Brain tissue was first diluted and homogenized at a ratio of 3 mL of PBS to 1 g of tissue. Five microliters of internal standard in methanol solution was added to 50 μ L of plasma or brain homogenate sample. Calibrators and assay quality controls were made by spiking SGE-301 into control mouse plasma or brain homogenate and preparing them as samples. One hundred fifty-five microliters of sample was then mixed with 200 μ L of deionized water and extracted with 1 mL of methyl-t-butyl ether. The organic layer was separated from the water layer and evaporated to dryness under nitrogen at 50°C for 15 minutes. The dry residue was reconstituted in 100 μ L of 50% acetonitrile + 0.1% formic acid in deionized water. Five microliters of reconstituted sample was injected on an ACE 3 Phenyl-300 50 x 1 mm HPLC column. Gradient elution was performed using an Eksigent LC200 HPLC system running a water:acetonitrile gradient from 50% acetonitrile to 95% acetonitrile over 2.3 minutes at 100 μ L/min.

Analyte detection was performed using a Sciex API4000 mass spectrometer running selected reaction monitoring of the analyte and internal standard in positive ion mode using a TurboV electrospray ion source. Sample concentrations were determined using the peak area ratio of analyte to internal standard and the least squares linear regression equation from the standard curve. Assay acceptance criteria for each LC-MS/MS run were +/- 20% accuracy compared to the nominal spiked concentration and +/- 20% CV.

Immunofluorescence and confocal studies with cultured live neurons

Primary hippocampal neurons were obtained from day 18 embryos of Wistar rats, as reported (Hughes *et al.*, 2010). Dissociated neurons were seeded on coverslips and grown in Corning® 35 mm x 10 mm dishes (Sigma-Aldrich, St Louis, MI, US) containing 1 mL of Neurobasal medium + B-27 Supplement (ThermoFisher, Waltham, MA, US). Seventeen-day *in vitro* cultures were then treated with patients' or controls' CSF (final

dilution 1:25 in the indicated media) along with SGE-301 (10 μ M) or vehicle (control) for 24 hours at 37°C. After washing with PBS, neurons were serially incubated with a human CSF NMDAR antibody sample (1:100, used as primary antibody) for 1 hour at 4°C, and the secondary antibody Alexa Fluor 488 goat anti-human IgG (A-11013 1:1000, ThermoFisher) for 1 hour at 4°C. Neurons were then washed with PBS, fixed with 4% paraformaldehyde, permeabilized with 0.3% Triton TM X-100, blocked with 1% BSA for 30 minutes, and serially incubated with rabbit anti-PSD95 (1:200, ab18258 Abcam, Cambridge, UK) overnight at 4°C, and the corresponding secondary antibody Alexa Fluor 594 goat anti-rabbit IgG (1:1000, A11012, ThermoFisher) for 1 hour at 4°C. Slides were mounted with ProLong Gold antifade reagent for 4 minutes, containing 6-diamidino-2-phenylindole dihydrochloride (DAPI, P36935; ThermoFisher) and results scanned with a Zeiss LSM 710 confocal microscope with EC-Plan NEOFLUAR CS 100 \times /1.3 NA oil immersion objective. For spot analysis we performed image deconvolution using the AutoQuantX3 software (Bitplane, Oxford Instruments, Abingdon, UK) followed by automatic segmentation using the spot detection algorithm from Imaris suite 7.6.4 (Bitplane). Synaptic localization was defined as colocalization of NMDAR with postsynaptic PSD95, applying an algorithm for spot colocalization of NMDAR and PSD95 using Imaris 7.6.4 (Bitplane). The density of spots was indicated as number of puncta per μ m-length of dendrite.

To determine the clusters of internalized antibody-bound receptors, neurons were treated as above with patients' CSF with SGE-301 or vehicle. Then neurons were washed with PBS, incubated with excess (1:20) secondary anti-human IgG Alexa Fluor 594 (red fluorescence, ThermoFisher) for 1 hour at 4°C, washed, fixed, permeabilized as above, and incubated with Alexa Fluor 488 goat anti-human IgG (1:1000, green fluorescence ThermoFisher) for 1 hour at 4°C. Slides were then mounted and the green fluorescence clusters quantified as above.

To determine whether prolonged treatment with SGE-301 modified the levels of NMDAR and phospho-S295-PSD95, neurons were treated as above for 48 hours with controls' CSF and SGE-301 or vehicle. Clusters of cell-surface synaptic and extrasynaptic NMDAR were immunolabeled as indicated, and neurons were then fixed and permeabilized as above and serially incubated with rabbit anti-phospho-S295-PSD95 (1:200, ab76108, Abcam) and mouse anti-PSD95 (1:200, 124 011, Synaptic Systems, Goettingen, Germany) overnight at 4°C, followed by the secondary antibodies Alexa Fluor 488 goat anti-rabbit IgG and Alexa Fluor 594 goat anti-mouse IgG (A-11034, A-11032, ThermoFisher) both at 1:500 dilution. Slides were then mounted and scanned, and the density of NMDARs, phospho-S295-PSD95 and PSD95 clusters was determined as above. Neurons treated for 24 hours with 25 μ M bicuculline (#14340, Sigma-Aldrich), which is an antagonist of GABA_A receptor that causes an increase of the levels of phospho-S295-PSD95 (Kim *et al.*, 2007) were used as control for this assay.

Electrophysiological studies

LTP and paired pulse facilitation in acute sections of hippocampus

Eighteen to 19 days after activation of the osmotic pumps and daily injection of drug or vehicle, mice were deeply anesthetized with isofluorane and decapitated. Brains were removed in ice-cold, high-sucrose extracellular artificial cerebrospinal fluid (aCSF1, in mM; 206 sucrose, 1.3 KCl, 1 CaCl₂, 10 MgSO₄, 26 NaHCO₃, 11 glucose, 1.25 NH₂PO₄, purged with 95% CO₂/5% O₂, pH 7.4) and subdivided into the hemispheres. Thick (380 μ m) coronal slices of hippocampus were obtained with a vibratome (VT1000S; Leica Microsystems, Wetzlar, Germany) and transferred into an incubation beaker with extracellular aCSF appropriate for neurophysiological recordings (aCSF2, in mM; 119 NaCl, 2.5 KCl, 2.5 CaCl₂, 1.25 NaH₂PO₄, 1.5 MgSO₄, 25 NaHCO₃, 11 glucose, purged with 95 % CO₂/5 % O₂, pH 7.4). Slices were kept at 32°C for 1 hour and subsequently at RT for at least 1 additional hour. For field potential measurements, single slices were then transferred into a measurement chamber perfused with aCSF2 at 2 ml/min

at 28-30°C (controls' CSF + vehicle: number of acute slices $n = 8$ prepared from brain hemisections of seven mice; patients' CSF + vehicle: $n = 6$ from hemisections of five mice; controls' CSF + SGE-301: $n = 10$ from hemisections of seven mice; patients' CSF + SGE-301: $n = 7$ from hemisections of six mice). A bipolar stimulation electrode (Platinum-Iridium stereotrode, PI2ST30.1A5, Science Products, Hofheim, Germany) was placed in the Schaffer collateral pathway. Recording electrodes were made with a puller (P-1000, Shutter Instrument Company, Novato, CA, US) from thick-walled borosilicate glass with a diameter of 1.5 mm (Sutter Instruments). The recording electrode filled with aCSF2 was placed in the dendritic branching of the CA1 region for local field potential measurement (field excitatory postsynaptic potential, fEPSP). A stimulus isolation unit A385 (World Precision Instruments, Hertfordshire, UK) was used to elicit stimulation currents between 25-700 μ A. Before baseline recordings for long-term potentiation (LTP), input-output (IO) curves were recorded for each slice at 0.03 Hz. The stimulation current was then adjusted in each recording to evoke fEPSPs at which the slope was at 50-60 % of maximally evoked fEPSP slope value. After baseline recording for 30 minutes with 0.03 Hz, LTP was induced by theta-burst stimulation (TBS; 10 theta bursts of four pulses of 100 Hz with an interstimulus interval of 200 ms repeated seven times with 0.03 Hz). After LTP induction, fEPSPs were recorded for 1 additional hour with 0.03 Hz. Paired-pulse fEPSPs in the test pathway were measured before baseline recordings with an interstimulus interval of 50 ms (controls' CSF + vehicle: number of acute slices $n = 20$ prepared from brain hemisections of eight mice; patients' CSF + vehicle: $n = 12$ from hemisections of six mice; controls' CSF + SGE-301: $n = 17$ from hemisections of eight mice; patients' CSF + SGE-301: $n = 14$ from hemisections of seven mice). All recordings were amplified and stored using amplifier AxoClamp 2B (Molecular Devices, San Jose, CA, US). Traces were analyzed using Axon pClamp software (Molecular Devices, version 10.6).

NMDAR-mediated spontaneous excitatory postsynaptic currents (sEPSC) in cultured neurons

To determine the effects of chronic exposure to SGE-301 on NMDAR currents we treated 18 days in vitro (d.i.v.) hippocampal neuronal cultures with controls' CSF (diluted 1:100) or controls' CSF + SGE-301 (10 μ M) for 48h prior to whole-cell patch clamp recordings of spontaneous NMDAR-mediated excitatory postsynaptic currents (sEPSCs). Recordings were made using thin-walled electrodes with a resistance of 3-5 M Ω , giving a final series resistance of 5-15 M Ω . Extracellular solution contained (in mM): 130 NaCl, 3.5 KCl, 2 CaCl₂, 15 glucose, 20 sorbitol and 10 HEPES, (Mg²⁺-free); osmolarity 300 mOsm/Kg and pH 7.4 with NaOH. In order to isolate NMDAR component, 100 μ M picrotoxin and 50 μ M NBQX were added to block GABA_AR-mediated IPSCs and AMPAR-mediated EPSCs, respectively. Intracellular pipette solution contained (in mM): 116 K-Gluconate, 6 KCl, 8 NaCl, 0.2 EGTA, 2 MgATP, 0.3 Na₃GTP and 10 HEPES; pH 7.25 with KOH. QX-314 at 2.5 mM was included into the pipette solution to block action potential firing in the recorded neuron. Spontaneous EPSCs were acquired at 2 kHz and filtered at 1 kHz at a holding potential of -70 mV. EPSCs were measured in periods ranging from 10 to 30 minutes. In experiments where the acute effect of SGE-301 was tested, a baseline period of 5 minutes in the absence of the drug was recorded followed by application of 10 μ M SGE-301 to the bath solution and a 10-15 minutes recording period after drug application. pClamp10/Clampfit10.6 software (Molecular Devices) were used to record, detect and analyze the amplitude, decay time constant and instantaneous frequency (from single sEPSCs).

Novel object location and locomotor activity

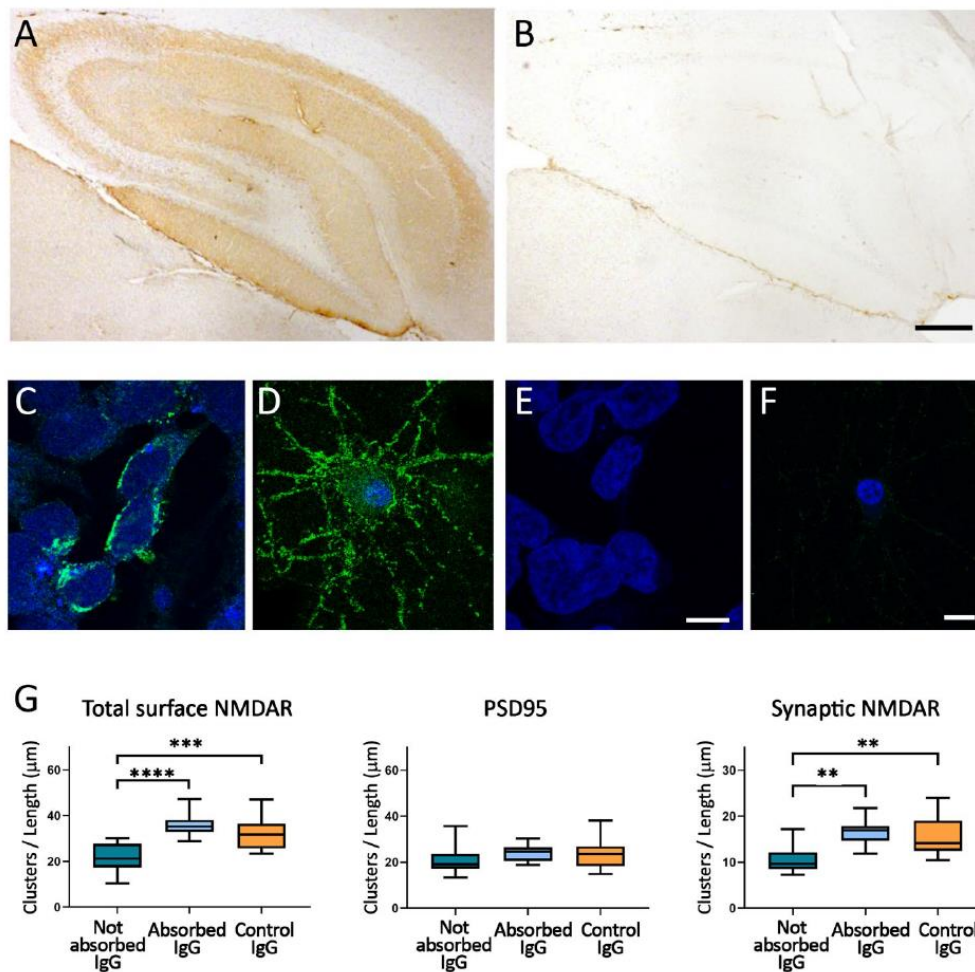
Both tasks were administered one day before surgical implantation of osmotic pumps and ventricular catheters, and once per week for four weeks after surgery (Fig. 1B).

Novel object location (NOL)

Animals were habituated to an empty, squared arena (45x45x40 cm, Panlab, Barcelona, Spain) with visual cues, and underwent two daily trials of 15 minutes each, for four days. The day of the test, animals were placed into the arena in presence of two equal objects positioned at two opposite corners and they were allowed to freely explore them for 9 minutes (familiarization phase). After a retention time of 3 hours, animals were returned to the arena, where one of the objects had been moved to a different corner. The animal was allowed to explore both objects for 9 minutes (test phase) and the time of exploration of each object was recorded. A discrimination index (NOL Index) was calculated using the following formula: Time of exploration of the moved object minus time of exploration of the not moved object divided by total time of exploration of both objects. A higher discrimination index indicates a better memory of the position of both objects. Object exploration is defined as any exploratory behavior triggered by the presence of the object (sniffing, biting, touching...) with the orientation of the nose toward the object within a distance of < 2 cm.

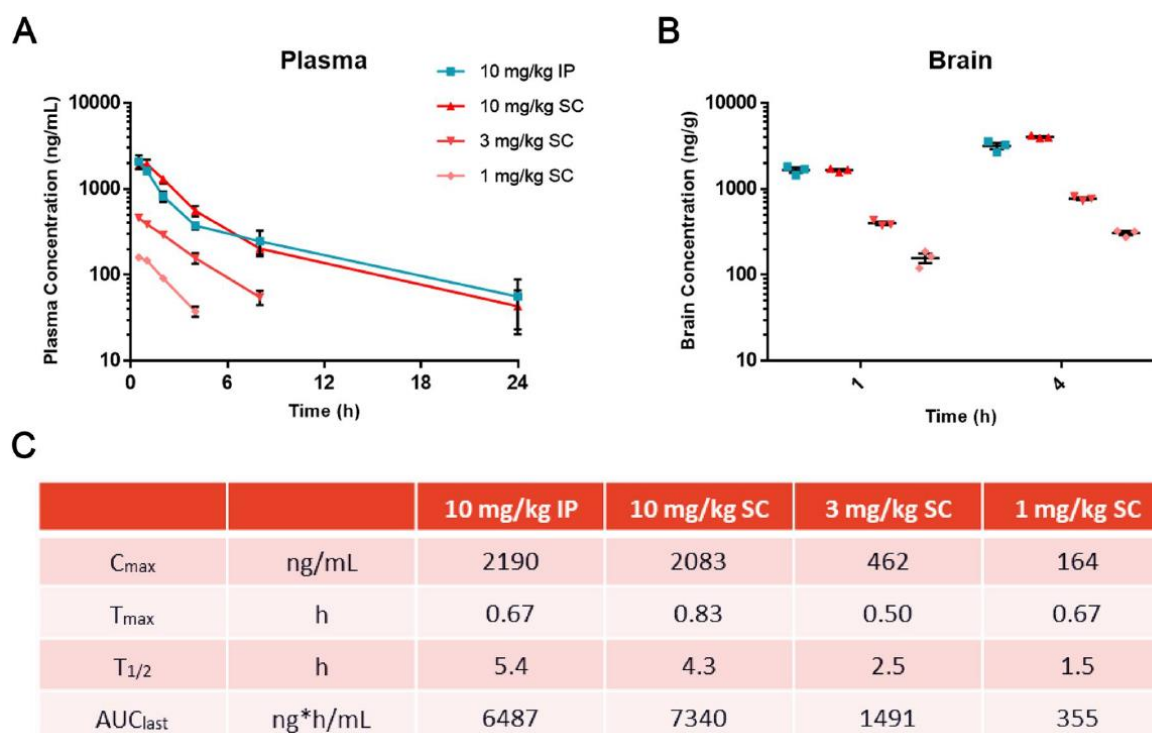
Locomotor activity

Animals were placed in locomotor activity boxes (11x21x18 cm, Imetronic, Passac, France) for 1 hour. The boxes are equipped with two rows of photocell beams that allow the measurement of small movements of the animal in each side of the box (local motor activity), the number of displacements from one side to the other of the box (horizontal activity) and the number of vertical explorations (rearings).



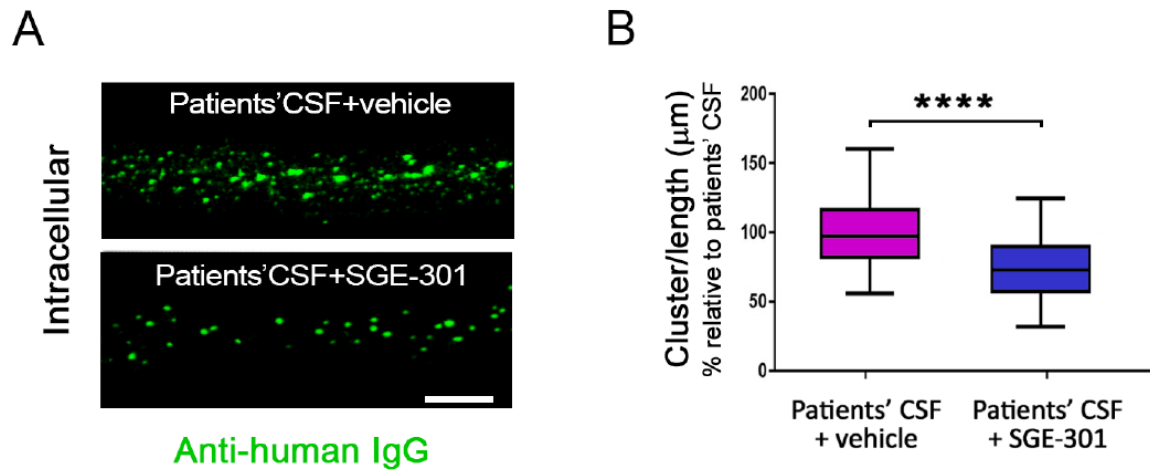
SUPPL FIG. 1: Absence of antibodies other than NMDAR in patients' CSF

Panels A and B show the immunostaining of rat brain by the pooled patients' CSF used in all experimental studies before (A) and after (B) immunoabsorption with NMDAR-expressing HEK293T cells. Scale bars = 200 μm. Panels C-F show the immunolabeling of NMDAR-expressing HEK293T cells and neurons by the pooled patients' CSF before (C and D) and after (E and F) immunoabsorption with NMDAR-expressing HEK293T cells. Scale bars = 10 μm. Panel G shows the effect of pooled patients' CSF antibodies on the density of total cell surface and synaptic NMDAR clusters before (not absorbed) and after (absorbed) immunoabsorption with NMDAR-expressing HEK293T cells. Note that the pooled patients' CSF causes the expected decrease of total cell surface and synaptic NMDAR, and that these effects are abrogated after immunoabsorption with NMDAR-expressing HEK cells. Box plots show the median, 25th and 75th percentiles; whiskers indicate the minimum or maximum values. Significance was assessed by one-way ANOVA ($p < 0.01$) and Bonferroni *post-hoc* correction test was applied: ** $p < 0.01$, *** $p < 0.001$, **** $p < 0.0001$.



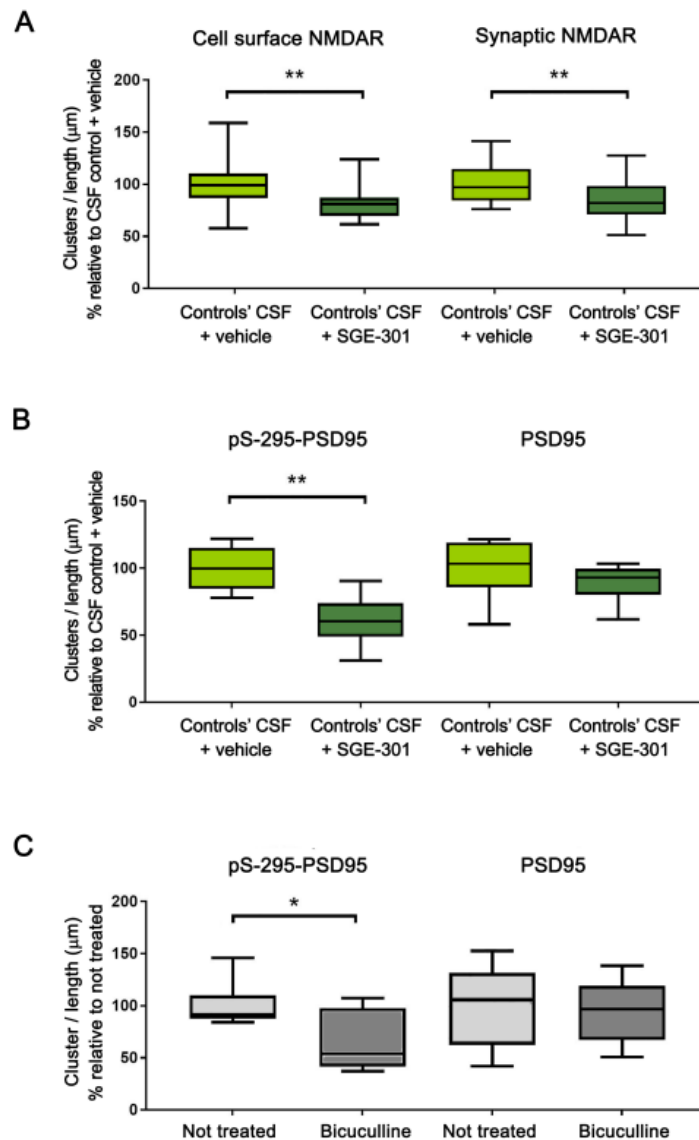
SUPPL FIG. 2: Plasma and brain exposures of SGE-301 after subcutaneous administration

For all *in vivo* experiments, animals were administered 10 mg/kg SGE-301 via subcutaneous administration. Plasma and brain levels achieved after subcutaneous (SC) administration were similar to those previously reported after intraperitoneal (IP) administration (Paul *et al.*, 2013). Data points represent mean \pm SEM levels of SGE-301. N= 4 mice per time point and matrix (e.g., 4 plasma 1 hour, 4 brain 1 hour, 4 plasma 4 hours, 4 brain 4 hours for a total of 16 animals).



SUPPL FIG. 3: SGE-301 decreases the number of antibody-bound internalized NMDAR

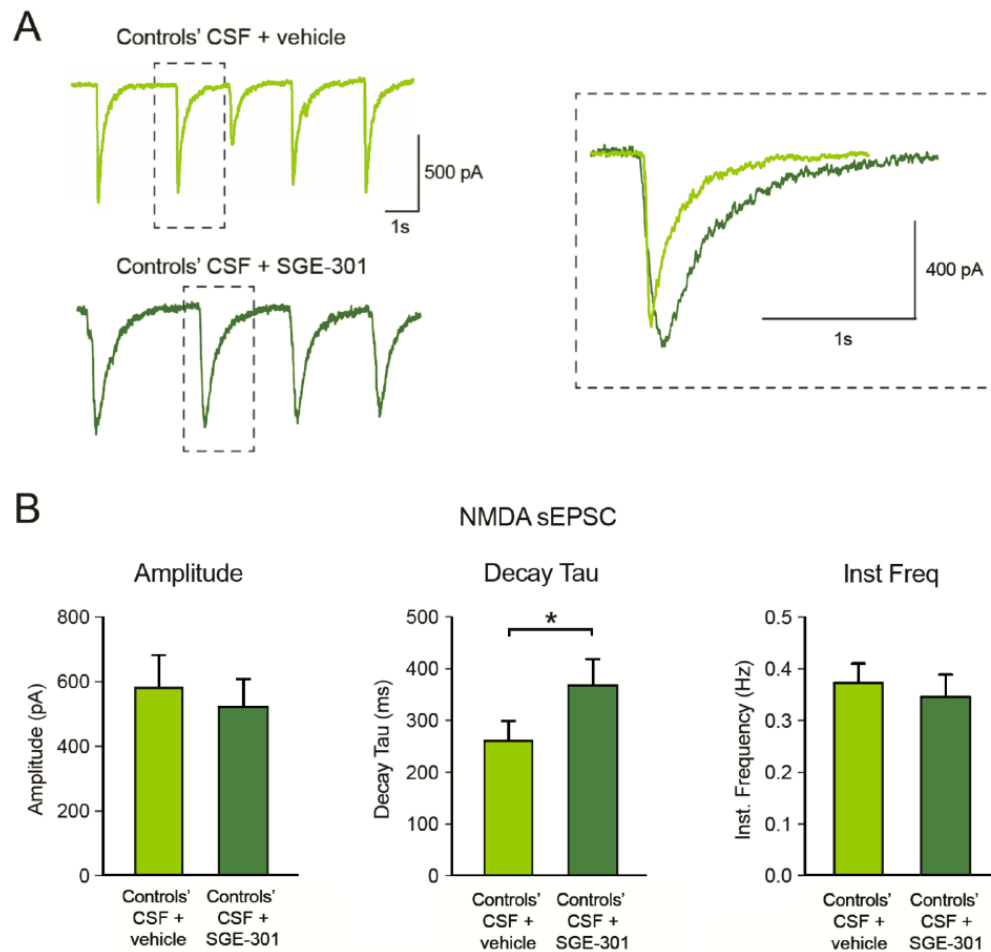
Panel A: Representative dendrites of neurons treated for 48 hours with patients' CSF with vehicle or SGE-301, showing the internalized antibody-bound NMDAR. Note that treatment with SGE-301 does not completely abrogate the internalization of receptors, Scale bars= 10 μm . Panel B: Quantification of internalized clusters of antibody-bound receptors. There is a significant decrease of internalized receptors. $n = 20$ dendrites per condition. Box plots show the median, 25th and 75th percentiles; whiskers indicate the minimum or maximum values. Significance of treatment effect was assessed by unpaired *t*-test. **** $p < 0.0001$.



SUPPL FIG. 4: Cultures of rat hippocampal neurons treated for 48 hours with SGE-301 show a reduction of clusters of NMDAR and phospho-S295-PSD95

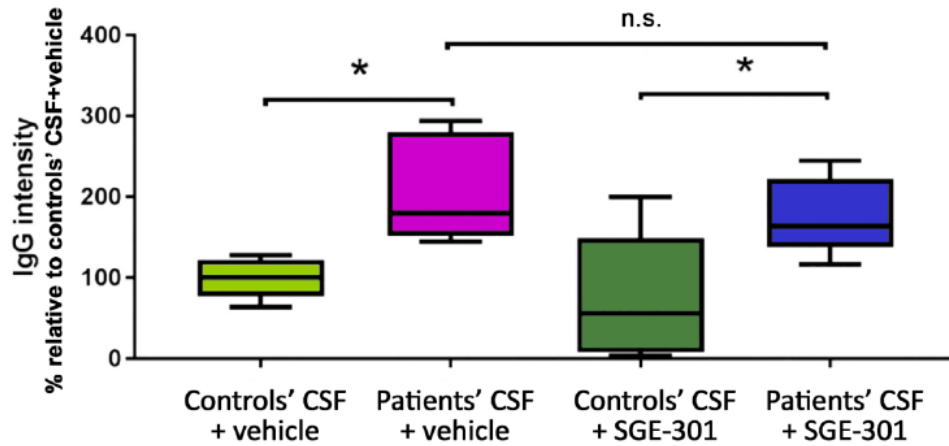
Panel A: Quantification of clusters of synaptic and extrasynaptic NMDAR in hippocampal cultures of neurons treated with controls' CSF along with vehicle or SGE-301. The presence of SGE-301 led to a significant reduction of clusters of NMDAR. Total surface NMDAR $**p = 0.0020$; synaptic NMDAR $**p = 0.0085$. Panel B: Quantification of clusters of phospho-S295-PSD95 and PSD95 in hippocampal cultures of neurons treated with controls' CSF along with vehicle or SGE-301. The presence of SGE-301 leads to a significant reduction of phospho-S295-PSD95, $**p < 0.01$. In this setting, SGE-301 did not lead to a significant reduction of PSD95 (in

contrast to the indicated reduction of PSD95 observed in mice hippocampus chronically treated with SGE-301, shown in Supplementary Fig. 5). Panel C: Quantification of clusters of phospho-S295-PSD95 and PSD95 in hippocampal cultures of neurons treated with bicuculline. In this setting, bicuculline caused a significant reduction of phospho-S295-PSD95, as reported (Kim *et al.*, 2007). * $p < 0.05$. For all studies, $n = 20$ dendrites per condition. Box plots show the median, 25th and 75th percentiles; whiskers indicate the minimum or maximum values. Significance of treatment effect was assessed by unpaired *t-test*.



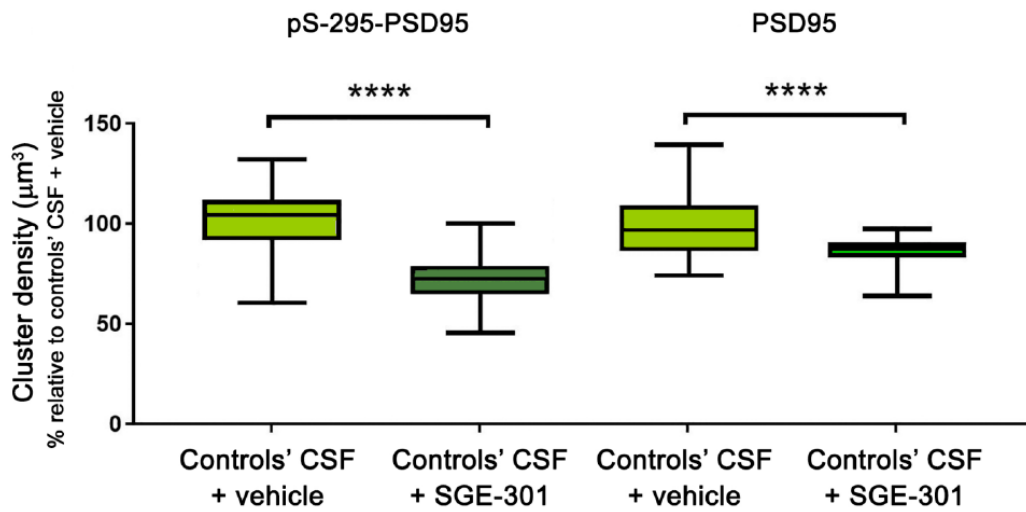
SUPPL FIG. 5: SGE-301 slows the decay phase of NMDAR-mediated spontaneous excitatory post-synaptic currents (sEPSC)

Panel A: Representative traces from spontaneous NMDAR-mediated EPSCs (sEPSC) recordings from hippocampal neuronal cultures treated with controls' CSF (light green trace) or controls' CSF and SGE-301 (dark green) for 48h prior to recordings. sEPSCs were recorded at -70 mV in the presence of NBQX and picrotoxin and in the absence of TTX. Co-treatment with SGE-301 did not modify sEPSC amplitude or frequency but slowed the recovery (increase in decay time constant). Right inset shows a superposition of two sEPSCs to illustrate the longer duration of sEPSC in neurons treated with SGE-301. Panel B: Mean amplitude, decay time constant (τ) and instantaneous frequency of NMDAR-mediated sEPSCs from neurons treated with controls' CSF (light green columns; $n=15$ neurons) or controls' CSF and SGE-301 (dark green columns; $n=13$). Controls' CSF vs controls' CSF + SGE-301: $*p < 0.05$ Student's t-test.



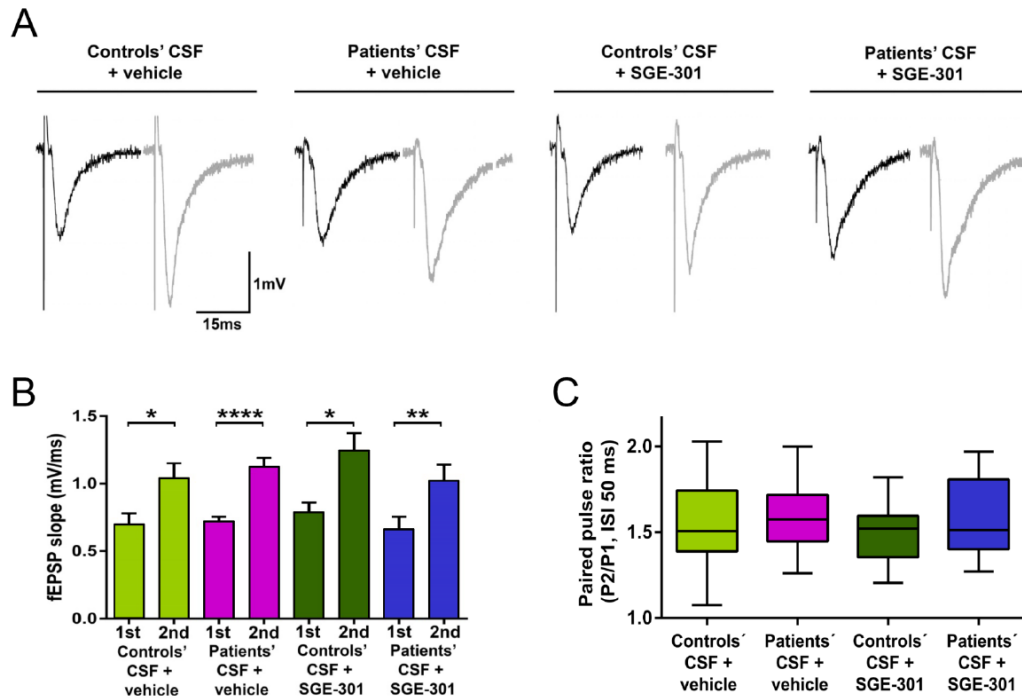
SUPPL FIG. 6: Administration of SGE-301 does not change the amount of patients' IgG present in mice hippocampus

Quantification of intensity of human IgG present in hippocampus of mice sacrificed on day 18. Mice infused with patients' CSF and treated with vehicle or SGE-301 show the same amount of IgG in the hippocampus, suggesting that SGE-301 does not block the binding of patients' antibodies to NMDAR. For all quantifications, mean intensity of IgG-immunostaining in the group of mice infused with controls' CSF and treated with vehicle was defined as 100%. Five animals of each experimental group were examined. Box plots show the median, 25th and 75th percentiles; whiskers indicate the minimum or maximum values.. Significance of treatment effect was assessed by one-way ANOVA ($p < 0.0001$) and *post-hoc* analyses were performed with Bonferroni correction; $*p < 0.05$.



SUPPL FIG. 7: Subcutaneous administration of SGE-301 leads in control mice to a reduction of clusters of phospho-S295-PSD95 and PSD95

Cluster density analysis of phospho-S295-PSD95 and PSD95 in brain tissue of animals infused with controls' CSF treated with vehicle or SGE-301. Note that animals treated with SGE-301 show a reduction of clusters of phospho-S295-PSD95 as well as PSD95. Five animals for each experimental group were examined. Box plots show the median, 25th and 75th percentiles; whiskers indicate the minimum or maximum values. Significance of treatment effect was assessed by unpaired *t*-test; *****p* < 0.0001.



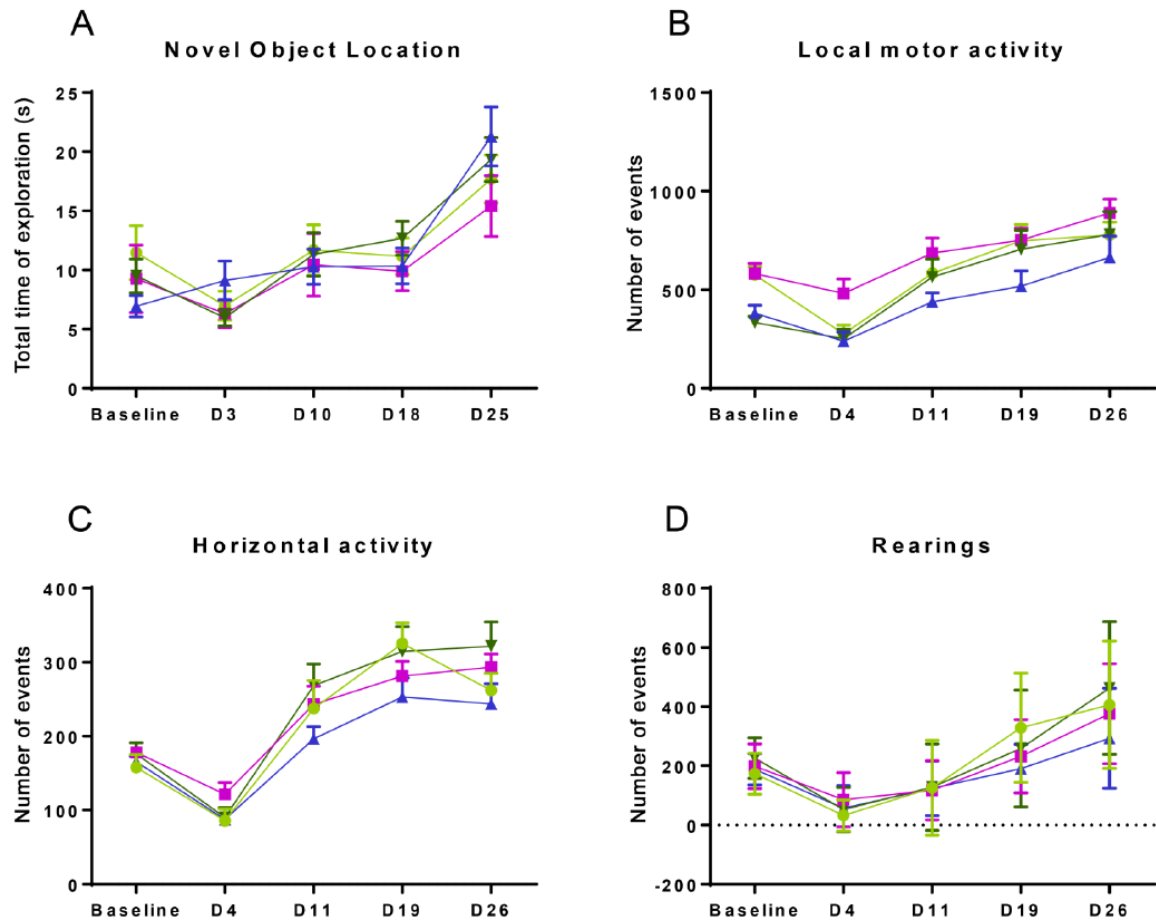
SUPPL FIG. 8: Paired-pulse facilitation is unaffected in animals infused with patients CSF and treated with or without SGE-301

Panel A: Example traces of fEPSPs in paired-pulse facilitation protocol applied to the Schaffer collateral - CA1 synaptic region. The fEPSP slope and amplitude in response to second stimulus (grey) are increased compared to the fEPSP slope and amplitude after the first stimulus (black) in all four groups of animals.

Panel B: Mean slope values of the fEPSPs in the response to the first (1st) and second (2nd) stimulus. All four experimental groups of animals show a significant increase in the fEPSP slope upon second stimulus.

Controls' CSF + vehicle (n= 20 recordings from eight animals, light green); patients' CSF + vehicle (n= 12 recordings from six animals, pink); controls' CSF + SGE-301 (n= 17 recordings from eight animals, dark green); patients' CSF + SGE-301 (n= 14 recordings from seven animals, blue). Data are shown as mean \pm SEM. Significance of the slope increase was assessed by unpaired *t*-test; **p* < 0.05, ***p* < 0.01, *****p* < 0.0001. Interstimulus interval is 50 ms.

Panel C: Paired-pulse facilitation, calculated as P2/P1 (pulse 2/pulse 1) fEPSP slope ratio, with interstimulus interval of 50 ms, is not significantly altered in any of the experimental groups of animals when compared with that of the group infused with controls' CSF + vehicle. The number of recordings and animals used are the same as those indicated in B. The significance of the results was assessed by one-way ANOVA (*p* > 0.05, not significant). Box plots show the median, 25th and 75th percentiles; whiskers indicate the 10th and 90th percentile.



SUPPL FIG. 9: Total time of exploration and locomotor activity were not affected by treatment with SGE-301

Panel A: The total time of exploration of the two objects presented in each NOL test session was similar in the four experimental groups of animals. Animals infused with controls' CSF and treated with vehicle (n = 11, light green); animals infused with patients' CSF and treated with vehicle (n = 10, pink); animals infused with controls' CSF and treated with SGE-301 (n = 12, dark green), and animals infused with patients' CSF and treated with SGE-301 (n = 10, blue). Data are presented as mean \pm SEM. Panels B-D: The locomotor activity was similar in the four experimental groups of animals, including measurement of local movements (B), displacement from one side to the other of the cage (C), and vertical explorations or rearings (D). Each colored line indicates the same experimental condition described in panel A. Number of animals: infused with controls' CSF and treated with vehicle, n = 11; infused with patients' CSF and treated with vehicle, n = 11; infused with controls' CSF and treated with SGE-301, n = 12, and infused with patients' CSF and treated with SGE-301, n = 11.

Supplementary Table: Values and statistics for figures 2-5

Fig 2 (Cluster density (cultures of hippocampal neurons))					
Total NMDAR	A) Controls' CSF + vehicle	B) Patients' CSF + vehicle	C) Controls' CSF + SGE-301	D) Patients' CSF + SGE-301	
Median	12.17	5.23	12.1	11.66	A vs B p<0.0001
75% Percentile	14.46	7.97	13.41	13.99	B vs D p<0.0001
25% Percentile	9.59	4.07	9.18	9.71	
PSD95	A) Controls' CSF + vehicle	B) Patients' CSF + vehicle	C) Controls' CSF + SGE-301	D) Patients' CSF + SGE-301	
Median	12.09	11.12	10.56	10.88	
75% Percentile	14.81	13.58	12.34	13.03	
25% Percentile	9.88	8.55	9.04	8.65	
Synaptic NMDAR	A) Controls' CSF + vehicle	B) Patients' CSF + vehicle	C) Controls' CSF + SGE-301	D) Patients' CSF + SGE-301	
Median	2.69	1.56	2.38	2.66	A vs B p<0.0001
75% Percentile	3.6	2.06	2.99	3.34	A vs C p<0.0001
25% Percentile	1.97	1.15	1.87	2.18	B vs D p<0.0170
Fig 3 (Cluster density (Brain tissue))					
Total NMDAR	A) Controls' CSF + vehicle	B) Patients' CSF + vehicle	C) Controls' CSF + SGE-301	D) Patients' CSF + SGE-301	
Median	99.27	79.69	85.61	101.1	A vs B p<0.0001
75% Percentile	107.5	84.7	93.81	109.3	A vs C p=0.0001
25% Percentile	91.99	67.17	80.15	89.94	B vs D p<0.0001
PSD95	A) Controls' CSF + vehicle	B) Patients' CSF + vehicle	C) Controls' CSF + SGE-301	D) Patients' CSF + SGE-301	
Median	98.91	101.4	94.91	99.91	A vs C p=0.0003
75% Percentile	107.9	104.9	98.91	113.9	C vs D p<0.0001
25% Percentile	91.91	93.91	82.92	91.91	
Synaptic NMDAR	A) Controls' CSF + vehicle	B) Patients' CSF + vehicle	C) Controls' CSF + SGE-301	D) Patients' CSF + SGE-301	
Median	98.56	73.12	82.66	98.56	A vs B p<0.0001
75% Percentile	114.5	85.84	95.38	117.6	A vs C p=0.0009
25% Percentile	82.66	60.41	76.3	76.3	B vs D p<0.0001
					C vs D p<0.0001
Fig 4 (fEPSP slope change %)					
	A) Controls' CSF + vehicle	B) Patients' CSF + vehicle	C) Controls' CSF + SGE-301	D) Patients' CSF + SGE-301	
Median	86,41	17,2	63,5	67,37	A vs B p=0.0013
75% Percentile	123,1	24,73	79,27	123,9	B vs D p=0.0060
25% Percentile	65,26	-0,4091	52,53	49,77	B vs C p=0.0443
Fig 5 (Novel Object Location Index)					
Baseline	A) Controls' CSF + vehicle	B) Patients' CSF + vehicle	C) Controls' CSF + SGE-301	D) Patients' CSF + SGE-301	
Mean	0,239	0,345	0,299	0,376	
SEM	0,052	0,053	0,044	0,056	
N	11	10	12	10	
D3	A) Controls' CSF + vehicle	B) Patients' CSF + vehicle	C) Controls' CSF + SGE-301	D) Patients' CSF + SGE-301	
Mean	0,298	0,225	0,322	0,216	
SEM	0,053	0,028	0,050	0,089	
N	11	10	12	10	
D10	A) Controls' CSF + vehicle	B) Patients' CSF + vehicle	C) Controls' CSF + SGE-301	D) Patients' CSF + SGE-301	
Mean	0,320	-0,041	0,311	0,260	A vs B p<0.0001
SEM	0,036	0,046	0,015	0,060	B vs D p=0.0001
N	11	10	12	10	B vs C p<0.0001
D18	A) Controls' CSF + vehicle	B) Patients' CSF + vehicle	C) Controls' CSF + SGE-301	D) Patients' CSF + SGE-301	
Mean	0,254	-0,008	0,272	0,283	A vs B p=0.0007
SEM	0,040	0,063	0,031	0,055	B vs D p=0.0002
N	11	10	12	10	B vs C p=0.0002
D25	A) Controls' CSF + vehicle	B) Patients' CSF + vehicle	C) Controls' CSF + SGE-301	D) Patients' CSF + SGE-301	
Mean	0,248	0,256	0,230	0,259	
SEM	0,017	0,044	0,015	0,043	
N	11	10	12	10	

REFERENCES

Hughes EG, Peng X, Gleichman AJ, Lai M, Zhou L, Tsou R, *et al.* Cellular and synaptic mechanisms of anti-NMDA receptor encephalitis. *J Neurosci* 2010; 30: 5866-75.

Kim MJ, Futai K, Jo J, Hayashi Y, Cho K, Sheng M. Synaptic accumulation of PSD-95 and synaptic function regulated by phosphorylation of serine-295 of PSD-95. *Neuron* 2007; 56: 488-502.

Paul SM, Doherty JJ, Robichaud AJ, Belfort GM, Chow BY, Hammond RS, *et al.* The major brain cholesterol metabolite 24(S)-hydroxycholesterol is a potent allosteric modulator of N-methyl-D-aspartate receptors. *J Neurosci* 2013; 33: 17290-300.

Paper IV

Allosteric modulation of NMDARs reverses patients' autoantibody effects in mice.

Marija Radosevic, Jesús Planagumà, Francesco Mannara, Araceli Mellado, Esther Aguilar, Lidia Sabater, Jon Landa, Anna García-Serra, **Estibaliz Maudes**, Xavier Gasull, Mike Lewis, Josep Dalmau.

Neurology: Neuroimmunology & Neuroinflammation.

2022, 9(1), e1122.

IF JCR 2022: 8.8 (D1).

Allosteric Modulation of NMDARs Reverses Patients' Autoantibody Effects in Mice

Marija Radosevic, PhD,* Jesús Planagumà, PhD,* Francesco Mannara, PhD,* Araceli Mellado, BS, Esther Aguilar, BS, Lidia Sabater, PhD, Jon Landa, MSc, Anna García-Serra, PhD, Estibaliz Maudes, MSc, Xavier Gasull, PhD, Mike Lewis, PhD,† and Josep Dalmau, MD, PhD†

Correspondence
Dr. Dalmau
jdalmau@clinic.cat

Neurol Neuroimmunol Neuroinflamm 2022;9:e1122. doi:10.1212/NXI.0000000000001122

Abstract

Background and Objectives

To demonstrate that an analog (SGE-301) of a brain-derived cholesterol metabolite, 24(S)-hydroxycholesterol, which is a selective positive allosteric modulator (PAM) of NMDA receptors (NMDARs), is able to reverse the memory and synaptic alterations caused by CSF from patients with anti-NMDAR encephalitis in an animal model of passive transfer of antibodies.

Methods

Four groups of mice received (days 1–14) patients' or controls' CSF via osmotic pumps connected to the cerebroventricular system and from day 11 were treated with daily subcutaneous injections of SGE-301 or vehicle (no drug). Visuospatial memory, locomotor activity (LA), synaptic NMDAR cluster density, hippocampal long-term potentiation (LTP), and paired-pulse facilitation (PPF) were assessed on days 10, 13, 18, and 26 using reported techniques.

Results

On day 10, mice infused with patients' CSF, but not controls' CSF, presented a significant visuospatial memory deficit, reduction of NMDAR clusters, and impairment of LTP, whereas LA and PPF were unaffected. These alterations persisted until day 18, the time of maximal deficits in this model. In contrast, mice that received patients' CSF but from day 11 were treated with SGE-301 showed memory recovery (day 13), and on day 18, all paradigms (memory, NMDAR clusters, and LTP) had reversed to values similar to those of controls. On day 26, no differences were observed among experimental groups.

Discussion

An oxysterol biology-based PAM of NMDARs is able to reverse the synaptic and memory deficits caused by CSF from patients with anti-NMDAR encephalitis. These findings suggest a novel adjuvant treatment approach that deserves future clinical evaluation.

*These authors contributed equally as co-first authors.

†These authors contributed equally as co-senior authors.

From the Institut d'Investigacions Biomèdiques August Pi i Sunyer (IDIBAPS) (M.R., J.P., F.M., A.M., E.A., L.S., J.L., A.G.-S., E.M., X.G., J.D.), Hospital Clínic, Universitat de Barcelona, Barcelona, Spain; Laboratori de Neurofisiologia (X.G.), Departament de Biomedicina, Facultat de Medicina i Ciències de la Salut, Institut de Neurociències, Universitat de Barcelona, Barcelona, Spain; Sage Therapeutics (M.L.), Department of Research and Nonclinical Development, Cambridge, MA; Department of Neurology (J.D.), University of Pennsylvania, Philadelphia, PA; Centro de Investigación Biomédica en Red de Enfermedades Raras (CIBERER) (J.D.), Madrid, Spain; and Institut de Recerca i Estudis Avançats (ICREA) (J.D.), Barcelona, Spain.

Go to [Neurology.org/NN](https://www.neurology.org/NN) for full disclosures. Funding information is provided at the end of the article.

The Article Processing Charge was funded by the authors.

This is an open access article distributed under the terms of the Creative Commons Attribution-NonCommercial-NoDerivatives License 4.0 (CC BY-NC-ND), which permits downloading and sharing the work provided it is properly cited. The work cannot be changed in any way or used commercially without permission from the journal.

Glossary

EPSC = excitatory postsynaptic current; HPBCD = 2-hydroxypropyl- β -cyclodextrin; LA = locomotor activity; LTP = long-term potentiation; NMDAR = NMDA receptor; NOL = novel object location; PAM = positive allosteric modulator; PPF = paired-pulse facilitation.

Anti-NMDA receptor (NMDAR) encephalitis is an immune-mediated disease characterized by a complex neuropsychiatric syndrome and the presence of CSF antibodies against the GluN1 subunit of NMDAR.¹ Although most patients improve with immunotherapy and tumor removal, when needed, one of the most challenging problems of this disease is the prolonged process of recovery.²⁻⁷ This problem particularly affects memory, attention, and executive functions that usually remain altered for many months after the acute phase has resolved.⁸⁻¹³ The reasons for this slow recovery are unclear, but it may be caused by a severe impairment of synaptic function due to persistent immune activation against NMDAR within the CNS,^{14,15} a limited efficacy of current immunotherapies, or a combination thereof.

To achieve a faster or sustained improvement, we postulated that patients with anti-NMDAR encephalitis may need, in addition to immunotherapy, adjuvant medication aimed to compensate or overcome the mechanisms altered by the antibodies. This approach would be similar to that used in patients with myasthenia gravis or the Lambert-Eaton myasthenic syndrome who receive immunotherapy along with acetylcholinesterase inhibitors or 3,4-diaminopyridine.^{16,17} Considering that in anti-NMDAR encephalitis, the antibodies cause a reduction of receptors and NMDAR-mediated currents,^{14,18} the potential treatment utility of positive allosteric modulators (PAMs) of NMDARs came to our attention.

There is evidence that a brain-derived cholesterol metabolite, 24(S)-hydroxycholesterol (24(S)-HC), is a potent, direct, and selective PAM of NMDARs.¹⁹ Several synthetic analogs of 24(S)-HC such as $\Delta 5,6$ -3 β -oxy-nor-cholesterol-dimethylcarbinol (SGE-201) and SGE-301 have similar mechanisms of action.¹⁹ An advantage of these compounds is their small size and lipophilicity that allow them to cross the blood-brain barrier and reach CNS concentrations that substantially potentiate NMDAR currents.¹⁹⁻²¹ In rats, administration of SGE-301 reversed the memory deficit caused by phencyclidine, a noncompetitive NMDAR antagonist,¹⁹ and in mice, it prevented the development of memory and synaptic alterations caused by cerebroventricular transfer of patients' NMDAR antibodies.²⁰ However, the potential treatment efficacy of SGE-301 in reversing the antibody-mediated effects once the memory and synaptic alterations have already occurred was not investigated. Here, we address this question in the model of cerebroventricular transfer of patients' CSF antibodies.

Methods

Animals, Surgery, and Patients' CSF

One hundred forty-one male C57BL/6J mice (Charles River), 8–10 weeks old, were used in the studies, including 44 for

assessment of memory and locomotor activity (LA), 50 for determination of clusters of NMDAR and PSD95 using confocal immunohistochemistry, and 47 for assessment of hippocampal long-term potentiation (LTP) and paired-pulse facilitation. Animal care, anesthesia, and the technique of cerebroventricular infusion of patients' CSF via subcutaneous osmotic pumps (Alzet; volume 100 microliter, flow rate 0.25 microliter/h for 14 days) have been described.¹⁸ The CSF infused was pooled from samples of 10 patients with high titer IgG GluN1 antibodies (all >1:320) and 10 patients with normal pressure hydrocephalus without antibodies (control); samples were dialyzed against phosphate-buffered saline and normalized to a physiologic concentration of 2 mg IgG/dL.²² The same samples were previously used in a report where the NMDAR antibody specificity and absence of other neuronal antibodies were demonstrated by immunoabsorption with HEK293 cells expressing GluN1, and abrogation of CSF-mediated NMDAR internalization after CSF was immunoabsorbed with GluN1.²⁰

Standard Protocol Approvals, Registrations, and Patient Consents

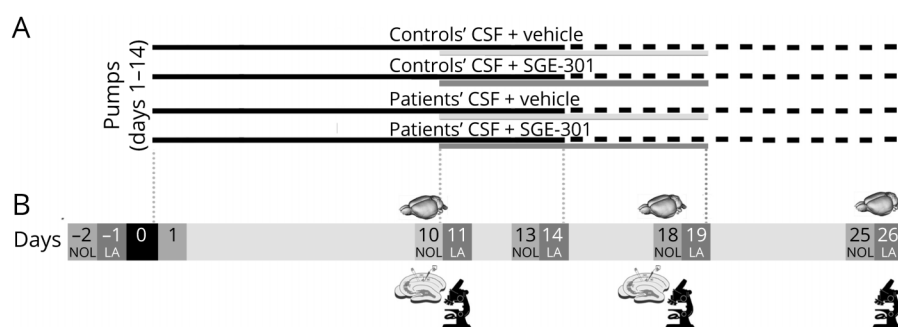
Written informed consent was obtained from patients, and the study was approved by the local institutional review board (Hospital Clinic, HCB/2018/0192). The Local Ethical Committee of the University of Barcelona following European (2010/63/UE) and Spanish (RD 53/2013) regulations approved the animal studies.

Preparation of SGE-301 and Experimental Design

Lyophilized SGE-301 was dissolved in a solution of 30% 2-hydroxypropyl- β -cyclodextrin (HPBCD, Sigma-Aldrich), and the dose (10 mg/kg) for subcutaneous administration was based on previously reported plasma and brain pharmacokinetic studies that demonstrated brain exposures sufficient to modulate activity in preclinical models of NMDAR hypofunction.^{19,20} A similar solution of 30% HPBCD, without drug, served as control (vehicle).

From days 1 to 14, mice were continuously infused in the cerebroventricular system with patients' or controls' CSF. From days 11 to 19, each experimental condition was divided into 2 additional groups depending on whether animals were treated with SGE-301 or vehicle (control) (Figure 1A). The treatment interval (days 11–19) was selected according to previous experience with this model, which consistently shows progressive impairment of memory along with a decrease of NMDAR clusters from days 10 to 18.^{18,20,22} Brain tissue studies were performed in subsets of mice killed at intermediate time points (days 10 and 18) and in the rest of animals killed on day 26 (Figure 1B).

Figure 1 Experimental Design



(A) Studies were performed in 4 experimental groups of mice that received a continuous infusion (days 1–14) of controls' or patients' CSF via subcutaneously implanted osmotic pumps connected to the cerebroventricular system along with daily subcutaneous injection of vehicle (no drug) or SGE-301 (10 mg/kg diluted in vehicle) from days 11 to 19. Note that before starting treatment on day 11, there are 2 experimental groups (mice infused with controls' CSF or patients' CSF). (B) Timing of memory and locomotor tasks. Baseline novel object location (NOL) and locomotor activity (LA) were obtained before the infusion of controls' or patients' CSF (days -2, -1). The same tests were applied on days 10–11, 13–14, 18–19, and 25–26 after onset of infusion of CSF. The effects of patients' antibodies on the levels of NMDARs or LTP were examined in subsets of mice killed on days 10–11, 18–19, or 26. LTP = long-term potentiation; NMDAR = NMDA receptor.

Immunohistochemistry, Immunoprecipitation, Confocal Microscopy, and Electrophysiological Studies

The presence of human IgG bound to brain tissue was quantified using immunofluorescence, as reported.²³ The NMDAR specificity of the IgG bound to brain was demonstrated by immunoprecipitation. In brief, homogenates of brain tissue were washed, incubated with protein A/G sepharose beads, precipitated, run in a gel, and blotted with an polyclonal rabbit GluN1 antibody (G8913, 1:200, Sigma-Aldrich, St. Louis, MO), as reported.²²

To determine the effects of patients' antibodies on the number of clusters of NMDAR, nonpermeabilized 5- μ m-thick brain sections (obtained on days 10, 18, and 26) were immunohistochemically studied as reported.¹⁸ In brief, sections were serially incubated with a human CSF NMDAR antibody (1:20, used as primary antibody), and the labeled NMDARs were determined with a secondary Alexa Fluor 488 goat anti-human IgG (1:1000, A-11013, Thermo Fisher, Waltham, MA). Sections were then permeabilized and incubated with a polyclonal rabbit anti-PSD95 (1:250, ab18258 Abcam, Cambridge, UK) followed by a secondary Alexa Fluor 594 goat anti-rabbit IgG (1:1000, A-11012, ThermoFisher). Slides were mounted and results scanned with the Zeiss LSM710 confocal microscope (Carl Zeiss, Jena, Germany) with the EC-Plan NEOFLUAR CS 100 \times /1.3 NA oil objective. For each animal, 5 identical image z-stacks (each stack comprising 50 optical images) from 3 hippocampal areas, CA1, CA3, and dentate gyrus (total 15 image z-stacks), were acquired.¹⁸ The mean density of clusters of NMDAR or PSD95 was obtained using a spot detection algorithm from Imaris suite v.8.1 (Oxford Instruments, Belfast, UK). The clusters of NMDAR that colocalized with PSD95 were defined as synaptic. Acute hippocampal sections in subsets of mice killed on days 10 or 11, and 18–20 after CSF infusion onset were used for electrophysiologic assessment of LTP and PPF, as reported.²²

Memory and Locomotor Activity Tasks

Visuospatial memory was determined by the discrimination index obtained from the novel object location (NOL) test, before the infusion of CSF (baseline) and on days 10, 13, 18, and 25 after infusion onset. LA was automatically determined using LA boxes (11 \times 21 \times 18 cm, Imetronic, Pessac, France) for 1 hour, at baseline, and on days 11, 14, 19, and 26, as reported¹⁸ (Figure 1B).

Statistical Analysis

Data from experiments measuring cluster densities of NMDAR and PSD95 in the brain were assessed using the Kruskal-Wallis test comparing ranks, as populations were not normally distributed according to the D'Agostino-Pearson test and Dunn corrections for multiple comparisons. The analysis of human IgG deposits and electrophysiologic data were assessed by 1-way ANOVA and unpaired *t* tests. NOL index and LA data were analyzed using repeated-measures 2-way ANOVA. All ANOVA tests included post hoc analyses with Bonferroni correction for multiple testing. In all statistical analyses, *p* value <0.05 was considered significant. For all experiments, the distribution of the data was assessed for outliers and normality. Statistical analyses were performed with GraphPad Prism v.8 (La Jolla, CA).

Data Availability

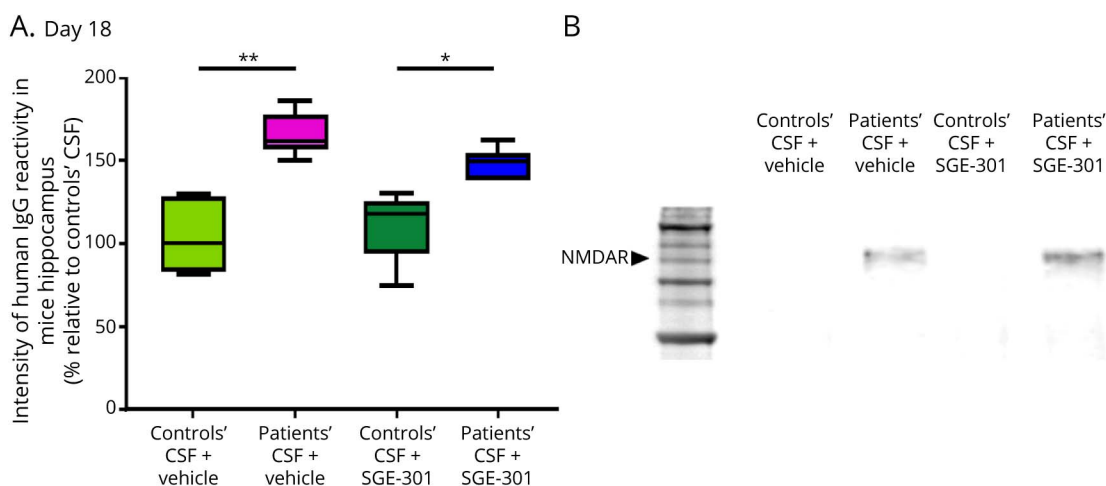
Data supporting these findings are available on reasonable request.

Results

Presence of NMDAR-Specific IgG in the Brains of Mice Infused With Patients' CSF

Compared with mice infused with controls' CSF, those infused with patients' CSF had a higher content of human IgG in the brain regardless of whether animals had been treated with SGE-301 or vehicle (Figure 2A). Immunoprecipitation

Figure 2 Presence of NMDAR-Specific IgG in the Brains of Mice Infused With Patients' CSF



(A) Quantification of human IgG immunofluorescence intensity in the brain of mice infused with patients' or controls' IgG shows an increased amount of human IgG in mice infused with patients' CSF regardless of whether mice received treatment with SGE-301 or vehicle. The median intensity of IgG immunofluorescence in the brain of mice infused with controls' CSF was defined as 100%. The number of mice per experimental group is 5. Data presented in box plots show the median and 25th, and 75th percentiles; whiskers indicate minimum and maximum. The significance of treatment effect was assessed by 1-way ANOVA. $*p = 0.0318$; $**p = 0.0064$. (B) Immunoprecipitation of NMDAR-bound IgG from mice brain exposed to patients' CSF or controls' CSF with or without SGE-301. The predicted molecular weight of 105 kDa (arrowhead) corresponds to the GluN1 subunit of the NMDAR. Each lane corresponds to the immunoprecipitation of 1 brain per each indicated condition. NMDAR = NMDA receptor.

studies showed that the IgG was specifically bound to NMDAR (Figure 2B). These findings are confirmatory of a previous study indicating that SGE-301 does not block the binding of patients' antibodies to NMDARs.²⁰

Treatment With SGE-301 Reversed the Structural and Functional Synaptic Effects of Patients' CSF

The effect of patients' or controls' CSF on the density of total cell surface or synaptic NMDAR clusters in hippocampus was examined in 50 mice, including 5 animals for each experimental group at 3 time points (days 10, 18, and 26). For each animal, 15 hippocampal areas were investigated (Figure 3A). A representative CA1 area of each experimental condition (e.g., 1 of the squares in A, right panel) on day 18 is shown at higher magnification in panel 3B. On days 10 and 18, animals infused with patients' CSF and treated with subcutaneous vehicle (without SGE-301) showed a significant decrease of total cell surface and synaptic NMDARs compared with animals infused with controls' CSF (Figure 3, C and D). In contrast, animals infused with the same patients' CSF but treated from day 11 with SGE-301 showed no changes in total or synaptic levels of NMDARs on day 18 (Figure 3D). On day 26 (12 days after the infusion of patients' CSF antibodies had stopped), the levels of total and synaptic NMDAR in all experimental groups had returned to the value of controls, as expected in this model (Figure 3E). No effects on the levels of PSD95 were observed in any of the time points investigated (days 10, 18, and 26) for all experimental groups (Figure 3B, red channel, and eFigure 1, links. www.com/NXI/A672).

Hippocampal electrophysiologic studies were performed in a total of 69 hippocampal slices from 47 mice representing the 4

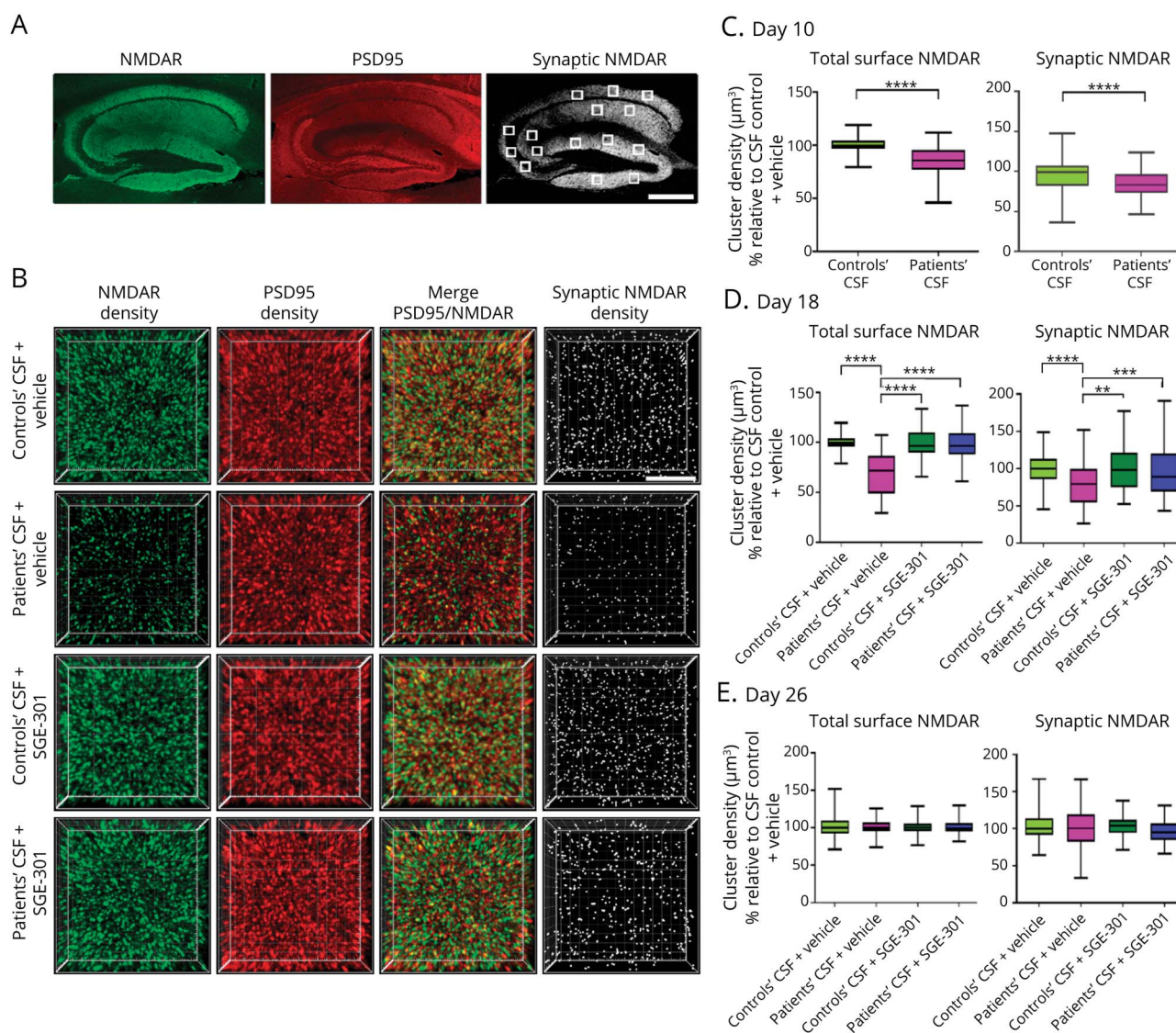
experimental groups (Figure 4A). On day 10 (before treatment with SGE-301 started), these studies showed that animals infused with patients' CSF had severe impairment of LTP compared with animals infused with controls' CSF (Figure 4, B, D, F). This impairment of hippocampal plasticity persisted until day 18 except for the group of animals that were treated with SGE-301. Indeed, animals that received the same patients' CSF and were treated from day 11 with SGE-301 had normalized LTP and memory function on day 18 (Figure 4, C, E, G).

In contrast to the severe impairment of LTP caused by patients' CSF in untreated animals, the field excitatory postsynaptic potential recordings following a standard paired-pulse protocol showed in all experimental groups (2 on day 10 and 4 on day 18) a significant facilitation consistent with increased pre-synaptic release probability (Figure 5). This finding indicates that the effects of patients' CSF antibodies are predominantly postsynaptic, as reported,^{20,22} and that SGE-301 did not significantly modify presynaptic release probability.

Treatment With SGE-301 Reversed the Memory Loss Caused by Patients' CSF

A total of 44 mice (10–12 per experimental group) were included in these studies. Compared with controls, animals infused with patients' CSF showed visuospatial memory deficits at first evaluation on day 10 (Figure 6). This memory deficit persisted until day 18 (which in this model is the time of maximal effects) and progressively recovered after the infusion of patients' CSF had stopped. In contrast, animals infused with the same patients' CSF but that from day 11 received treatment with subcutaneous SGE-301 showed a rapid recovery of memory, which as of day 13 became similar to that

Figure 3 Treatment With SGE-301 Reverses the Reduction of NMDARs Caused by Patients' CSF in the Hippocampus



(A) Hippocampus of the mouse immunolabeled for NMDAR (green) and PSD95 (red). Images were merged to demonstrate colocalizing clusters (defined as synaptic NMDAR, white color). The 15 small white squares indicate the analyzed areas in CA1, CA3, and dentate gyrus (5 each). Each square is a 3D stack of 50 sections. Scale bar = 400 μm . (B) Four magnified squares (3D projection) of a CA1 region of hippocampus representing the 4 experimental conditions and showing the analysis of density of total cell surface NMDAR, PSD95, and synaptic NMDAR clusters on day 18. The images (NMDAR, green; PSD95, red) were postprocessed and used to calculate the density of the clusters (density = spots/ μm^3). Scale bar = 5 μm . Quantification of the density of total surface NMDAR and synaptic NMDAR clusters on day 10 (C), day 18 (D), and day 26 (E) in a pooled analysis of the 15 hippocampal areas (CA1, CA3, and dentate gyrus) for each experimental condition. Mean density of clusters in animals treated with controls' CSF + vehicle was defined as 100%. For each condition, 5 animals were examined. Box plots show the median and 25th and 75th percentiles; whiskers indicate the minimum and maximum values. Significance of the treatment effect was assessed using the Kruskal-Wallis test, **** p < 0.0001; *** p < 0.001; ** p = 0.008. NMDAR = NMDA receptor.

of controls. These animals not only showed earlier memory recovery but also remained without memory deficits even though from day 11 to 14 they continued receiving patients' CSF antibodies. The total time of exploration of the 2 objects (not moved + novel location) was similar in animals of the 4 experimental groups (data not shown). No abnormal behavior or side effects were observed in animals infused with controls' CSF and treated with SGE-301. The LA was also similar in the 4 groups (data not shown).

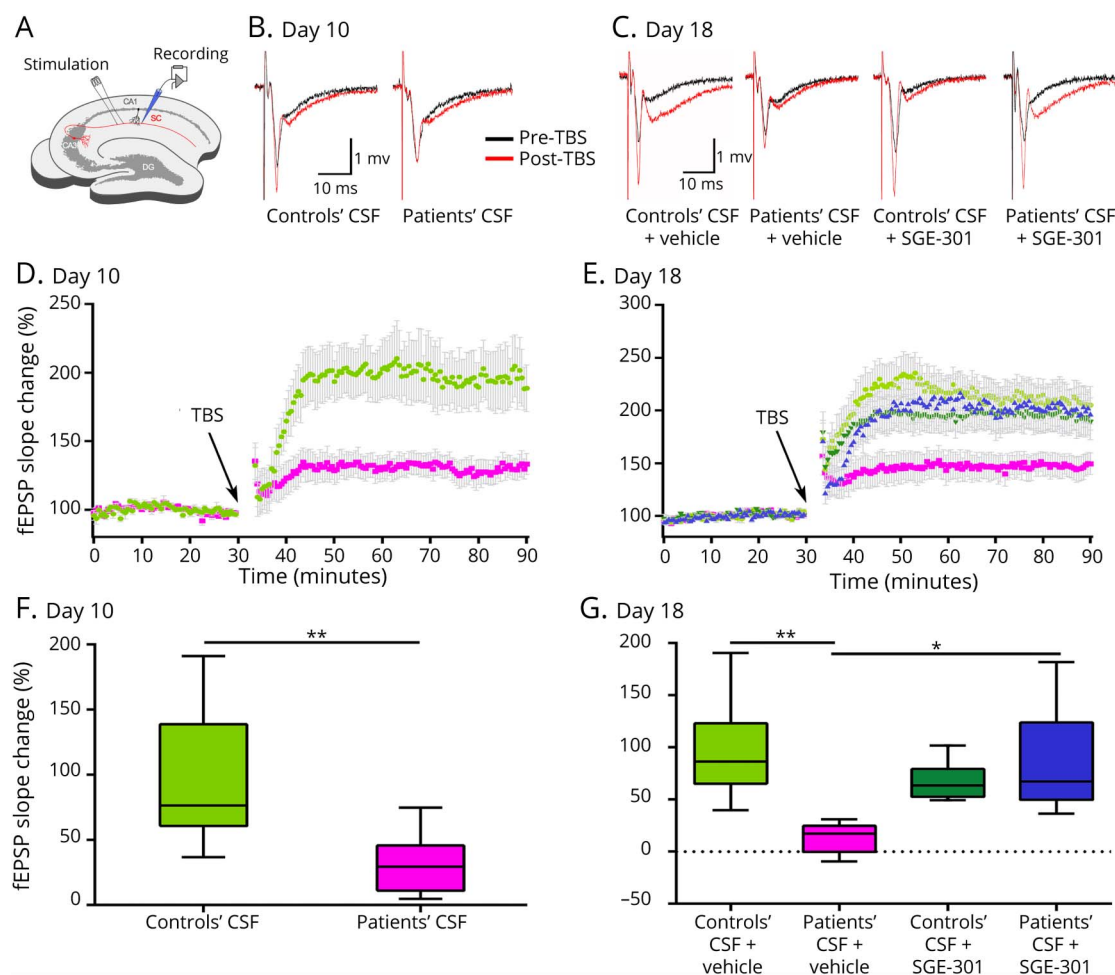
Taken together, treatment with SGE-301 resulted in an improvement of memory deficits and restoration of synaptic

levels of NMDAR and LTP that had been impaired by CSF from patients with anti-NMDAR encephalitis. The treatment effect was particularly notable on day 18, when all paradigms (memory, clusters of NMDAR, and LTP) are consistently impaired in this model but, as shown here, were reversed to normal after treatment with SGE-301.

Discussion

We show that SGE-301, a synthetic analog of a major brain-derived cholesterol metabolite, 24(S)-HC, reversed the pathogenic effects of CSF from patients with anti-NMDAR

Figure 4 Treatment With SGE-301 Reverses the Impairment of LTP Caused by Patients' CSF

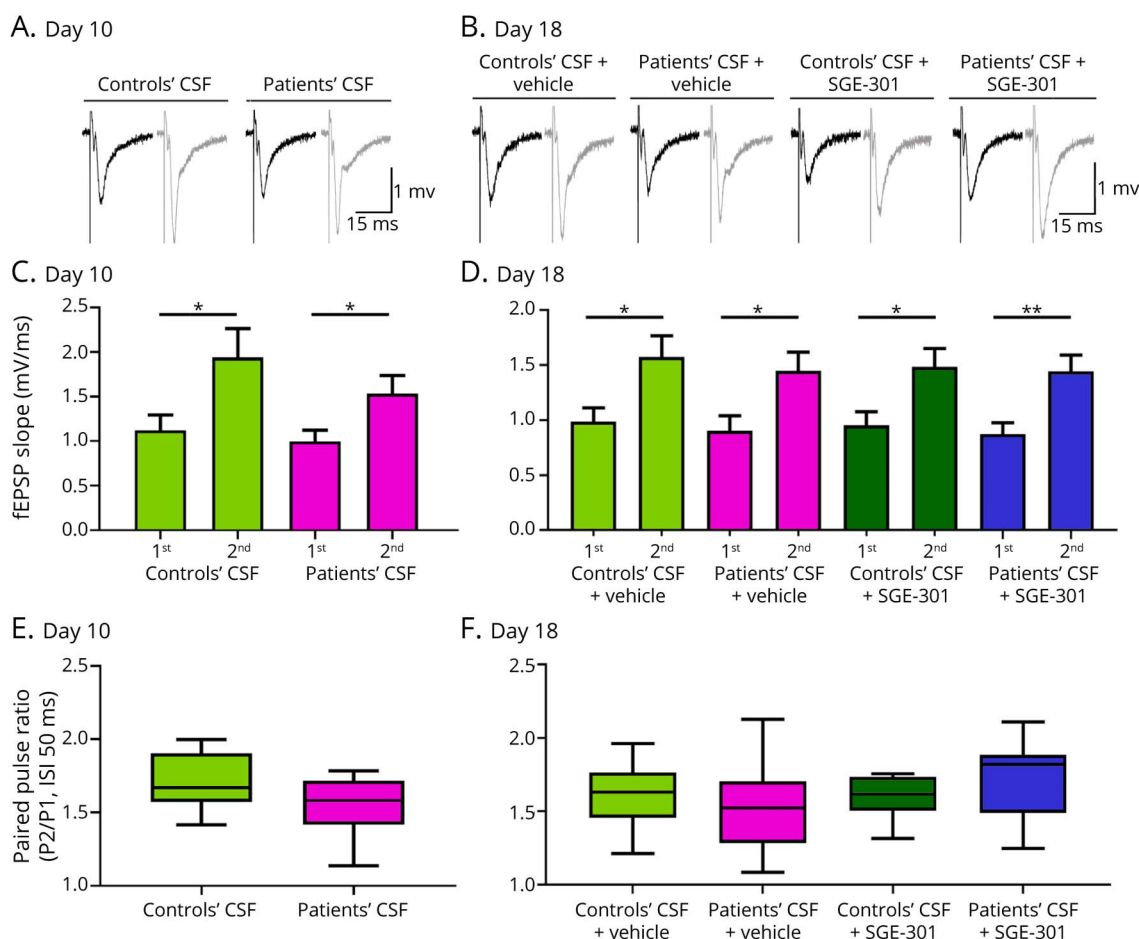


(A) The Schaffer collateral pathway (SC, red) was stimulated, and field potentials were recorded in the CA1 region of the hippocampus. Long-term potentiation (LTP) was induced by theta-burst stimulation (TBS); DG = dentate gyrus; CA = cornu ammonis. (B and C) Example traces of individual recordings showing baseline field excitatory postsynaptic potentials (fEPSPs) before LTP induction (black traces) and after LTP (red traces) (B) at day 10 and (C) day 18. (D and E) Time course of fEPSP recordings at day 10 (D) and day 18 (E) showing robust changes in the fEPSP slope in the animals infused with controls' CSF treated or not with SGE-301 (dark or light green traces) and in the animals infused with patients' CSF treated with SGE-301 (day 18, blue trace). Animals infused with the same patients' CSF but not treated with SGE-301 showed a marked impairment of LTP induction (pink traces in D and E). The fEPSP slopes of all animals for each of the groups are presented as mean \pm SEM. (F and G) Quantification of the fEPSP slope change showing a significant reduction of the fEPSP slope in animals infused with patients' CSF not treated with SGE-301 compared with animals infused with the same patients' CSF treated with SGE-301 or animals infused with controls' CSF (treated or untreated with SGE-301). Number of slices and animals used on day 10: controls' CSF, number of acute slices $n = 7$ from 6 mice; patients' CSF, $n = 8$ from 6 mice. Day 18: controls' CSF + vehicle, $n = 8$ from 6 mice; patients' CSF + vehicle, $n = 9$ from 7 mice; controls' CSF + SGE-301, $n = 8$ from 6 mice; and patients' CSF + SGE-301, $n = 8$ from 6 mice. Box plots show the median and 25th and 75th percentiles; whiskers indicate minimum and maximum values. Significance was assessed using 1-way ANOVA, and the Bonferroni post hoc correction test was applied. Day 10: $^{**}p = 0.0063$ and day 18: $^{*}p = 0.0039$, $^{*}p = 0.0229$.

encephalitis, including the antibody-mediated reduction of NMDAR clusters and impairment of visuospatial memory and synaptic plasticity. These findings are important considering that the main treatment options currently available for anti-NMDAR encephalitis are limited to escalation of immunotherapy and symptom management (e.g., psychosis, seizures, autonomic dysregulation, or hypoventilation) with non-disease-specific treatments.²⁴ Although this treatment approach is successful in improving or resolving the symptoms of the acute phase of the disease in 75%–80% of patients, virtually all patients transition to a second stage characterized by prolonged deficits of memory, attention, and executive functions. These deficits usually show a slow progressive improvement over

many months, or in some patients, they remain as persistent sequelae.^{2,3,7,13,25,26} The mechanisms underlying this protracted stage of the disease are less known than those of the acute stage; for example, the signs of inflammation (CSF pleocytosis and MRI changes) usually observed in the initial stage are no longer present despite that NMDAR antibodies are detectable in CSF.²⁷ The usefulness of immunotherapy during this second stage is also unclear, and there are no guidelines for treatment. Some investigators maintain treatment with first- or second-line immunotherapies for 1–2 years or use mycophenolate mofetil or azathioprine,²⁸ whereas others (including ourselves) use symptomatic treatment and a close follow-up to promptly retreat with immunotherapy if there is clinical worsening.

Figure 5 Paired-Pulse Facilitation Is Unaffected in Animals Infused With Patients' CSF and Treated With or Without SGE-301



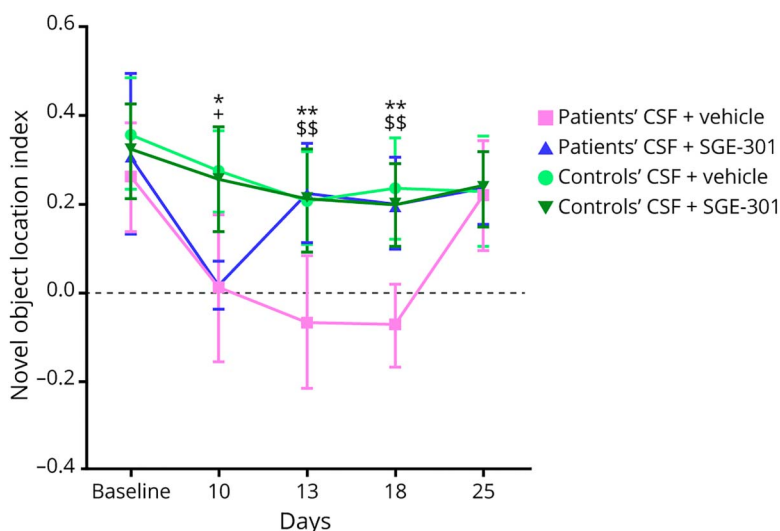
(A and B) Example traces of fEPSPs in the paired-pulse facilitation protocol applied to the Schaffer collateral—CA1 synaptic region on days 10 (A) and 18 (B). In all experimental groups, the fEPSP slope and amplitude in the response to the second stimulus (gray) are increased compared with the fEPSP slope and amplitude after the first stimulus (black). The interstimulus interval is 50 ms. (C and D) Mean slope values of fEPSP responses obtained after the first (1st) stimulus and second (2nd) stimulus on days 10 (C) and 18 (D). All experimental groups of animals show a significant increase in the fEPSP slope after the second stimulus. Number of slices and animals used on day 10: controls' CSF ($n = 8$ recordings from 5 animals); patients' CSF ($n = 10$ recordings from 7 animals). Day 18: controls' CSF + vehicle ($n = 14$ recordings from 9 animals, light green); patients' CSF + vehicle ($n = 14$ recordings from 9 animals, pink); controls' CSF + SGE-301 ($n = 10$ recordings from 8 animals, dark green); patients' CSF + SGE-301 ($n = 13$ recordings from 9 animals, blue). Data are shown as mean \pm SEM. Significance of the fEPSP slope increase on the second stimulus was assessed by unpaired t tests. Day 10: controls' CSF, $*p = 0.0424$; patients' CSF $*p = 0.0380$. Day 18: controls' CSF + vehicle, $*p = 0.0162$; patients' CSF + vehicle, $*p = 0.0424$; controls' CSF + SGE-301, $*p = 0.0194$; patients' CSF + SGE-301, $**p < 0.0039$. (E and F) Paired-pulse facilitation, calculated as P2/P1 (pulse 2/pulse 1) fEPSP slope ratio, is not altered in any of the experimental groups of animals on days 10 (E) and 18 (F) when compared with that of the group infused with controls' CSF + vehicle. The number of recordings and animals used are the same as those indicated above. Box plots show the median and 25th and 75th percentiles; whiskers indicate minimum and maximum values. The significance of the results was assessed using 1-way ANOVA. fEPSP = field excitatory postsynaptic potential.

The model of cerebroventricular transfer of patients' CSF that we have used here shows more similarities to the second stage than to the initial stage of anti-NMDAR encephalitis. In this model, animals receive patients' CSF NMDAR antibodies which, as previously reported,^{18,20,22} bind and internalize NMDARs, without inflammatory changes, but causing an impairment of memory and hippocampal plasticity for as long as the antibodies are present in the brain. The model has been useful in demonstrating the pathogenicity of patients' antibodies and offers the possibility of testing compounds of potential therapeutic utility, such as SGE-301.

Although the exact mechanism of action of SGE-301 has not been fully characterized, we and others previously reported that

it increases channel's open probability and slows the decay phase of the spontaneous excitatory postsynaptic currents (EPSCs), potentiating NMDAR-mediated EPSCs.^{19,20,29} In a study in which cultured rat hippocampal neurons were exposed for 48 hours to patients' CSF or controls' CSF and during the last 24 hours, each condition was treated with SGE-301 or vehicle (no drug); those that were treated with SGE-301 showed increased NMDAR function compared with the untreated.²⁹ In a previous report, we showed that SGE-301 antagonized the antibody-mediated reduction of NMDARs in cultured neurons and prevented the development of memory deficits in a model of cerebroventricular transfer of patients' CSF similar to that used here.²⁰ Of interest, SGE-301 did not block the antibody binding to the brain but significantly decreased (without fully

Figure 6 SGE-301 Reverses the Memory Deficit Caused by Patients' CSF



Mice infused with patients' CSF and treated with vehicle (pink line) showed a significant reduction of the Novel Object Location (NOL) index. This memory deficit was reversed in the group of mice infused with the same patients' CSF but treated from day 11 with SGE-301 (blue line). Note that by day 13, the NOL index of these treated animals has recovered to levels similar to those of controls. No significant memory changes were noted in the groups of mice infused with controls' CSF and treated with vehicle (light green line) or SGE-301 (dark green line). Number of animals: controls' CSF + vehicle, $n = 11$; patients' CSF + vehicle, $n = 10$; controls' CSF + SGE-301, $n = 12$; patients' CSF + SGE-301, $n = 11$. A higher NOL index represents better visuospatial memory. Data are presented as mean \pm 95% CI. Significance of assessment was performed by repeated-measures 2-way analysis of variance (ANOVA; $p < 0.0001$) with Bonferroni post hoc correction. Day 10 (pretreatment with SGE or vehicle): patients' CSF vs controls' CSF that will both start treatment with vehicle, $*p = 0.0186$; patients' CSF vs controls' CSF that will both start treatment with SGE-301, $+p = 0.0314$. Day 13: patients' CSF + vehicle vs controls' CSF + vehicle, $**p = 0.0081$; patients' CSF + vehicle vs patients' CSF + SGE-301, $$$p = 0.0041$. Day 18: patients' CSF + vehicle vs controls' CSF + vehicle, $**p = 0.0016$; patients' CSF + vehicle vs patients' CSF + SGE-301, $$$p = 0.0090$.

preventing) antibody-mediated NMDAR internalization. In addition, treatment with SGE-301 prevented the development of LTP impairment caused by patients' CSF antibodies.²⁰ These and the current findings suggest that SGE-301 also increases the recruitment of NMDAR to the synapse to restore the levels and function of synaptic NMDARs. The exact mechanism that facilitates this recruitment is currently unknown and should be the focus of future investigations.

These studies, however, did not allow the assessment of whether SGE-301 is able to reverse the memory and synaptic alterations caused by patients' CSF because SGE-301 (used subcutaneously and at the same dose as here) was administered simultaneously with the ventricular infusion of patients' antibodies, and none of the animals developed clinical or synaptic alterations.²⁰ Thus, we have adapted the model so that the administration of SGE-301 starts after synaptic and memory alterations have already developed. Of interest, between days 10 and 18, which in this model is the period of progressive development of severe memory and synaptic alterations, SGE-301 was able to reverse all antibody-mediated pathogenic effects (memory deficit, reduction of synaptic clusters of NMDARs, and LTP impairment) despite that during 4 days (days 10–14), animals continued receiving the infusion of patients' CSF.

We believe that the animal model used here is the best currently available model to assess the pathogenic effect of patients' CSF antibodies and the utility of drugs aimed to reverse this effect. Yet, the study has limitations inherent to this model. For example, we mainly focused on visuospatial memory as a surrogate marker of behavior because in this model, the memory deficit is the most severely affected paradigm and consistently shows a highly predictable alteration detectable from days 10 to 18 of patients' CSF infusion. This provides a good time interval of 9

days and an intermediate point of assessment (day 13) to determine the treatment efficacy of SGE-301 and to estimate the speed of recovery (e.g., by day 13, the memory deficit was already reversed and remained unaffected until the end of the experiment). The fact that the structural and functional synaptic alterations that underlie the symptoms of this model were also reversed supports the potential utility of PAMs of NMDARs as adjuvant treatment in the second stage of anti-NMDAR encephalitis. It is unclear whether SGE-301 may be effective in improving symptoms in the acute phase or first stage of the disease. In clinical practice, however, assessment of any adjuvant treatment in the acute phase will be challenging because of the presence of concurrent symptoms (seizures, dyskinesias, autonomic instability, or decreased level of consciousness), complications, and use of multiple different treatments.^{1,3,30}

Overall, the current findings along with those of previous studies^{19,20,29} support the potential clinical utility of PAMs of NMDAR in patients with anti-NMDAR encephalitis and deserve future testing in the context of a clinical trial. There are ongoing studies with an oxysterol biology-based PAM closely related to SGE-301 (SAGE-718) optimized for clinical applications (e.g., oral bioavailability) that showed a good tolerability profile in healthy volunteers in a double-blind, placebo-controlled phase 1 single ascending disease study³¹ and is currently being used in a trial of Huntington disease (which at early stages, associates with hypofunction of NMDARs). Another task for the future is to assess the efficacy of oxysterol-based PAMs in an experimental setting that reproduces the acute inflammatory phase of anti-NMDAR encephalitis, such as in a model of active immunization with NMDARs.

Acknowledgment

The authors thank Michael C. Quirk and Albert J. Robichaud from Sage Therapeutics, Cambridge, MA, USA, for their

critical review of the manuscript, and Mercedes Alba and Eva Caballero (IDIBAPS, Hospital Clínic, University of Barcelona) for their technical support.

Study Funding

Plan Nacional de I+D+I and cofinanced by the ISCIII—Subdirección General de Evaluación y Fomento de la Investigación Sanitaria and the Fondo Europeo de Desarrollo Regional (ISCIII-FEDER; FIS 20/00197, FIS 20/00280, FIS 018/00067, and FIS 17/00296); Project Integrative of Excellence (PIE16/00014); CIBERER (#CB15/00010); “la Caixa” Banking Foundation (ID 100010434, under the agreement LCF/PR/HR17/S2150001); ERA-NET NEURON/Instituto Carlos III (AC18-00009); The Safra Foundation, and Fundació CELLEX; RETICs Ofsted RD16/0008/0014; FI-AGAUR grant program by the Generalitat de Catalunya (2020FI_B2 00208); Maria de Maeztu MDM-2017-0729; and Basque Government Doctoral Fellowship Programme (PRE_2020_2_0219).

Disclosure

J.D. receives royalties from Athena Diagnostics for the use of Ma2 as an autoantibody test and from Euroimmun for the use of NMDA as an antibody test. He received a licensing fee from Euroimmun for the use of GABAB receptor, GABAA receptor, DPPX, and IgLON5 as autoantibody tests; he has received a research grant from Sage Therapeutics. M.L. works at Sage Therapeutics. M.R., J.P., F.M., A.M., E.A., L.S., J.L., A.G-S., E.M., and X.G. report no disclosures. Go to [Neurology.org/NN](https://www.neurology.org/NN) for full disclosures.

Publication History

Received by *Neurology: Neuroimmunology & Neuroinflammation* September 3, 2021. Accepted in final form October 21, 2021.

Appendix Authors

Name	Location	Contribution
Marija Radosevic, PhD	Institut d'Investigacions Biomèdiques August Pi i Sunyer (IDIBAPS), Hospital Clínic, Universitat de Barcelona, Barcelona, Spain	Drafting/revision of the manuscript for content, including medical writing for content; major role in the acquisition of data; study concept or design; and analysis or interpretation of data
Jesús Planagumà, PhD	Institut d'Investigacions Biomèdiques August Pi i Sunyer (IDIBAPS), Hospital Clínic, Universitat de Barcelona, Barcelona, Spain	Drafting/revision of the manuscript for content, including medical writing for content; major role in the acquisition of data; study concept or design; and analysis or interpretation of data
Francesco Mannara, PhD	Institut d'Investigacions Biomèdiques August Pi i Sunyer (IDIBAPS), Hospital Clínic, Universitat de Barcelona, Barcelona, Spain	Drafting/revision of the manuscript for content, including medical writing for content; major role in the acquisition of data; study concept or design; and analysis or interpretation of data

Appendix (continued)

Name	Location	Contribution
Araceli Mellado, BS	Institut d'Investigacions Biomèdiques August Pi i Sunyer (IDIBAPS), Hospital Clínic, Universitat de Barcelona, Barcelona, Spain	Major role in the acquisition of data
Esther Aguilar, BS	Institut d'Investigacions Biomèdiques August Pi i Sunyer (IDIBAPS), Hospital Clínic, Universitat de Barcelona, Barcelona, Spain	Major role in the acquisition of data
Lidia Sabater, PhD	Institut d'Investigacions Biomèdiques August Pi i Sunyer (IDIBAPS), Hospital Clínic, Universitat de Barcelona, Barcelona, Spain	Analysis or interpretation of data; additional contributions: acquisition of data
Jon Landa, MSc	Institut d'Investigacions Biomèdiques August Pi i Sunyer (IDIBAPS), Hospital Clínic, Universitat de Barcelona, Barcelona, Spain	Additional contributions: acquisition of data
Anna García-Serra, PhD	Institut d'Investigacions Biomèdiques August Pi i Sunyer (IDIBAPS), Hospital Clínic, Universitat de Barcelona, Barcelona, Spain	Additional contributions: acquisition of data
Estibaliz Maudes, MSc	Institut d'Investigacions Biomèdiques August Pi i Sunyer (IDIBAPS), Hospital Clínic, Universitat de Barcelona, Barcelona, Spain	Additional contributions: acquisition of data
Xavier Gasull, PhD	Institut d'Investigacions Biomèdiques August Pi i Sunyer (IDIBAPS), Hospital Clínic, Universitat de Barcelona, Barcelona, Spain; Laboratori de Neurofisiologia, Departament de Biomedicina, Facultat de Medicina i Ciències de la Salut, Institut de Neurociències, Universitat de Barcelona, Barcelona, Spain	Analysis or interpretation of data
Mike Lewis, PhD	Sage Therapeutics, Department of Research and Nonclinical Development, Cambridge, MA	Drafting/revision of the manuscript for content, including medical writing for content; study concept or design; and analysis or interpretation of data
Josep Dalmau, MD, PhD	Institut d'Investigacions Biomèdiques August Pi i Sunyer (IDIBAPS), Hospital Clínic, Universitat de Barcelona, Barcelona, Spain; Department of Neurology, University of Pennsylvania, Philadelphia, PA; Institució Catalana de Recerca i Estudis Avançats (ICREA), Barcelona, Spain	Drafting/revision of the manuscript for content, including medical writing for content; study concept or design; and analysis or interpretation of data

References

- Dalmau J, Gleichman AJ, Hughes EG, et al. Anti-NMDA-receptor encephalitis: case series and analysis of the effects of antibodies. *Lancet Neurol*. 2008;7(12):1091-1098.

2. Florance NR, Davis RL, Lam C, et al. Anti-N-methyl-D-aspartate receptor (NMDAR) encephalitis in children and adolescents. *Ann Neurol*. 2009;66(1):11-18.
3. Titulaer MJ, McCracken L, Gabilondo I, et al. Treatment and prognostic factors for long-term outcome in patients with anti-NMDA receptor encephalitis: an observational cohort study. *Lancet Neurol*. 2013;12(2):157-165.
4. Ariño H, Muñoz-Lopetegi A, Martínez-Hernández E, et al. Sleep disorders in anti-NMDAR encephalitis. *Neurology*. 2020;95(6):e671-e684.
5. Wang W, Li JM, Hu FY, et al. Anti-NMDA receptor encephalitis: clinical characteristics, predictors of outcome and the knowledge gap in southwest China. *Eur J Neurol*. 2016;23(3):621-629.
6. Zhang Y, Liu G, Jiang M, Chen W, He Y, Su Y. Clinical characteristics and prognosis of severe anti-N-methyl-D-aspartate receptor encephalitis patients. *Neurocrit Care*. 2018;29(2):264-272.
7. Xu X, Lu Q, Huang Y, et al. Anti-NMDAR encephalitis: a single-center, longitudinal study in China. *Neurol Neuroimmunol Neuroinflamm*. 2020;7(1):e633.
8. Dalmau J, Lancaster E, Martinez-Hernandez E, Rosenfeld MR, Balice-Gordon R. Clinical experience and laboratory investigations in patients with anti-NMDAR encephalitis. *Lancet Neurol*. 2011;10(1):63-74.
9. Finke C, Kopp UA, Prüss H, Dalmau J, Wandinger KP, Ploner CJ. Cognitive deficits following anti-NMDA receptor encephalitis. *J Neurol Neurosurg Psychiatry*. 2012;83(2):195-198.
10. Shim Y, Kim SY, Kim H, et al. Clinical outcomes of pediatric Anti-NMDA receptor encephalitis. *Eur J Paediatr Neurol*. 2020;29:87-91.
11. Blum RA, Tomlinson AR, Jetté N, Kwon CS, Easton A, Yeshokumar AK. Assessment of long-term psychosocial outcomes in anti-NMDA receptor encephalitis. *Epilepsy Behav*. 2020;108:107088.
12. Tomlinson AR, Blum RA, Jetté N, Kwon CS, Easton A, Yeshokumar AK. Assessment of care transitions and caregiver burden in anti-NMDA receptor encephalitis. *Epilepsy Behav*. 2020;108:107066.
13. de Bruijn M, Aarsen FK, van Oosterhout MP, et al. Long-term neuropsychological outcome following pediatric anti-NMDAR encephalitis. *Neurology*. 2018;90(22):e1997-e2005.
14. Hughes EG, Peng X, Gleichman AJ, et al. Cellular and synaptic mechanisms of anti-NMDA receptor encephalitis. *J Neurosci*. 2010;30(17):5866-5875.
15. Zrzavy T, Endmayr V, Bauer J, et al. Neuropathological variability within a spectrum of NMDAR-encephalitis. *Ann Neurol*. 2021;90:725-737.
16. Wirtz PW, Titulaer MJ, Gerven JM, Verschuuren JJ. 3,4-diaminopyridine for the treatment of Lambert-Eaton myasthenic syndrome. *Expert Rev Clin Immunol*. 2010;6(6):867-874.
17. Newsom-Davis J. Therapy in myasthenia gravis and Lambert-Eaton myasthenic syndrome. *Semin Neurol*. 2003;23(2):191-198.
18. Planagumà J, Leypoldt F, Mannara F, et al. Human N-methyl D-aspartate receptor antibodies alter memory and behaviour in mice. *Brain*. 2015;138(pt 1):94-109.
19. Paul SM, Doherty JJ, Robichaud AJ, et al. The major brain cholesterol metabolite 24(S)-hydroxycholesterol is a potent allosteric modulator of N-methyl-D-aspartate receptors. *J Neurosci*. 2013;33(44):17290-17300.
20. Mannara F, Radosevic M, Planagumà J, et al. Allosteric modulation of NMDA receptors prevents the antibody effects of patients with anti-NMDAR encephalitis. *Brain*. 2020;143(9):2709-2720.
21. Shu HJ, Zeng CM, Wang C, Covey DF, Zorumski CF, Mennerick S. Cyclodextrins sequester neuroactive steroids and differentiate mechanisms that rate limit steroid actions. *Br J Pharmacol*. 2007;150(2):164-175.
22. Planagumà J, Haselmann H, Mannara F, et al. Ephrin-B2 prevents N-methyl-D-aspartate receptor antibody effects on memory and neuroplasticity. *Ann Neurol*. 2016;80(3):388-400.
23. Moscato EH, Peng X, Jain A, Parsons TD, Dalmau J, Balice-Gordon RJ. Acute mechanisms underlying antibody effects in anti-N-methyl-D-aspartate receptor encephalitis. *Ann Neurol*. 2014;76(1):108-119.
24. Dalmau J, Armangué T, Planagumà J, et al. An update on anti-NMDA receptor encephalitis for neurologists and psychiatrists: mechanisms and models. *Lancet Neurol*. 2019;18(11):1045-1057.
25. Viacoz A, Desestret V, Ducray F, et al. Clinical specificities of adult male patients with NMDA receptor antibodies encephalitis. *Neurology*. 2014;82(7):556-563.
26. Irani SR, Bera K, Waters P, et al. N-methyl-D-aspartate antibody encephalitis: temporal progression of clinical and paraclinical observations in a predominantly non-paraneoplastic disorder of both sexes. *Brain*. 2010;133(pt 6):1655-1667.
27. Gresa-Arribas N, Titulaer MJ, Torrents A, et al. Antibody titres at diagnosis and during follow-up of anti-NMDA receptor encephalitis: a retrospective study. *Lancet Neurol*. 2014;13:167-177.
28. Nosadini M, Mohammad SS, Toldo I, Sartori S, Dale RC. Mycophenolate mofetil, azathioprine and methotrexate usage in paediatric anti-NMDAR encephalitis: a systematic literature review. *Eur J Paediatr Neurol*. 2019;23(1):7-18.
29. Warikoo N, Brunwasser SJ, Benz A, et al. Positive allosteric modulation as a potential therapeutic strategy in anti-NMDA receptor encephalitis. *J Neurosci*. 2018;38(13):3218-3229.
30. de Montmollin E, Demeret S, Brule N, et al. Anti-N-methyl-d-aspartate receptor encephalitis in adult patients requiring intensive care. *Am J Respir Crit Care Med*. 2017;195(4):491-499.
31. Koenig A, Murck H, Paskavitz J, et al. Double-blind, placebo-controlled phase 1 single ascending dose study of SAHE-718. *International College of Neuropsychopharmacology (CINP) 2019 Congress*. Athens, Greece, 2019.

Paper V

Positive allosteric modulation of NMDARs prevents the altered surface dynamics caused by patients' antibodies.

Estibaliz Maudes, Zoë Jamet, Laura Marmolejo, Josep Dalmau,
Laurent Groc.

Neurology: Neuroimmunology & Neuroinflammation.

2024, 11(4), e200261.

IF JCR 2022: 8.8 (D1).

Positive Allosteric Modulation of NMDARs Prevents the Altered Surface Dynamics Caused by Patients' Antibodies

Estibaliz Maudes, MSc, Zoë Jamet, PhD, Laura Marmolejo, MSc, Josep O. Dalmau, MD, PhD, and Laurent Groc, PhD

Correspondence

Dr. Groc
laurent.groc@u-bordeaux.fr

Neurol Neuroimmunol Neuroinflamm 2024;11:e200261. doi:10.1212/NXI.000000000200261

Abstract

Objectives

A positive allosteric modulator of the NMDAR, SGE-301, has been shown to reverse the alterations caused by the antibodies of patients with anti-NMDAR encephalitis (NMDARe). However, the mechanisms involved beyond receptor modulation are unclear. In this study, we aimed to investigate how this modulator affects NMDAR membrane dynamics.

Methods

Cultured hippocampal neurons were treated with SGE-301 or vehicle, alongside with immunoglobulins G (IgG) from patients with NMDARe or healthy controls. NMDAR surface dynamics were assessed with single-molecule imaging by photoactivated localization microscopy.

Results

NMDAR trajectories from neurons treated with SGE-301 were less confinement, with increased diffusion coefficients. This effect mainly occurred at synapses because extrasynaptic diffusion and confinement were minimally affected by SGE-301. Treatment with patients' IgG reduced NMDAR surface dynamics and increased their confinement. Remarkably, SGE-301 incubation antagonized patients' IgG effects in both synaptic and extrasynaptic membrane compartments, restoring diffusion and confinement values similar to those from neurons exposed to control IgG.

Discussion

We demonstrate that SGE-301 upregulates NMDAR surface diffusion and antagonizes the pathogenic effects of patients' IgG on NMDAR membrane organization. These findings suggest a potential therapeutic strategy for NMDARe.

Introduction

Anti-NMDA receptor encephalitis (NMDARe) is a neurologic disease mediated by antibodies (NMDAR-Ab) against the GluN1 subunit of the NMDAR. Patients develop severe neuropsychiatric symptoms that improve with immunotherapy, but the improvement can be remarkably slow, often taking several months for cognitive and psychiatric recovery. Other than immunotherapy, there are no specific treatments that boost clinical recovery.¹ In the rodent hippocampus, patients' NMDAR-Ab alter the NMDAR surface dynamics and synaptic content, affecting synaptic plasticity and behaviors.²⁻⁴

The synthetic oxysterol SGE-301, a positive allosteric modulator (PAM) of the NMDAR, increases NMDAR open channel probability and prolongs spontaneous excitatory currents.^{5,6}

From the Neuroimmunology Program (E.M., L.M., J.O.D.), Fundació Clinic per la Recerca Biomèdiques August Pi i Sunyer (FCRB-IDIBAPS), University of Barcelona, Spain; and University of Bordeaux (Z.J., L.G.), CNRS, Interdisciplinary Institute for Neuroscience, IINS, UMR 5297, Bordeaux, France.

Go to [Neurology.org/NN](https://www.neurology.org/NN) for full disclosures. Funding information is provided at the end of the article.

The Article Processing Charge was funded by the authors.

This is an open access article distributed under the terms of the Creative Commons Attribution-NonCommercial-NoDerivatives License 4.0 (CC BY-NC-ND), which permits downloading and sharing the work provided it is properly cited. The work cannot be changed in any way or used commercially without permission from the journal.

In neurons exposed to patients' NMDAR-Ab, this molecule did not block the binding of antibodies but prevented the reduction of cell surface NMDAR without fully abrogating receptor internalization.⁶ Moreover, in mice infused with NMDAR-Ab, SGE-301 antagonized and reversed all pathogenic effects, including membrane receptor content and behavioral alterations.^{7,8} Yet, the mechanisms underpinning these beneficial effects are not fully understood, leading to postulate that in addition to act as PAM, SGE-301 changes the NMDAR surface dynamics. Here, we address this hypothesis examining how SGE-301 modulates NMDAR membrane dynamics.

Methods

Patients' Purified IgG

IgG was purified from pooled serum from 6 patients with NMDARe and 2 healthy blood donors using protein A/G agarose beads' columns (Pierce, Rockford, IL) and stored at -80°C until use. The reactivity of purified IgG against NMDAR was confirmed as reported.⁹

Primary Cell Culture, Transfection, and Treatments

Hippocampal cultured neurons were prepared from E18 Sprague-Dawley rats, as reported.² Neurons were transfected at 10 days in vitro with Homer-GFP and GluN1-mEos3.2 using calcium phosphate transfection.¹⁰ SGE-301 was prepared as reported.⁷ Neurons were incubated for 12 hours in medium containing vehicle (dimethyl sulfoxide) or SGE-301. To assess the ability of SGE-301 and to prevent the effects of patient's NMDAR-Ab, neurons were incubated with 100 $\mu\text{g}/\text{mL}$ of control or patients' IgG, in combination with SGE-301 or vehicle.

Single-Particle Tracking by Photoactivation Localization Microscopy (PALM)

Neurons were imaged in an open chamber (Ludin chamber, Life Imaging Services) with 1 mL of Tyrode solution at 37°C . The chamber was mounted on a Nikon Ti Eclipse microscope (Nikon France S.A.S.) equipped with a Perfect Focus System, an iLas² TIRF arm (Gataca Systems), an Apo TIRF 100X oil-immersion objective, and an ORCA-Fusion BT sCMOS camera (Hamamatsu) with a final pixel size of 65 nm. Transfected cells were detected with a Homer-GFP signal, and GluN1-mEos3.2 was photoactivated using a 405 nm laser. The resulting photoconverted single-molecule fluorescence was excited with a 561 nm laser. Both 405 nm and 561 nm lasers illuminated the sample simultaneously. Acquisition was performed using Metamorph software, with 2000 frames and exposure time of 50 ms with a TIRF illumination to track surface GluN1-mEos. Detection and reconnection of trajectories were performed with PALM Tracer plugin for Metamorph. Homer-GFP was used as a synaptic marker to discriminate synaptic and extrasynaptic NMDAR trajectories. Mean square displacement (MSD) and diffusion coefficient were calculated as previously described.²

Data and Statistical Analyses

Violin plots have dashed lines and dotted lines and the median and quartiles $\pm 25\text{--}75\%$, respectively. All other group values are expressed as mean \pm SEM. Each data series was obtained from 4 independent cell cultures. Normality was assessed by the Shapiro-Wilk test. Statistical comparisons were performed with 1- or 2-way ANOVA with multiple comparisons corrected by the false discovery rate (Benjamini, Krieger, and Yekutieli). The significance level was defined as $p < 0.05$.

Ethical Approval

The use of patients' samples for research purposes and animal procedures complied with European 210/63/UE and Spanish RD53/2013 requirements and were approved by the local ethical committees of the Universities of Barcelona (Spain) and Bordeaux (France).

Results

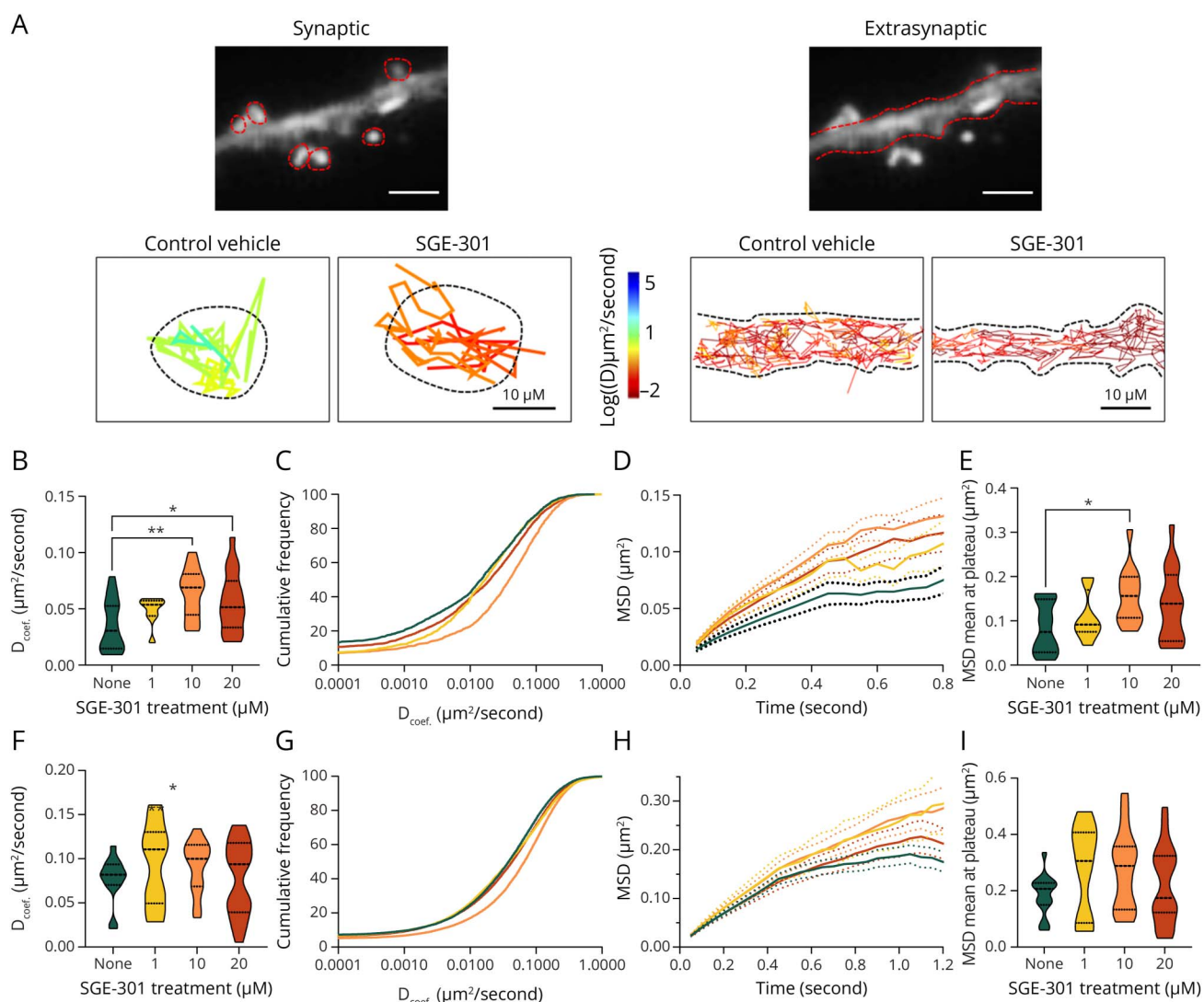
SGE-301 Increases Surface NMDAR Dynamics

To determine the effects of SGE-301 on NMDAR surface dynamics, we used the PALM approach to track synaptic and extrasynaptic NMDAR in hippocampal neurons treated with vehicle or various concentrations of SGE-301 (Figure 1A). The surface diffusion of synaptic NMDAR was significantly increased in neurons exposed to concentrations $\geq 10 \mu\text{M}$ (Figure 1B). The cumulative distributions of diffusion coefficients were shifted to the right in the presence of SGE-301 above $10 \mu\text{M}$ (Figure 1C). Furthermore, NMDAR trajectories were less confined in the presence of SGE-301 (Figure 1, D and E). These findings indicate that SGE-301, at a minimal concentration of $10 \mu\text{M}$, upregulates the surface dynamics of synaptic NMDAR. However, the surface diffusion and confinement of extrasynaptic NMDAR trajectories remain mainly unaltered in the presence of SGE-301 (Figure 1, F–I). These data demonstrate that SGE-301 upregulates NMDAR surface dynamics mainly at the synapse.

SGE-301 Counteracts Patient's NMDAR-Ab-Induced Alteration of NMDAR Dynamics

To determine whether SGE-301 could prevent the pathogenic effects of patients' antibodies on the surface dynamics of NMDAR,² neurons were exposed for 12 hours to either control or NMDAR-Abs ($100 \mu\text{g}/\text{mL}$) in addition to vehicle or SGE-301 ($10 \mu\text{M}$) (Figure 2A). In the synapse, patients' NMDAR-Ab reduced the diffusion of NMDAR (2-way-ANOVA, $p < 0.05$) (Figure 2, B and C). Of interest, SGE-301 increased the diffusion of NMDAR (2-way-ANOVA, $p < 0.01$), normalizing the NMDAR diffusion values between control and NMDAR-Ab conditions (Figure 2, B and C). Noteworthy, there was no interaction between the 2 factors ($p = 0.94$), indicating that the effect of SGE-301 occurred, irrespective of the presence of NMDAR-Ab. The NMDAR-Ab-induced decrease in synaptic NMDAR confinement was also abrogated by SGE-301 (Figure 2, D and E). Thus, SGE-

Figure 1 SGE-301 Induces More Mobile and Less Confined NMDAR Trajectories



301 antagonizes the reduced dynamics of NMDAR in synapses exposed to patients' NMDAR-Ab.

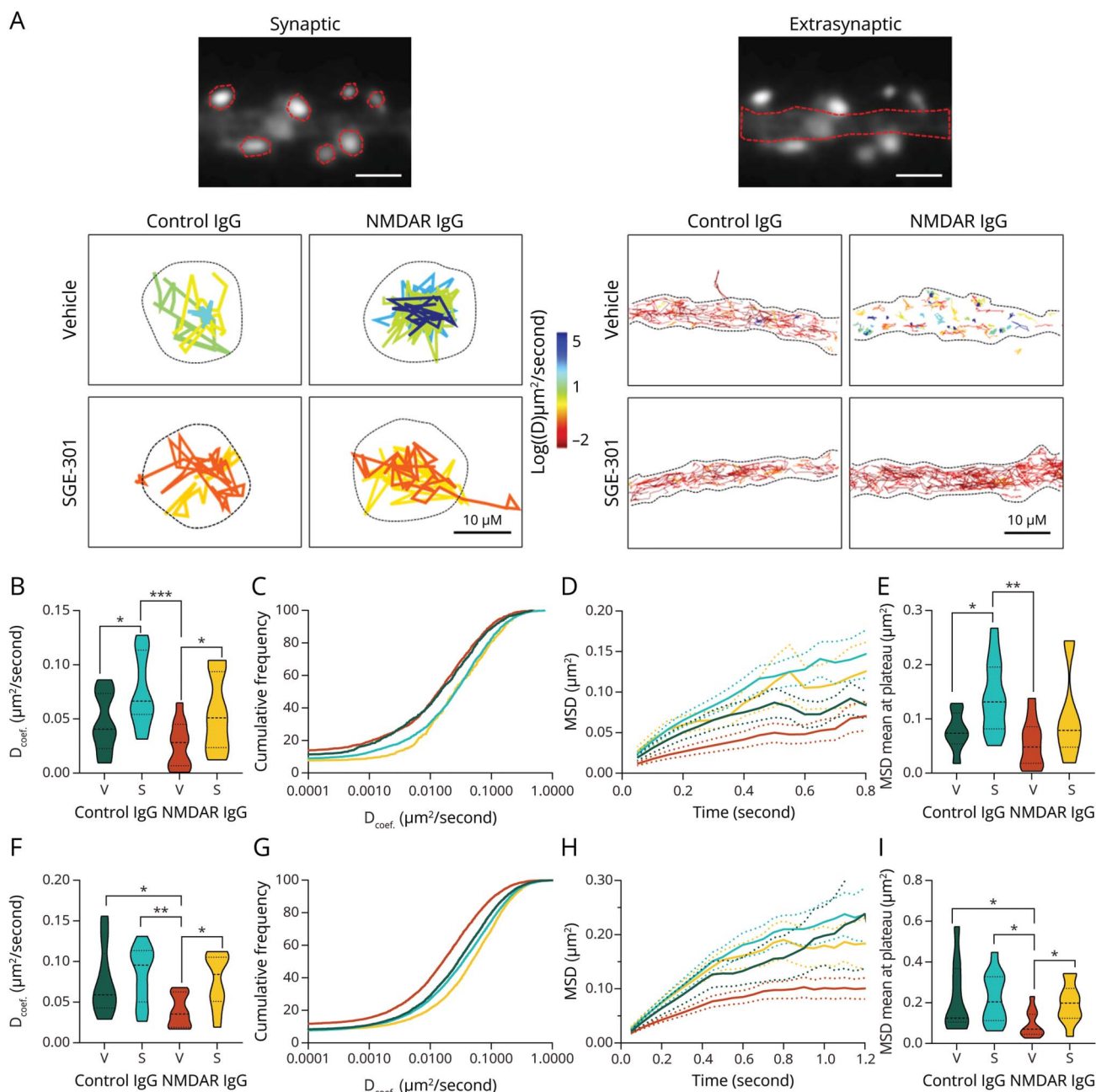
As expected, patients' NMDAR-Ab decreased extrasynaptic NMDAR surface diffusion (Figure 2, F and G; 2-way-ANOVA, *p* < 0.05). Yet, SGE-301 increased the diffusion of NMDAR (2-way-ANOVA, *p* < 0.05), equalizing NMDAR diffusion values between control and NMDAR-Ab conditions (Figure 2, F and G). The same effects were observed for the NMDAR confinement (Figure 2, H and I). Altogether, these data demonstrate that SGE-301 has the

potency to counteract the reduced dynamics of membrane NMDAR, outside and inside synapses, when exposed to patients' NMDAR-Ab.

Discussion

Normal NMDAR surface dynamics are instrumental for long-term synaptic plasticity.¹¹ Previous studies demonstrated that NMDAR surface dynamics are impaired by NMDAR-Ab from patients with NMDARE.^{2,12,13} In the presence of NMDAR-Ab, the nanoscale organization and dynamics of NMDAR are

Figure 2 SGE-301 Prevents the Effect of Anti-NMDAR Encephalitis Patients' Antibodies on the Receptor's Surface Dynamics



disrupted, contributing to the deficit in NMDAR-mediated synaptic transmission and plasticity.^{2,3,12–14} Identifying ways to directly act on NMDAR nanoscale organization and dynamics would thus represent a novel treatment strategy for this disorder.

Here, we demonstrate that SGE-301, at doses $>10 \mu$ M, upregulates NMDAR surface diffusion mainly in the postsynaptic compartment. Of interest, this upregulation is sufficient to normalize NMDAR diffusion in neurons exposed to patients' NMDAR-Ab.

Previous studies showed that SGE-301 increased NMDAR channel open probability, acting on a site independent of other allosteric modulators.⁵ Consequently, SGE-301 increases NMDAR function and prolongs spontaneous excitatory postsynaptic currents.^{6,7} In neurons exposed to patients' NMDAR-Ab, SGE-301 did not block the binding of antibodies but prevented the reduction of cell surface NMDAR without fully abrogating receptor internalization, suggesting that it might also change the surface dynamics.^{7,8} The current findings confirm this hypothesis and, together with the reported effects of SGE-301 on ionotropic currents,^{6,7} suggest a functional interplay between the state of the receptor and its membrane dynamics. Yet, the mechanism through which SGE-301 changes NMDAR diffusion remains unknown. SGE-301 may alter NMDAR's conformation, reducing the interaction with anchoring proteins, or its oxysterol properties may affect the plasma membrane tuning the diffusion.

Of clinical interest, SGE-301 is capable of compensating the detrimental effect of NMDAR-Ab on the receptor dynamics. This finding coupled with previous evidence that SGE-301 reverses the behavioral alterations caused by patients' NMDAR-Ab in animal models^{7,8} might have implications for the treatment of NMDARe, particularly the residual cognitive and psychiatric symptoms. Considering that SAGE-718 (a PAM closely related to SGE-301 designed for oral bioavailability) showed a good tolerability profile in healthy volunteers,¹⁵ future studies should assess the potential therapeutic benefit of oxysterol-based NMDAR PAMs in the postacute stage of NMDARe.

Acknowledgment

The authors thank Sage Therapeutics for providing SGE-301. Moreover, the authors thank the Bordeaux Imaging Center, a service unit of the CNRS-INSERM and Bordeaux University, member of the national infrastructure France BioImaging (ANR-10-INBS-04-01), and the Cell Biology Facility for cell culture production. The authors extend our gratitude to Esther Aguilar (FCRB-IDIBAPS) for her technical support and our lab members for engaging in constructive discussions.

Study Funding

The authors report no targeted funding.

Disclosure

E. Maudes is a recipient of the Basque Government Doctoral Fellowship Program (PRE_2022_2_0065), and this project was conducted as a part of her stay in Bordeaux funded by the exchange programs EGONLABUR (EP_2023_1_0041) and EMBO Scientific Exchange Grants. L. Groc received funding from the Centre National de la Recherche Scientifique, Era-Net Neuron Mental Disorders Program (Project Autoscale; to L.G. and J.D), the European Research Council Synergy grant (ENSEMBLE, 951294 to L.G), and Fondation pour la Recherche Médicale (FDT202204014778 to Z.J.). J.O. Dalmau received funding from Sage Therapeutics. All other

authors report no disclosures relevant to the manuscript. Go to Neurology.org/NN for full disclosures.

Publication History

Received by *Neurology: Neuroimmunology & Neuroinflammation* February 7, 2024. Accepted in final form March 27, 2024. Submitted and externally peer reviewed. The handling editor was Deputy Editor Scott S. Zamvil, MD, PhD, FAAN.

Appendix Authors

Name	Location	Contribution
Estibaliz Maudes, MSc	Neuroimmunology Program, Fundació Clinic per la Recerca Biomèdiques August Pi i Sunyer (FCRB-IDIBAPS), University of Barcelona, Spain	Drafting/revision of the manuscript for content, including medical writing for content; major role in the acquisition of data; study concept or design; analysis or interpretation of data
Zoë Jamet, PhD	University of Bordeaux, CNRS, Interdisciplinary Institute for Neuroscience, IINS, UMR 5297, Bordeaux, France	Drafting/revision of the manuscript for content, including medical writing for content; major role in the acquisition of data; analysis or interpretation of data
Laura Marmolejo, MSc	Neuroimmunology Program, Fundació Clinic per la Recerca Biomèdiques August Pi i Sunyer (FCRB-IDIBAPS), University of Barcelona, Spain	Drafting/revision of the manuscript for content, including medical writing for content; analysis or interpretation of data
Josep O. Dalmau, MD, PhD	Neuroimmunology Program, Fundació Clinic per la Recerca Biomèdiques August Pi i Sunyer (FCRB-IDIBAPS), University of Barcelona, Spain	Drafting/revision of the manuscript for content, including medical writing for content; study concept or design; analysis or interpretation of data
Laurent Groc, PhD	University of Bordeaux, CNRS, Interdisciplinary Institute for Neuroscience, IINS, UMR 5297, Bordeaux, France	Drafting/revision of the manuscript for content, including medical writing for content; study concept or design; analysis or interpretation of data

References

1. Titulaer MJ, McCracken L, Gabilondo I, et al. Treatment and prognostic factors for long-term outcome in patients with anti-NMDA receptor encephalitis: an observational cohort study. *Lancet Neurol.* 2013;12(2):157-165. doi:10.1016/S1474-4422(12)70310-1

2. Mikasova L, De Rossi P, Bouchet D, et al. Disrupted surface cross-talk between NMDA and Ephrin-B2 receptors in anti-NMDA encephalitis. *Brain.* 2012;135(Pt 5):1606-1621. doi:10.1093/brain/awu092

3. Hughes EG, Peng X, Gleichman AJ, et al. Cellular and synaptic mechanisms of anti-NMDA receptor encephalitis. *J Neurosci.* 2010;30(17):5866-5875. doi:10.1523/JNEUROSCI.0167-10.2010

4. Planagumà J, Leyboldt F, Mannara F, et al. Human N-methyl D-aspartate receptor antibodies alter memory and behaviour in mice. *Brain.* 2015;138(Pt 1):94-109. doi:10.1093/brain/awu310

5. Paul SM, Doherty JJ, Robichaud AJ, et al. The major brain cholesterol metabolite 24(S)-hydroxycholesterol is a potent allosteric modulator of N-methyl-D-aspartate receptors. *J Neurosci.* 2013;33(44):17290-17300. doi:10.1523/JNEUROSCI.2619-13.2013

6. Warikoo N, Brunwasser SJ, Benz A, et al. Positive allosteric modulation as a potential therapeutic strategy in anti-NMDA receptor encephalitis. *J Neurosci.* 2018;38(13):3218-3229. doi:10.1523/JNEUROSCI.3377-17.2018

7. Mannara F, Radosevic M, Planagumà J, et al. Allosteric modulation of NMDA receptors prevents the antibody effects of patients with anti-NMDAR encephalitis. *Brain.* 2020;143(9):2709-2720. doi:10.1093/brain/awaa195

8. Radosevic M, Planagumà J, Mannara F, et al. Allosteric modulation of NMDARs reverses patients' autoantibody effects in mice. *Neurol Neuroimmunol Neuroinflamm.* 2022;9(1):e1122. doi:10.1212/NXI.0000000000001122

9. Dalmau J, Gleichman AJ, Hughes E, et al. Anti-NMDA-receptor encephalitis: case series and analysis of the effects of antibodies. *Lancet Neurol.* 2008;7(12):1091-1098. doi:10.1016/S1474-4422(08)70224-2
10. Jiang M, Chen G. High Ca²⁺-phosphate transfection efficiency in low-density neuronal cultures. *Nat Protoc.* 2006;1(2):695-700. doi:10.1038/nprot.2006.86
11. Groc L, Choquet D. Linking glutamate receptor movements and synapse function. *Science.* 2020;368(6496):eaay4631. doi:10.1126/science.aay4631
12. Jezequel J, Johansson EM, Dupuis JP, et al. Dynamic disorganization of synaptic NMDA receptors triggered by autoantibodies from psychotic patients. *Nat Commun.* 2017;8(1):1791. doi:10.1038/s41467-017-01700-3
13. Jezequel J, Johansson EM, Leboyer M, Groc L. Pathogenicity of antibodies against NMDA receptor: molecular insights into autoimmune psychosis. *Trends Neurosci.* 2018;41(8):502-511. doi:10.1016/j.tins.2018.05.002
14. Ladepeche L, Planagumà J, Thakur S, et al. NMDA receptor autoantibodies in autoimmune encephalitis cause a subunit-specific nanoscale redistribution of NMDA receptors. *Cell Rep.* 2018;23(13):3759-3768. doi:10.1016/j.celrep.2018.05.096
15. Hill M, Blanco M-J, Salituro F, et al. SAGE-718: a first-in-class N-Methyl-d-Aspartate Receptor positive allosteric modulator for the potential treatment of cognitive impairment. *J Med Chem.* 2022;65(13):9063-9075. doi:10.1021/acs.jmedchem.2c00313

Paper VI

*Neuro-immunobiology in a mouse model of anti-NMDAR
encephalitis and assessment of treatment approaches.*

Estibaliz Maudes, Jesús Planagumà, [†] Laura Marmolejo, [†] Marija
Radosevic, Ana Beatriz Serafim, Esther Aguilar, Carlos Sindreu, Jon
Landa, Anna García-Serra, Francesco Mannara, Marina Cunqueiro,
Anna Smith, Chiara Milano, Paula Peixoto-Moledo, Mar Guasp,
Raquel Ruiz-Garcia, Sarah M. Gray, Marianna Spatola, Pablo Loza-
Alvarez, Lidia Sabater, Carlos Matute, Josep Dalmau.

[†] These authors contributed equally

Submitted to Brain. 2024.

IF JCR 2022: 14.5 (D1).

Neuro-immunobiology and treatment assessment in a mouse model of anti-NMDAR encephalitis

Estibaliz Maudes,¹ Jesús Planagumà,^{1,2,†} Laura Marmolejo,^{1,†} Marija Radosevic,¹ Ana Beatriz Serafim,¹ Esther Aguilar,¹ Carlos Sindreu,¹ Jon Landa,¹ Anna García-Serra,^{1,3} Francesco Mannara,¹ Marina Cunquero,² Anna Smith,¹ Chiara Milano,^{1,4} Paula Peixoto-Moledo,¹ Mar Guasp,¹ Raquel Ruiz-Garcia,¹ Sarah M. Gray,⁵ Marianna Spatola,¹ Pablo Loza-Alvarez,² Lidia Sabater,¹ Carlos Matute,⁶ Josep Dalmau¹

[†]**These authors contributed equally to this work.**

Abstract

Anti-N-methyl-*D*-aspartate receptor (NMDAR) encephalitis is a disorder mediated by autoantibodies against the GluN1 subunit of NMDAR. It occurs with severe neuropsychiatric symptoms that often improve with immunotherapy. Clinical studies and animal models based on patients' antibody transfer or NMDAR immunization suggest that the autoantibodies play a major pathogenic role. Yet, there is an important need of models offering an all-inclusive neuro-immunobiology of the disease together with a clinical course long enough to facilitate the assessment of potential new treatments. Toward this end, eight-week-old female mice (C57BL/6J) were immunized (days 1 and 28) with GluN1₃₅₆₋₃₈₅ peptide or saline with AddaVax adjuvant and pertussis toxin. After symptom development (~day 35), subsets of mice were treated with an anti-CD20 (day 35), a positive allosteric modulator (PAM) of NMDAR (NMDAR-PAM, SGE-301) from days 45 to 71, or both. GluN1-antibody synthesis, epitope spreading, effects of antibodies on density and function of NMDAR, brain immunological infiltrates, microglial activation and NMDAR phagocytosis, and antibody synthesis in cultured inguinal and deep cervical lymph nodes (DCLN) were assessed with techniques including immunohistochemistry, calcium imaging, confocal and super-resolution microscopy, electrophysiology, or flow cytometry. Changes of memory and behaviour were

assessed with a panel of behavioural tests, and clinical/subclinical seizures with brain-implanted electrodes. Immunized mice, but not controls, developed serum and CSF NMDAR-antibodies (IgG1 predominant) against the immunizing peptide and other GluN1 regions (epitope spreading) resulting in a decrease of synaptic and extrasynaptic NMDAR clusters and reduction of hippocampal plasticity. These findings were associated with brain inflammatory infiltrates, mainly B- and plasma cells, microglial activation, colocalization of NMDAR-IgG complexes with microglia, and presence of these complexes within microglial endosomes. Cultures of DCLC showed GluN1-antibody production. These findings were associated with psychotic-like behaviour (predominant at disease onset), memory deficit, depressive-like behaviour, abnormal movements (15% of mice), and lower threshold for developing pentylenetetrazole-induced seizures (hypoactivity, myoclonic jerks, continuous tonic-clonic) which correlated with regional cFOS expression. Most symptoms and neurobiological alterations were reversed by the anti-CD20 and PAM, alone or combined. Initial repopulation of B cells, by the end of the study, was associated with re-emergence of clinical-neurobiological alterations, which were abrogated by PAM. Overall, this model offers an all-inclusive neuro-immunobiology of the disease, allowing testing novel treatments, supporting the potential therapeutic role of NMDAR-PAM, and suggesting an immunological paradigm of systemic antigen presentation and brain NMDAR epitope spreading, which along the DCLN might contribute to fine-tune the polyclonal immune response.

Author affiliations:

¹Neuroimmunology Program, Fundació Clínic per la Recerca Biomèdica – Institut d'Investigacions Biomèdiques August Pi i Sunyer (FCRB-IDIBAPS), University of Barcelona, Spain; ² ICFO-Institut de Ciències Fotòniques, Barcelona Institute of Science and Technology (BIST), Spain; ³ Psychooncology and Digital Health Group, IConnecta't, ICO-IDIBELL, Spain; ⁴ Department of Clinical and Experimental Medicine, University of Pisa, Pisa, Spain; ⁵ Sage Therapeutics, Cambridge, MA, USA; ⁶ Achucarro Basque Center for Neuroscience, Biomedical Research Networking Center on Neurodegenerative Diseases and Department of Neurosciences, University of the Basque Country, Leioa, Spain

Correspondence to:

Josep Dalmau, Neuroimmunology Program, Fundació Clínic per la Recerca Biomèdica – Institut d'Investigacions Biomèdiques August Pi i Sunyer (FCRB-IDIBAPS), University of Barcelona, Casanova, 143; CELLEX3A, Barcelona 08036, Spain. E-mail: jdalmau@clinic.cat

Running title: Comprehensive NMDAR immunization model

Keywords: NMDAR encephalitis; active immunization; SGE-301; immunotherapy; animal model; treatments

Introduction

Anti-N-methyl-*D*-aspartate receptor (NMDAR) encephalitis is an autoimmune brain disease of rapid presentation and prolonged clinical course characterized by severe psychiatric and neurological symptoms in association with IgG antibodies against the GluN1 subunit of NMDARs.¹ Most patients are young adults and children, predominantly female (4:1), who in a matter of days or weeks develop behavioural change, psychosis, memory impairment, and variable presence of abnormal movements, seizures, decreased level of consciousness or dysautonomia.² Known triggers of the disease are tumors, mainly teratomas, and less frequently herpes simplex encephalitis, but in about 60% of patients the trigger is unknown.³ ⁴ Treatments aimed to remove the antibodies and antibody-producing cells (e.g., anti-CD20 such as rituximab) often result in improvement, but for most patients the recovery is slow, remaining with memory and cognitive deficits for several months.⁵ Because the pathophysiology of the post-acute stage is unknown, the treatment approach to shorten the period of recovery and improve clinical outcome is currently one of the most important challenges of the disease.⁶

In cultures of rodent hippocampal neurons, patients' antibodies disrupt the surface dynamics of NMDARs and internalize them, causing a reduction of their surface content and NMDAR-mediated currents.^{7, 8} Similar effects are obtained with passive transfer of patients' antibodies to the cerebroventricular system of mice, causing transient psychotic-like behaviour, memory impairment, and seizures or reduced seizure threshold.⁹⁻¹¹ These studies confirm the pathogenicity of patients' autoantibodies but do not represent a *bona fide* model of anti-NMDAR encephalitis, and are unable to provide further insights into the immunopathology and clinical course of the disease.

Additional approaches to model the disease are based on immunization of rodents with native NMDAR or peptides of the GluN1 subunit, resulting in phenotypes that range from fulminant, sometimes lethal, encephalitis (with severe seizures and stereotyped movements) to milder phenotypes that depending on the model, include memory impairment, behavioural change (depressive, anxiety-like), or reduction of seizure threshold.¹²⁻¹⁷ These models occur with the development of NMDAR antibodies and support the concept that NMDAR autoimmunity is sufficient to cause multifaceted symptoms. However, there is an unmet need of models that can offer an all-inclusive assessment of the neurobiology and immunobiology of the disease and a clinical course long enough to facilitate the evaluation of potential therapies on all these paradigms.

Even though animal models are imperfect reproductions of human diseases, they offer insights into the pathogenic mechanisms and potential new treatments, which for anti-NMDAR encephalitis is of paramount importance. Towards this end, we developed a mouse model of anti-NMDAR encephalitis that allows behavioural, neurobiological and immunobiological assessments during an extended course. Additionally, we tested the model with several treatment approaches including an anti-CD20, which represents a frequent treatment in patients; a positive allosteric modulator (PAM) of NMDAR (SGE-301) that has potential for clinical use,^{18, 19} and both combined, and determined how these treatments modified the clinical and biological paradigms of the disease.

Materials and methods

Animals

Female C57BL6/J mice (Charles River) were housed in cages of four in our animal facility (Unitat d'Experimentació Animal de Medicina, Centres Científics i Tecnològics, Universitat de Barcelona) at a controlled temperature ($21 \pm 1^{\circ}\text{C}$) and humidity ($55 \pm 10\%$) with illumination at 12-h cycles, and food and water *ad libitum*. Experiments were performed during the light phase, and animals were habituated to the room for 30 min before each experiment. All procedures were done according to standard ethical guidelines (European Communities Directive 2010/63/EU), approved by the local ethical committee (CEE-316/22), and reported in accordance with the ARRIVE guidelines (Supplementary Material).

Immunization and treatments

On days 1 and 28, eight-week-old mice were subcutaneously injected with 200 μg of the GluN1_{356–385} peptide or saline and AddaVax (InvivoGen, San Diego, USA) adjuvant. All animals received 100 ng of Bordetella pertussis toxin intraperitoneally at the time of immunization and 48 h later. To assess different treatments, a subset of mice received 250 μg of anti-CD20 intravenously on day 35, another subset received from day 47 until 71 (end of the study) daily intraperitoneal injections of a NMDAR-PAM (SGE-301), and a third subset received both, anti-CD20 and PAM (Fig. 1A). Each subset had the corresponding controls including intravenous injection of saline, intraperitoneal injection of vehicle, or both. A total of 275 animals were used in the study. Mice were randomly allocated to NMDAR or control groups. The preparation and concentration of SGE-301 (10 mg/kg) were similar as those previously reported.¹⁸

GluN1 antibody detection and characterization

Serum was obtained from blood collected from the submandibular vein, and CSF from the cisterna magna of deeply anesthetized mice prior to sacrifice on day 42 or 71. The presence of GluN1 antibodies was determined with rat brain immunohistochemistry, cell-based assay (CBA) of GluN1/GluN2b, and live immunolabeling of cultures of dissociated rat hippocampal neurons, as reported.^{2, 8} The titre of NMDAR antibodies was calculated by CBA with serial dilutions of samples until the reactivity was no longer visible (units reported as dilution factor). Mice NMDAR antibody class and subclass were determined with the indicated CBA of GluN1/GluN2b and antibodies against each subclass of mouse IgG (IgG1, 2, 3) (Supplementary material).

The occurrence of antibodies targeting epitope regions other than that of the immunizing GluN1_{356–385} peptide (epitope spreading) was determined with CBA of a truncated GluN1 construct without the peptide sequence,²⁰ and with western blot of the immunizing peptide and neuronal lysates probed with mice serum non-absorbed and pre-absorbed with the immunizing peptide (Supplementary Material).

A preliminary assessment of functional effects of IgG from GluN1 immunized mice (NMDAR mice) was conducted using quantitative immunocytochemical analysis of clusters of NMDARs in live rat hippocampal neurons exposed for 24 h to IgG of NMDAR mice or controls, and calcium imaging of similar cultures of neurons under the same experimental conditions (Supplementary Material). The specificity of the NMDAR-IgG effect in calcium imaging experiments was determined with IgG pre-absorbed with GluN1-expressing HEK293 cells. The techniques of immunocytochemical quantitation of NMDAR clusters, IgG isolation, and immunoabsorption have been previously reported,^{8, 21, 22} and the calcium imaging experiment is described in Supplementary Material.

Determination of IgG presence in the brain, immunoprecipitation of IgG bound to NMDAR, and assessment of complement deposition was assessed as previously reported and described in Supplementary Material.²³

Brain, spleen, and lymph node dissection

On days 42 and 71, subsets of mice were deeply anaesthetized, and their spleen was harvested. Mice were then euthanized by cardiac perfusion with saline, and the brain was removed. For immunohistochemical and confocal microscopy studies, the right hemisphere was fixed with 4% paraformaldehyde for 1h, cryopreserved in 40% glucose for 48h, embedded in optimal cutting temperature compound, and snapped frozen in isopentane chilled with liquid nitrogen. The left hemisphere was fresh frozen for immunoprecipitation studies, acutely sectioned for electrophysiology, or processed to obtain immune cells for flow cytometry.

Inguinal and deep cervical lymph nodes of immunized mice and controls were obtained at day 42. Lymph node cells were dissociated and kept in culture with X-vivo 15 (02-053Q, Lonza, Basel, Switzerland) supplemented with 10% fetal bovine serum for 24 h, and with the presence of 0,1 µg/µl of GluN1₃₅₆₋₃₈₅ peptide for 3 days. The media was then assessed (diluted 1:2) for the presence of GluN1 antibodies with a cell-based assay (CBA) expressing GluN1/GluN2b.

Analysis of brain and spleen immune cells

Flow cytometry: Brain tissue was homogenized with gentleMACS Dissociator (130-096-427, Miltenyi Biotec) while immersed in 2ml of HBSS buffer (w/o Ca²⁺ and Mg²⁺, 14175-053, Thermo Fisher Scientific) containing 100 U/mL collagenase IV (C5138, Sigma) and 50 U/mL DNase I (D5025-150 KU, Sigma). The tissue was then filtered on a cell strainer (70

µm) and the cells were separated from myelin and debris with a 30% Percoll gradient (17-0891-01, GE Healthcare) in HBSS without Ca^{2+} and Mg^{2+} , centrifuged at 950 g during 25 min without brakes. Cells were collected from the bottom of the tube after centrifugation and washed with HBSS buffer. The isolation of immune cells from the spleen is provided in Supplementary Material.

Brain immune cell infiltrates or splenocytes were incubated with the following fluorophore-conjugated antibodies during 20 min at 4 °C: CD11b (clone M1/70, eFluor 450, 48011282), CD45 (clone 30-F11, APC, 17045182), CD3 (clone 17A2, Alexa Fluor 488, 53003282), CD4 (clone RM4-5, PE-Cyanine5.5, 35004282), CD8 (clone 53-6.7, Brilliant Ultra Violet 737, 367008182), CD19 (clone 1D3, PE-Cyanine5, 15019382), IgD (clone 11-26, Super Bright 600, 63599382), CD27 (clone LG.7F9, Super Bright 702, 67027182), CD138 (clone 300506, PE, MA523527). All the antibodies were purchased from Invitrogen (Waltham, MA, USA). Data was acquired in a Cytex Aurora cytometer and analysed using SpectroFlo software (Cytex Biosciences, Fremont, CA, USA).

Brain immunohistochemistry: Additional studies of brain T cell infiltrates were performed by immunostaining using antibodies specific for CD4 and CD8 T cells as described in Supplementary Material.

ELISpot: Determination of GluN1_{356–385} specific T cells in splenocytes was performed with ELISpot, described in Supplementary Material.

NMDAR cluster density and microglia studies

To determine the cluster density of cell-surface NMDAR and postsynaptic density protein 95 (PDS95), 5 µm-thick brain sections of NMDAR mice and controls were incubated with a human CSF enriched with GluN1 antibodies (used as a primary antibody) for 1h at room temperature (RT), followed by the secondary Alexa Fluor 488 goat anti-human IgG (1:1000,

A-11013, Thermo Fisher) for 1h at RT, as reported.⁹ Tissue sections were then permeabilized with 0.3% Triton X-100 for 10 min at RT and incubated with rabbit polyclonal anti-PSD95 (1:250, ab18258, Abcam, Cambridge, UK) overnight at 4°C, followed by the corresponding secondary Alexa Fluor 594 goat anti-rabbit IgG (1:1000, A-11012, Thermo Fisher) for 1h at RT.

Microglia was assessed in brain sections using a monoclonal rat antibody against CD68 (1:200, MCA1957GA, Bio-Rad, Hercules, CA, USA) to label macrophage/microglia and a polyclonal rabbit antibody against Iba-1 (1:1000, 019-19741, Wako Chemicals, Neuss, Germany) to label activated microglia. To assess whether microglia co-localized with IgG bound to NMDAR, we used a triple staining (anti-CD68, anti-mouse IgG, anti-NMDAR) each as indicated above, for 2h at RT, followed by the corresponding secondary antibodies for 1h at RT: goat anti-rat Alexa Fluor 594 (1/500, A-1100), goat anti-mouse Alexa Fluor 488 (1:500, A-11001), and goat anti-human Alexa Fluor 647 (1:500, A-21445) all from Thermo Fisher (Waltham, USA).

Slides were then mounted in ProLong Gold antifade (P36935, Thermo Fisher) and scanned under a Zeiss LSM710 confocal microscope (Carl Zeiss, Jena, Germany) with the EC-Plan NEOFLUAR CS 100x/1.3 NA oil objective. Cluster analysis was performed as reported.⁹ In brief, standardized z-stacks including 50 optical images were acquired from the CA1, CA3, dentate gyrus (DG) and cortex. Images were then deconvolved using Huygens Essential 23.10 software (Scientific Volume Imaging, Hilversum, NL), and a spot detection algorithm from Imaris 8.1 software (Oxford instruments, Belfast, UK) was used. Density of clusters was expressed as spots/ μm^3 . Three-dimensional colocalization of clusters was done using a spot colocalization algorithm (Imaris 8.1, Oxford instruments). Synaptic localization was defined as colocalization of NMDAR with PSD95. Microglia activation was defined as colocalization of Iba-1 with CD68. Phagocytosis of the complex IgG-NMDAR was defined

by the triple colocalization of CD68, mouse IgG, and NMDAR, and confirmed with Stimulated Emission Depletion (STED) microscopy (Supplementary Material).

Hippocampal long-term potentiation, and paired-pulse facilitation

Acute sections of the hippocampus on day 42 and 71 were used to assess long-term plasticity by the classical paradigm of stimulation at the Schaffer collateral pathway and recording the field potentials at CA3-CA1 synapses, as previously described.^{18, 19} A detailed description can be found in Supplementary Material.

Behavioural testing, seizure susceptibility, and abnormal movements

A panel of standardized behavioural and memory tests was applied by investigators blinded to the experimental conditions (Fig. 1A). They included: memory (Novel Object Location [NOL]), psychotic-like behaviour (Pre-Pulse Inhibition [PPI]), anxiety (Black and White [BW]), depressive-like behaviour (Tail Suspension Test [TST]), and locomotor activity (LA). These tests are described in Supplementary Material and have been reported.^{9, 10} Mice were subjected to PPI, BW and TST just once prior to being sacrificed on day 42 or 71. Mice sacrificed on day 71 underwent NOL test from the beginning of the battery. To determine seizure susceptibility, the GABA_AR antagonist pentylenetetrazol (PTZ, Sigma) was given intraperitoneally (40 mg/kg) to a subgroup of NMDAR and control mice on days 38-43. Seizure development and scaling was confirmed by recordings via intracerebral electrodes synchronized to a video camera, and by cFos immunostaining (Supplementary Material). The presence of abnormal movements was visually assessed, without quantification, during recordings or the indicated behavioural tests.

Statistical analysis

Comparisons of total and synaptic NMDAR clusters, IgG deposits, field excitatory postsynaptic potentials (fEPSP) slope change, brain infiltrates, splenic B cells, T cell activation, microglia activation, and behavioural tests across of all treatment groups were conducted using a mixed-effects model. This model included immunization, treatment, and time as fixed effects, with the subject included as a random effect to account for inter-subject variability. The area under the curve of calcium curves was also analyzed with a mixed-effects model, where IgG type was a fixed effect and hippocampal culture a random effect to account for culture replicate viability. These analyses were performed using the lme4 package in R, with p-values adjusted for multiple comparisons using Bonferroni correction. Comparison of hippocampal NMDAR and PSD95 clusters, and microglia phagocytosis were performed using a nested t-test. PPI test, BW test and TST for untreated control and NMDAR mice were compared using a two-way analysis of variance with Bonferroni correction for multiple comparisons. Seizure susceptibility was evaluated using a chi-squared test. All experiments were assessed for outliers with the ROUT method applying $Q = 1\%$. In all analyses, we used a 2-sided type I error of 5%. All tests and graphs were performed using GraphPad Prism (version 8; GraphPad Inc., San Diego, CA) and R studio (v4.0.0).

Data availability

The data that support the findings of this study are available from the corresponding author, upon request.

Results

NMDAR mice produce GluN1 antibodies with effects similar to those of anti-NMDAR encephalitis

NMDAR mice, but not controls, developed serum and CSF NMDAR antibodies that were demonstrated with rat brain immunostaining (Fig. 1B-C), CBA with HEK293 cells expressing GluN1/GluN2B subunits of NMDAR, and live immunolabelling of cultures of rat hippocampal neurons (Fig. 1D). The predominant GluN1 immunoglobulin class and subclass was examined in a representative group of 10 mice, showing IgG1 in all, and IgG2 in 4 (40%) (data not shown). Immunoabsorption of the antibodies with GluN1₃₅₆₋₃₈₅ peptide abrogated the reactivity with the peptide but not with GluN1 regions outside the peptide sequence, suggesting epitope spreading (Fig. 1E); this was confirmed with CBA of a GluN1 construct that did not contain the peptide sequence (Supplementary Fig. 1). In cultured rat hippocampal neurons, IgG from NMDAR mice, but not from controls, caused a significant reduction of cell-surface NMDAR clusters (Supplementary Fig. 2). Moreover, neurons pre-treated with IgG from NMDAR mice showed a significant reduction of NMDA-induced calcium influx compared with neurons pre-treated with IgG from controls. This effect was abrogated if the IgG from NMDAR mice had been pre-absorbed with NMDARs (Fig. 1F-G, Supplementary Video 1). Overall, these findings show that NMDAR mice developed polyclonal antibodies highly similar in all paradigms tested to those reported in the human disease.^{8, 9, 24} Moreover, the presence of GluN1 antibodies was confirmed in the media of cultured cells from deep cervical lymph nodes, but not inguinal lymph nodes, of NMDAR mice (Supplementary Fig. 3).

Preliminary assessment of anti-CD20 and PAM treatments used in the model

In previous studies with passive transfer of patients' NMDAR antibodies to mice, and in cultured neurons, we previously established the effects of the NMDAR-PAM (SGE-301).^{18, 19, 25} Since we had not previously tested the anti-CD20 used in the current model, we preliminary confirmed that it was able to deplete systemic B cells in mice. Flow cytometry on splenocytes from all subsets of NMDAR and control mice showed that administration of anti-CD20 at day 35 caused a significant reduction of B cells measured at day 42, which was no longer detected by day 71, indicating B cell repopulation (Supplementary Fig. 4A-B).

Additional studies with IFN- γ ELISpot on splenocytes from NMDAR mice showed activation of GluN1-specific T cells on day 42, which was abrogated by the anti-CD20, suggesting a contribution of GluN1-specific CD20+ T cells in B cell activation (Supplementary Fig. 4C).

Brain-bound IgG from NMDAR mice precipitates NMDAR

Quantitation of the IgG bound to brain was performed by immunohistochemistry on tissue obtained at days 42 and 71 in the indicated subsets of NMDAR mice and controls. Compared to controls, NMDAR mice had a significant increase of brain IgG at days 42 and 71, which was substantially decreased or not significant in mice treated with anti-CD20, but not NMDAR-PAM (Supplementary Fig. 5A-C). The absent effect of NMDAR-PAM on IgG binding was in line with previous reports that used a mouse model of passive transfer of patients' NMDAR antibodies, in which NMDAR-PAM antagonized and reversed the pathogenic effect of antibodies without affecting antibody binding to NMDAR.^{18, 19}

The specificity of the brain-bound IgG for NMDAR was confirmed by precipitation of brain IgG, which co-precipitated NMDAR (Supplementary Fig. 5D).

NMDAR mice show a decrease of NMDARs and impaired hippocampal plasticity, reversible with treatment

Having shown that NMDAR mice develop an anti-NMDAR-specific immune response and that the associated antibodies bind to brain NMDARs, we determined whether the neuronal surface content of NMDAR clusters was modified in the cerebral cortex and hippocampus of mice examined at days 42 and 71 (Fig. 2A). Confocal quantification of NMDAR clusters showed a significant reduction of total and synaptic surface clusters at day 71 in the hippocampus, dentate, and cerebral cortex of NMDAR mice, but not in controls (Fig. 2B-G). In the hippocampus, the reduction of total and synaptic NMDAR clusters was detectable at day 42 (Fig. 2B-C).

By contrast, all but one subset of NMDAR mice treated with anti-CD20, NMDAR-PAM, or both, showed unaltered levels of total and synaptic NMDAR clusters at days 42 and 71 compared to those of controls. The only subset of treated NMDAR mice that on day 71 had reduced synaptic NMDAR clusters (noted in the dentate) was the group that received anti-CD20 (Fig. 2D-E).

Studies of long-term potentiation (LTP) in the hippocampus showed that untreated NMDAR mice had a significant impairment of plasticity at days 42 and 71 compared to that of controls (Fig. 3A-D). By contrast, all but one subset of NMDAR mice treated with anti-CD20, NMDAR-PAM, or both, showed unaltered LTP at days 42 and 71 compared to controls (Fig. 3B and 3E-H). Similar to the analysis of NMDAR clusters, only the subset of NMDAR mice treated with anti-CD20 showed LTP impairment at day 71 (Fig. 3B, F). Presynaptic release probability, as assessed by paired-pulse facilitation,¹⁸ was unaffected (data not shown).

These findings together with the indicated reduction of NMDAR clusters in cultured neurons exposed to IgG of NMDAR mice, suggest the NMDAR immune response causes a

reduction of cell-surface NMDARs and that treatment with anti-CD20, NMDAR-PAM, or both, reverses this effect. Although anti-CD20 was effective in preventing all alterations at day 42, it was no longer as effective by day 71, coinciding with B cell repopulation (shown in the next section). The restoring of NMDAR cluster content in animals treated with NMDAR-PAM is similar to the reported effects of this PAM in cultured neurons exposed to patients' NMDAR antibodies and in a model of passive transfer of patients' antibodies.^{18, 19}

NMDAR mice have brain infiltrates of B and plasma cells with distinct treatment-response timings

The presence of brain immune cell infiltrates was determined by flow cytometry at days 42 and 71 in all subsets of NMDAR mice and controls (Fig. 4A). The brain of untreated NMDAR mice showed at days 42 and 71 a significant increase of pan-B cells (CD3-CD19+), memory B cells (CD3-CD19+CD27+), and plasma cells (CD19-CD138+) compared with the brain of untreated control mice (Fig. 4B-D). By contrast, the subsets of NMDAR mice treated with anti-CD20 showed at day 42 a significant reduction of brain pan-B cells and memory B cells, with cell counts not different from those of control mice, whereas by day 71 the presence of memory B cells had increased in NMDAR mice compared to controls (Fig. 4B-C). Conversely, the effects of anti-CD20 on brain plasma cells were not observed at day 42 (NMDAR mice had more brain plasma cells than controls), but by day 71 the number of plasma cells was markedly reduced in NMDAR mice and not different from that of controls (Fig. 4D).

We did not find a substantial component of CD4 or CD8 T cells in the brain of NMDAR mice and controls by flow cytometry. Using brain immunohistochemistry, infrequent infiltrates of T cells (CD4>CD8) were identified in the meninges and brain parenchyma of both subsets of mice, with increased number of CD4+ T cells in NMDAR mice that was not

significant (data not shown). Moreover, we did not find complement deposition in the brain of NMDAR mice (data not shown), which is similar to reported patients' autopsy findings.^{26,}

27

In parallel studies, antibody titres were determined in serum of mice before being sacrificed at days 42 and 71. In NMDAR mice, anti-CD20 alone or followed by PAM caused a partial reduction in serum NMDAR antibody titres on day 42, which was more marked on day 71. No reduction in antibody titres was observed in mice only treated with PAM (Supplementary Fig. 6). CSF from NMDAR mice treated with anti-CD20 showed less reactivity than CSF from untreated mice on day 42 and 71, although the reactivity was not completely abolished (Supplementary Fig. 6).

NMDAR mice have brain microglial activation that co-localizes with IgG-bound to receptors

A significant co-localization of CD68 and Iba-1 (microglial activation) was noted on day 71 in the hippocampus of untreated NMDAR mice, and a similar trend was observed in the cerebral cortex (Fig. 5A-B). Microglial activation was not observed in subsets that received treatment with anti-CD20 or NMDAR-PAM. Because microglia might be involved in phagocytosis of NMDAR targeted by autoantibodies, we determined by confocal microscopy the triple co-localization of CD68, IgG and NMDAR in the hippocampus of untreated NMDAR mice and controls at day 71 (Fig. 5C). The findings showed a significant increase of this triple co-localization in the hippocampus of NMDAR mice (Fig. 5D-E). Super-resolution STED microscopy in several representative areas of triple co-localization demonstrated the presence of IgG and GluN1 in CD68-expressing endosomes of microglial cells, suggesting phagocytosis of antibody-targeted NMDARs (Fig. 5F-G). Overall, these findings support a

pathogenic role of the microglia in the brain autoimmune process, likely contributing to the reduction of NMDARs.

NMDAR mice show multiple symptoms of anti-NMDAR encephalitis that respond to treatment

Compared to the corresponding controls, all four subsets of NMDAR mice (untreated, treated with anti-CD20, NMDAR-PAM, or both) developed a significant decrease of memory (Object Location index) that was detected at first evaluation (day 34) and persisted until the last evaluation (day 68) unless mice were treated (Fig. 6A). The subsets of mice that were treated with anti-CD20, NMDAR-PAM, or both, showed a significant improvement of memory at day 47 that was maintained until the last assessment (day 68) except for the subset that received anti-CD20 alone which showed relapsing memory impairment by the time of B cell repopulation (Fig. 6A). Because all mice subsets received from days 45-71 daily injections of NMDAR-PAM or vehicle, we also assessed the memory changes in NMDAR mice and controls that did not receive any treatment or injections. In these two groups the findings were similar to those in the groups of NMDAR mice and controls that received injections with vehicle alone, suggesting that the stress caused by daily injections did not affect memory (data not shown).

In addition to memory impairment, untreated NMDAR mice developed early and transient psychotic-like behaviour (PPI test on day 36, but not day 64), and late depressive-like behaviour (TST on day 71, but not day 42) (Fig. 6B-D). Anxiety (BW test) was not affected in NMDAR mice or controls that did not receive any treatment or injections (Fig. 6C).

Since the administration of NMDAR-PAM was done with daily intraperitoneal injections that can result in stress and affect behavioural tests, the later assessment (as off day 45) of all paradigms of behaviour was controlled with subsets of mice that received daily injections of vehicle (Fig. 6E-G). Compared with these vehicle-injected controls, NMDAR mice showed psychotic-like behaviour (Fig. 6E), increased level of anxiety (Fig. 6F) and depressive like behaviour (Fig. 6G), which were all abrogated or improved by treatment with anti-CD20, NMDAR-PAM or both. These findings compared with the subset of untreated and not injected NMDAR mice which by the last assessment no longer have psychotic-like behaviour and did not show anxiety (Fig. 6B-D), suggest that NMDAR mice that received daily injections (either vehicle or treatment) had a potentiation or unmasking of NMDAR-related symptoms, which were successfully treated (psychotic-behaviour, anxiety) or improved (depressive-behaviour) with anti-CD20, NMDAR-PAM, and both.

In addition to memory and abnormal behaviours, 7 of 50 (14%) NMDAR mice, but not controls, exhibited motor stereotypies such as circling, self-biting, and walking backwards (Supplementary Video 2). None of these motor behaviours were observed after treatment with anti-CD20, NMDAR-PAM, or both. In addition, NMDAR mice showed a decrease in seizure threshold induced by pentylenetetrazol on day 42, which resulted in visible motor seizures (Supplementary Fig. 7). We did not find changes in locomotor activity in any subsets of NMDAR mice or controls, untreated or treated (data not shown). Altogether, NMDAR mice showed sequential psychiatric and neurologic alterations with persisting memory impairment, resembling the sequential clinical features of the human disease.

Discussion

We introduce a mouse model of anti-NMDAR encephalitis that associates with a T cell dependent GluN1 IgG response and results in a reduction of cell-surface receptor content and NMDAR function, similar to the effects reported for antibodies of patients with anti-NMDAR encephalitis. To that end, we used a 30 amino acid peptide derived from the major GluN1 antigenic region of the human disease (containing amino acids N368/G369)²⁸ in a novel immunization protocol that produced a robust synthesis of GluN1 polyclonal antibodies. These antibodies, predominantly of IgG1 subclass, targeted not only the immunizing GluN1 peptide but also epitope regions outside the peptide sequence, indicating epitope spreading.

These findings have not been previously investigated in models of anti-NMDAR encephalitis, and suggest a paradigm of immune-response different from that reported in myelin-oligodendrocyte glycoprotein (MOG)-experimental autoimmune encephalomyelitis (EAE) in which peptide immunization induces an EAE model that is mainly T cell mediated (B cell independent).^{29, 30} The longer GluN1 peptide length used in our model (30 amino acids), instead of shorter peptides (9-14 amino acid MOG fragments) used in the B cell independent EAE, together with the adjuvant AddaVax, which primes B cell responses may have played a role in the robust humoral response of our model. Indeed, AddaVax, a squalene-oil-in-water adjuvant, is known to be more effective in generating high antibody titres and CD4+T cell responses than Freund's complete adjuvant or aluminium-based adjuvants³¹⁻³³ and has fewer side-effects.³⁴ Our studies with IFN- γ ELISpot on splenocytes from NMDAR mice confirmed the activation of GluN1-specific T cells, which was significantly decreased by the anti-CD20, suggesting an important contribution of GluN1-specific CD20+T cells in B cell activation, as reported in an EAE model.³⁵

IgG isolated from NMDAR mice caused a reduction of NMDAR clusters and NMDAR-dependent calcium currents in cultured rat hippocampal neurons, similar to the alterations reported for the IgG of patients,^{8, 24} confirming that mice autoantibodies have direct effects on NMDARs. As a result, immunized mice, but not controls, showed NMDAR-specific brain-bound IgG, reduced content of synaptic and extrasynaptic NMDAR clusters, and significant impairment of hippocampal plasticity (LTP) similar to the alterations reported with passive cerebroventricular transfer of patients' antibodies to mice.^{9, 18} However, different from the passive transfer model in which the duration of effects was shorter (~14 days) until antibodies were cleared,^{10, 18} the current model showed NMDAR-related alterations for the entire duration of the study (71 days), providing the opportunity to assess different treatment strategies targeting at distinct disease mechanisms.

Another advantage of active immunization over passive transfer models is the possibility to study components of the immune response other than the antibody effects, such as brain inflammatory infiltrates, complement-mediated neuronal injury, and microglial activation. Analysis of brain inflammatory infiltrates, showed predominance of B cells and plasma cells, very infrequent T cells, absence of complement, and extensive microglial activation, overall resembling most of the findings reported in autopsies of patients.^{1, 26, 27, 36} A potential difference is that in patients, the frequency of T cells although low, might be higher than that observed in our model. Microglial activation is a consistent finding in patients' autopsies,^{1, 27} suggesting it plays a pathogenic role.³⁷ In the current study, NMDAR mice but not controls, showed a significant co-localization of CD68 (a phagocytic marker expressed by microglia/perivascular macrophages) with IgG and NMDARs. This triple co-localization, when assessed at the nanoscale level with super-resolution STED microscopy, was found to occur in endosomal/lysosomal structures, suggesting microglial phagocytosis of IgG-bound NMDARs.

Overall, these findings were accompanied by psychotic-like behaviour, memory deficits, depressive-like behaviour, variable presence of stereotyped movements (e.g., circling, self-biting, and walking backwards), and enhanced susceptibility to develop seizures (demonstrated with intracerebral electrodes). Interestingly, NMDAR mice not receiving treatment or injections of vehicle, developed psychotic-like behaviour earlier than depressive-like behaviour (as occurs in many patients),^{5, 38} whereas memory impairment persisted during the entire follow-up, and stereotyped movements occurred without stage preference. By contrast, psychotic-like behaviour remained detectable during the entire follow-up in untreated NMDAR mice stressed by daily (days 45-71) injections of vehicle.

The feasibility of the model to assess potential treatments, was tested with an anti-CD20 (equivalent to rituximab), and a synthetic analogue of 24(S)-hydroxycholesterol (SGE-301).³⁹ SGE-301 is a potent and selective NMDAR-PAM that crosses the blood-brain-barrier and has been shown to antagonize and reverse the synaptic and behavioural alterations caused by patients' NMDAR antibodies in cultured neurons and passive transfer models.^{18, 19, 25, 40}

NMDAR mice treated with the anti-CD20 showed rapid depletion of peripheral and brain B cell counts, accompanied by a decrease in brain-bound IgG, and recovery of NMDAR cluster density, hippocampal plasticity (LTP), and memory. These effects started wearing off about 5 weeks after treatment, when mice showed B cell repopulation and increased memory B cell infiltrates in the brain, accompanied by reduction of NMDAR clusters (initially detected in the DG), worsening synaptic plasticity, and return of memory impairment. These findings highlight the importance of B cell entry into the CNS, as suggested by neuropathological studies in patients,²⁷ and a previous model examining the brain inflammatory infiltrates in untreated mice.¹³ Murine models of other disorders treated with anti-CD20 have shown variable duration of B cell depletion, ranging from 8 weeks post-treatment with three administrations of 200 µg of anti-CD20⁴¹ to 6 weeks after two

administrations of 150 µg of anti-CD20.⁴² In our model, B cell repopulation occurred 5 weeks after a single 250 µg administration of anti-CD20, suggesting the depletion period is dose-dependent. These findings are in line with those in clinical practice which show the need of repeat cycles of rituximab to obtain therapeutic B cell depletion. The time lag between treatment administration and effects on symptoms and antibody levels is consistent with the findings in the EAE model in which symptom recovery associates better with B cell reduction than with the reduction of MOG antibody levels.²⁹ Similarly, in our model, the decrease in brain plasma cells represented a delayed response, likely due to these cells not expressing CD20.

Of potential clinical interest, late daily treatment with NMDAR-PAM (SGE-301) restored NMDAR density, hippocampal LTP, and memory and behavioural functions, without modifying the levels of B cells or antibody synthesis. The mechanisms underlying these PAM effects are poorly understood, but previous studies by us and others showed that SGE-301 increased NMDAR function (e.g., open channel probability).^{18, 39, 40} In addition, single NMDAR molecule tracking in cultures of neurons exposed to patients' NMDAR antibodies demonstrated that SGE-301 upregulated NMDAR surface diffusion in the post-synaptic compartment, which compensated for the antibody-mediated decrease in NMDAR surface dynamics and reduction of NMDAR clusters.²⁵ Taken together, these findings suggest that SGE-301 or similar NMDAR-PAMs (e.g., some designed for oral bioavailability) could be an effective adjuvant treatment for anti-NMDAR encephalitis, particularly during the prolonged post-acute stage, when cognitive and psychiatric symptoms persist, and maintenance or escalation of immunotherapy may not be needed.⁶ In our model the early use of an anti-CD20 combined with a later administration of SGE-301 resulted in abrogation of all clinical and neurobiological alterations.

This study has several considerations and limitations. Because the model examines multiple clinical and biological paradigms, requiring multiple subsets of NMDAR mice and controls without and with several treatments, we designed the follow-up for 10 weeks after initial immunization. We chose this experimental design with the rationale that if active immunization recapitulated the clinical disease course, the model would provide important immune and neurobiological insights and be well positioned to test the effect of clinical standard care (anti-CD20) and an experimental NMDAR-PAM (SGE-301) that had been efficacious in a passive transfer model of patients' antibodies. Our data strongly support this preclinical model of anti-NMDAR encephalitis as means to examine the course of the disease, and we believe the model can be followed for increasing amounts of time to investigate more long-term aspects of the disease. Indeed, further studies (not included here) in which we followed antibody titers for 4 months, showed that 8 of 10 untreated NMDAR mice remained with high antibody titers (similar to those of day 71); the other two animals only showed a mild spontaneous reduction of titers. Although we confirmed the presence of antibodies in CSF, the small amounts of CSF were a logistic problem that precluded several studies; thus, most investigations were performed with IgG isolated from serum. Mice showed propensity to develop seizures and status epilepticus, but not spontaneous seizures, which is a frequent feature in patients.⁵ The subsets of untreated mice with brain implanted electrodes were examined on day 42; we did not explore whether this lower seizure threshold could be treated with anti-CD20 or NMDAR-PAM, which is a task for the future. Finally, although changes in immunological, neurobiological, and behavioural paradigms usually occurred in parallel (e.g., B cell repopulation and re-emerging of neurobiological and memory problems), the correlation with serum antibody titers was not perfect, an observation also made in patients.²⁰

Our current demonstration that GluN1 peptide immunization leads to a polyclonal NMDAR antibody response, microglial/macrophage phagocytosis of IgG-NMDAR complexes, and synthesis of NMDAR antibodies in deep cervical lymph nodes, together with reports showing synthesis of autoantibodies in deep cervical lymph nodes of some anti-NMDAR patients,⁴³ and microglial phagocytosis of autoantibody-NMDAR complexes in mixed neuron/microglia cultures,³⁷ suggest an immunological paradigm. After immunological activation at regional lymph nodes close to the immunization site, NMDAR antibodies produced systemically and by brain infiltrating B cells/plasma cells cause a reduction of neuronal NMDAR (as occur in the human disease)^{8, 27} accompanied by phagocytosis of NMDAR-IgG complexes by microglia/macrophages. These brain antigen-presenting cells likely contribute to epitope spreading by presenting new fragments of phagocytised NMDAR to CD4 T cells, resulting in a NMDAR-specific polyclonal B cell/antibody response, probably at deep cervical lymph nodes.^{44, 45} Evidence of naïve T-cell priming and epitope spreading in the brain have been shown in models of EAE and other autoimmune encephalomyelitis.⁴⁶

Our model can now be adapted in many ways, for example extending the follow-up, increasing the number of administrations of anti-CD20, using simultaneously anti-CD20 and NMDAR-PAM, or considering new therapies (e.g., CAR T cell technology). It also offers the opportunity to explore at the cellular and circuitry levels the alterations underlying the prolonged memory and behavioral changes, typical of the post-acute stage of anti-NMDAR encephalitis.^{6, 47} Finally, an important task for the future is to determine how a systemically triggered neuronal immune response (as occur in patients with teratoma) reaches the CNS, and the role of brain antigen-presenting cells (microglia/macrophages) and deep cervical lymph nodes in fine tuning the immune response (e.g., epitope spreading, antibody affinity).

Acknowledgements

Moreover, we extend our gratitude to Mercedes Alba and Eva Caballero, Balma Serrano and Rafael Marín (FCRB-IDIBAPS), Maria Marsal, Merche Ribas, and Gustavo Castro (ICFO) for their technical support.

Funding

This study was funded by Instituto de Salud Carlos III (ISCIII) through the projects PI20/00197 to J.D. and PI20/00280 to J.P., Fundació CELLEX, “la Caixa” Foundation under the project code HR22-00221 to J.D and HR19-52160003 to P.L-A, and Ministerio de Economía y Competitividad - Severo Ochoa program for Centres of Excellence in R&D (CEX2019-000910-S, [MCIN/ AEI/10.13039/501100011033]). E.M. was a recipient of the Basque Government Doctoral Fellowship Program (PRE_2022_2_0065). AB.S. is a recipient of the PhD Fellowship Program of the Fundação para a Ciência e Tecnologia (2022.13131.BD). A.G-S. was a recipient of Agència de Gestió d'Ajuts Universitaris i de Recerca (FI-AGAUR) grant by La Generalitat de Catalunya (2019FI_B100212). M.C is a recipient of the PhD Fellowship from Fondo Social Europeo (PRE2020-095721).

Competing interests

J.D. receives royalties from Athena Diagnostics for the use of Ma2 as an autoantibody test and from Euroimmun for the use of NMDA as an antibody test. He received a licensing fee from Euroimmun for the use of GABAB receptor, GABAA receptor, DPPX and IgLON5 as autoantibody tests; he has received a research grant from Sage Therapeutics. S.G is an employee and shareholder of Sage Therapeutics.

References

1. Dalmau J, Tuzun E, Wu HY, et al. Paraneoplastic anti-N-methyl-D-aspartate receptor encephalitis associated with ovarian teratoma. *Ann Neurol* 2007;61:25-36.
2. Dalmau J, Gleichman AJ, Hughes EG, et al. Anti-NMDA-receptor encephalitis: case series and analysis of the effects of antibodies. *Lancet Neurol* 2008;7:1091-1098.
3. Florance NR, Davis RL, Lam C, et al. Anti-N-methyl-D-aspartate receptor (NMDAR) encephalitis in children and adolescents. *Ann Neurol* 2009;66:11-18.
4. Armangue T, Olive-Cirera G, Martinez-Hernandez E, et al. Neurologic complications in herpes simplex encephalitis: clinical, immunological and genetic studies. *Brain* 2023;146:4306-4319.
5. Titulaer MJ, McCracken L, Gabilondo I, et al. Treatment and prognostic factors for long-term outcome in patients with anti-NMDA receptor encephalitis: an observational cohort study. *Lancet Neurol* 2013;12:157-165.
6. Guasp M, Rosa-Justicia M, Munoz-Lopetegi A, et al. Clinical characterisation of patients in the post-acute stage of anti-NMDA receptor encephalitis: a prospective cohort study and comparison with patients with schizophrenia spectrum disorders. *Lancet Neurol* 2022;21:899-910.
7. Mikasova L, P. DR, Bouchet D, et al. Disrupted surface cross-talk between NMDA and Ephrin-B2 receptors in anti-NMDA encephalitis. *Brain* 2012;135:1606-1621.
8. Hughes EG, Peng X, Gleichman AJ, et al. Cellular and synaptic mechanisms of anti-NMDA receptor encephalitis. *J Neurosci* 2010;30:5866-5875.
9. Planaguma J, Leypoldt F, Mannara F, et al. Human N-methyl D-aspartate receptor antibodies alter memory and behaviour in mice. *Brain* 2015;138:94-109.
10. Carceles-Cordon M, Mannara F, Aguilar E, Castellanos A, Planaguma J, Dalmau J. NMDAR antibodies alter dopamine receptors and cause psychotic behavior in mice. *Ann Neurol* 2020;88:603-613.

11. Wright S, Hashemi K, Stasiak L, et al. Epileptogenic effects of NMDAR antibodies in a passive transfer mouse model. *Brain* 2015;138:3159-3167.
12. Jones BE, Tovar KR, Goehring A, et al. Autoimmune receptor encephalitis in mice induced by active immunization with conformationally stabilized holoreceptors. *Sci Transl Med* 2019;11.
13. Wagnon I, Helie P, Bardou I, et al. Autoimmune encephalitis mediated by B-cell response against N-methyl-d-aspartate receptor. *Brain* 2020;143:2957-2972.
14. Ding Y, Zhou Z, Chen J, et al. Anti-NMDAR encephalitis induced in mice by active immunization with a peptide from the amino-terminal domain of the GluN1 subunit. *J Neuroinflammation* 2021;18:53.
15. Linnoila J, Jalali Motlagh N, Jachimiec G, et al. Optimizing animal models of autoimmune encephalitis using active immunization. *Front Immunol* 2023;14:1177672.
16. He S, Sun C, Zhu Q, et al. A juvenile mouse model of anti-N-methyl-D-aspartate receptor encephalitis by active immunization. *Front Mol Neurosci* 2023;16:1211119.
17. Yu L, Wen Y, Yang J, et al. Autoimmune receptor encephalitis in ApoE(-/-) mice induced by active immunization with NMDA1. *Mol Med Rep* 2023;28.
18. Mannara F, Radosevic M, Planaguma J, et al. Allosteric modulation of NMDA receptors prevents the antibody effects of patients with anti-NMDAR encephalitis. *Brain* 2020;143:2709-2720.
19. Radosevic M, Planaguma J, Mannara F, et al. Allosteric Modulation of NMDARs Reverses Patients' Autoantibody Effects in Mice. *Neurol Neuroimmunol Neuroinflamm* 2021;9(1):e1122.
20. Gresa-Arribas N, Titulaer MJ, Torrents A, et al. Antibody titres at diagnosis and during follow-up of anti-NMDA receptor encephalitis: a retrospective study. *Lancet Neurol* 2014;13:167-177.

21. Matute C, Palma A, Serrano-Regal MP, et al. N-methyl-D-aspartate receptor antibodies in autoimmune encephalopathy alter oligodendrocyte function. *Ann Neurol* 2020;87:670-676.
22. Maudes E, Mannara F, Garcia-Serra A, et al. Human Metabotropic Glutamate Receptor 5 Antibodies Alter Receptor Levels and Behavior in Mice. *Ann Neurol* 2022; 92:81-86.
23. Garcia-Serra A, Radosevic M, Pupak A, et al. Placental transfer of NMDAR antibodies causes reversible alterations in mice. *Neurol Neuroimmunol Neuroinflamm* 2021;8:e1061.
24. Cunqueiro M, Aguilar E, Loza-Alvarez P, Planaguma J. Hippocampal Neuronal Cultures to Detect and Study New Pathogenic Antibodies Involved in Autoimmune Encephalitis. *J Vis Exp* 2022 Jun 2:(184).
25. Maudes E, Jamet Z, Marmolejo L, Dalmau JO, Groc L. Positive Allosteric Modulation of NMDARs Prevents the Altered Surface Dynamics Caused by Patients' Antibodies. *Neurol Neuroimmunol Neuroinflamm* 2024;11:e200261.
26. Martinez-Hernandez E, Horvath J, Shiloh-Malawsky Y, Sangha N, Martinez-Lage M, Dalmau J. Analysis of complement and plasma cells in the brain of patients with anti-NMDAR encephalitis. *Neurology* 2011;77:589-593.
27. Zrzavy T, Endmayr V, Bauer J, et al. Neuropathological Variability within a Spectrum of NMDAR-Encephalitis. *Ann Neurol* 2021;90:725-737.
28. Gleichman AJ, Spruce LA, Dalmau J, Seeholzer SH, Lynch DR. Anti-NMDA receptor encephalitis antibody binding is dependent on amino acid identity of a small region within the GluN1 amino terminal domain. *J Neurosci* 2012;32:11082-11094.
29. Weber MS, Prod'homme T, Patarroyo JC, et al. B-cell activation influences T-cell polarization and outcome of anti-CD20 B-cell depletion in central nervous system autoimmunity. *Ann Neurol* 2010;68:369-383.

30. Lyons JA, San M, Happ MP, Cross AH. B cells are critical to induction of experimental allergic encephalomyelitis by protein but not by a short encephalitogenic peptide. *Eur J Immunol* 1999;29:3432-3439.
31. Ott G, Barchfeld GL, Chernoff D, Radhakrishnan R, van Hoogevest P, Van Nest G. MF59. Design and evaluation of a safe and potent adjuvant for human vaccines. *Pharm Biotechnol* 1995;6:277-296.
32. Zhang J, Miao J, Han X, et al. Development of a novel oil-in-water emulsion and evaluation of its potential adjuvant function in a swine influenza vaccine in mice. *BMC Vet Res* 2018;14:415.
33. Wang Y, Tai W, Yang J, et al. Receptor-binding domain of MERS-CoV with optimal immunogen dosage and immunization interval protects human transgenic mice from MERS-CoV infection. *Hum Vaccin Immunother* 2017;13:1615-1624.
34. Leenaars PP, Koedam MA, Wester PW, Baumans V, Claassen E, Hendriksen CF. Assessment of side effects induced by injection of different adjuvant/antigen combinations in rabbits and mice. *Lab Anim* 1998;32:387-406.
35. Ochs J, Nissimov N, Torke S, et al. Proinflammatory CD20(+) T cells contribute to CNS-directed autoimmunity. *Sci Transl Med* 2022;14:eabi4632.
36. Bien CG, Vincent A, Barnett MH, et al. Immunopathology of autoantibody-associated encephalitides: clues for pathogenesis. *Brain* 2012;135:1622-1638.
37. Rahman KA, Orlando M, Boulos A, et al. Microglia actively remove NR1 autoantibody-bound NMDA receptors and associated post-synaptic proteins in neuron microglia co-cultures. *Glia* 2023;71:1804-1829.
38. Kayser MS, Titulaer MJ, Gresa-Arribas N, Dalmau J. Frequency and characteristics of isolated psychiatric episodes in anti-N-methyl-d-aspartate receptor encephalitis. *JAMA Neurol* 2013;70:1133-1139.
39. Paul SM, Doherty JJ, Robichaud AJ, et al. The major brain cholesterol metabolite 24(S)-hydroxycholesterol is a potent allosteric modulator of N-methyl-D-aspartate receptors. *J Neurosci* 2013;33:17290-17300.

40. Warikoo N, Brunwasser SJ, Benz A, et al. Positive allosteric modulation as a potential therapeutic strategy in anti-NMDA receptor encephalitis. *J Neurosci* 2018;38:3218-3229.
41. Hausler D, Hausser-Kinzel S, Feldmann L, et al. Functional characterization of reappearing B cells after anti-CD20 treatment of CNS autoimmune disease. *Proc Natl Acad Sci U S A* 2018;115:9773-9778.
42. Yu S, Ellis JS, Dunn R, Kehry MR, Braley-Mullen H. Transient depletion of B cells in young mice results in activation of regulatory T cells that inhibit development of autoimmune disease in adults. *Int Immunol* 2012;24:233-242.
43. Al-Diwani A, Theorell J, Damato V, et al. Cervical lymph nodes and ovarian teratomas as germinal centres in NMDA receptor-antibody encephalitis. *Brain* 2022;145:2742-2754.
44. Laman JD, Weller RO. Drainage of cells and soluble antigen from the CNS to regional lymph nodes. *J Neuroimmune Pharmacol* 2013;8:840-856.
45. Laman JD, Weller RO. Editorial: route by which monocytes leave the brain is revealed. *J Leukoc Biol* 2012;92:6-9.
46. McMahon EJ, Bailey SL, Castenada CV, Waldner H, Miller SD. Epitope spreading initiates in the CNS in two mouse models of multiple sclerosis. *Nat Med* 2005;11:335-339.
47. Heine J, Kopp UA, Klag J, Ploner CJ, Pruss H, Finke C. Long-Term Cognitive Outcome in Anti-N-Methyl-D-Aspartate Receptor Encephalitis. *Ann Neurol* 2021;90:949-961.

Figures

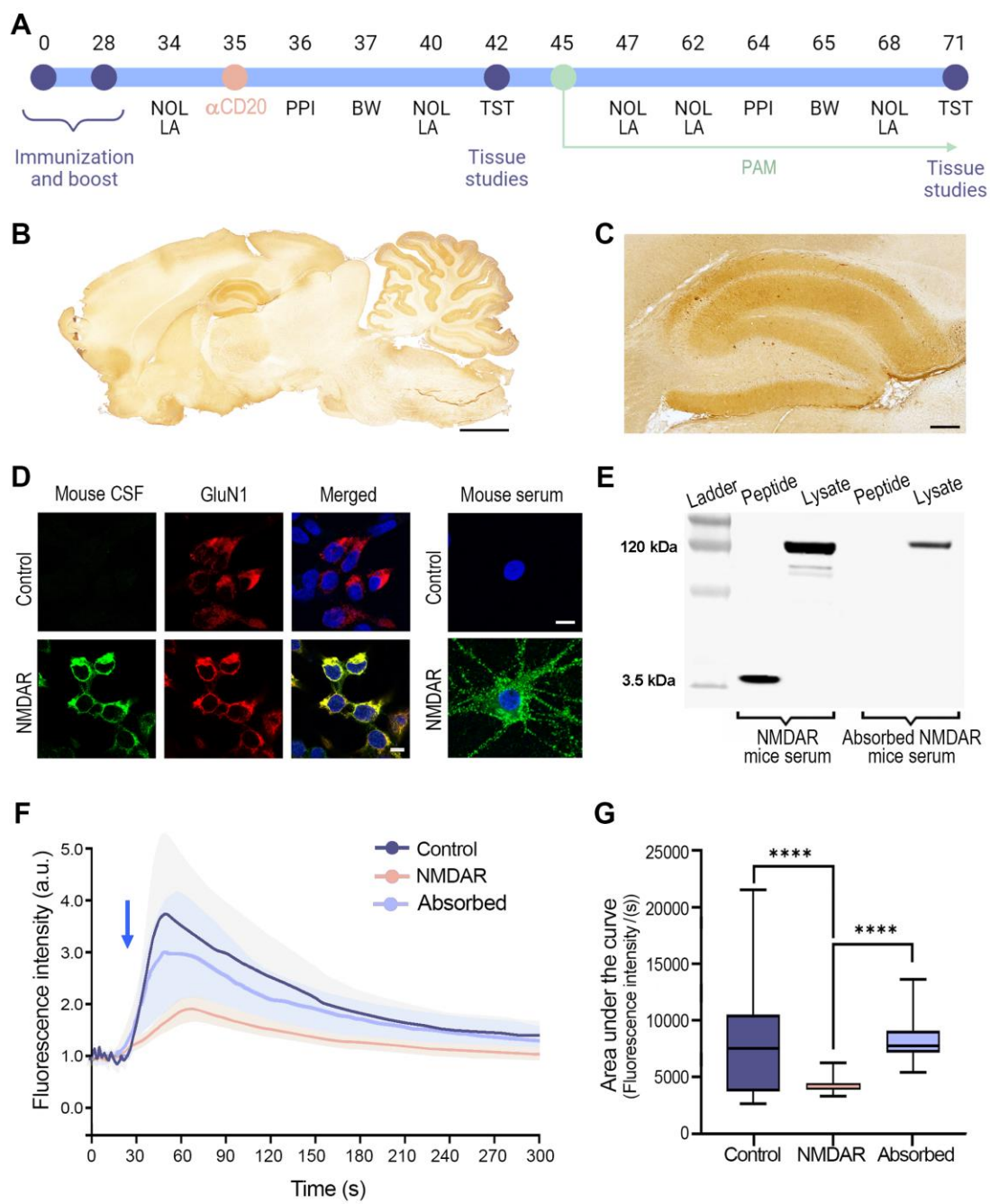


Figure 1: Immunization with GluN1₃₅₆₋₃₈₅ results in pathogenic GluN1 antibody production

(A) Schematic representation of the immunization, treatment, behavioural tasks and tissue study timeline. NOL: Novel Object Location; PPI: Prepulse Inhibition; BM: Black and White test; TST: Tail Suspension Test. On days 42 and 71 subsets of mice were sacrificed and their blood, spleen, lymph nodes, brain, and CSF were harvested for tissue and cellular studies. (B) Sagittal section of rat brain immunostained with IgG purified from a pool of 5 NMDAR mice showing a pattern of neuropil staining similar to that described for patients' NMDAR IgG. Scale bar = 2 mm. (C) Magnification showing the immunostaining of the hippocampus. Scale bar = 250 μ m. (D) Left side: cell-based assay with HEK293 cells expressing GluN1/GluN2b showing reactivity with CSF from an NMDAR mouse (green), which colocalizes (yellow) with the commercial GluN1 antibody (red); CSF from a control mouse shows no reactivity. Right side: live neuron immunofluorescence showing intense cell-surface immunolabelling (green) with serum of an NMDAR mouse, but not with control serum. (E) Immunoblot of GluN1₃₅₆₋₃₈₅ peptide and neuronal lysate probed with non-absorbed and peptide-absorbed NMDAR mice serum. Compared with non-absorbed NMDAR mice serum, the peptide-absorbed mice serum is no longer reactive with the peptide, but retains reactivity with the neuronal lysate. (F) NMDAR mice IgG reduce NMDA-induced calcium influx in rat neurons expressing GCaMP5G. The plot shows one of three independent experiments representing the fluorescence intensity upon NMDA stimulation (blue arrow) for neuronal cultures treated with NMDAR mice IgG (pink), control mice IgG (dark blue), and NMDAR mice IgG pre-absorbed with NMDAR (light blue). Data are represented as mean \pm SEM. (G) Analysis of the area under the curve of calcium fluorescence over-time for the three experimental groups (controls n = 56 cells; NMDAR mice n = 103 cells; NMDAR mice absorbed n = 43 cells). Box plots show the median, 25th and 75th percentile. Whiskers indicate the minimum and maximum values. Assessment of significance was performed by one-way analysis of variance (ANOVA, $p < 0.0001$). A value of $p < 0.05$ was considered statistically significant.

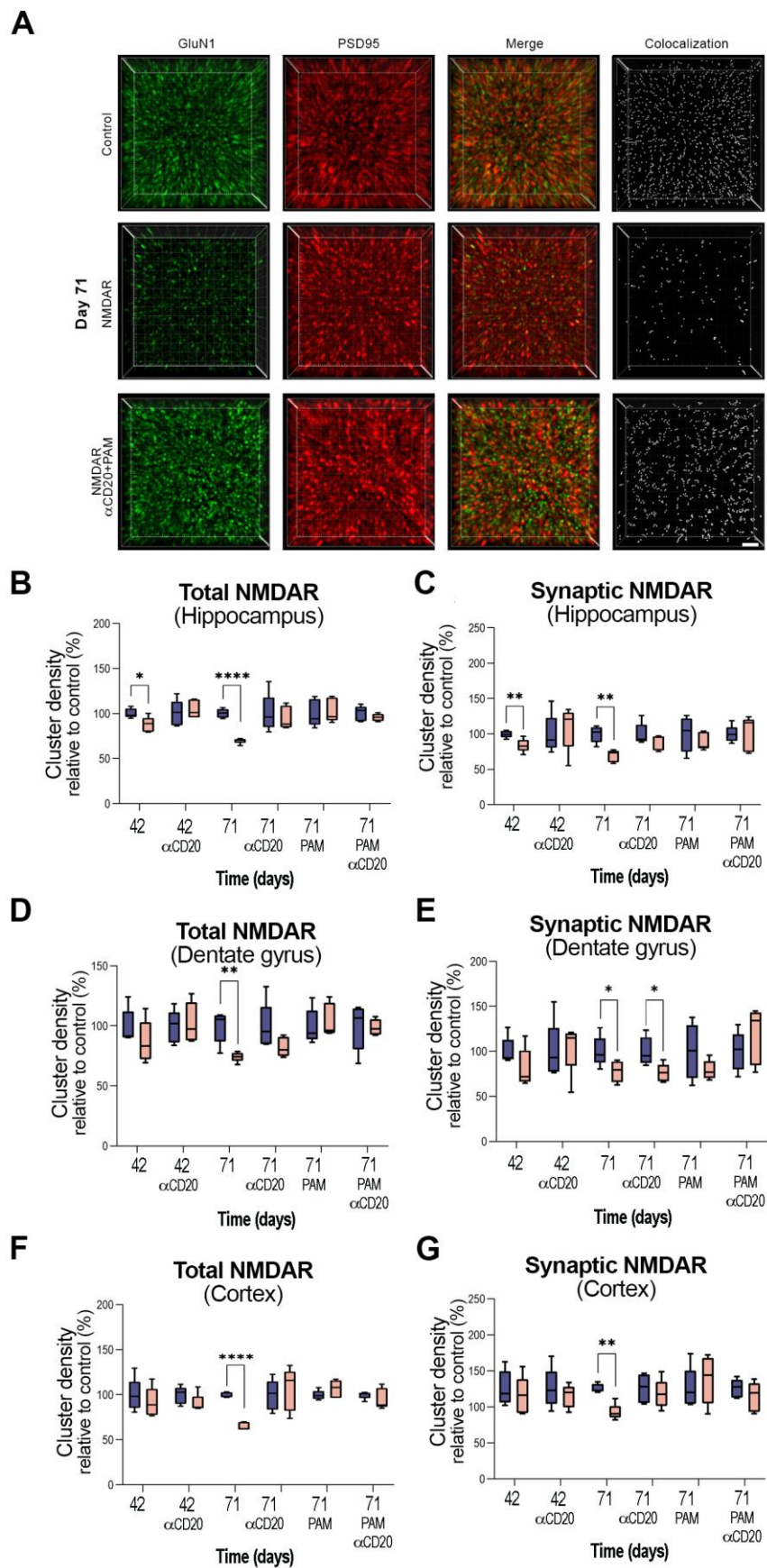


Figure 2: Treatments with anti-CD20 and NMDAR-PAM restore the levels of NMDARs in NMDAR mice

(A) 3D projection and analysis of the density of total cell-surface NMDAR (GluN1) clusters, PSD95, and synaptic NMDAR clusters (defined as those that co-localized with PSD95) in a representative area of CA1 of the hippocampus at day 71. Top row corresponds to the CA1 region of a control mouse; middle row, NMDAR mouse; lower row, NMDAR mouse treated with anti-CD20 and a positive allosteric modulator (PAM, SGE301) of NMDAR. Merged images were postprocessed and used to calculate the density of clusters (density = spots/ μm^3). Scale bar = 2 μm . For each animal 42 square images similar to those shown in A were examined (9 from CA1, 9 from CA3, 9 from dentate, and 15 from cortex). Quantification of the density of NMDAR clusters showing (B) total and (C) synaptic NMDAR clusters in a pooled analysis of hippocampal areas (CA1, CA3), (D) total and (E) synaptic NMDAR clusters in the dentate gyrus, and (F) total and (G) synaptic NMDAR clusters in the cortex. For the 3 brain regions assessed, untreated NMDAR mice show a significant reduction of synaptic and extrasynaptic clusters on day 71, and substantial or significant reduction of clusters on day 42. Treatment with anti-CD20, NMDAR-PAM, or both combined, restored the levels of NMDAR, but on day 71 NMDAR mice only treated with anti-CD20 started showing a new reduction of NMDAR (significant in dentate gyrus) coinciding with B cell repopulation (see Fig 4C). Mean density of clusters in control conditions was defined as 100%. For each experimental condition 5 controls (blue) and 5 NMDAR mice (pink) were examined. Box plots show the median, and 25th and 75th percentile; whiskers indicate the minimum or maximum values. Significance was assessed by a mixed nested model and a value of $p < 0.05$ was considered significant.

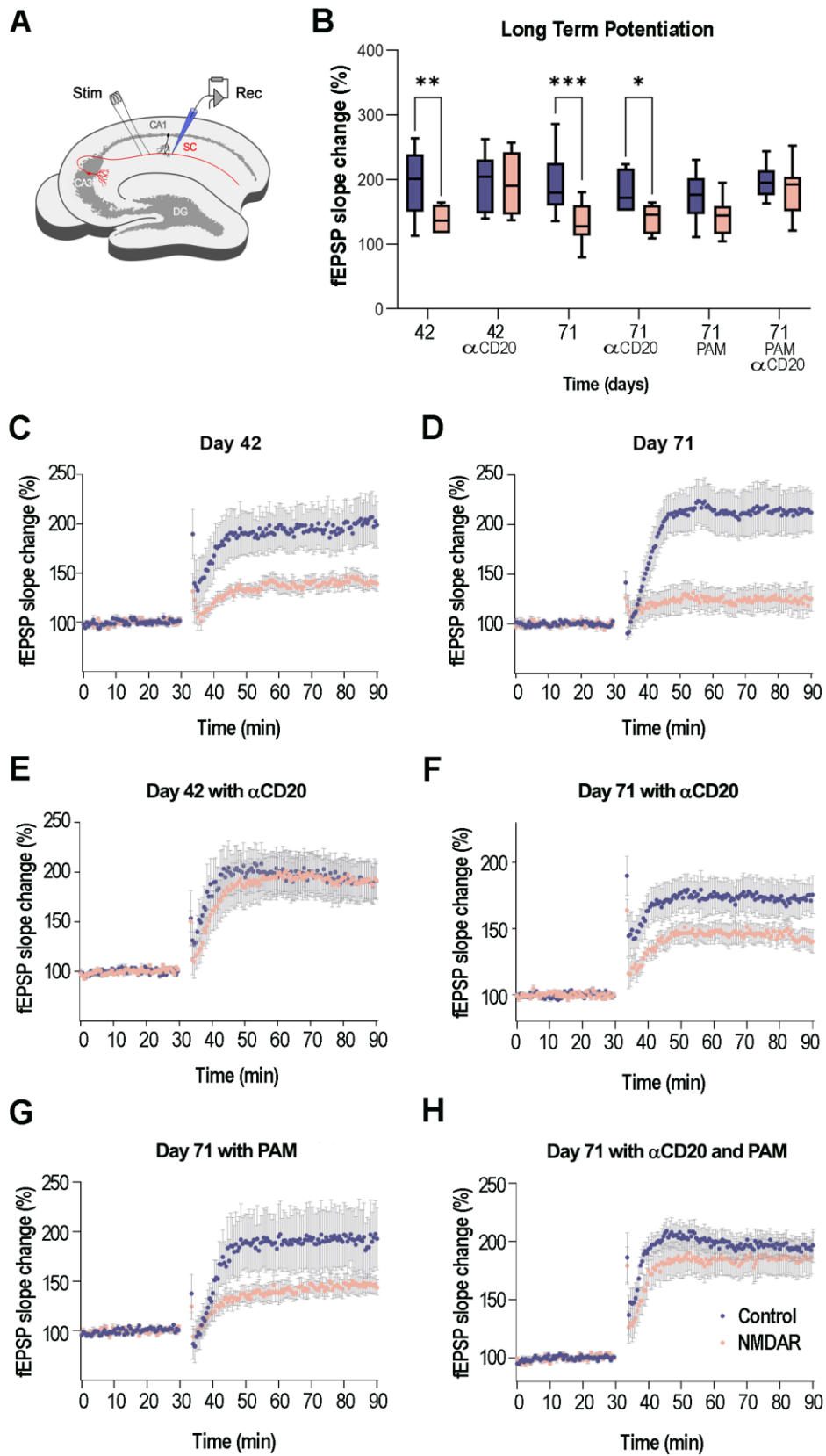


Figure 3: Hippocampal long-term potentiation (LTP) in NMDAR mice, and effects of different treatments

The Schaffer collateral pathway (SC, red) was stimulated (Stim) and field potentials were recorded (Rec) in the CA1 region of the hippocampus. LTP was induced by theta burst stimulation. **(B)** Compared with controls (blue), untreated NMDAR mice (pink) showed a significant reduction of field excitatory postsynaptic potential (fEPSP) slope change on days 42 and 71. NMDAR mice treated with anti-CD20 showed early recovery of fEPSP (day 42) but new reduction of fEPSP on day 71, coinciding with B-cell repopulation (see Fig. 4C). Box plot shows the median, 25th and 75th percentiles; whiskers indicate minimum and maximum values. Significance was assessed with a nested mixed model. A value of $p < 0.05$ was considered significant. **(C)** Time course of fEPSP recordings in control (blue) and NMDAR mice (pink) on day 42 (controls $n = 6$, NMDAR $n = 7$); **(D)** day 71 (controls $n = 8$, NMDAR $n = 9$); **(E)** day 42 treated with anti-CD20 (controls $n = 6$, NMDAR $n = 6$); **(F)** day 71 treated with anti-CD20 (controls $n = 8$, NMDAR $n = 7$); **(G)** day 71 treated with NMDAR-PAM (SGE-301) (controls $n = 6$, NMDAR $n = 8$); and **(H)** day 71 treated with both anti-CD20 and NMDAR-PAM (controls $n = 6$, NMDAR $n = 6$). The fEPSP values of all animals for each of the groups are presented as mean \pm standard error of the mean (SEM).

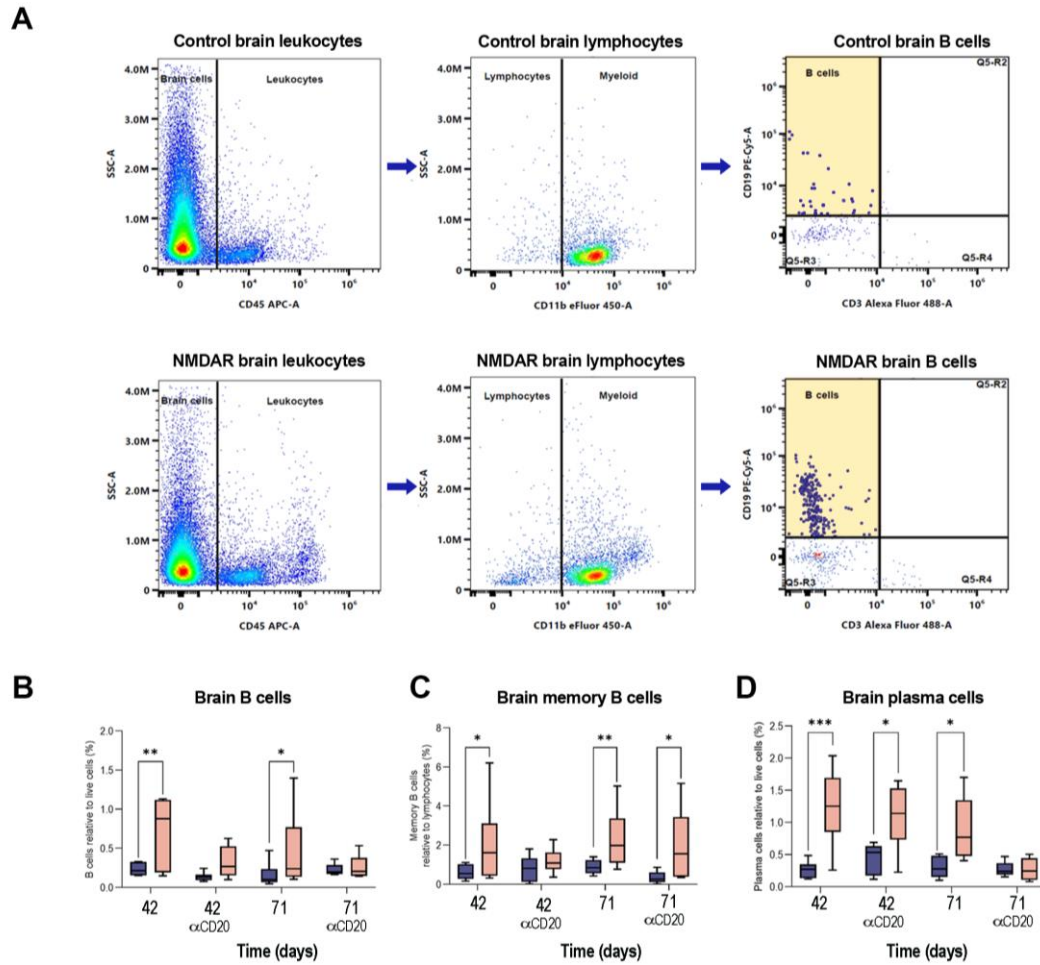


Figure 4: Presence of B cells and plasma cells in the brain of NMDAR mice, and effects of different treatments

(A) Flow cytometry scatter plots showing the presence of B cells and plasma cells in the brain of a representative NMDAR mouse and control mouse, illustrating the gating strategy to analyze the presence of the cell infiltrates. Live cells were gated for CD45 to select leukocytes and for CD11b to select lymphocytes. B cells were gated as CD3⁻ and CD19⁺. Quantification of brain B cells (B), memory B cells (C), and plasma cells (D) in control (blue, n=10) and NMDAR mice (pink, n=10) for all experimental conditions. Untreated NMDAR mice had a significant brain increase of total B cells, memory B cells, and plasma cells on days 42 and 71. NMDAR mice treated with anti-CD20 treatment showed a decrease of brain B cells on day 42 and plasma cells on day 71, but memory B cells started to repopulate on day 71. Box plot shows the median, 25th and 75th percentiles; whiskers indicate minimum and maximum values. Significance was assessed with a mixed model. A value of $p < 0.05$ was considered significant.

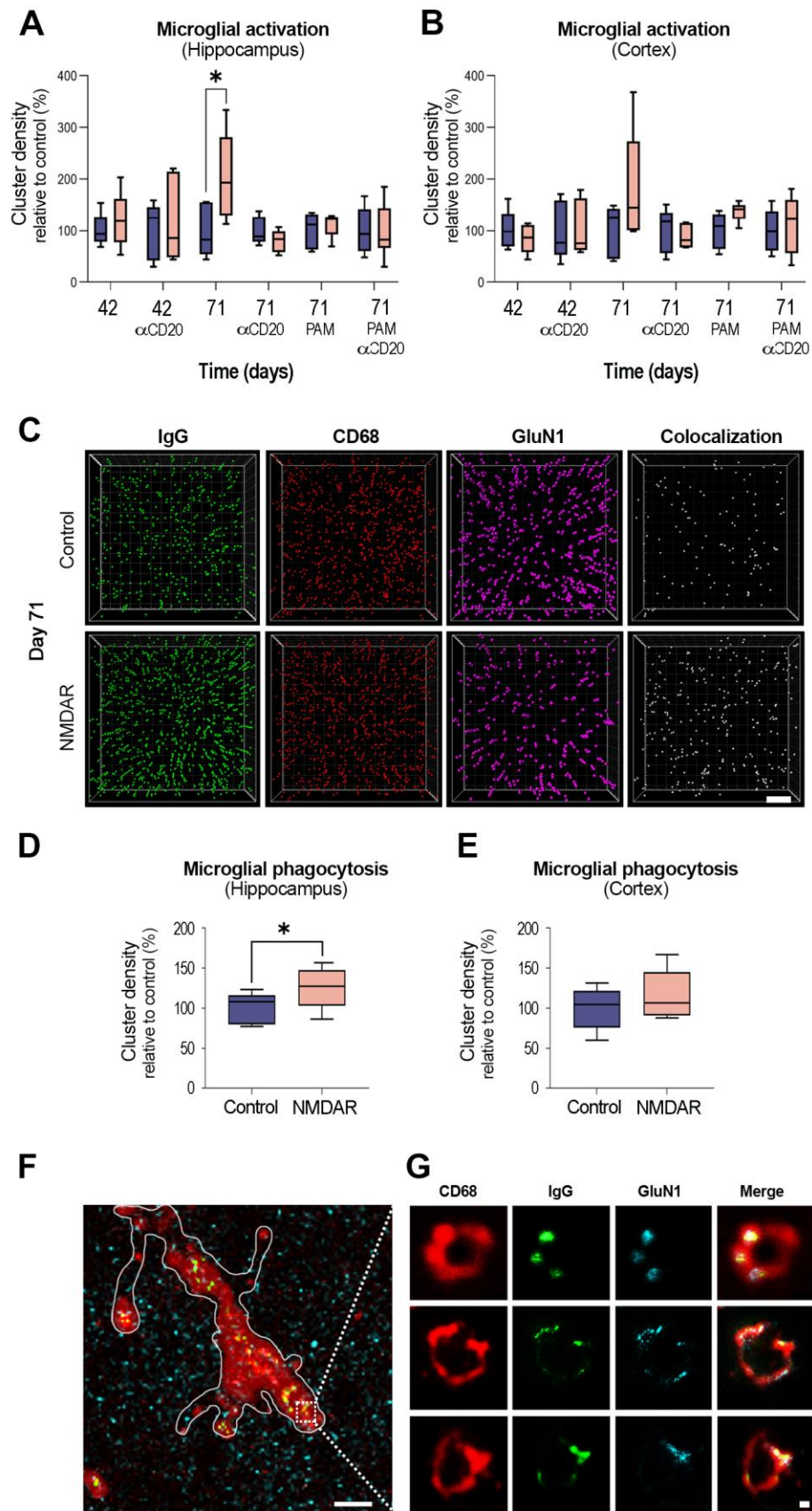


Figure 5: Microglia activation and phagocytosis of NMDARs bound to IgG

Quantification of microglia activation (defined as the co-localization of Iba-1 and CD68) in the hippocampus (**A**) and cortex (**B**) of NMDAR mice and controls; the areas of the hippocampus (CA1, CA3, and dentate) and cortex are the same as those examined in Figure 2. (**C**) 3D projection and analysis of the density of clusters of IgG, CD68, total cell-surface GluN1, and their triple co-localization in a representative CA1 square region of an NMDAR and control mice at day 71. Merged images were postprocessed and used to calculate density clusters (density = spots/ μm^3). Scale bar = 2 μm . Quantification of triple co-localization of clusters (IgG, CD68, GluN1 = defined as microglial phagocytosis of NMDAR) in the indicated regions of hippocampus (**D**) and cortex (**E**) of untreated NMDAR and control mice on day 71. Mean density of clusters in control conditions was defined as 100%. For each experimental condition 5 controls (blue) and 5 NMDAR mice (pink) were examined. Box plots show the median, and 25th and 75th percentile; whiskers indicate the minimum or maximum values. Significance of microglia activation was assessed by a mixed nested model, and microglia phagocytosis by t-student. A value of $p < 0.05$ was considered significant. Super-resolution imaging of a microglial cell (**F,G**) with Stimulated Emission Depletion (STED) microscopy shows that the triple co-localization (white) of CD68 (red), IgG (green), and GluN1 (cyan) occurs in the endosomes. **F** scale bar = 2 μm ; **G** scale bar = 100 nm.

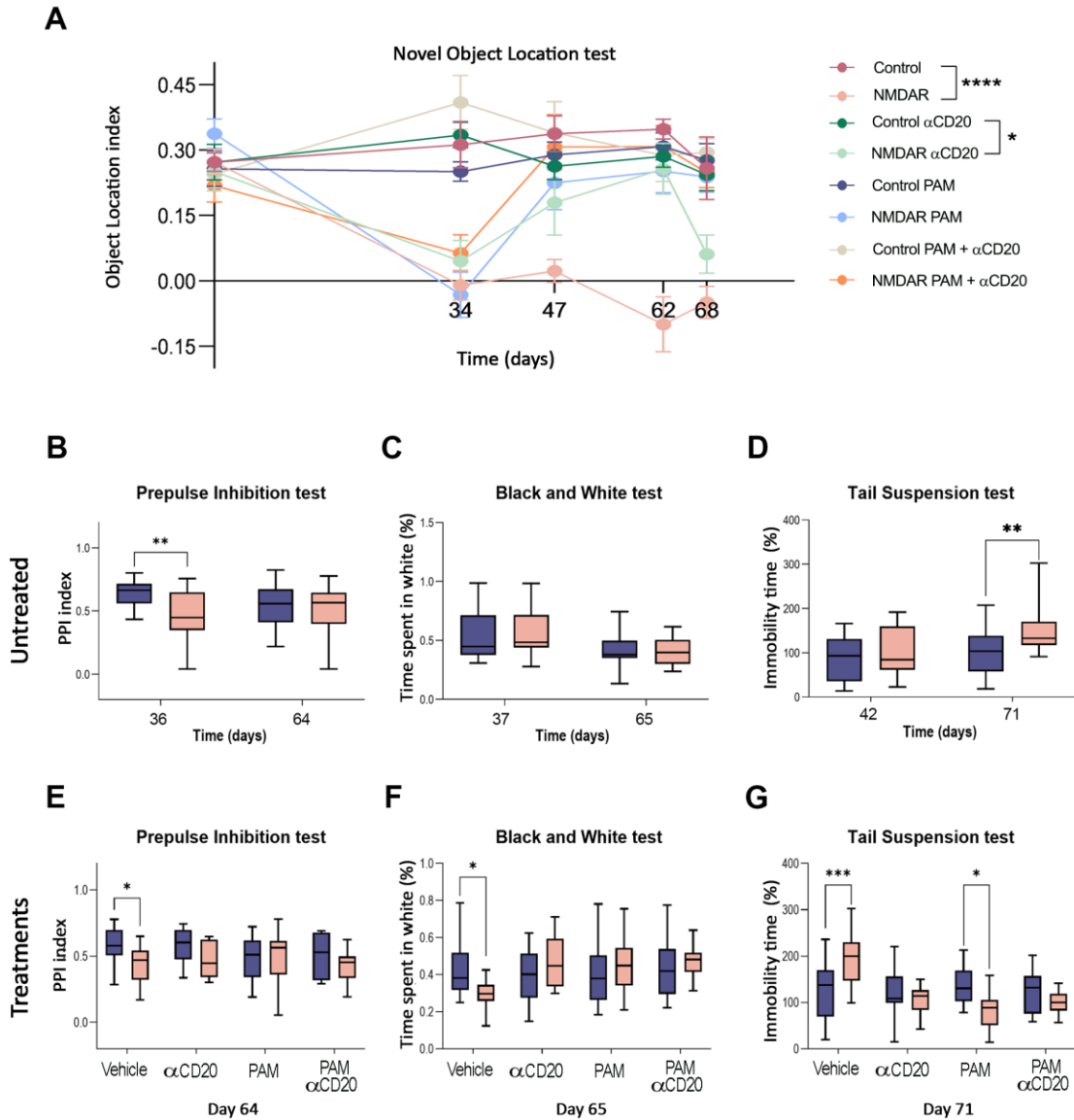


Figure 6: Behavioural and memory alterations in NMDAR mice, and effects of different treatments

(A) Memory assessment with the Novel Object Location (NOL) test in NMDAR mice and controls that received vehicle (no treatment), anti-CD20, NMDAR-PAM, and both treatments. On day 34, all NMDAR mice, but not controls, showed a significant decrease of memory. Treatment with anti-CD20 restored memory levels in NMDAR mice (days 47, 62), although by day 68, coinciding with B cell repopulation (see Fig. 4C), they showed relapsing memory impairment. NMDAR mice treated with NMDAR-PAM alone or the sequential administration of anti-CD20 and NMDAR-PAM showed

improved memory from day 47 until the end of the study. Each experimental group included 12 animals. **(B-D)** Behavioural assessments in untreated NMDAR mice and controls that did not receive daily injections of vehicle: **(B)** compared to controls (blue), untreated NMDAR mice (pink) showed psychotic-like behaviour (prepulse inhibition test) on day 36, but not on day 64. Day 36, NMDAR mice n = 22, controls n = 23; day 64, NMDAR mice n = 23, controls n = 23. **(C)** Untreated NMDAR mice and controls showed similar levels of anxiety during the study (black and white test). Day 37, NMDAR mice n = 22, controls n = 23; day 65, NMDAR mice n = 24, controls n = 23. **(D)** Compared to controls, untreated NMDAR mice showed depressive-like behaviour (tail suspension test) on day 71, but not on day 42. Day 42, NMDAR mice n = 22, controls n = 23; day 71, NMDAR mice n = 24, controls n = 23. **(E-F)** Behavioural assessments (as in B-D) in NMDAR mice and controls that received no treatment (daily injection of vehicle) or one of the following treatments: anti-CD20, daily injection of NMDAR-PAM, or sequential combination of both treatments. Compared with controls (blue), untreated NMDAR mice (red) showed psychotic-like behaviour on day 64 **(E)**, anxiety on day 65 **(F)** and depressive-like behaviour on day 71 **(G)**. None of these alterations occurred in animals that received treatment with anti-CD20, NMDAR-PAM, or both. Each of the experimental groups in E-G included 12 animals. Box plots show the median, and the 25th and 75th percentile; whiskers indicate the minimum or maximum values. Line plots are represented as the mean \pm SEM. Significance was assessed using a mixed model for the analysis of the tests of treated mice and two-way ANOVA with post hoc analysis, including multiple comparison corrections for the tests of untreated mice. A value of $p < 0.05$ was considered statistically significant.

Supplementary material

Supplementary methods

Animal experiments	3
Polyclonal antibody response and epitope spreading in NMDAR mice	3
Peptide and neuronal lysate immunoblot	3
Cell-based assays with GluN1 mutants.....	3
Determination of IgG subtype	4
Pathogenicity of antibodies from NMDAR mice.....	5
Cultures of primary rat hippocampal neurons.....	5
Calcium video microscopy.....	5
Determination of effects of antibodies on NMDAR clusters in hippocampal neurons.....	5
Determination of IgG deposits and precipitation of NMDAR-bound to antibodies	6
Electrophysiology	7
Determination of complement deposition in brain	8
Stimulated Emission Depletion (STED) microscopy	8
Determination of brain T cells by immunohistochemistry.....	9
Isolation of splenocytes	10
Behavioral tasks	10
Novel Object Location (NOL) test.....	10
Locomotor Activity (LA).....	11
Pre-pulse inhibition of the acoustic startle response (PPI) test	11
Black and White (BW).....	11

Tail Suspension Test (TST)	12
Seizure susceptibility study	12
Pentylentetrazol-induced seizures	12
cFos immunostaining	13
Electrophysiological recordings in vivo.....	14
Supplementary figures	
Supplementary Figure 1: Mice immunized with GluN1356-385 peptide produce polyclonal antibodies beyond the epitope region of the immunizing peptide	16
Supplementary Figure 2: NMDAR mice serum cause a reduction of cell-surface NMDAR clusters in cultured rat hippocampal neurons.	16
Supplementary Figure 3: Cells from deep cervical lymph nodes from NMDAR mice produce GluN1 antibodies.	17
Supplementary Figure 4: Effects of anti-CD20 on splenocytes and lymphocytes	17
Supplementary Figure 5: Presence of IgG bound to NMDAR in brain of NMDAR mice	18
Supplementary Figure 6: Effects of anti-CD20 on antibody titers.....	18
Supplementary Figure 7: NMDAR mice show a decrease in seizure threshold induced by pentylentetrazol.	19
Supplementary videos	
Supplementary Video 1: Reduction of NMDA-induced calcium currents in neurons treated with IgG from NMDAR mice	20
Supplementary Video 2: Motor stereotypies in NMDAR mice.	20

Supplementary methods

Animal experiments

A total of 275 female C57BL6/J mice (Charles River) were used for all experiments. Sample size was calculated based on previously published studies using passive transfer of patients' antibodies and similar experiments.¹⁻³ Each mouse was considered as a experimental unit. Mice were randomly allocated to an experimental group based on a random number generator. Confounders were minimised by having two control and two NMDAR mice housed in the same cage for all experimental conditions. Investigators were blinded to the experimental allocation during behavioral and tissue investigations until data analysis.

Polyclonal antibody response and epitope spreading in NMDAR mice

Peptide and neuronal lysate immunoblot

The immunizing peptide GluN1₃₅₆₋₃₈₅ and hippocampal neuronal culture lysates were run in a gel, transferred to a nitrocellulose membrane (1704158, Bio-Rad, Hercules, CA), and incubated with pooled serum from 5 representative NMDAR mice (1:200) intact or pre-absorbed with the peptide (0.25 µg/µl) for 2 h at room temperature (RT). The reactivity was developed following a standard enhanced chemiluminescence developing kit (RPN2108, GE Healthcare, Chicago, IL).

Cell-based assays using GluN1 mutants

The GluN1 mutants have been previously described^{4, 5} and are shown in Supplementary Fig. 1. In brief, G369I and G369S are single point mutations where glycine 369 was replaced by an isoleucine or serine, respectively. The “top lobe construct” carries a deletion of residues 26-140 and 275-349 in the top lobe of the amino-terminal domain (ATD). The deleted-construct carries a deletion of residues 12-385, containing all amino acids present in the

immunizing peptide GluN1₃₅₆₋₃₈₅. HEK cells transfected with these mutants were used for immunocytochemistry following the same cell-based assay and serum dilutions used to test mouse samples with native GluN1. Briefly, HEK293 cells transfected with GluN1/GluN2b in equimolar ratios, or the indicated mutants, were grown for 24h after transfection. All cells were routinely grown in the presence of ketamine (500 μ M) to prevent cell death after transfection. Transfected cells were then fixed with 4% paraformaldehyde for 5 min at RT, permeabilized with 0.3% Triton X-100 for 5 min at RT, and incubated with mouse serum diluted 1:40 and a commercial rabbit polyclonal antibody against the c-terminal region of GluN1 (dilution 1:5000, G8913, Sigma) overnight at 4 °C. Cells were then washed with PBS, and incubated with the corresponding fluorescence secondary antibodies (Alexa Fluor 488 goat anti-mouse and Alexa Fluor 594 goat anti-rabbit, both diluted 1:1000 and from Invitrogen) for 1 h at RT.

Determination of IgG subtype

IgG subtype of antibodies from NMDAR mice was determined by CBA with HEK293 cells transfected with GluN1/GluN2b. Transfected cells were fixed and permeabilized as indicated above, and incubated with mouse serum diluted 1:40 and a commercial rabbit polyclonal antibody against GluN1 (dilution 1:5000, G8913, Sigma) overnight at 4 °C. Cells were then washed with PBS and incubated with specific Alexa Fluor 488 goat anti-mouse IgG1 (A21121), IgG2a (A21131), IgG2b (A21141), or IgG3 (A21151) and Alexa Fluor 594 goat anti-rabbit (all diluted 1:1000 and from Invitrogen) for 1 h at RT.

Pathogenicity of antibodies from NMDAR mice

Cultures of primary hippocampal neurons

Primary hippocampal neurons were obtained from day 18 embryos of Wistar rats, as reported.⁶ Dissociated neurons were seeded on coverslips and grown in Corning® 35 mm x 10 mm dishes (Sigma-Aldrich, St Louis, MI, US) containing 1 ml of Neurobasal medium + B-27 Supplement (ThermoFisher, Waltham, MA, US).

Calcium video microscopy

Calcium video microscopy was performed on 7-day *in vitro* primary cultures of dissociated rat hippocampal neurons transduced with the viral vector pAAV2-CAG-GCaMP5G at 2.5×10^{10} GC/mL as previously reported.⁷ Five days after transduction, cells were treated with purified IgG from NMDAR mice or controls. One day later, cells were transferred to a chamber of an inverted fluorescent microscope equipped with a mercury lamp and a FITC filter cube (Eclipse TE20000-U, Nikon, Tokyo, Japan) and an ORCA flash4.0 v3 digital CMOS camera (Hamamatsu, Hamamatsu, Japan). The cell chamber was kept at 37°C with 5% CO₂. Cells were treated with NBQX to block AMPA and KA receptors, and specifically visualize NMDAR dependent Ca²⁺ signal (fluorescence). A movie of 5 min with frames recorded every 100 ms was acquired. Shortly after starting the acquisition, 100 µM of NMDA and 1 µM of Glycine were added to the dish. The fluorescence signal over time was extracted by ImageJ.

Determination of effects of antibodies on NMDAR clusters in hippocampal neurons

To assess the effect of mice antibodies on NMDAR cluster density, serum from a pool of 5 NMDAR or control mice was added to the culture media (1:100) for 24 h. After removing the media and extensively washing with phosphate buffered saline (PBS), neurons were live incubated with human NMDAR IgG (1:200) for 30 min at room temperature to label the

clusters on cell surface, as reported.² Subsequently, neurons were fixed with 4% PFA for 10 min, incubated with Alexa Fluor 488 goat anti-human IgG (1:1000, 109-545-088, Jackson ImmunoResearch, Newmarket, UK) for 1 h RT, and permeabilized with 0.3% Triton X-100 for 5 min. This was followed by incubation with a rabbit anti-PSD95 antibody (1:200, ab18258, Abcam, Cambridge, UK) for 1 h and subsequent incubation with Alexa Fluor 594 goat anti-rabbit IgG (1:1000, A-11012, Thermo Fisher Scientific). Cell surface clusters were captured using confocal microscopy (LSM710, Carl Zeiss, Jena, Germany). Images were deconvolved using Huygens Essential version 23.10 (Scientific Volume Imaging, The Netherlands) and quantified using Imaris 8.1 software (Oxford Instruments.).

Determination of IgG deposits and precipitation of NMDAR-bound to IgG

To determine the presence of mouse IgG in the brain, 5 µm-thick sagittal brain sections were blocked with 5% goat serum and immunostained for mouse IgG using Alexa Fluor 488 goat anti-mouse (1:500, A-11001, Thermo Fisher Scientific, Waltham, MA, USA) overnight at 4°C, as reported.⁸ Slides were then mounted in ProLong Gold antifade (P36935, Thermo Fisher) and scanned under a Zeiss LSM710 confocal microscope (Carl Zeiss, Jena, Germany) with the EC-Plan NEOFLUAR CS 100x/1.3 NA oil objective.

To establish that the brain IgG was specifically bound to NMDARs, control and NMDAR mice brains were washed, homogenized in n-dodecyl-phosphocholine 0.1% lysis buffer containing protease inhibitors (1:50, #P8340, Sigma-Aldrich) and ultracentrifuged (200,000 g). The supernatant was then incubated with protein A/G sepharose beads (20423, Thermo Fisher), precipitated, run in a gel, and blotted with a commercial GluN1 polyclonal rabbit antibody (G8913, 1:200, Sigma-Aldrich, St. Louis, MO, USA).

Electrophysiology

Electrophysiological studies on acute sections of mice brains were performed as reported.^{2, 3} In brief, mice were deeply anesthetized with isoflurane and decapitated. Brains were removed in ice-cold, high sucrose extracellular artificial cerebrospinal fluid (aCSF1, in mM: 206 sucrose, 1.3 KCl, 1 CaCl₂, 10 MgSO₄, 26 NaHCO₃, 11 glucose, 1.25 NaH₂PO₄; purged with 95% CO₂/5% O₂, pH 7.4), and subdivided into hemispheres. Thick (380 μ m) coronal slices of hippocampus were obtained with a vibratome (VT1000S; Leica Microsystems, Wetzlar, Germany) and transferred into an incubation beaker with extracellular aCSF appropriate for neurophysiological recordings (aCSF2, in mM: 119 NaCl, 2.5 KCl, 2.5 CaCl₂, 1.25 NaH₂PO₄, 1.5 MgSO₄, 25 NaHCO₃, 11 glucose, purged with 95% CO₂/5% O₂, pH 7.4). Slices were kept at 32°C for 1h and subsequently at RT for at least 1 additional h. For field potential measurements, single slices were then transferred into a measurement chamber perfused with aCSF2 at 2 ml/min at 28-30°C. A bipolar stimulation electrode (Platinum-Iridium stereotrode, PI2ST30.1A5, Science Products GmbH, Hofheim, Germany) was placed in the Schaffer collateral pathway. Recording electrodes were made with a puller (P-1000, Sutter Instrument Company, Novato, CA, USA) from thick-walled borosilicate glass with a diameter of 1.5 mm (BF150-86-10, Sutter Instrument). The recording electrode filled with aCSF2 was placed in the dendritic branching of the CA1 region for local field potential measurement (field excitatory postsynaptic potential, fEPSP). A stimulus isolation unit A385 (World Precision Instruments, Sarasota, FL, USA) was used to elicit stimulation currents between 25-700 μ A. Before baseline recordings for long-term potentiation (LTP), input-output curves were recorded for each slice at 0.03 Hz. The stimulation current was then adjusted in each recording to evoke fEPSPs at which the slope was at 50-60% of maximally evoked fEPSP slope value. After baseline recording for 30 mins with 0.03 Hz, LTP was induced by theta-burst stimulation (TBS; 10 theta bursts of four pulses of 100 Hz with an

interstimulus interval of 200 ms, repeated seven times with 0.03 Hz). After LTP induction, fEPSPs were recorded for 1 additional hour with 0.03 Hz. Recordings with unstable baseline measurements (variations higher than 20% in baseline fEPSPs) were discarded. Paired-pulse fEPSPs in the test pathway were measured before baseline recordings with an interstimulus interval of 50 ms. All recordings were amplified and stored using amplifier AxonClamp P2 (Molecular Devices, San José, CA, USA). Traces were analyzed using Axon pClamp software (Molecular Devices, version 10.6).

Determination of complement deposition in the brain

To determine the presence of complement deposition, 5 µm-thick brain sections were permeabilized with 0.3% Triton X-100 for 10 min at RT and blocked with 5% goat serum. Then, slides were immunostained with a polyclonal rabbit anti-mouse C5b-9 antibody (1:200, ab55811, Abcam) for 2h at RT followed by the secondary antibody Alexa Fluor 488 goat anti-rabbit IgG for 1h at RT. Slides were then mounted in ProLong Gold antifade (P36935, Thermo Fisher) and scanned under a Zeiss LSM710 confocal microscope (Carl Zeiss, Jena, Germany) with the EC-Plan NEOFLUAR CS 100x/1.3 NA oil objective.

Stimulated Emission Depletion (STED) microscopy

To obtain a super-resolution image of microglia phagocytosis we utilized stimulated emission depletion (STED) microscopy. We conjugated the antibodies against GluN1 (human NMDAR IgG) with Alexa Fluor 594 (A20004, Thermo Fisher Scientific), and the antibodies against CD68 (MCA1957GA, Bio-Rad) with Abberior Star 635P (07679, Sigma-Aldrich). Alexa Fluor 488 goat anti-mouse (A-11001, Invitrogen, Carlsbad, CA, USA) was used to label mouse IgG.

Non-permeabilized brain sections were then sequentially incubated at 4°C with the three indicated labelled antibodies (3 hours each at the following dilutions: 1:100 for Alexa Fluor

488 goat anti-mouse IgG; 1:10 for Alexa Fluor 594 human NMDAR IgG; and 1:20 for Abberior Star 635P anti-CD68). After incubation, the slides were washed and mounted with ProLong Gold (P36930; Molecular Probes, Eugene, OR) and scanned under a gated-STED microscope (TCS-SP8 STED 3X; Leica Microsystems, Wetzlar, Germany). For the fluorophores Alexa Fluor 488, Alexa Fluor 594 and Abberior Star 635P, we used excitation lines of 488, 594 and 635nm, and depletion lines (STED) of 592, 660 and 775nm, respectively. Fluorescence light was collected with HyD SMD molecule detectors on an HC PL APO CS2 100×/1.40 OIL objective (Leica Microsystems).

Determination of brain T cells by immunohistochemistry

To determine the presence of T cells by brain tissue immunohistochemistry, 5 µm-thick brain sections were permeabilized with Triton X-100 for 10 min at RT and blocked with 5% goat serum. Then, slides were immunostained with rabbit anti-mouse CD3 (1:200, ab16669, Abcam), rabbit anti-mouse CD4 (1:200, bs-0766R, Bioss), or rabbit anti-mouse CD8a (1:200, PA5-81344, Invitrogen) over night at 4°C, and followed by the secondary antibody Alexa Fluor 488 goat anti-rabbit IgG for 1h at RT. Slides were then mounted in ProLong Gold antifade (P36935, Thermo Fisher) and scanned under a Zeiss LSM710 confocal microscope (Carl Zeiss, Jena, Germany) with the EC-Plan NEOFLUAR CS 100x/1.3 NA oil objective.

Isolation of splenocytes

Spleen from euthanized mice were harvested and placed in HBSS buffer (w/o Ca²⁺ and Mg²⁺, 14175-053, Thermo Fisher Scientific). The spleens were then minced and passed through a 70 µm cell strainer to create a single-cell suspension. The cell suspension was layered over Ficoll-Plaque PLUS (Cytiva, GE17-1440-02, Sigma Aldrich) and centrifuged at 800 g during 20 min without brakes. The mononuclear cell layer was collected and washed with HBSS buffer.

Behavioural tasks

Novel Object Location (NOL) test

NOL test is a paradigm to study memory. Animals were habituated to an empty, squared arena (45x45 cm, Panlab, Spain) with visual cues, and underwent two daily trials of 15 mins each, for four days. The day of the test, animals were placed into the arena in presence of two equal objects positioned at two opposite corners and they were allowed to explore the objects for 9 min (familiarization phase). After a retention time of 3 h, animals were reintroduced to the arena, where one of the objects had been moved to a different corner. The animal was allowed to explore the objects for 9 mins (test phase) and the time of exploration of each object was recorded. A discrimination index (NOL Index) was calculated using the following formula: Time of exploration of the moved object minus time of exploration of the not moved object, divided by total time of exploration of both objects. A higher discrimination index indicates a better memory of the position of both objects. Object exploration is defined as any exploratory behaviour triggered by the presence of the object (sniffing, biting, touching) with the orientation of the nose toward the object within a distance of < 2 cm.²

Locomotor Activity (LA) test

Mice were assessed in LA boxes (9x20x11 cm, Imetronic, Passac, France), equipped with 2 rows of photocell detectors and placed in a low-luminosity environment (20-25 lux), as previously described.⁹ Mice locomotor activity was recorded for 1 hour as horizontal activity and vertical activity.

Pre-pulse inhibition of the acoustic startle response (PPI) test

The PPI test is a classic paradigm to measure alternations in sensorimotor gating, which have been shown to occur in models of psychotic-like behavior.¹⁰ Mice were habituated to being restrained using a plexiglass cylinder within a startle box (Panlab, Barcelona) in the presence

of white noise (60 dB) and light for 15 min, for 3 days. The day of the test, after 5 min of habituation, a series of 10 trials of pulses (8 KHz, 115 dB, 40 milliseconds [ms]) was administered and the startle response (SR) was measured for 1000 ms (intertrial interval 29 seconds) in order to establish the basal response. The animal was subsequently exposed to a total of 40 trials randomly administered and equally divided into 4 different stimuli: pulse alone (8 KHz, 115 dB, 40 ms), prepulse alone (10 KHz, 80 dB, 20 ms), prepulse-pulse, and no stimulus (absence of pulse). Both habituation and test were always performed in presence of background white noise (60 dB) and light. The amount of inhibition of the SR due to the administration of the prepulse prior to the pulse was calculated as:

$$SR \text{ inhibition (\%)} = 1 - (\text{average SR following prepulse-pulse stimulus} / \text{average SR following pulse alone stimulus}) \times 100$$

Black and White (BW) test

BW test is a classic paradigm to measure anxiety-like behaviour in rodents; it measures the conflict between the innate exploratory behaviour and natural aversion to brightly illuminated areas.¹¹ The box includes a small black compartment and a big white compartment separated by a connecting gate (LE810, Panlab, Spain). The compartments are independently illuminated: the white one with a white led (500 lux) and the black one with a red led (10 lux). At the start of the session, mice were placed in the back compartment, head facing a corner. The latency of first entry into the white compartment and section reached in each entry, together with time spent, squares crossed, and number of entries into both compartments were recorded, tracked by Smart 3.0 software (Panlab, Spain) and used to evaluate anxiety.

Tail Suspension Test (TST)

TST is a classic task to measure depressive-like behaviour in rodents.¹² Mice are suspended by the tail in the automated tail-suspension box (76-1227, Harvard Apparatus, Massachusetts, USA). During a 6 min interval, energy, power, and total time of immobility are recorded. Long periods of immobility are characteristic of a depressive-like state.

Seizure susceptibility study

Pentylenetetrazol-induced seizures

Mice were handled for 2-3 days (corresponding to 10-15 days after the immune boost) before being placed in a square box (33x33 cm) with shallow bedding and <100 lux indirect light. After a 10 min baseline, the GABA_AR antagonist pentylenetetrazole (PTZ, 2 mg/mL in saline) was injected at a dose of 40 mg/kg, intraperitoneally. Actimetry was tracked using Smart 3.0 software over the entire 1h session. A second frontal video camera was used for behavioral labeling off-line. All spontaneous actions were carefully observed at x 0.25-0.5 playback speed, annotated, and their association with PTZ treatment determined using the pointwise mutual information value. Labels distinctive of PTZ (laying on belly, crawling, pivoting, crunch posture with splayed hindlimb, head nodding, pacing, myoclonic jerks, clonus with loss of posture, forelimb sitting, freezing) appeared in a non-random order, and could be grouped into three main stages of seizure severity: hypoactivity, periodic jerks, and tonic-clonic. *In vivo* recordings and cFos induction (see below) confirmed this behavioral classification, as well as the occurrence of time-locked ictal activity during myoclonic jerks and tonic-clonic epochs. Jerks consisted of a combined downward motion of the head, jerk of the body and upward tail extension, all emerging in less than a second. A typical tonic-clonic episode lasted several seconds and followed a sequence of high-frequency jerks that made the mouse fall on its side, followed by righting, forelimb clonus and freezing. The incidence of

seizure stages in control and immunized mice was performed blindly during the 50 min following PTZ injection. We tested the accuracy of detecting seizures behaviorally by comparing video and electrophysiological data in 7 implanted mice, and obtained >95 % coincidence for jerks and 100 % for tonic-clonic epochs.

cFos immunostaining

90 min after PTZ injection, mice were anesthetized and transcardially perfused with ice-cold formaldehyde as previously described.¹³ Coronal cryostat sections (25 μ m-thick) were stained free-floating. After blocking in 2% BSA, 5% fetal bovine serum and 0.1 % Tween-20 in PBS, sections were incubated in rabbit cFos antibody (1:2000 dilution, ABE-457, Millipore) overnight at 4 °C. For visualization, we used tyramide-mediated amplification following manual instructions (Invitrogen). Briefly, after rinses, sections were incubated with goat poly-
HRP anti-rabbit antibody for 1h at RT, rinsed again, and incubated in reaction solution containing Tyr-AlexaFluor555 diluted 1:50 for 10 min in the dark. Sections were then counterstained with mouse anti-NeuN antibody (1:500, Millipore) overnight, and visualized with goat anti-mouse AlexaFluor488 (1:500, Invitrogen) for 2 h at RT. Epifluorescent images were acquired within linear range and exposure parameters fixed across groups and brain regions. Changes in cFos levels in neurons were analyzed with FIJI. NeuN staining was thresholded using the Moments function, a selection was then created and applied to the cFos channel to measure the grayscale intensity within. The cFos/NeuN signal ratio was normalized to that in vehicle-injected mice to generate a cFos matrix according to seizure severity using GraphPad 10.

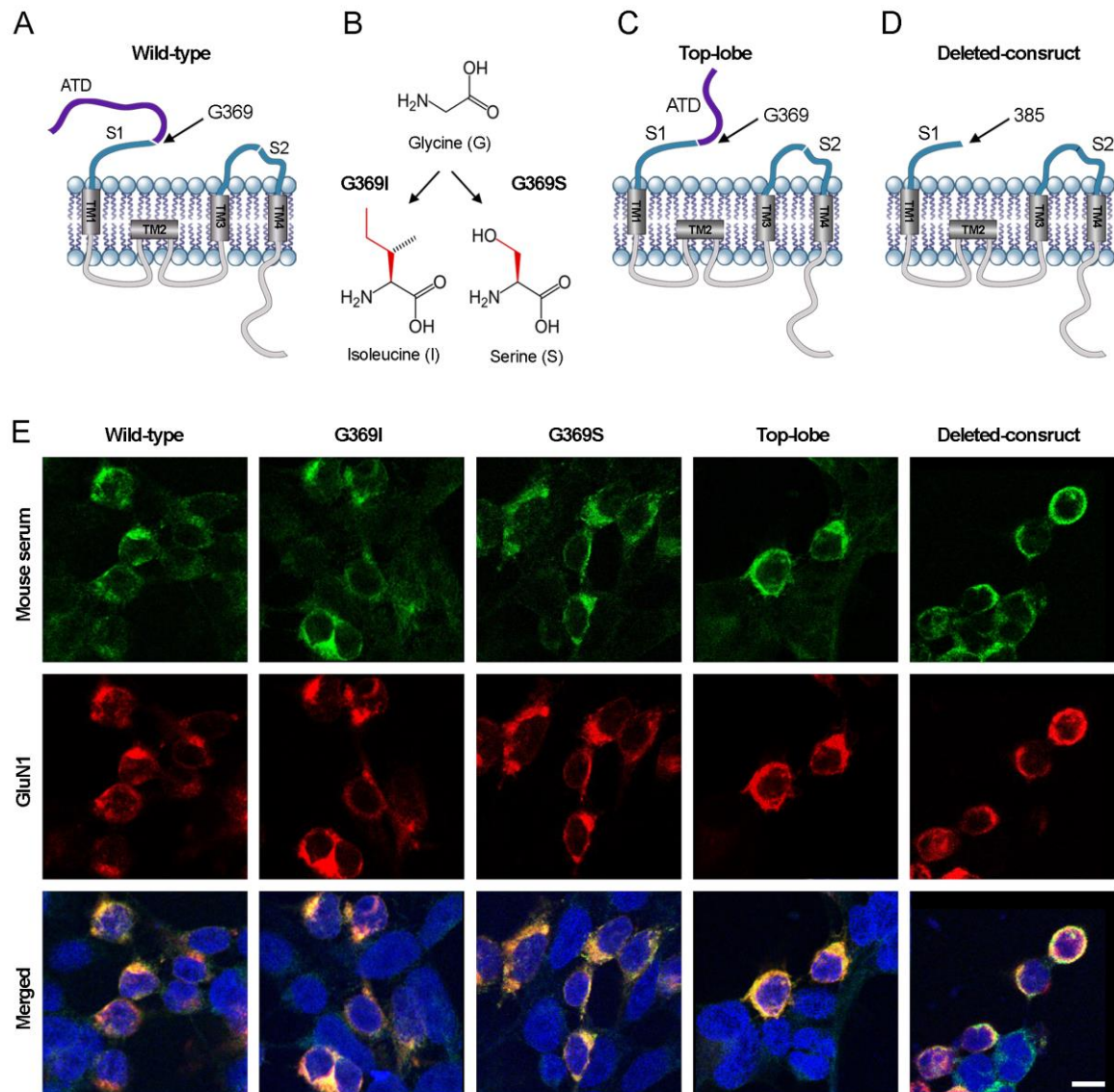
Electrophysiological recordings in vivo

A bundle of 10-14 recording wires (Sandvik #PX000003) was glued onto a thin metal stick on one end, and cut to protrude 2.5-3 mm. On the other end, wires were stripped and

individually wound to the pins of a 16-channel female connector (Omnetics #NSD-18-VV-GS). A silver wire (A-M systems #786000) was soldered to the ground pin. A drop of silver paint (RS Pro #123-9911) was applied to all wired pins, and then covered with abundant silicone glue (Dow #3145 RTV). The distal bundle tip was gold-plated to bring the wire impedance down to 100 KOhms. Briefly, the recording assembly was connected to a NanoZ kit (Neuralynx), tips were immersed in a diluted gold solution (final 2 % gold with 0.1% PEG; Neuralynx), and electroplated with repeated cycles of -0.05 uA to match progressively lower impedances.

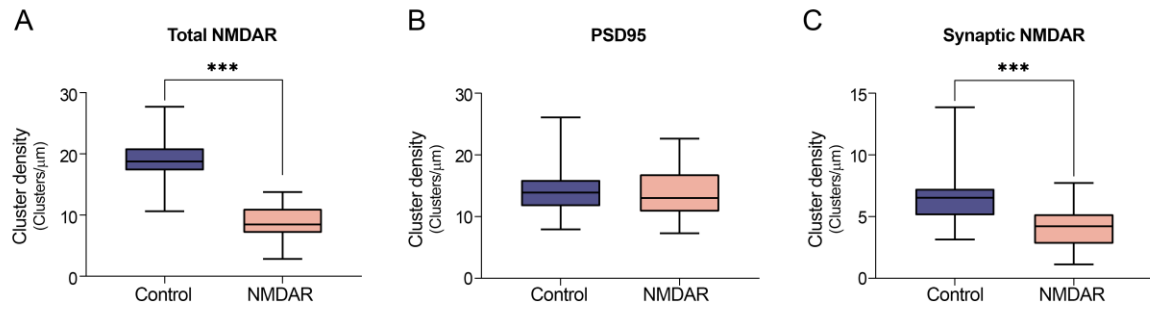
In order to implant the recording drive in the right dorsal hippocampus, mice were anesthetized with isoflurane, immobilized in a stereotactic apparatus, and injected subcutaneously with bupivacaine (2 mg/kg). A 1 mm craniotomy was made, and the drive was slowly inserted (mm from bregma: -2 AP, 2 ML, -2 DV). The drive was secured with Superbond cement, and skin sutured. Mice received post-operative analgesia (meloxicam 5 mg/kg) for the next 3 days, and allowed to recover for a week before recording in a noise- and sound-insulated square box. Mice were tethered and allowed to freely move inside the box while signal was continuously acquired. Electrical signals were pre-amplified by connecting the drive to a headstage and acquired with an openephys board. A Bpod system connected to a PC was used to control and synchronize the videocamera (33 fps) and the electrophysiological signal with transistor-transistor logic (TTL) synchronization. Signals were analyzed in Python (3.7). They were first down sampled to 1 kHz, bandpass filtered between 0.1-300 Hz, and line noise removed using the notch filter.

Supplementary figures



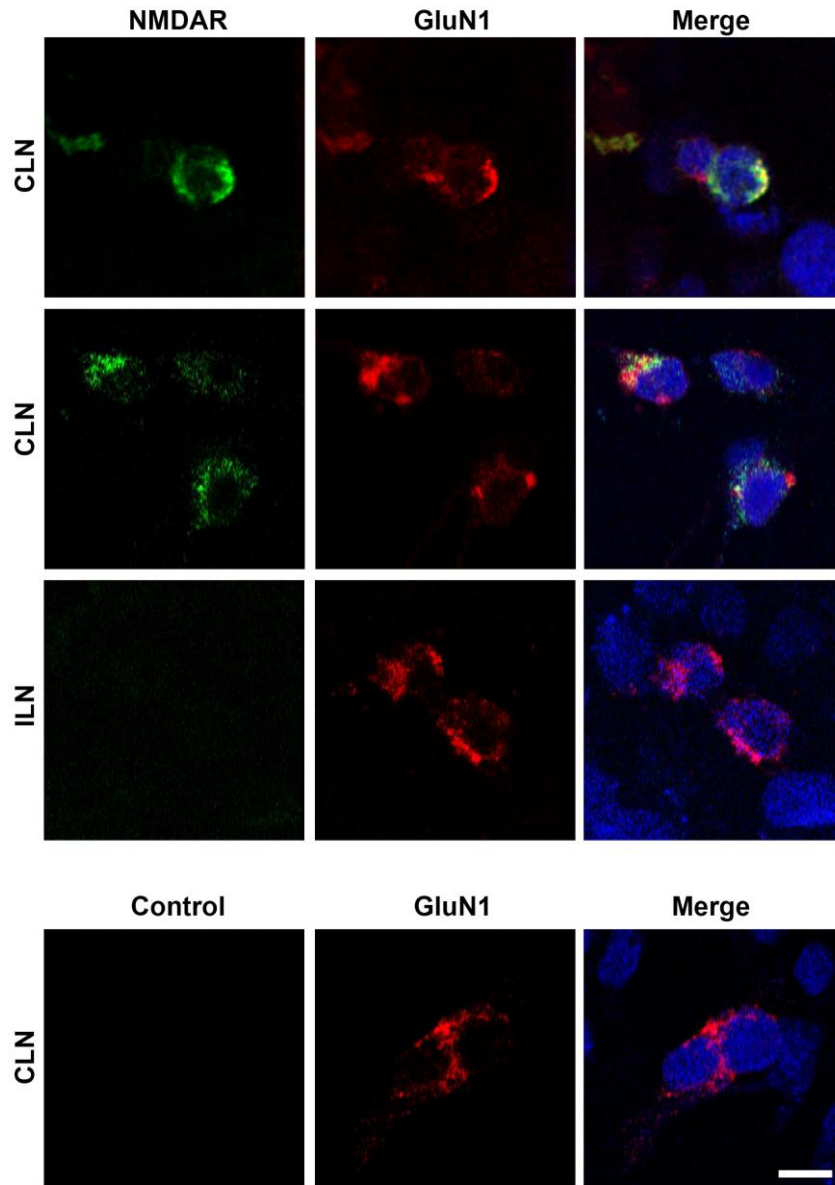
Supplementary Figure 1: Mice immunized with GluN1₃₅₆₋₃₈₅ peptide produce polyclonal antibodies beyond the epitope region of the immunizing peptide

Schematic representation of (A) native GluN1, (B) G369I and G369S, (C) amino terminal domain (ATD) top-lobe deleted, and (D) ATD deleted mutant constructs. (E) Cell-based assays with HEK293 cells expressing the indicated native or mutant GluN1 constructs and GluN2b, showing reactivity with serum of a representative NMDAR mouse (green), which colocalizes (yellow) with the reactivity of a commercial GluN1 antibody (red). All mice serum tested (n=10), but not controls, showed reactivity with all GluN1 constructs (not shown).



Supplementary Figure 2: NMDAR mice serum cause a reduction of cell-surface NMDAR clusters in cultured rat hippocampal neurons

(A) Total (synaptic and extrasynaptic) NMDAR clusters, (B) PSD95, and (C) synaptic NMDAR cluster density in cultures of rat dissociated hippocampal neurons treated with IgG purified from pooled serum of 5 control and 5 NMDAR mice. Results show a significant decrease in total and synaptic NMDAR cluster density in neurons treated with NMDAR IgG. 30 dendrites were analyzed per condition. Box plots show the median, 25th and 75th percentiles; whiskers indicate the minimum and maximum values. Significance was assessed using a t-test. A p-value of < 0.05 was considered statistically significant.

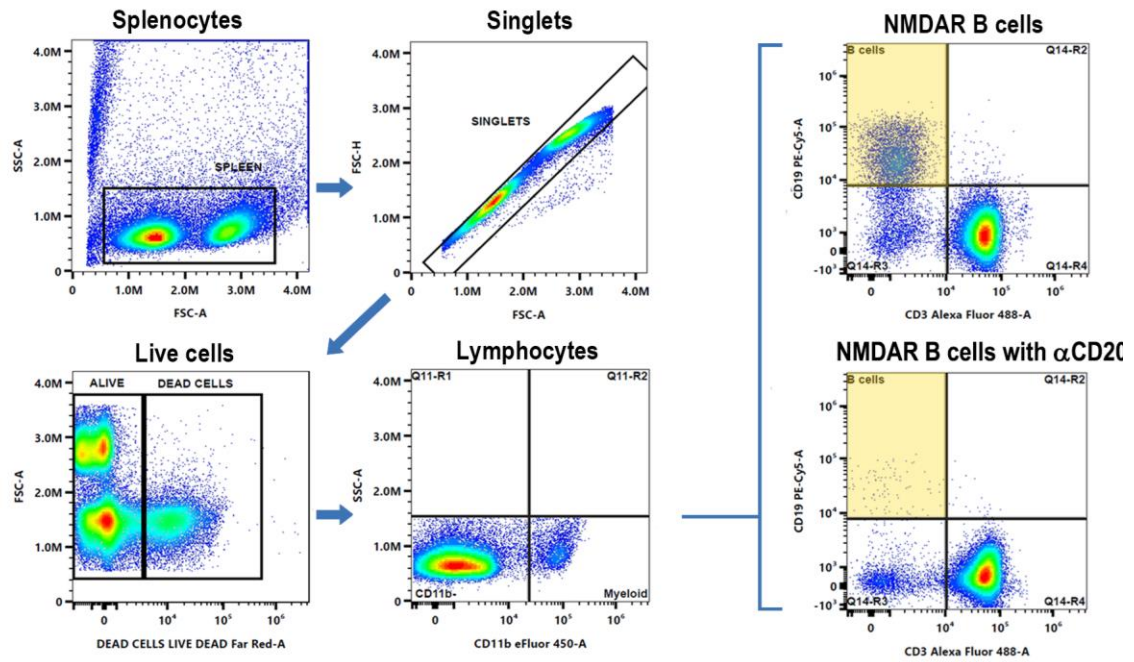


Supplementary Figure 3: Cells from deep cervical lymph nodes from NMDAR mice produce GluN1 antibodies

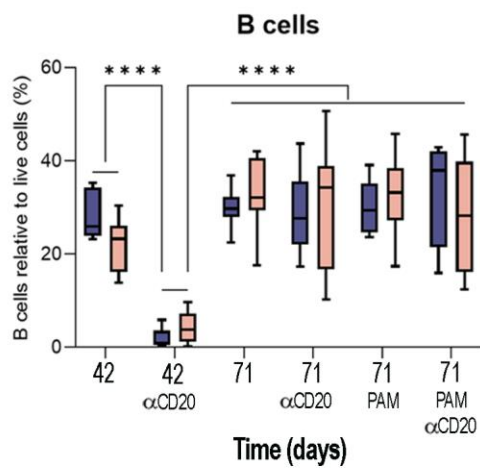
Cell-based assays with HEK293 cells expressing GluN1/GluN2b showing reactivity with antibodies secreted in the culture media by cells dissociated from deep cervical lymph nodes (CLN) of a representative NMDAR mouse (green). The reactivity of secreted antibodies colocalizes (yellow) with the reactivity of a commercial GluN1 antibody (red). Culture media of cells dissociated from inguinal lymph nodes (ILN) of the same NMDAR mouse, and CLN of a control mouse, do not show NMDAR reactivity.

A

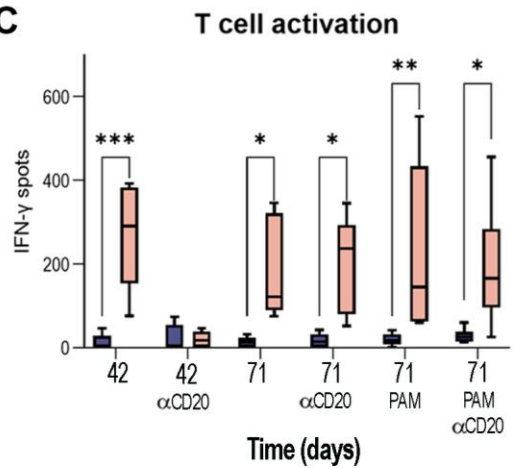
Gating strategy for spleen samples



B

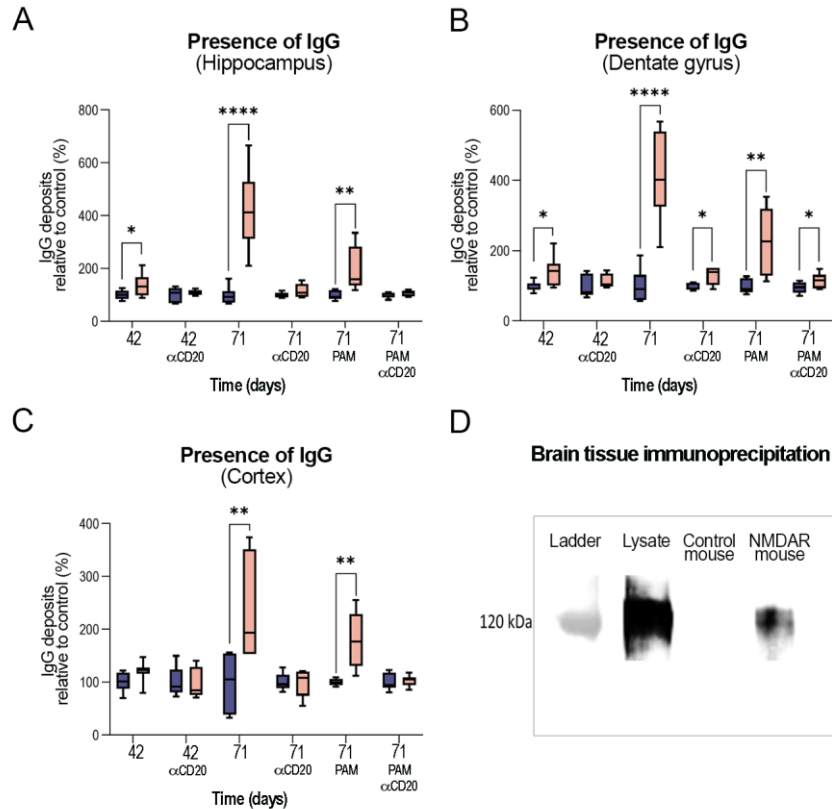


C



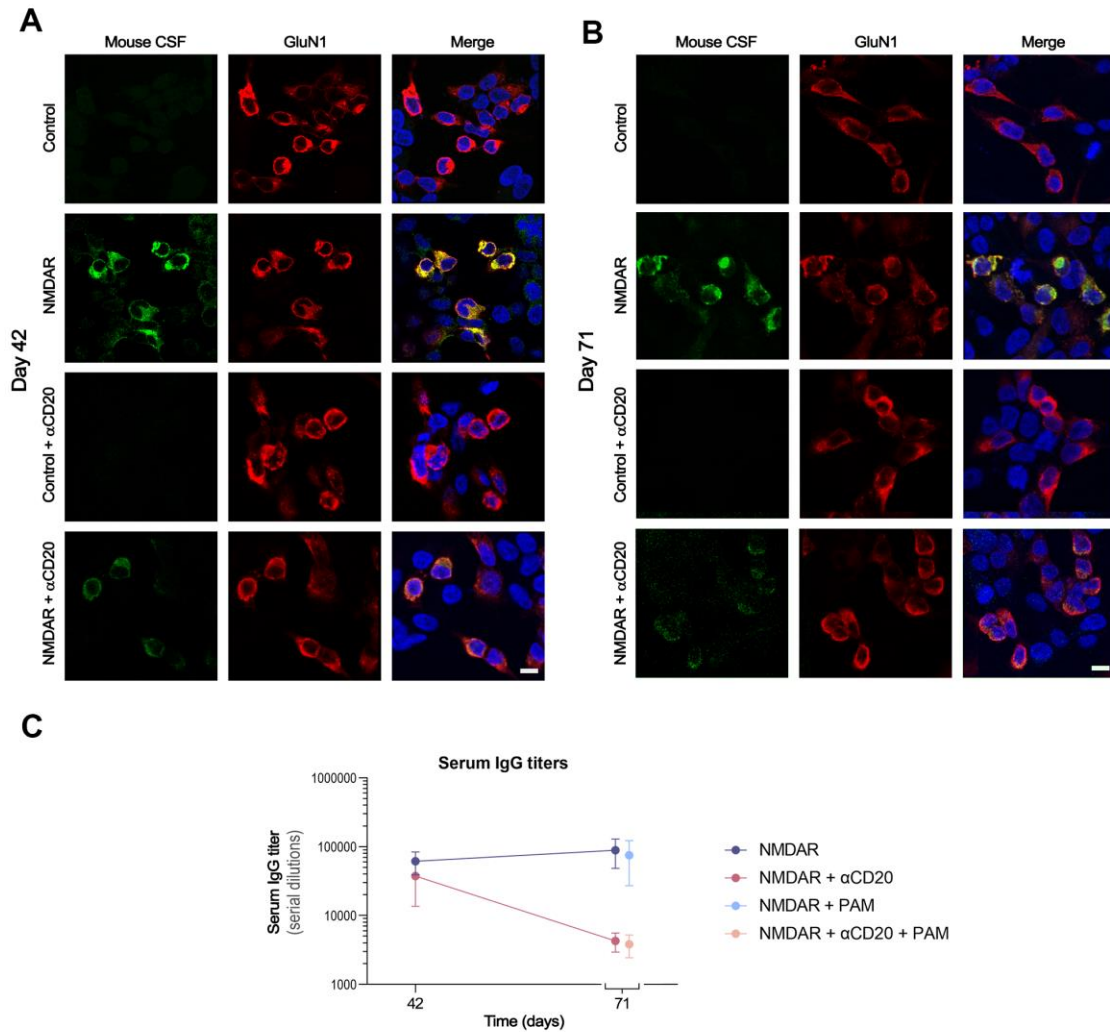
Supplementary Figure 4: Effects of anti-CD20 on splenocytes and lymphocytes

(A) Representative flow cytometry scatter plots illustrating the gating strategy used to identify B cells from spleen samples. Initial gating was performed on forward and side scatter properties to exclude debris. Subsequent gates were applied to select singlets and live cells. Next, cells negative for CD11b were selected as lymphocytes. B cells were gated as CD3⁻ and CD19⁺ cells. Scatter plots show splenic B cells from a representative untreated NMDAR mouse and an NMDAR mouse treated with anti-CD20, exemplifying B cell depletion caused by anti-CD20. (B) Quantitation of splenic B cells in control (blue, n = 10) and NMDAR mice (pink, n = 10) under all experimental conditions. There is a significant decrease in B cells (day 42) in mice treated with anti-CD20, indicating effective B cell depletion, which by day 71 is no longer present (B cell repopulation). NMDAR-PAM (SGE-301) does not alter B cell number. (C) Quantitative analysis of the ELISpot experiment, indicative of IFN- γ production by splenocytes in response to GluN1₃₅₆₋₃₈₆ stimulation, in control (blue, n = 10) and NMDAR mice (pink, n = 10) under all experimental conditions. There is a significant increase of IFN- γ production in NMDAR mice, indicating T-cell activation, which is abrogated by anti-CD20 treatment on day 42. NMDAR-PAM does not alter T-cell activation. Box plots show the median, 25th and 75th percentiles; whiskers indicate the minimum and maximum values. Significance was assessed using a mixed model. A p-value of < 0.05 was considered statistically significant.



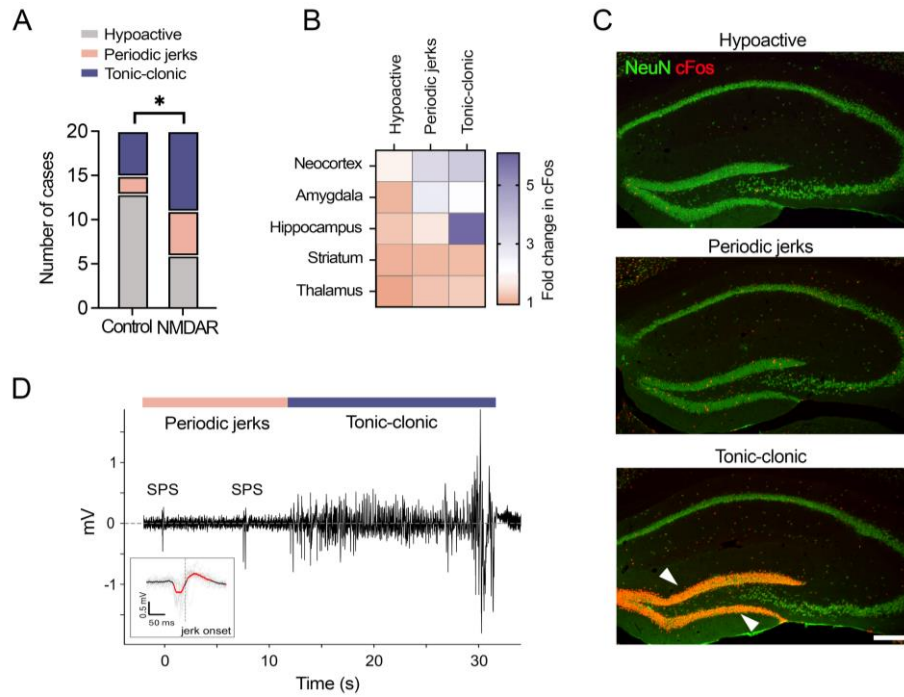
Supplementary Figure 5: Presence of IgG bound to NMDAR in brain of NMDAR mice

Quantitation of mouse IgG brain deposits in controls (blue) and NMDAR mice (pink) across all experimental groups: **(A)** pooled analysis of hippocampal areas, **(B)** dentate gyrus, and **(C)** cortex. Compared to controls, NMDAR mice have a significant increase in IgG deposits, which is substantially decreased in mice treated with anti-CD20, but not NMDAR-PAM. For each experimental condition 5 controls and 5 NMDAR mice were examined. For each animal 42 square images similar to those indicated in Fig 2A were examined (9 from CA1, 9 from CA3, 9 from dentate, and 15 from cortex). Box plots show the median, 25th and 75th percentiles; whiskers indicate the minimum and maximum values. Significance was assessed using a nested mixed model. A value of $p < 0.05$ was considered statistically significant. **(D)** Immunoprecipitation of brain IgG in a representative NMDAR mouse and control, showing that in the NMDAR mouse the IgG is bound to NMDARs.



Supplementary Figure 6: Effects of anti-CD20 on antibody titers

HEK293 cells expressing GluN1/GluN2b show reactivity with CSF from untreated NMDAR mice (green) at day 42 (**A**) and day 71 (**B**) after initial immunization. Mouse CSF reactivity colocalizes (yellow) with the reactivity of a commercial GluN1 antibody (red). CSF from NMDAR mice treated with anti-CD20 show a substantial decrease of immunoreactivity, although samples remain positive at both time-points (day 42 > day 71, the later barely visible). (**C**) Graphic representation of the change in serum titres (measured by CBA with serial serum dilutions) for all treatment groups of NMDAR mice (n = 6 for each experimental group). Anti-CD20 treatment reduces serum IgG titers by day 71. NMDAR PAM (SGE-301) does not alter IgG titers.



Supplementary Figure 7: NMDAR mice show a decrease in seizure threshold induced by pentylenetetrazol

(A) The distribution of maximal seizure stages shown in control and peptide immunized mice was quantified from data extending 1h after pentylenetetrazol (PTZ) injection (n=20/group). The fraction of mice showing generalized seizures (i.e. hypoactive versus jerks and tonic-clonic) was significantly larger in immunized mice, Chi square test, $P = 0.026$. (B) Quantification of cFos induction, a proxy of recent neural activation, across several brain regions in mice that reached different behavioral seizure stages (i.e. hypoactivity, myoclonic jerks, or continuous tonic-clonic seizures). Two-way ANOVA revealed an interaction between regional change in cFos and seizure stage, $F(8, 30) = 9.3$, $P < 0.0001$ (n = 3 mice / group), indicating different patterns of neural activation depending on seizure stage. (C) Representative images of hippocampus double stained for cFos and the neural marker NeuN following different seizure stages. Arrows point to dentate gyrus granule cells where cFos induction was maximal after tonic-clonic seizures. Scale bar = 250 μm . (D) Example trace of the local field potential recorded in the hippocampus of a freely moving mouse. Sharp population spikes (SPS) were time locked with behavioral jerks, and transitioned to high-frequency spikes during the tonic-clonic episode. Inset, magnified average SPS aligned to jerk onset. Red points indicate voltage amplitudes significantly larger than baseline.

Supplementary video

Supplementary Video 1: Reduction of NMDA-induced calcium currents in neurons treated with IgG from NMDAR mice

Representative video of calcium imaging showing that neurons pre-treated with IgG from NMDAR mice show a significant reduction of NMDA-induced calcium influx compared to neurons pre-treated with IgG from controls. Scale bar = 10 μm .

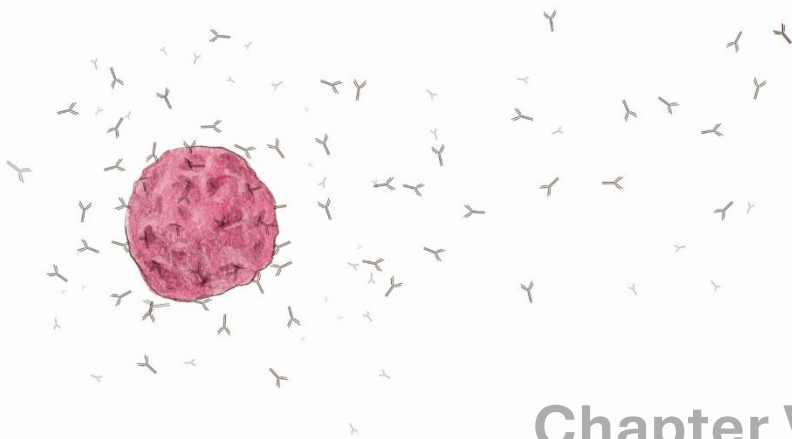
Supplementary Video 2: Motor stereotypies in NMDAR mice

Video of four NMDAR mice showing different types of stereotypic movements and behaviours, such as walking backwards, self-biting, and circling.

References

1. Planaguma J, Leypoldt F, Mannara F, et al. Human N-methyl D-aspartate receptor antibodies alter memory and behaviour in mice. *Brain* 2015;138:94-109.
2. Mannara F, Radošević M, Planaguma J, et al. Allosteric modulation of NMDA receptors prevents the antibody effects of patients with anti-NMDAR encephalitis. *Brain* 2020;143:2709-2720.
3. Radošević M, Planaguma J, Mannara F, et al. Allosteric Modulation of NMDARs Reverses Patients' Autoantibody Effects in Mice. *Neurol Neuroimmunol Neuroinflamm* 2022;9.
4. Gleichman AJ, Spruce LA, Dalmau J, Seeholzer SH, Lynch DR. Anti-NMDA receptor encephalitis antibody binding is dependent on amino acid identity of a small region within the GluN1 amino terminal domain. *J Neurosci* 2012;32:11082-11094.
5. Gresa-Arribas N, Titulaer MJ, Torrents A, et al. Antibody titres at diagnosis and during follow-up of anti-NMDA receptor encephalitis: a retrospective study. *Lancet Neurol* 2014;13:167-177.
6. Hughes EG, Peng X, Gleichman AJ, et al. Cellular and synaptic mechanisms of anti-NMDA receptor encephalitis. *J Neurosci* 2010;30:5866-5875.
7. Cunqueiro M, Aguilar E, Loza-Alvarez P, Planaguma J. Hippocampal Neuronal Cultures to Detect and Study New Pathogenic Antibodies Involved in Autoimmune Encephalitis. *J Vis Exp* 2022.
8. Garcia-Serra A, Radošević M, Pupak A, et al. Placental transfer of NMDAR antibodies causes reversible alterations in mice. *Neurol Neuroimmunol Neuroinflamm* 2021;8.
9. Berrendero F, Mendizabal V, Robledo P, et al. Nicotine-induced antinociception, rewarding effects, and physical dependence are decreased in mice lacking the preproenkephalin gene. *J Neurosci* 2005;25:1103-1112.

10. Jones CA, Watson DJ, Fone KC. Animal models of schizophrenia. *Br J Pharmacol* 2011;164:1162-1194.
11. Bura SA, Burokas A, Martin-Garcia E, Maldonado R. Effects of chronic nicotine on food intake and anxiety-like behaviour in CB(1) knockout mice. *Eur Neuropsychopharmacol* 2010;20:369-378.
12. Aso E, Ozaita A, Valdizan EM, et al. BDNF impairment in the hippocampus is related to enhanced despair behavior in CB1 knockout mice. *J Neurochem* 2008;105:565-572. Sans-Dublanc A, Razzauti A, Desikan S, Pascual M, Monyer H, Sindreu C. Septal GABAergic inputs to CA1 govern contextual memory retrieval. *Sci Adv* 2020;6.



Chapter VII

Discussion

Antibody-mediated encephalitis constitute a novel group of autoimmune neurological diseases, where neuronal cell surface proteins or receptors are targeted by autoantibodies. This thesis focused on studying the pathogenic mechanisms of these autoantibodies through cellular and animal models and explored new therapeutic strategies.

The **first study** of this thesis aimed to develop an animal model of passive transfer of neuronal antibodies, similar to the model previously established in our laboratory for antibodies against NMDAR. The goal was to eventually apply my training to further investigate anti-NMDAR encephalitis, which is the most frequent autoimmune encephalitis and leads most of the research in the field. In this study, antibodies from patients with anti-mGluR5 encephalitis were passively transferred to mice via cerebroventricular infusion. The findings confirmed that the infusion of patients' IgG led to memory loss and increased anxiety, associated with a significant reduction in mGluR5 clusters in the hippocampus.¹³³ These effects were reversible once the antibody infusion via subcutaneously implanted pumps stopped. Thus, together with previously published studies showing that patients' antibodies caused a reduction of mGluR5 clusters in cultured neurons,⁸⁴ the findings of this publication provided robust evidence of the antibody pathogenicity linking memory and anxiety alterations with a reduction of mGluR5 levels.

For this model we opted to use pooled IgG from several patients, rather than IgG from a single patient, or patient-derived monoclonal antibodies. This approach better represents the diverse repertoire of

pathogenic antibodies in the disease, thereby allowing for the generalization of the findings. mGluR5 plays a crucial role in memory formation. In rodents, pharmacological potentiation of mGluR5 is linked to improved learning and memory, whereas genetic deletion leads to impaired learning. These observations align with the effects observed in our animal model, where the decrease in mGluR5 impaired memory. It has been suggested that the role of mGluR5 in memory acquisition is largely mediated through the enhancement of NMDAR responses.¹⁵⁵ However, whether the effects of mGluR5 antibodies on memory also involve NMDAR modulation remains to be determined in future studies.

In addition to memory impairment, mice infused with patients' IgG exhibited increased anxiety, mirroring the clinical phenotype of anti-mGluR5 encephalitis.⁷⁹ The role of mGluR5 in anxiety responses is complex and not fully understood. For instance, pharmacological modulation of mGluR5 with negative allosteric modulators has been shown to reduce anxiety levels in mice, while genetic deletion of mGluR5 in older mice, is associated with increased anxiety.^{156,157} These contrasting results may be due to significant variability in the effects of mGluR5 on anxiety circuits, depending on receptor location, cell type, and age.¹⁵⁶ In our model, we focused on the antibody effects in the hippocampus, a region involved in both memory and stress responses, and clinically and radiologically implicated in anti-mGluR5 encephalitis.

Following the passive cerebroventricular transfer techniques, I focused on several approaches (cellular and animal modelling) to better understand the physiopathology and treatment of anti-NMDAR

encephalitis. Thus, the second objective of the thesis was to assess the effect of antibodies from patients with anti-NMDAR encephalitis on cultures of oligodendrocytes. The rationale for this **second study** was to identify a mechanism explaining the paradoxical findings that despite normal clinical MRI results, advanced MRI sequences show substantial abnormalities in white matter integrity and connectivity in most patients with this disease. Indeed, in a study of 577 patients with anti-NMDAR encephalitis, 67% had normal clinical MRI findings, while the remaining patients displayed mild or transient subcortical FLAIR abnormalities, with subcortical white matter as frequently involved as grey matter.¹⁵⁸ However, a detailed examination using diffusion tensor imaging sequences, an MRI technique used to detect white matter fibers and their connectivity, revealed widespread changes in white matter integrity correlating with disease severity in a cohort of 24 patients. In another series of 46 patients with anti-NMDAR encephalitis, superficial white matter changes occurred more frequently in those who had not clinically recovered than in those who had recovered or in healthy participants.⁷⁰ Thus, anti-NMDAR encephalitis is associated with characteristic alterations of functional connectivity and widespread changes in white matter integrity, despite often apparently normal routine clinical MRI findings.⁶⁹

Our findings revealed that oligodendrocytes treated with CSF from patients with anti-NMDAR encephalitis, or recombinant monoclonal antibodies derived from patients' plasma cells, showed a significant reduction in NMDAR activation.¹⁰⁰ This pathogenic effect, which was not seen when cells were treated with control samples, was

abrogated if patients' CSF was absorbed with HEK cells expressing NMDAR, confirming the pathogenic role of the autoantibodies. Interestingly, patients' CSF did not affect the function of other receptors, indicating a specific impairment in NMDAR activation. These antibody-mediated effects were linked to reduced GLUT1 expression in oligodendrocyte processes. Because expression of GLUT1 is important for axonal function, the findings suggest a pathogenic mechanism additional to the reported antibody effects on neuronal NMDARs.

In oligodendrocytes, NMDARs control the supply of energy substrates to support the proper function of axons via GLUT1 translocation to the oligodendrocyte membrane.⁷¹ Thus, the amplitude of the action potentials during high-frequency stimulation is decreased and recovers more slowly in axons of mice lacking NMDAR in oligodendrocytes. In addition, prolonged loss of NMDAR function in oligodendrocytes leads to axonal pathology and inflammation in white matter tracts resulting in neurological symptoms and motor dysfunction. Therefore, the relevance of our second publication is that it provides a potential antibody-mediated mechanism for the white matter abnormalities frequently identified in patients with anti-NMDAR encephalitis.

The third goal of the thesis was to explore potential therapies for anti-NMDAR encephalitis beyond immunotherapies. For this, in the **third study**, we focused on cultured neurons exposed to patients' antibodies and an animal model of passive transfer of patients' antibodies to mice, to assess whether a positive allosteric modulator (PAM) of the NMDAR could antagonize the effects of patients' antibodies.

24(S)-hydroxycholesterol, a brain-derived oxysterol, is a very potent, direct, and selective PAM of NMDAR. Several synthetic analogues, such as SGE-301, share similar properties. Previous studies have shown that SGE-301 increases NMDAR channel open probability by acting on a site independent of other allosteric modulators, consequently enhancing NMDAR function and prolonging spontaneous excitatory postsynaptic currents.⁷⁶ Moreover, application of SGE-301 to cultures of neurons exposed to CSF from patients with anti-NMDAR encephalitis prevented the antibody-mediated dysfunction of NMDARs.⁷⁷

In our study we demonstrated that mice infused with patients' CSF developed memory deficits accompanied by a decrease in NMDAR clusters and impairment of synaptic plasticity. All antibody-mediated effects were prevented in the animals treated with SGE-301.¹⁵⁹ Further investigations into the potential mechanisms related to these effects showed that SGE-301 does not interfere with the binding of patients' antibodies to NMDAR, but prevents the reduction of cell-surface NMDARs without completely stopping receptor internalization.¹⁵⁹

However, this study did not assess whether SGE-301 could reverse the memory and synaptic alterations caused by patients' CSF because it was administered simultaneously with the ventricular infusion of the antibodies, and none of the animals developed clinical or synaptic alterations. Therefore, in the **fourth study**, the model was adapted so that the administration of SGE-301 commenced after the development of synaptic and memory alterations. Importantly, between days 10 and 18, which in this model

is the period of progressive development of severe memory and synaptic alterations, SGE-301 could reverse all antibody-mediated pathogenic effects, including memory deficits, reduction of NMDAR density, and synaptic plasticity impairment.¹⁶⁰

The findings of these two studies suggested that the mechanisms of action of SGE301 are multiple and extend beyond the indicated effects on channel function. For example, it remained unclear how, without competing with the binding of antibodies to NMDAR and without fully abrogating the antibody-mediated internalization of NMDARs, SGE-301 was able to restore the cell-surface NMDAR cluster content. Therefore, we postulated that SGE301 could also be restoring the surface dynamics of NMDARs.

With this in mind, the **fifth publication** aimed to investigate the effect of SGE-301 on the membrane dynamics of NMDARs as a potential mechanism of action. We showed that SGE-301, at doses $>10\ \mu\text{M}$, significantly increases NMDAR surface diffusion, mainly in the postsynaptic compartment.¹⁶¹ Furthermore, NMDAR trajectories were less confined in the presence of SGE-301.¹⁶¹ To determine whether SGE-301 could prevent the pathogenic effects of patients' antibodies on the surface dynamics of NMDAR, neurons were exposed to either control or patients' IgG in addition to vehicle or SGE-301. As expected, patients' IgG reduced the diffusion of NMDAR and increased the confinement. Interestingly, SGE-301 alone was sufficient to normalize NMDAR diffusion in neurons exposed to patients' antibodies.¹⁶¹

Our results, alongside the documented modulation of SGE-301 on ionotropic currents,⁷⁶ suggest a dynamic interplay between the state of the receptor and its membrane dynamics. Yet, the exact mechanism by which SGE-301 alters NMDAR diffusion remains unknown. SGE-301 may modify NMDAR's conformation, reducing the interaction with anchoring proteins, or the oxysterol properties of SGE-301 could affect plasma membrane diffusion.

Animal models of passive transfer have been instrumental in probing the pathogenicity of patients' antibodies. However, these models do not allow exploring the immunobiology of the disease, as they lack brain inflammatory infiltrates, participation of T-cell mechanisms and engagement of microglia. These aspects are vital in autoimmune encephalitis given its autoimmune etiology. Moreover, the clinical and synaptic changes offered by passive transfer models are infusion-dependent, lasting only 14 days, which is a significant limitation for assessing the long-term effectiveness of potential new treatments. Therefore, the final objective of the thesis was to develop a new mouse model of anti-NMDAR encephalitis through active immunization, as shown in the **sixth study**.

This study introduces a novel murine model of anti-NMDAR encephalitis through active immunization that associates with a T cell dependent GluN1 IgG response and results in a reduction of cell-surface receptor content and NMDAR function, similar to the effects reported for the antibodies of patients with anti-NMDAR encephalitis (Maudes et al. *unpublished*).

To this end, we used a 30 amino acid peptide derived from the major GluN1 antigenic region of the human disease (containing amino acids N368/G369) in a novel immunization protocol. In our approach we immunized mice with 200 µg of the peptide and AddaVax, a squalene-oil-in-water adjuvant known to be more effective at generating high antibody titers and T-helper responses than other commonly used adjuvants, as Freund's Complete Adjuvant (FCA) or aluminium-based adjuvants.^{162,163} AddaVax also causes fewer undesirable side effects in mice, such as chronic-pain, granulomas, abscesses, and systemic reactions.¹⁶⁴ We followed a 28-day boost protocol previously shown to induce the highest IgG1 titers post-immunization.¹⁶⁵ This protocol produced a robust synthesis of GluN1 polyclonal antibodies. These antibodies, predominantly of IgG1 subclass, targeted not only the immunizing GluN1 peptide but also epitope regions outside the peptide sequence, indicating epitope spreading.

These findings have not been previously investigated in models of anti-NMDAR encephalitis, and suggest a paradigm of immune-response different from that reported in myelin-oligodendrocyte glycoprotein (MOG)-experimental autoimmune encephalomyelitis (EAE) in which peptide immunization induces an EAE model that is mainly T cell mediated (B cell independent).¹⁴⁶ The length of the GluN1 peptide used in our model (30 amino acids) instead for example, shorter peptides (9-14 amino acid MOG fragments) reported in the B cell independent EAE, together with the adjuvant used here, AddaVax, which primes B cell responses may have played a role in the robust humoral response of our model. Our studies with

IFN- γ ELISpot on splenocytes from NMDAR mice confirmed the activation of GluN1-specific T cells, which was significantly decreased by the anti-CD20, suggesting an important contribution of GluN1-specific CD20+T cells in B cell activation, as reported previously in an EAE model.¹⁶⁶

IgG isolated from NMDAR mice caused a reduction of NMDAR clusters and NMDAR-dependent calcium currents in cultured rat hippocampal neurons, similar to the alterations reported for the IgG of patients, confirming that mice autoantibodies have direct effects on NMDARs. As a result, immunized mice, but not controls, showed NMDAR-specific brain-bound IgG, reduced content of synaptic and extrasynaptic NMDAR clusters, and significant impairment of hippocampal plasticity (LTP) similar to the alterations reported with passive cerebroventricular transfer of patients' antibodies to mice.¹²⁹ However, different from the passive transfer model in which the duration of effects was short (~14 days) until antibodies were cleared, the current model showed NMDAR-related alterations for the entire duration of the study (71 days), providing the opportunity to assess different treatment strategies targeting at distinct disease mechanisms.

Another advantage of active immunization over passive transfer models is the possibility to study components of the immune response other than the antibody effects, such as brain inflammatory infiltrates, complement-mediated neuronal injury, and microglial activation. Analysis of brain inflammatory infiltrates showed predominance of B cells and plasma cells, infrequent T cells, absence of complement, and extensive microglial activation, overall

resembling most of the findings reported in autopsies of patients. A potential difference is that in patients, the frequency of T cells although low, might be higher than that observed in our model. Microglial activation is a consistent finding in patients' autopsies,⁶⁷ suggesting it plays a pathogenic role.¹⁶⁷ In the current study, NMDAR mice but not controls, showed a significant co-localization of CD68 (a phagocytic marker expressed by microglia/perivascular macrophages) with IgG and NMDARs. This triple co-localization, when assessed at the nanoscale level with super-resolution STED microscopy, was found to occur in endosomal/lysosomal structures, suggesting microglial phagocytosis of IgG-bound NMDARs.

Overall, these findings were accompanied by psychotic-like behaviour, memory deficits, depressive-like behaviour, variable presence of stereotyped movements (e.g., circling, self-biting, and walking backwards), and enhanced susceptibility to develop seizures (demonstrated with intracerebral electrodes). Interestingly, NMDAR mice not receiving treatment or injections of vehicle, developed psychotic-like behaviour earlier than depressive-like behaviour (as occurs in many patients), whereas memory impairment persisted during the entire follow-up, and stereotyped movements occurred without stage preference. By contrast, psychotic-like behaviour remained detectable during the entire follow-up in untreated NMDAR mice stressed by daily (days 45-71) injections of vehicle.

The feasibility of the model to assess potential treatments was tested with an anti-CD20 immunotherapy, and SGE-301. NMDAR mice treated with anti-CD20 showed acute depletion of peripheral and brain B cell counts, accompanied by a decrease in brain-bound IgG,

and recovery of NMDAR cluster density, hippocampal plasticity (LTP), memory and other behavioral paradigms. These effects started wearing off about 5 weeks after treatment, when mice showed B cell repopulation and increased memory B cell infiltrates in the brain, alongside reduction of NMDAR clusters (initially detected in the DG), worsening synaptic plasticity, and return of memory impairment. These findings highlight the importance of B cell entry into the CNS, as suggested by neuropathological studies in patients, and a previous model examining the brain inflammatory infiltrates in untreated mice. Murine models of other disorders treated with anti-CD20 have shown variable duration of B cell depletion, ranging from 8 weeks post-treatment with three administrations of 200 µg of anti-CD20 to 6 weeks after two administrations of 150 µg of anti-CD20.^{168,169} In our model, B cell repopulation occurred 5 weeks after a single 250 µg administration of anti-CD20, suggesting the depletion period is dose-dependent. These findings are in line with those in clinical practice which show the need of repeat cycles of rituximab to obtain therapeutic B cell depletion. The time lag between treatment administration and effects on symptoms and antibody levels is consistent with the findings in the EAE model in which symptom recovery associates better with B cell reduction than with the reduction of MOG antibody levels.¹⁴⁶ Similarly, in our model, the decrease in brain plasma cell infiltrates represented a delayed response, likely due to these cells not expressing CD20.

Of potential clinical interest, late daily treatment with a SGE-301 restored normal NMDAR density, hippocampal LTP, and memory and behavioural alterations, without modifying the levels of B cells or

antibody synthesis. These findings suggest that SGE-301 or similar NMDAR PAMs (e.g., some designed for oral bioavailability) could be an effective adjuvant treatment for anti-NMDAR encephalitis, particularly during the prolonged post-acute stage, when cognitive and psychiatric symptoms persist, and maintenance or escalation of immunotherapy may not be needed. In our model the early use of an anti-CD20 combined with a later administration of SGE-301 resulted in abrogation of all clinical and neurobiological alterations of the disease.

This study has several considerations and limitations. Since the model examines multiple clinical and biological paradigms, requiring multiple subsets of NMDAR mice and controls without and with several treatments, we designed the follow-up for 10 weeks after initial immunization. We chose this experimental design with the rationale that if active immunization recapitulated the clinical disease course, the model would provide important immune and neurobiological insights and be well positioned to test the effect of clinical standard of care (anti-CD20 immunotherapy) and SGE-301. Our data strongly supports this preclinical model as means to examine the clinical disease course and believe it can be followed for increasing amounts of time to investigate more long-term aspects of the disease. Moreover, although we confirmed the presence of antibodies in CSF, the small amounts of CSF were a logistical problem that precluded several studies; thus, most investigations were performed with IgG isolated from serum. Mice showed propensity to develop seizures and status epilepticus, but did not show spontaneous seizures, which is frequent in patients. Finally,

although changes in immunological, neurobiological, and behavioural paradigms usually occurred in parallel (e.g., B cell repopulation and re-emerging of neurobiological and memory problems), the correlation with serum antibody titers was not perfect, an observation also made in patients.

Together with a report showing in some patients with anti-NMDAR encephalitis antibody synthesis in deep cervical lymph nodes,¹⁷⁰ and a study with mixed cultures of neurons/microglia suggesting IgG-NMDAR microglial phagocytosis,¹⁶⁷ our demonstration that GluN1 peptide immunization leads to a polyclonal antibody response, microglial IgG-NMDAR phagocytosis, and synthesis of antibodies in deep cervical lymph nodes, suggests an immunological paradigm. After immunological activation at systemic lymph nodes corresponding to the immunization site, NMDAR antibodies produced systemically and by brain infiltrating B cells/plasma cells cause a reduction of neuronal NMDAR (as seen in cultured neurons and passive transfer models with human antibodies), but there is also phagocytosis of NMDAR-IgG complexes by microglia (antigen presenting cells) that likely contributes to epitope spreading by presentation of new NMDAR fragments to CD4 T cells resulting in polyclonal B cell activation, most likely at deep cervical lymph nodes.

This model can now be adapted in many ways, for example extending the follow-up, increasing the number of administrations of the anti-CD20, administering simultaneously both treatments, or even considering new treatments. It also offers the opportunity to further investigate how a systemically triggered neuronal immune response (as occur in patients with teratoma) reaches the CNS, and the role of

brain antigen-presenting cells and deep cervical lymph nodes in further adapting the anti-neuronal immunity. The model can also be used for the adoptive transfer of immune cells (e.g., splenocytes or expanded GluN1-specific T cells of NMDAR mice) into nude mice, offering the opportunity to assess CAR T cell therapy approaches on all the clinical and biological paradigms we have examined here. Overall, the results from the **sixth study** not only fill a crucial gap in the existing literature on anti-NMDAR encephalitis, but also set a foundation for future research into the recovery process of the disease and novel therapeutic approaches.

Chapter VIII

Conclusions

1. Antibodies from patients with anti-mGluR5 encephalitis infused into the cerebroventricular system of mice cause memory impairment, increased anxiety and decreased neuronal cell-surface mGluR5 clusters. These findings support the pathogenicity of antibodies in anti-mGluR5 encephalitis.
2. Antibodies from patients with anti-NMDAR encephalitis specifically alter the function of NMDAR in oligodendrocytes causing a decrease of expression of GLUT1. These findings suggest a link between antibody-mediated dysfunction of NMDAR in oligodendrocytes and the alterations of white matter integrity reported in patients with anti-NMDAR encephalitis.
3. In cultures of neurons, SGE-301, an oxysterol-based PAM of NMDAR, significantly decreases, without fully preventing, the internalization of antibody-bound NMDARs.
4. In a well-established mouse model of cerebroventricular transfer of patients' CSF antibodies, SGE-301 antagonizes and reverses the synaptic and behavioral pathogenic effect of the antibodies without preventing antibody binding to NMDARs.
5. SGE-301 upregulates the surface dynamics of NMDAR, mainly in the postsynaptic compartment, and this effect normalizes NMDAR diffusion in neurons exposed to patients' antibodies.
6. Immunization of mice with the peptide GluN1₃₅₆₋₃₈₅ and the adjuvant AddaVax adjuvant reproduces most of the neurobiological, immunological and behavioral alterations that occur in anti-NMDAR encephalitis.

7. In this new murine model, treatment with either anti-CD20 or SGE-301 resulted in significant improvement of the symptoms and associated neurobiological alterations caused by anti-NMDAR encephalitis. The combination of treatment with anti-CD20 and SGE-301) was the most efficient approach to obtain recovery from all the alterations, suggesting that SGE-301 could potentially serve as adjuvant treatment for the disease.

Chapter IX

Bibliography

1. Venkatesan A, Michael BD, Probasco JC, Geocadin RG, Solomon T. Acute encephalitis in immunocompetent adults. *Lancet (London, England)*. 2019;393(10172):702-716. doi:10.1016/S0140-6736(18)32526-1
2. Granerod J, Cousens S, Davies NWS, Crowcroft NS, Thomas SL. New estimates of incidence of encephalitis in England. *Emerg Infect Dis*. 2013;19(9):1455-1462. doi:10.3201/eid1909.130064
3. Boucher A, Herrmann JL, Morand P, et al. Epidemiology of infectious encephalitis causes in 2016. *Med Mal Infect*. 2017;47(3):221-235. doi:10.1016/j.medmal.2017.02.003
4. Granerod J, Tam CC, Crowcroft NS, Davies NWS, Borchert M, Thomas SL. Challenge of the unknown. A systematic review of acute encephalitis in non-outbreak situations. *Neurology*. 2010;75(10):924-932. doi:10.1212/WNL.0b013e3181f11d65
5. Venkatesan A. Epidemiology and outcomes of acute encephalitis. *Curr Opin Neurol*. 2015;28(3):277-282. doi:10.1097/WCO.0000000000000199
6. Granerod J, Ambrose HE, Davies NW, et al. Causes of encephalitis and differences in their clinical presentations in England: a multicentre, population-based prospective study. *Lancet Infect Dis*. 2010;10(12):835-844. doi:10.1016/S1473-3099(10)70222-X
7. Hjalmarsson A, Blomqvist P, Sköldenberg B. Herpes simplex encephalitis in Sweden, 1990-2001: incidence, morbidity, and mortality. *Clin Infect Dis an Off Publ Infect Dis Soc Am*. 2007;45(7):875-880. doi:10.1086/521262
8. Graus F, Cordon-Cardo C, Posner JB. Neuronal antinuclear antibody in sensory neuronopathy from lung cancer. *Neurology*. 1985;35(4):538-543. doi:10.1212/wnl.35.4.538
9. Graus F, Elkon KB, Cordon-Cardo C, Posner JB. Sensory neuronopathy and small cell lung cancer. Antineuronal antibody that also reacts with the tumor. *Am J Med*. 1986;80(1):45-52. doi:10.1016/0002-9343(86)90047-1
10. Graus F, Dalmau J. Paraneoplastic neurological syndromes in the era of immune-checkpoint inhibitors. *Nat Rev Clin Oncol*. 2019;16(9):535-548. doi:10.1038/s41571-019-0194-4
11. Graus F, Keime-Guibert F, Reñe R, et al. Anti-Hu-associated paraneoplastic encephalomyelitis: analysis of 200 patients. *Brain*. 2001;124(Pt 6):1138-1148. doi:10.1093/brain/124.6.1138

12. Rees JH, Hain SF, Johnson MR, et al. The role of [18F]fluoro-2-deoxyglucose-PET scanning in the diagnosis of paraneoplastic neurological disorders. *Brain*. 2001;124(Pt 11):2223-2231. doi:10.1093/brain/124.11.2223
13. Hormigo A, Lieberman F. Nuclear localization of anti-Hu antibody is not associated with in vitro cytotoxicity. *J Neuroimmunol*. 1994;55(2):205-212. doi:10.1016/0165-5728(94)90011-6
14. Tanaka K, Tanaka M, Onodera O, Igarashi S, Miyatake T, Tsuji S. Passive transfer and active immunization with the recombinant leucine-zipper (Yo) protein as an attempt to establish an animal model of paraneoplastic cerebellar degeneration. *J Neurol Sci*. 1994;127(2):153-158. doi:10.1016/0022-510x(94)90067-1
15. Verschuuren JJ, Dalmau J, Hoard R, Posner JB. Paraneoplastic anti-Hu serum: studies on human tumor cell lines. *J Neuroimmunol*. 1997;79(2):202-210. doi:10.1016/s0165-5728(97)00124-0
16. Albert ML, Darnell JC, Bender A, Francisco LM, Bhardwaj N, Darnell RB. Tumor-specific killer cells in paraneoplastic cerebellar degeneration. *Nat Med*. 1998;4(11):1321-1324. doi:10.1038/3315
17. Bernal F, Graus F, Pifarré A, Saiz A, Benyahia B, Ribalta T. Immunohistochemical analysis of anti-Hu-associated paraneoplastic encephalomyelitis. *Acta Neuropathol*. 2002;103(5):509-515. doi:10.1007/s00401-001-0498-0
18. Rosenfeld MR, Dalmau J. Diagnosis and management of paraneoplastic neurologic disorders. *Curr Treat Options Oncol*. 2013;14(4):528-538. doi:10.1007/s11864-013-0249-1
19. Rotte A, Jin JY, Lemaire V. Mechanistic overview of immune checkpoints to support the rational design of their combinations in cancer immunotherapy. *Ann Oncol Off J Eur Soc Med Oncol*. 2018;29(1):71-83. doi:10.1093/annonc/mdx686
20. Johnson DB, Manouchehri A, Haugh AM, et al. Neurologic toxicity associated with immune checkpoint inhibitors: a pharmacovigilance study. *J Immunother cancer*. 2019;7(1):134. doi:10.1186/s40425-019-0617-x
21. Fonseca E, Cabrera-Maqueda JM, Ruiz-García R, et al. Neurological adverse events related to immune-checkpoint inhibitors in Spain: a retrospective cohort study. *Lancet Neurol*. 2023;22(12):1150-1159. doi:10.1016/S1474-4422(23)00335-6
22. Dalmau J, Graus F. *Autoimmune Encephalitis and Related Disorders of the Nervous System*. Cambridge University Press; 2022.

23. Simpson JA. Myasthenia Gravis: A New Hypothesis. *Scott Med J*. 1960;5(10):419-436. doi:10.1177/003693306000501001
24. Patrick J, Lindstrom J. Autoimmune response to acetylcholine receptor. *Science*. 1973;180(4088):871-872. doi:10.1126/science.180.4088.871
25. Toyka K V, Brachman DB, Pestronk A, Kao I. Myasthenia gravis: passive transfer from man to mouse. *Science*. 1975;190(4212):397-399. doi:10.1126/science.1179220
26. Lindstrom J. Immunological studies of acetylcholine receptors. *J Supramol Struct*. 1976;4(3):389-403. doi:10.1002/jss.400040310
27. Drachman DB. Myasthenia gravis (second of two parts). *N Engl J Med*. 1978;298(4):186-193. doi:10.1056/NEJM197801262980404
28. Lennon VA, Lambert EH, Whittingham S, Fairbanks V. Autoimmunity in the Lambert-Eaton myasthenic syndrome. *Muscle Nerve*. 1982;5(9S):S21-5.
29. Lang B, Newsom-Davis J, Prior C, Wray D. Antibodies to motor nerve terminals: an electrophysiological study of a human myasthenic syndrome transferred to mouse. *J Physiol*. 1983;344:335-345. doi:10.1113/jphysiol.1983.sp014943
30. Lennon VA, Kryzer TJ, Griesmann GE, et al. Calcium-channel antibodies in the Lambert-Eaton syndrome and other paraneoplastic syndromes. *N Engl J Med*. 1995;332(22):1467-1474. doi:10.1056/NEJM199506013322203
31. Motomura M, Johnston I, Lang B, Vincent A, Newsom-Davis J. An improved diagnostic assay for Lambert-Eaton myasthenic syndrome. *J Neurol Neurosurg Psychiatry*. 1995;58(1):85-87. doi:10.1136/jnnp.58.1.85
32. Waerness E. Neuromyotonia and bronchial carcinoma. *Electromyogr Clin Neurophysiol*. 1974;14(5-6):527-535.
33. Partanen VS, Soininen H, Saksa M, Riekkinen P. Electromyographic and nerve conduction findings in a patient with neuromyotonia, normocalcemic tetany and small-cell lung cancer. *Acta Neurol Scand*. 1980;61(4):216-226. doi:10.1111/j.1600-0404.1980.tb01486.x
34. Halbach M, Hömberg V, Freund HJ. Neuromuscular, autonomic and central cholinergic hyperactivity associated with thymoma and acetylcholine receptor-binding antibody. *J Neurol*. 1987;234(6):433-436. doi:10.1007/BF00314093

35. Sinha S, Newsom-Davis J, Mills K, Byrne N, Lang B, Vincent A. Autoimmune aetiology for acquired neuromyotonia (Isaacs' syndrome). *Lancet (London, England)*. 1991;338(8759):75-77. doi:10.1016/0140-6736(91)90073-x
36. Hart IK, Maddison P, Newsom-Davis J, Vincent A, Mills KR. Phenotypic variants of autoimmune peripheral nerve hyperexcitability. *Brain*. 2002;125(Pt 8):1887-1895. doi:10.1093/brain/awf178
37. Bruno R, Sabater L, Tolosa E, et al. Different patterns of nicotinic acetylcholine receptor subunit transcription in human thymus. *J Neuroimmunol*. 2004;149(1-2):147-159. doi:10.1016/j.jneuroim.2003.11.022
38. Gilhus NE, Tzartos S, Evoli A, Palace J, Burns TM, Verschuuren JJGM. Myasthenia gravis. *Nat Rev Dis Prim*. 2019;5(1):30. doi:10.1038/s41572-019-0079-y
39. Buckley C, Douek D, Newsom-Davis J, Vincent A, Willcox N. Mature, long-lived CD4+ and CD8+ T cells are generated by the thymoma in myasthenia gravis. *Ann Neurol*. 2001;50(1):64-72. doi:10.1002/ana.1017
40. Marx A, Pfister F, Schalke B, Saruhan-Direskeneli G, Melms A, Ströbel P. The different roles of the thymus in the pathogenesis of the various myasthenia gravis subtypes. *Autoimmun Rev*. 2013;12(9):875-884. doi:10.1016/j.autrev.2013.03.007
41. Wolfe GI, Kaminski HJ, Aban IB, et al. Long-term effect of thymectomy plus prednisone versus prednisone alone in patients with non-thymomatous myasthenia gravis: 2-year extension of the MGTX randomised trial. *Lancet Neurol*. 2019;18(3):259-268. doi:10.1016/S1474-4422(18)30392-2
42. O'Neill JH, Murray NM, Newsom-Davis J. The Lambert-Eaton myasthenic syndrome. A review of 50 cases. *Brain*. 1988;111 (Pt 3):577-596. doi:10.1093/brain/111.3.577
43. Pascuzzi RM, Bodkin CL. Myasthenia Gravis and Lambert-Eaton Myasthenic Syndrome: New Developments in Diagnosis and Treatment. *Neuropsychiatr Dis Treat*. 2022;18:3001-3022. doi:10.2147/NDT.S296714
44. Sillevs Smitt P, Kinoshita A, De Leeuw B, et al. Paraneoplastic cerebellar ataxia due to autoantibodies against a glutamate receptor. *N Engl J Med*. 2000;342(1):21-27. doi:10.1056/NEJM200001063420104

45. Irani SR, Alexander S, Waters P, et al. Antibodies to Kv1 potassium channel-complex proteins leucine-rich, glioma inactivated 1 protein and contactin-associated protein-2 in limbic encephalitis, Morvan's syndrome and acquired neuromyotonia. *Brain*. 2010;133(9):2734-2748. doi:10.1093/brain/awq213
46. Ances BM, Vitaliani R, Taylor RA, et al. Treatment-responsive limbic encephalitis identified by neuropil antibodies: MRI and PET correlates. *Brain*. 2005;128(Pt 8):1764-1777. doi:10.1093/brain/awh526
47. Vitaliani R, Mason W, Ances B, Zwerdling T, Jiang Z, Dalmau J. Paraneoplastic encephalitis, psychiatric symptoms, and hypoventilation in ovarian teratoma. *Ann Neurol*. 2005;58(4):594-604. doi:10.1002/ana.20614
48. Dalmau J, Tüzün E, Wu HY, et al. Paraneoplastic anti-N-methyl-D-aspartate receptor encephalitis associated with ovarian teratoma. *Ann Neurol*. 2007;61(1):25-36. doi:10.1002/ana.21050
49. Graus F, Titulaer MJ, Balu R, et al. A clinical approach to diagnosis of autoimmune encephalitis. *Lancet Neurol*. 2016;15(4):391-404. doi:10.1016/S1474-4422(15)00401-9
50. Dalmau J, Geis C, Graus F. Autoantibodies to Synaptic Receptors and Neuronal Cell Surface Proteins in Autoimmune Diseases of the Central Nervous System. *Physiol Rev*. 2017;97(2):839-887. doi:10.1152/physrev.00010.2016
51. Dalmau J, Armangué T, Planagumà J, et al. An update on anti-NMDA receptor encephalitis for neurologists and psychiatrists: mechanisms and models. *Lancet Neurol*. 2019;18(11):1045-1057. doi:10.1016/S1474-4422(19)30244-3
52. Gleichman AJ, Spruce LA, Dalmau J, Seeholzer SH, Lynch DR. Anti-NMDA receptor encephalitis antibody binding is dependent on amino acid identity of a small region within the GluN1 amino terminal domain. *J Neurosci*. 2012;32(32):11082-11094. doi:10.1523/JNEUROSCI.0064-12.2012
53. Hansen KB, Yi F, Perszyk RE, et al. Structure, function, and allosteric modulation of NMDA receptors. *J Gen Physiol*. 2018;150(8):1081-1105. doi:10.1085/jgp.201812032
54. Johnson JW. Acid tests of N-methyl-D-aspartate receptor gating basics. *Mol Pharmacol*. 2003;63(6):1199-1201. doi:10.1124/mol.63.6.1199

55. Laube B, Kuhse J, Betz H. Evidence for a tetrameric structure of recombinant NMDA receptors. *J Neurosci Off J Soc Neurosci*. 1998;18(8):2954-2961. doi:10.1523/JNEUROSCI.18-08-02954.1998
56. Karakas E, Furukawa H. Crystal structure of a heterotetrameric NMDA receptor ion channel. *Science*. 2014;344(6187):992-997. doi:10.1126/science.1251915
57. Traynelis SF, Wollmuth LP, McBain CJ, et al. Glutamate receptor ion channels: structure, regulation, and function. *Pharmacol Rev*. 2010;62(3):405-496. doi:10.1124/pr.109.002451
58. Franchini L, Carrano N, Di Luca M, Gardoni F. Synaptic GluN2A-Containing NMDA Receptors: From Physiology to Pathological Synaptic Plasticity. *Int J Mol Sci*. 2020;21(4). doi:10.3390/ijms21041538
59. Lee CH, Lü W, Michel JC, et al. NMDA receptor structures reveal subunit arrangement and pore architecture. *Nature*. 2014;511(7508):191-197. doi:10.1038/nature13548
60. Mayer ML, Westbrook GL, Guthrie PB. Voltage-dependent block by Mg²⁺ of NMDA responses in spinal cord neurones. *Nature*. 1984;309(5965):261-263. doi:10.1038/309261a0
61. Forrest D, Yuzaki M, Soares HD, et al. Targeted disruption of NMDA receptor 1 gene abolishes NMDA response and results in neonatal death. *Neuron*. 1994;13(2):325-338. doi:10.1016/0896-6273(94)90350-6
62. McHugh TJ, Blum KI, Tsien JZ, Tonegawa S, Wilson MA. Impaired hippocampal representation of space in CA1-specific NMDAR1 knockout mice. *Cell*. 1996;87(7):1339-1349. doi:10.1016/s0092-8674(00)81828-0
63. Tüzün E, Zhou L, Baehring JM, Bannykh S, Rosenfeld MR, Dalmau J. Evidence for antibody-mediated pathogenesis in anti-NMDAR encephalitis associated with ovarian teratoma. *Acta Neuropathol*. 2009;118(6):737-743. doi:10.1007/s00401-009-0582-4
64. Armangue T, Spatola M, Vlagea A, et al. Frequency, symptoms, risk factors, and outcomes of autoimmune encephalitis after herpes simplex encephalitis: a prospective observational study and retrospective analysis. *Lancet Neurol*. 2018;17(9):760-772. doi:10.1016/S1474-4422(18)30244-8
65. Bien CG, Vincent A, Barnett MH, et al. Immunopathology of autoantibody-associated encephalitides: clues for pathogenesis. *Brain*. 2012;135(Pt 5):1622-1638. doi:10.1093/brain/aws082

66. Camdessanché JP, Streichenberger N, Cavillon G, et al. Brain immunohistopathological study in a patient with anti-NMDAR encephalitis. *Eur J Neurol*. 2011;18(6):929-931. doi:10.1111/j.1468-1331.2010.03180.x
67. Zrzavy T, Endmayr V, Bauer J, et al. Neuropathological Variability within a Spectrum of NMDAR-Encephalitis. *Ann Neurol*. 2021;90(5):725-737. doi:10.1002/ana.26223
68. Dalmau J, Lancaster E, Martinez-Hernandez E, Rosenfeld MR BGR. Clinical experience and laboratory investigations in patients with anti-NMDAR encephalitis Prof Josep Dalmau , Department of Neuroscience , University of Pennsylvania School of Medicine (Prof R Balice-Gordon , PhD), Philadelphia , PA , USA The syndrome. *Lancet Neurol*. 2011;10(1):63-74. doi:10.1016/S1474-4422(10)70253-2.Clinical
69. Finke C, Kopp UA, Scheel M, et al. Functional and structural brain changes in anti-N-methyl-D-aspartate receptor encephalitis. *Ann Neurol*. 2013;74(2):284-296. doi:10.1002/ana.23932
70. Phillips OR, Joshi SH, Narr KL, et al. Superficial white matter damage in anti-NMDA receptor encephalitis. *J Neurol Neurosurg Psychiatry*. 2018;89(5):518-525. doi:10.1136/jnnp-2017-316822
71. Saab AS, Tzvetavona ID, Trevisiol A, et al. Oligodendroglial NMDA Receptors Regulate Glucose Import and Axonal Energy Metabolism. *Neuron*. 2016;91(1):119-132. doi:10.1016/j.neuron.2016.05.016
72. Titulaer MJ, McCracken L, Gabilondo I, et al. Treatment and prognostic factors for long-term outcome in patients with anti-N-Methyl-D-Aspartate (NMDA) receptor encephalitis: a cohort study. *Lancet Neurol*. 2013;12(2):157-165. doi:10.1016/S1474-4422(12)70310-1.Treatment
73. Nicolle DCM, Moses JL. A Systematic Review of the Neuropsychological Sequelae of People Diagnosed with Anti N-Methyl-D-Aspartate Receptor Encephalitis in the Acute and Chronic Phases. *Arch Clin Neuropsychol Off J Natl Acad Neuropsychol*. 2018;33(8):964-983. doi:10.1093/arclin/acy005
74. Guasp M, Rosa-Justicia M, Muñoz-Lopetegi A, et al. Clinical characterisation of patients in the post-acute stage of anti-NMDA receptor encephalitis: a prospective cohort study and comparison with patients with schizophrenia spectrum disorders. *Lancet Neurol*. 2022;21(10):899-910. doi:10.1016/S1474-4422(22)00299-X

75. Planagumà J, Haselmann H, Mannara F, et al. Ephrin-B2 prevents N-methyl-D-aspartate receptor antibody effects on memory and neuroplasticity. *Ann Neurol.* 2016;80(3):388-400. doi:10.1002/ana.24721
76. Paul SM, Doherty JJ, Robichaud AJ, et al. The major brain cholesterol metabolite 24(S)-hydroxycholesterol is a potent allosteric modulator of N-methyl-D-aspartate receptors. *J Neurosci Off J Soc Neurosci.* 2013;33(44):17290-17300. doi:10.1523/JNEUROSCI.2619-13.2013
77. Warikoo N, Brunwasser SJ, Benz A, et al. Positive allosteric modulation as a potential therapeutic strategy in anti-NMDA receptor encephalitis. *J Neurosci.* 2018;38(13):3218-3229. doi:10.1523/JNEUROSCI.3377-17.2018
78. Carr I. The Ophelia syndrome: memory loss in Hodgkin's disease. *Lancet (London, England).* 1982;1(8276):844-845. doi:10.1016/s0140-6736(82)91887-6
79. Lancaster E, Martinez-Hernandez E, Titulaer MJ, et al. Antibodies to metabotropic glutamate receptor 5 in the Ophelia syndrome. *Neurology.* 2011;77(18):1698-1701. doi:10.1212/WNL.0b013e3182364a44
80. Nicoletti F, Bockaert J, Collingridge GL, et al. Metabotropic glutamate receptors: from the workbench to the bedside. *Neuropharmacology.* 2011;60(7-8):1017-1041. doi:10.1016/j.neuropharm.2010.10.022
81. Nasrallah C, Cannone G, Briot J, et al. Agonists and allosteric modulators promote signaling from different metabotropic glutamate receptor 5 conformations. *Cell Rep.* 2021;36(9):109648. doi:10.1016/j.celrep.2021.109648
82. Sengmany K, Gregory KJ. Metabotropic glutamate receptor subtype 5: molecular pharmacology, allosteric modulation and stimulus bias. *Br J Pharmacol.* 2016;173(20):3001-3017. doi:10.1111/bph.13281
83. Guo K, Liu X, Gong X, et al. Autoimmune encephalitis with mGluR5 antibodies: A case series from China and review of the literature. *Front Immunol.* 2023;14:1146536. doi:10.3389/fimmu.2023.1146536
84. Spatola M, Sabater L, Planaguma J, et al. Encephalitis with mGluR5 antibodies: Symptoms and antibody effects. *Neurology.* Published online 2018:1-10. doi:10.1212/WNL.0000000000005614

85. Vidarsson G, Dekkers G, Rispens T. IgG subclasses and allotypes: from structure to effector functions. *Front Immunol.* 2014;5:520. doi:10.3389/fimmu.2014.00520
86. Hughes EG, Peng X, Gleichman AJ, et al. Cellular and synaptic mechanisms of anti-NMDA receptor encephalitis. *J Neurosci.* 2010;30(17):5866-5875. doi:10.1523/JNEUROSCI.0167-10.2010
87. Lai M, Hughes EG, Peng X, et al. AMPA receptor antibodies in limbic encephalitis alter synaptic receptor location. *Ann Neurol.* 2009;65(4):424-434. doi:10.1002/ana.21589
88. Petit-Pedrol M, Armangue T, Peng X, et al. Encephalitis with refractory seizures, status epilepticus, and antibodies to the GABAA receptor: a case series, characterisation of the antigen, and analysis of the effects of antibodies. *Lancet Neurol.* 2014;13(3):276-286. doi:10.1016/S1474-4422(13)70299-0
89. Landa J, Guasp M, Míguez-Cabello F, et al. Encephalitis with Autoantibodies against the Glutamate Kainate Receptors GluK2. *Ann Neurol.* 2021;90(1):101-117. doi:10.1002/ana.26098
90. Lancaster E, Lai M, Peng X, et al. Antibodies to the GABA(B) receptor in limbic encephalitis with seizures: case series and characterisation of the antigen. *Lancet Neurol.* 2010;9(1):67-76. doi:10.1016/S1474-4422(09)70324-2
91. Sabater L, Gaig C, Gelpi E, et al. A novel non-rapid-eye movement and rapid-eye-movement parasomnia with sleep breathing disorder associated with antibodies to IgLON5: a case series, characterisation of the antigen, and post-mortem study. *Lancet Neurol.* 2014;13(6):575-586. doi:10.1016/S1474-4422(14)70051-1
92. Ohkawa T, Fukata Y, Yamasaki M, et al. Autoantibodies to epilepsy-related LGI1 in limbic encephalitis neutralize LGI1-ADAM22 interaction and reduce synaptic AMPA receptors. *J Neurosci Off J Soc Neurosci.* 2013;33(46):18161-18174. doi:10.1523/JNEUROSCI.3506-13.2013
93. Pinatel D, Hivert B, Boucraut J, et al. Inhibitory axons are targeted in hippocampal cell culture by anti-Caspr2 autoantibodies associated with limbic encephalitis. *Front Cell Neurosci.* 2015;9:265. doi:10.3389/fncel.2015.00265
94. Jarius S, Metz I, König FB, et al. Screening for MOG-IgG and 27 other anti-glial and anti-neuronal autoantibodies in “pattern II multiple sclerosis” and brain biopsy findings in a MOG-IgG-positive case. *Mult Scler.* 2016;22(12):1541-1549. doi:10.1177/1352458515622986

95. Stathopoulos P, Dalakas MC. The role of complement and complement therapeutics in neuromyelitis optica spectrum disorders. *Expert Rev Clin Immunol.* 2022;18(9):933-945. doi:10.1080/1744666X.2022.2105205
96. Kreye J, Wenke NK, Chayka M, et al. Human cerebrospinal fluid monoclonal N-methyl-D-aspartate receptor autoantibodies are sufficient for encephalitis pathogenesis. *Brain.* 2016;139(10):2641-2652. doi:10.1093/brain/aww208
97. Moscato EH, Peng X, Jain A, Parsons TD, Dalmau J, Balice-Gordon RJ. Acute mechanisms underlying antibody effects in anti-N-methyl-D-aspartate receptor encephalitis. *Ann Neurol.* 2014;76(1):108-119. doi:10.1002/ana.24195
98. Mikasova L, De Rossi P, Bouchet D, et al. Disrupted surface cross-talk between NMDA and Ephrin-B2 receptors in anti-NMDA encephalitis. *Brain.* 2012;135(5):1606-1621. doi:10.1093/brain/aws092
99. Carceles-Cordon M, Mannara F, Aguilar E, Castellanos A, Planagumà J, Dalmau J. NMDAR Antibodies Alter Dopamine Receptors and Cause Psychotic Behavior in Mice. *Ann Neurol.* 2020;88(3):603-613. doi:10.1002/ana.25829
100. Matute C, Palma A, Serrano-Regal MP, et al. N-Methyl-D-Aspartate Receptor Antibodies in Autoimmune Encephalopathy Alter Oligodendrocyte Function. *Ann Neurol.* 2020;87(5):670-676. doi:10.1002/ana.25699
101. Peng X, Hughes EG, Moscato EH, Parsons TD, Dalmau J, Balice-Gordon RJ. Cellular plasticity induced by anti- α -amino-3-hydroxy-5-methyl-4-isoxazolepropionic acid (AMPA) receptor encephalitis antibodies. *Ann Neurol.* 2015;77(3):381-398. doi:10.1002/ana.24293
102. Petit-pedrol M, Armangue T, Peng X, et al. Articles Encephalitis with refractory seizures , status epilepticus , and antibodies to the GABA A receptor : a case series , characterisation of the antigen , and analysis of the effects of antibodies. *Lancet Neurol.* 2014;4422(13):14-16. doi:10.1016/S1474-4422(13)70299-0
103. Spatola M, Petit Pedrol M, Maudes E, et al. Clinical features, prognostic factors, and antibody effects in anti-mGluR1 encephalitis. *Neurology.* 2020;95(22):e3012-e3025. doi:10.1212/WNL.0000000000010854
104. Coesmans M, Smitt PAS, Linden DJ, et al. Mechanisms underlying cerebellar motor deficits due to mGluR1-autoantibodies. *Ann Neurol.* 2003;53(3):325-336. doi:10.1002/ana.10451

105. Ruiz-García R, Martínez-Hernández E, Joubert B, et al. Paraneoplastic cerebellar ataxia and antibodies to metabotropic glutamate receptor 2. *Neurol Neuroimmunol neuroinflammation*. 2020;7(2). doi:10.1212/NXI.0000000000000658
106. Sinmaz N, Tea F, Pilli D, et al. Dopamine-2 receptor extracellular N-terminus regulates receptor surface availability and is the target of human pathogenic antibodies from children with movement and psychiatric disorders. *Acta Neuropathol Commun*. 2016;4(1):126. doi:10.1186/s40478-016-0397-1
107. Crisp SJ, Dixon CL, Jacobson L, et al. Glycine receptor autoantibodies disrupt inhibitory neurotransmission. *Brain*. 2019;142(11):3398-3410. doi:10.1093/brain/awz297
108. Rauschenberger V, von Wardenburg N, Schaefer N, et al. Glycine Receptor Autoantibodies Impair Receptor Function and Induce Motor Dysfunction. *Ann Neurol*. 2020;88(3):544-561. doi:10.1002/ana.25832
109. Lalic T, Pettingill P, Vincent A, Capogna M. Human limbic encephalitis serum enhances hippocampal mossy fiber-CA3 pyramidal cell synaptic transmission. *Epilepsia*. 2011;52(1):121-131. doi:10.1111/j.1528-1167.2010.02756.x
110. Patterson KR, Dalmau J, Lancaster E. Mechanisms of Caspr2 Antibodies in Autoimmune Encephalitis and Neuromyotonia. Published online 2017. doi:10.1002/ana.25120
111. Fernandes D, Santos SD, Coutinho E, et al. Disrupted AMPA Receptor Function upon Genetic- or Antibody-Mediated Loss of Autism-Associated CASPR2. *Cereb Cortex*. 2019;29(12):4919-4931. doi:10.1093/cercor/bhz032
112. Hara M, Ariño H, Petit-Pedrol M, et al. DPPX antibody-associated encephalitis: Main syndrome and antibody effects. *Neurology*. 2017;88(14):1340-1348. doi:10.1212/WNL.0000000000003796
113. Piegras J, Höltje M, Michel K, et al. Anti-DPPX encephalitis: pathogenic effects of antibodies on gut and brain neurons. *Neurology*. 2015;85(10):890-897. doi:10.1212/WNL.0000000000001907
114. Gresa-Arribas N, Planagumà J, Petit-Pedrol M, et al. *Human Neurexin-3a Antibodies Associate with Encephalitis and Alter Synapse Development*; 2016.

115. Sabater L, Planagumà J, Dalmau J, Graus F. Cellular investigations with human antibodies associated with the anti-IgLON5 syndrome. *J Neuroinflammation*. 2016;13(1):226. doi:10.1186/s12974-016-0689-1
116. Landa J, Gaig C, Plagumà J, et al. Effects of IgLON5 Antibodies on Neuronal Cytoskeleton: A Link between Autoimmunity and Neurodegeneration. *Ann Neurol*. 2020;88(5):1023-1027. doi:10.1002/ana.25857
117. Landa J, Serafim AB, Gaig C, et al. Patients' IgLON5 autoantibodies interfere with IgLON5-protein interactions. *Front Immunol*. 2023;14:1151574. doi:10.3389/fimmu.2023.1151574
118. Landa J, Guasp M, Petit-Pedrol M, et al. Seizure-related 6 homolog like 2 autoimmunity: Neurologic syndrome and antibody effects. *Neurol Neuroimmunol neuroinflammation*. 2021;8(1). doi:10.1212/NXI.0000000000000916
119. Roberts A, Perera S, Lang B, Vincent A, Newsom-Davis J. Paraneoplastic myasthenic syndrome IgG inhibits 45Ca^{2+} flux in a human small cell carcinoma line. *Nature*. 1985;317(6039):737-739. doi:10.1038/317737a0
120. Lang B, Pinto A, Giovannini F, Newsom-Davis J, Vincent A. Pathogenic autoantibodies in the lambert-eaton myasthenic syndrome. *Ann N Y Acad Sci*. 2003;998:187-195. doi:10.1196/annals.1254.019
121. Geis C, Weishaupt A, Hallermann S, et al. Stiff person syndrome-associated autoantibodies to amphiphysin mediate reduced GABAergic inhibition. *Brain*. 2010;133(11):3166-3180. doi:10.1093/brain/awq253
122. Dalmau J, Lancaster E, Martinez-Hernandez E, Rosenfeld MR, Balice-Gordon R. Clinical experience and laboratory investigations in patients with anti-NMDAR encephalitis. *Lancet Neurol*. 2011;10(1):63-74. doi:10.1016/S1474-4422(10)70253-2
123. Groc L, Heine M, Cousins SL, et al. NMDA receptor surface mobility depends on NR2A-2B subunits. *Proc Natl Acad Sci U S A*. 2006;103(49):18769-18774. doi:10.1073/pnas.0605238103
124. Newpher TM, Ehlers MD. Glutamate receptor dynamics in dendritic microdomains. *Neuron*. 2008;58(4):472-497. doi:10.1016/j.neuron.2008.04.030

125. Dupuis JP, Groc L. Surface trafficking of neurotransmitter receptors: From cultured neurons to intact brain preparations. *Neuropharmacology*. 2020;169:107642. doi:10.1016/j.neuropharm.2019.05.019
126. Gréa H, Bouchet D, Rogemond V, et al. Human Autoantibodies Against N-Methyl-D-Aspartate Receptor Modestly Alter Dopamine D1 Receptor Surface Dynamics. *Front psychiatry*. 2019;10:670. doi:10.3389/fpsyt.2019.00670
127. Ladépêche L, Planagumà J, Thakur S, et al. NMDA Receptor Autoantibodies in Autoimmune Encephalitis Cause a Subunit-Specific Nanoscale Redistribution of NMDA Receptors. *Cell Rep*. 2018;23(13):3759-3768. doi:10.1016/j.celrep.2018.05.096
128. Rose NR, Bona C. Defining criteria for autoimmune diseases (Witebsky's postulates revisited). *Immunol Today*. 1993;14(9):426-430. doi:10.1016/0167-5699(93)90244-F
129. Planagumà J, Leyboldt F, Mannara F, et al. Human N-methyl D-aspartate receptor antibodies alter memory and behaviour in mice. *Brain*. 2015;138(1):94-109. doi:10.1093/brain/awu310
130. Malviya M, Barman S, Golombeck KS, et al. NMDAR encephalitis: passive transfer from man to mouse by a recombinant antibody. *Ann Clin Transl Neurol*. 2017;4(11):768-783. doi:10.1002/acn3.444
131. Haselmann H, Mannara F, Werner C, et al. Human Autoantibodies against the AMPA Receptor Subunit GluA2 Induce Receptor Reorganization and Memory Dysfunction. *Neuron*. 2018;100(1):91-105.e9. doi:10.1016/j.neuron.2018.07.048
132. Palmer CL, Cotton L, Henley JM. The molecular pharmacology and cell biology of alpha-amino-3-hydroxy-5-methyl-4-isoxazolepropionic acid receptors. *Pharmacol Rev*. 2005;57(2):253-277. doi:10.1124/pr.57.2.7
133. Maudes E, Mannara F, García-Serra A, et al. Human Metabotropic Glutamate Receptor 5 Antibodies Alter Receptor Levels and Behavior in Mice. *Ann Neurol*. 2022;92(1):81-86. doi:10.1002/ana.26362
134. Petit-Pedrol M, Sell J, Planagumà J, et al. LGI1 antibodies alter Kv1.1 and AMPA receptors changing synaptic excitability, plasticity and memory. *Brain*. 2018;141(11):3144-3159. doi:10.1093/brain/awy253

135. Ramberger M, Berretta A, Tan JMM, et al. Distinctive binding properties of human monoclonal LGI1 autoantibodies determine pathogenic mechanisms. *Brain*. 2020;143(6):1731-1745. doi:10.1093/brain/awaa104
136. Joubert B, Petit-Pedrol M, Planagumà J, et al. Human CASPR2 Antibodies Reversibly Alter Memory and the CASPR2 Protein Complex. *Ann Neurol*. 2022;91(6):801-813. doi:10.1002/ana.26345
137. Dawes JM, Weir GA, Middleton SJ, et al. Immune or Genetic-Mediated Disruption of CASPR2 Causes Pain Hypersensitivity Due to Enhanced Primary Afferent Excitability. *Neuron*. 2018;97(4):806-822.e10. doi:10.1016/j.neuron.2018.01.033
138. Martín-García E, Mannara F, Gutiérrez-Cuesta J, et al. Intrathecal injection of P/Q type voltage-gated calcium channel antibodies from paraneoplastic cerebellar degeneration cause ataxia in mice. *J Neuroimmunol*. 2013;261(1-2):53-59. doi:10.1016/j.jneuroim.2013.05.003
139. Liao YJ, Safa P, Chen YR, Sobel RA, Boyden ES, Tsien RW. Anti-Ca²⁺ channel antibody attenuates Ca²⁺ currents and mimics cerebellar ataxia in vivo. *Proc Natl Acad Sci U S A*. 2008;105(7):2705-2710. doi:10.1073/pnas.0710771105
140. Sommer C, Weishaupt A, Brinkhoff J, et al. Paraneoplastic stiff-person syndrome: passive transfer to rats by means of IgG antibodies to amphiphysin. *Lancet (London, England)*. 2005;365(9468):1406-1411. doi:10.1016/S0140-6736(05)66376-3
141. Geis C, Grünewald B, Weishaupt A, et al. Human IgG directed against amphiphysin induces anxiety behavior in a rat model after intrathecal passive transfer. *J Neural Transm*. 2012;119(8):981-985. doi:10.1007/s00702-012-0773-3
142. Rivers TM, Sprunt DH, Berry GP. OBSERVATIONS ON ATTEMPTS TO PRODUCE ACUTE DISSEMINATED ENCEPHALOMYELITIS IN MONKEYS. *J Exp Med*. 1933;58(1):39-53. doi:10.1084/jem.58.1.39
143. Kabat EA, Wolf A, Bezer AE. THE RAPID PRODUCTION OF ACUTE DISSEMINATED ENCEPHALOMYELITIS IN RHESUS MONKEYS BY INJECTION OF HETEROLOGOUS AND HOMOLOGOUS BRAIN TISSUE WITH ADJUVANTS. *J Exp Med*. 1947;85(1):117-130. doi:10.1084/jem.85.1.117
144. Van Epps HL. Thomas Rivers and the EAE model. *J Exp Med*. 2005;202(1):4. doi:10.1084/jem.2021fta

145. Constantinescu CS, Farooqi N, O'Brien K, Gran B. Experimental autoimmune encephalomyelitis (EAE) as a model for multiple sclerosis (MS). *Br J Pharmacol.* 2011;164(4):1079-1106. doi:10.1111/j.1476-5381.2011.01302.x
146. Weber MS, Prod'homme T, Patarroyo JC, et al. B-cell activation influences T-cell polarization and outcome of anti-CD20 B-cell depletion in central nervous system autoimmunity. *Ann Neurol.* 2010;68(3):369-383. doi:10.1002/ana.22081
147. Jones BE, Tovar KR, Goehring A, et al. Autoimmune receptor encephalitis in mice induced by active immunization with conformationally stabilized holoreceptors. *Sci Transl Med.* 2019;11(500). doi:10.1126/scitranslmed.aaw0044
148. Wagnon I, Hélie P, Bardou I, et al. Autoimmune encephalitis mediated by B-cell response against N-methyl-D-aspartate receptor. *Brain.* 2020;143(10):2957-2972. doi:10.1093/brain/awaa250
149. Ding Y, Zhou Z, Chen J, et al. Anti-NMDAR encephalitis induced in mice by active immunization with a peptide from the amino-terminal domain of the GluN1 subunit. *J Neuroinflammation.* 2021;18(1):53. doi:10.1186/s12974-021-02107-0
150. Pan H, Oliveira B, Saher G, et al. Uncoupling the widespread occurrence of anti-NMDAR1 autoantibodies from neuropsychiatric disease in a novel autoimmune model. *Mol Psychiatry.* 2019;24(10):1489-1501. doi:10.1038/s41380-017-0011-3
151. Linnoila J, Jalali Motlagh N, Jachimiec G, et al. Optimizing animal models of autoimmune encephalitis using active immunization. *Front Immunol.* 2023;14:1177672. doi:10.3389/fimmu.2023.1177672
152. He S, Sun C, Zhu Q, et al. A juvenile mouse model of anti-N-methyl-D-aspartate receptor encephalitis by active immunization. *Front Mol Neurosci.* 2023;16:1211119. doi:10.3389/fnmol.2023.1211119
153. Yu L, Wen Y, Yang J, et al. Autoimmune receptor encephalitis in ApoE(-/-) mice induced by active immunization with NMDA1. *Mol Med Rep.* 2023;28(6). doi:10.3892/mmr.2023.13120
154. Linnoila JJ, Rosenfeld MR, Dalmau J. Neuronal Surface Antibody-Mediated Autoimmune Encephalitis. 2014;1(212).

155. Matta JA, Ashby MC, Sanz-Clemente A, Roche KW, Isaac JTR. mGluR5 and NMDA receptors drive the experience- and activity-dependent NMDA receptor NR2B to NR2A subunit switch. *Neuron*. 2011;70(2):339-351. doi:10.1016/j.neuron.2011.02.045
156. Inta D, Vogt MA, Luoni A, et al. Significant increase in anxiety during aging in mGlu5 receptor knockout mice. *Behav Brain Res*. 2013;241(1):27-31. doi:10.1016/j.bbr.2012.11.042
157. Cai G, Wang X, Che Y, Yang J, Wu S. Basimglurant, an mGluR5-Selective Negative Allosteric Modulator, Dose Not Reduce Pain but Alleviate Pain Related Anxiety-Like Behavior (P4.065). *Neurology*. 2016;86(16 Supplement):P4.065. http://n.neurology.org/content/86/16_Supplement/P4.065.abstract
158. Bacchi S, Franke K, Wewegama D, Needham E, Patel S, Menon D. Magnetic resonance imaging and positron emission tomography in anti-NMDA receptor encephalitis: A systematic review. *J Clin Neurosci*. Published online 2018. doi:10.1016/j.jocn.2018.03.026
159. Mannara F, Radosevic M, Planagumà J, et al. Allosteric modulation of NMDA receptors prevents the antibody effects of patients with anti-NMDAR encephalitis. *Brain*. 2020;143(9):2709-2720. doi:10.1093/brain/awaa195
160. Radosevic M, Planagumà J, Mannara F, et al. Allosteric Modulation of NMDARs Reverses Patients' Autoantibody Effects in Mice. *Neurol - Neuroimmunol Neuroinflammation*. 2022;9(1):e1122. doi:10.1212/nxi.0000000000001122
161. Maudes E, Jamet Z, Marmolejo L, Dalmau JO, Groc L. Positive Allosteric Modulation of NMDARs Prevents the Altered Surface Dynamics Caused by Patients' Antibodies. *Neurol Neuroimmunol neuroinflammation*. 2024;11(4):e200261. doi:10.1212/NXI.000000000000200261
162. Ott G, Barchfeld GL, Chernoff D, Radhakrishnan R, van Hoogevest P, Van Nest G. MF59. Design and evaluation of a safe and potent adjuvant for human vaccines. *Pharm Biotechnol*. 1995;6:277-296. doi:10.1007/978-1-4615-1823-5_10
163. Zhang J, Miao J, Han X, et al. Development of a novel oil-in-water emulsion and evaluation of its potential adjuvant function in a swine influenza vaccine in mice. *BMC Vet Res*. 2018;14(1):415. doi:10.1186/s12917-018-1719-2

164. Leenaars PP, Koedam MA, Wester PW, Baumans V, Claassen E, Hendriksen CF. Assessment of side effects induced by injection of different adjuvant/antigen combinations in rabbits and mice. *Lab Anim.* 1998;32(4):387-406. doi:10.1258/002367798780599884
165. Wang Y, Tai W, Yang J, et al. Receptor-binding domain of MERS-CoV with optimal immunogen dosage and immunization interval protects human transgenic mice from MERS-CoV infection. *Hum Vaccin Immunother.* 2017;13(7):1615-1624. doi:10.1080/21645515.2017.1296994
166. Ochs J, Nissimov N, Torke S, et al. Proinflammatory CD20(+) T cells contribute to CNS-directed autoimmunity. *Sci Transl Med.* 2022;14(638):eabi4632. doi:10.1126/scitranslmed.abi4632
167. Rahman KA, Orlando M, Boulous A, et al. Microglia actively remove NR1 autoantibody-bound NMDA receptors and associated post-synaptic proteins in neuron microglia co-cultures. *Glia.* 2023;71(8):1804-1829. doi:10.1002/glia.24369
168. Häusler D, Häusser-Kinzel S, Feldmann L, et al. Functional characterization of reappearing B cells after anti-CD20 treatment of CNS autoimmune disease. *Proc Natl Acad Sci U S A.* 2018;115(39):9773-9778. doi:10.1073/pnas.1810470115
169. Yu S, Ellis JS, Dunn R, Kehry MR, Braley-Mullen H. Transient depletion of B cells in young mice results in activation of regulatory T cells that inhibit development of autoimmune disease in adults. *Int Immunol.* 2012;24(4):233-242. doi:10.1093/intimm/dxs003
170. Al-Diwani A, Theorell J, Damato V, et al. Cervical lymph nodes and ovarian teratomas as germinal centres in NMDA receptor-antibody encephalitis. *Brain.* 2022;145(8):2742-2754. doi:10.1093/brain/awac088

Chapter X

Annex

Resumen científico

Introducción

Las encefalitis mediadas por anticuerpos representan una nueva categoría de trastornos inflamatorios del cerebro causados por anticuerpos que atacan proteínas de la superficie celular neuronal. La forma más prevalente es la encefalitis anti-receptor N-metil-D-aspartato (NMDAR), caracterizada por autoanticuerpos contra la subunidad GluN1 del NMDAR, lo que provoca síntomas neuropsiquiátricos graves que a menudo mejoran con la inmunoterapia. A diferencia de las imágenes por resonancia magnética rutinaria, los estudios de imagen avanzados han demostrado cambios extensos en la sustancia blanca en pacientes, lo cual podría explicarse porque los oligodendrocitos, responsables de la síntesis de mielina, expresan NMDAR. La mayoría de los pacientes experimentan una recuperación lenta, con déficits persistentes de memoria y cognición, y el enfoque de tratamiento óptimo sigue siendo incierto. Nuevos enfoques terapéuticos, como el modulador alostérico positivo del NMDAR SGE-301, deben testarse como tratamientos complementarios a la inmunoterapia. Existe una necesidad crítica de modelos que proporcionen una comprensión neuro-inmunobiológica integral de la enfermedad y ofrezcan un curso clínico lo suficientemente largo como para facilitar la evaluación de posibles nuevos tratamientos.

Otra forma menos común de encefalitis mediada por anticuerpos es la encefalitis anti-receptor metabotrópico de glutamato 5 (mGluR5). Este trastorno está menos caracterizado, y el efecto de los anticuerpos de los pacientes aún no se ha evaluado en modelos animales.

Objetivos

1) Determinar la patogenicidad de los anticuerpos de pacientes con encefalitis anti-mGluR5 en un modelo de infusión cerebroventricular en ratones; **2)** Investigar el efecto de los anticuerpos de pacientes con encefalitis anti-NMDAR en cultivos de oligodendrocitos; **3)** Evaluar si el SGE-301 previene y restaura los efectos patológicos de los anticuerpos de pacientes con encefalitis anti-NMDAR en un modelo de ratón; **4)** Elucidar el mecanismo de acción del SGE-301 estudiando la dinámica del NMDAR en la membrana de las neuronas; **5)** Desarrollar un modelo animal de encefalitis anti-NMDAR para caracterizar la neuro-inmunobiología de la enfermedad y probar diferentes tratamientos, incluyendo inmunoterapia y el SGE-301.

Métodos

Para desarrollar un modelo de ratón para la encefalitis anti-mGluR5, los anticuerpos de los pacientes se infundieron cerebroventricularmente en ratones macho C57BL/6J de diez semanas durante 14 días. Se evaluaron la memoria y la ansiedad, y se determinaron los efectos sobre la densidad de mGluR5 en el hipocampo. Para estudiar el efecto de los anticuerpos de pacientes con encefalitis anti-NMDAR en oligodendrocitos, se expusieron

cultivos de oligodendrocitos al líquido cefalorraquídeo (LCR) de los pacientes, y se evaluó la actividad de los NMDAR. Para evaluar el potencial terapéutico del SGE-301, ratones adultos que recibieron infusión cerebroventricular de LCR de pacientes con encefalitis anti-NMDAR fueron tratados diariamente con SGE-301 durante 14 días desde el inicio de la infusión de anticuerpos o al comienzo de los síntomas. Se evaluó la memoria, la plasticidad sináptica y la densidad de NMDAR en el hipocampo de los ratones. Para investigar el mecanismo molecular del SGE-301, se trataron neuronas hipocámpales cultivadas con SGE-301 junto con anticuerpos de pacientes con encefalitis anti-NMDAR, y se evaluó la dinámica del NMDAR en la membrana de neuronas mediante microscopía de seguimiento de partículas. Para desarrollar un nuevo modelo de ratón para la encefalitis anti-NMDAR mediante inmunización activa, se inmunizó a ratones hembra de ocho semanas (C57BL/6J) con un péptido del GluN1 y el adyuvante AddaVax. El modelo fue caracterizado exhaustivamente, incluyendo la presencia de anticuerpos contra NMDAR, cambios en la memoria y el comportamiento, efectos de los anticuerpos sobre la densidad y función de NMDAR, plasticidad sináptica e infiltrados inmunológicos cerebrales. En este modelo se validó con la inmunoterapia comúnmente utilizada en pacientes (anti-CD20) y se evaluó el potencial terapéutico del SGE-301.

Resultados

- 1) Los ratones infundidos con anticuerpos de pacientes con encefalitis anti-mGluR5 mostraron deterioro de la memoria, mayor ansiedad y disminución de mGluR5 en la superficie neuronal. Después de la eliminación de los anticuerpos, tanto los cambios conductuales como moleculares volvieron a las condiciones normales.
- 2) En oligodendrocitos incubados con LCR de pacientes con encefalitis anti-NMDAR, las respuestas del NMDAR se redujeron significativamente. Estos efectos fueron específicos para el NMDAR.
- 3) En ratones infundidos con LCR de pacientes con encefalitis anti-NMDAR, la administración diaria subcutánea de SGE-301 previno y recuperó el deterioro de la memoria y las hipocampales sinápticas causadas por los anticuerpos NMDAR.
- 4) Las trayectorias del NMDAR en neuronas tratadas con SGE-301 se incrementaron, principalmente en la sinapsis. El tratamiento con anticuerpos de pacientes con encefalitis anti-NMDAR redujo la dinámica del NMDAR y aumentó su confinamiento. El SGE-301 antagonizó los efectos de los anticuerpos de los pacientes tanto en los compartimentos sinápticos como extrasinápticos, restaurando la dinámica normal del NMDAR en la membrana de neuronas.

- 5) Los ratones inmunizados con el péptido GluN1 desarrollaron anticuerpos contra NMDAR en suero y LCR, lo que resultó en la disminución de la densidad de NMDAR en el cerebro de los ratones y una reducción de la plasticidad sináptica. Estos hallazgos se asociaron con infiltrados inflamatorios cerebrales, activación de microglía, comportamiento psicótico, déficit de memoria, comportamiento depresivo, movimientos anormales y un umbral más bajo para desarrollar convulsiones. La mayoría de los síntomas y alteraciones neurobiológicas se revirtieron con el tratamiento con inmunoterapia anti-CD20 y SGE-301.

Conclusiones

Mis estudios han contribuido a comprender mejor la fisiopatología de la encefalitis anti-mGluR5 y anti-NMDAR. El primer estudio proporciona evidencia robusta de la patogenicidad de los anticuerpos contra mGluR5, asociando en un modelo animal la reducción de la densidad de mGluR5 en el hipocampo y la subsecuente aparición de síntomas neuropsiquiátricos. El segundo estudio sugiere una conexión entre la disfunción mediada por los anticuerpos contra NMDAR en los oligodendrocitos y las alteraciones de la sustancia blanca reportadas en pacientes con encefalitis anti-NMDAR. El tercer y cuarto estudio ofrecen evidencia, en un modelo de ratón bien establecido de transferencia cerebroventricular de anticuerpos de pacientes con encefalitis anti-NMDAR, de que el SGE-301 antagoniza y revierte los efectos sinápticos y patogénicos de los anticuerpos. El quinto estudio arroja luz sobre el mecanismo molecular de este nuevo fármaco. El sexto estudio ofrece un nuevo modelo de ratón de encefalitis anti-NMDAR mediante inmunización

activa que refleja la mayoría de las alteraciones neuro-inmunobiológicas de la enfermedad y demuestra que el tratamiento conjunto con inmunoterapia y SGE-301 es la mejor estrategia para recuperar los síntomas y las alteraciones neurobiológicas asociadas. Esto resalta la importancia de explorar fármacos similares como tratamientos adyuvantes para la encefalitis anti-NMDAR.

Resumen divulgativo

¿De qué trata esta investigación?

Esta investigación se centra en el estudio de unas enfermedades llamadas encefalitis mediadas por anticuerpos, causadas cuando el sistema inmunológico ataca erróneamente a componentes importantes del cerebro mediante anticuerpos. Existen varios tipos de encefalitis mediadas por anticuerpos. En esta investigación nos hemos centrado en dos: la más común es la encefalitis anti-NMDAR, donde los anticuerpos atacan a un receptor de señales neurológicas conocido como NMDAR. El segundo tipo es la encefalitis anti-mGluR5, en la que los anticuerpos atacan otro receptor llamado mGluR5.

¿Por qué es importante?

Comprender estas enfermedades es crucial porque provocan síntomas graves como pérdida de memoria, problemas psiquiátricos y otras complicaciones neurológicas. Los tratamientos actuales ayudan a la mayoría de los pacientes, pero la recuperación puede ser muy lenta e incompleta, porque algunos pacientes continúan con problemas de memoria durante meses o incluso años.

¿Qué hemos hecho?

Hemos utilizado cultivos celulares y modelos animales de ratón para estudiar cómo estos anticuerpos dañan el cerebro. También hemos probado un nuevo tratamiento llamado SGE-301, que podría ofrecer una nueva opción para contrarrestar los efectos de los anticuerpos contra NMDAR.

¿Qué hemos descubierto?

Nuestros estudios han demostrado que los anticuerpos contra NMDAR y mGluR5 dañan el cerebro y provocan síntomas neurológicos. Además, hemos visto que el nuevo tratamiento SGE-301 es efectivo mejorando muchos de estos efectos en nuestros modelos celulares y animales. Esto sugiere que fármacos similares a SGE-301, que se aprueben para su uso en pacientes, podrían ser un tratamiento prometedor para esta encefalitis.

¿Qué implicaciones tiene esto para el futuro?

Estos hallazgos nos ayudan a entender mejor la base biológica detrás de los síntomas que observamos en los pacientes con encefalitis mediada por anticuerpos. Además, podrían conducir a mejores tratamientos para los pacientes, mejorando sus posibilidades de recuperación y calidad de vida. Este avance subraya la importancia de seguir investigando los mecanismos de estas enfermedades y su tratamiento.

Other publications

Landa J, Serafim AB, Alba M, Maudes E, Molina-Porcel L, Garcia-Serra A, Mannara F, Dalmau J, Graus F, Sabater L. IgLON5 deficiency produces behavioral alterations in a knockout mice model. *Frontiers in Immunology*. 2024;15: 1347948.

Joubert B, Petit-Pedrol M, Planagumà J, Mannara F, Radosevic M, Marsal M, Maudes E, García-Serra A, Aguilar E, Andrés-Bilbé A, Gasull X, Loza-Alvarez P, Sabater L, Rosenfeld MR, Dalmau J. Human CASPR2 antibodies reversibly alter memory and the CASPR2 protein complex. *Annals of Neurology*. 2022;91:801-813.

Guasp M, Martín-Aguilar L, Sabater L, Bioque M, Armangué T, Martínez-Hernández E, Landa J, Maudes E, Borràs R, Muñoz-Lopetegí A, Saiz A, Castro-Fornieles J, Graus F, Parellada E, Querol L, Dalmau J. Neurofilament light chain levels in anti-NMDAR encephalitis and primary psychiatric psychosis. *Neurology*. 2022;98:e1489-1498.

García-Serra A, Radosevic M, Ríos J, Aguilar E, Maudes E, Landa J, Sabater L, Martinez-Hernandez E, Planagumà J, Dalmau J. Blocking placental class G immunoglobulin transfer prevents NMDA receptor antibody effects in newborn mice. *Neurology-Neuroimmunology Neuroinflammation*. 2021;8:6.

Guasp M, Giné-Servén E, Maudes E, Rosa-Justicia M, Martínez-Hernández E, Boix-Quintana E, Bioque M, Casado V, Módena-Ouarzi Y, Guanyabens N, Muriana D, Sugranyes G, Pacchiarotti I, Davi-Loocos E, Torres-Rivas C, Ríos J, Sabater L, Saiz A, Graus F, Castro-

Fornieles J, Parellada E, Dalmau J. Clinical, neuroimmunologic, and CSF investigations in first episode psychosis. *Neurology*. 2021;97:e61-e75.

García-Serra A, Radosevic M, Pupak A, Brito V, Ríos J, Aguilar E, Maudes E, Ariño H, Spatola M, Mannara F, Pedreño M, Joubert B, Ginés S, Planagumà J, Dalmau J. Placental transfer of NMDAR antibodies causes reversible alterations in mice. *Neurology-Neuroimmunology Neuroinflammation*. 2021;8:1.

Spatola M, Petit Pedrol M, Maudes E, Simabukuro M, Muñiz-Castrillo S, Pinto A, Wandinger K, Spiegler J, Schramm P, Almeida Dutra L, Iorio , Kornblum C, Bien CG, Höftberger R, Leypoldt F, Titulaer MJ, Sillevs Smitt J, Honnorat J, Rosenfeld MR, Graus F, Dalmau J. Clinical features, prognostic factors, and antibody effects in anti-mGluR1 encephalitis. *Neurology*. 2020;95:e3012-3025.

Maudes E,* Landa J,* Muñoz-Lopetegi A, Armangue T, Alba M, Saiz A, Graus F, Dalmau J, Sabater L. Clinical significance of Kelch-like protein 11 antibodies. *Neurology-Neuroimmunology Neuroinflammation*. 2020;7:3.

Martinez-Hernandez E, Guasp M, García-Serra A, Maudes E, Ariño H, Sepulveda M, Armangué T, Ramos AP, Ben-Hur T, Iizuka T, Saiz A, Graus F, Dalmau J. Clinical significance of anti-NMDAR concurrent with glial or neuronal surface antibodies. *Neurology*. 2020;94:e2302-e2310.

Agradecimientos

Recuerdo un día, hace más de veinte años, en la cocina de casa, después de comer, cuando le pregunté a mi madre cómo funcionaba su enfermedad, la Esclerosis Múltiple. Entonces ella, con la misma naturalidad con la que me explicó un día que los números son infinitos, comenzó a dibujar en un folio neuronas y oligodendrocitos, y me explicó lo que era la mielina. Recuerdo cómo me fascinó, y ese fue un punto sin retorno. Siempre he sido de ideas muy claras, pero la idea de estudiar neuroinmunología quizá haya sido una de las más claras y vivas en mí desde entonces. Una idea que nació de una curiosidad inmensa hacia este campo tan fascinante y también el deseo de poder, con mi granito de arena, ayudar y contribuir al bienestar de pacientes como mi madre. Así como mi motivación y aliciente durante estos más de cinco años en el laboratorio han bebido del propósito de poder ayudar, la lista de todos los que me habéis ayudado y apoyado para conseguirlo es interminable.

En primer lugar, muchísimas gracias a Josep, por haber depositado tu confianza en mí. Me siento profundamente afortunada de todo lo que he aprendido de ti, aunque sigo sintiendo que siempre te queda por enseñarme. Creo que no voy a poder tener otro mentor con la pasión que sientes por la ciencia y la perseverancia y cariño que pones a cada proyecto.

Gracias a Carlos, nuestra colaboración siempre me ha hecho sentir con medio pie en casa. Gracias porque tus contribuciones y críticas constructivas siempre han mejorado todos nuestros proyectos.

Thank you, Myrna, for the wise advice and for teaching me how to solve difficult problems with elegance. También quiero agradecer a Francesc Graus y Albert Saiz por todos los momentos en los que he podido aprender de vuestra experiencia. Ha sido un regalo poder coincidir con vosotros.

Gracias a todo el laboratorio, sois una mina de oro. Cada uno de vosotros suma un granito de arena para formar esta tesis. He tenido una suerte incalculable de haber podido aprender tanto de un equipo científico tan profesional y trabajador, que también ha sido para mí una gran familia.

Gracias a Esther por compartir conmigo tu criterio, por nuestros momentos de crítica desfogadora, por todas las inmunofluorescencias con las que has hecho que mi proyecto fuera posible, y porque la visión que tienes de mí me hace confiar en que voy por buen camino. A María por orquestar el laboratorio con una elegancia y un control que parece que no cuesta esfuerzo, aunque sea mentira. Recuerda esperarme en Badalona para nuestro plan.

A Merche por convertir cada comida en un debate social diferente, por buscar soluciones sencillas a problemas complejos y por los abrazos de madre. Gracias a Lidia por compartir conmigo toda tu sabiduría técnica, pero también vital. Me guardo todos tus consejos. Gracias a Jesús por el talante afrontando toda la complejidad que progresivamente ha ido adquiriendo nuestro proyecto. A Eva por tu compromiso trabajando y por los consejos sobre gatitos.

Gracias a Lorena por los ánimos estas últimas semanas; ojalá hubiéramos podido coincidir más. A Víctor por tus palabras de calma en el momento necesario que me han convencido de que lo tengo todo bajo control. Gracias a Laia por tus apariciones estelares para compartir siempre una charla distendida.

Gracias al tremendo equipo médico del laboratorio, he aprendido muchísimo de vosotras. Gracias incalculables a Marianna por todo el cariño que pusiste en enseñarme durante mis primeros meses en el laboratorio y por la generosidad con la que siempre has confiado en mí. Gracias a Eugenia porque infundes paz, entereza y buena energía, siempre recordándonos razones para celebrar. A Elianet por esa sonrisa permanente

con la que nos saludas cada día. Gracias a Gemma por ser tan genuinamente empática. A Thaís por las palmeras de kínder gigantes. A Raquel por ser tan cercana. A Mar G. por la tenacidad hacia los proyectos y la generosidad aclarando todas mis dudas médicas, profesionales y personales. Ai due neurologi più divertenti e sorridenti di tutta Italia. Claudia e Chiara è stata una gioia condividere questi mesi con voi. Ti auguro molto successo. Gracias, Chiara, por ser una compañera de piso tan atenta y comprensiva conmigo y con toda mi gente.

Gracias a todos de los que aún se habla en el laboratorio porque os fuisteis demasiado pronto: Araceli, Marta P., Li-Wen, Anna S., Pietro, Simone... Gracias a Marija por la predisposición intachable al trabajo en equipo. A Mar P. por acogerme cuando era inexperta y enseñarme todos los detalles científicos y no científicos de laboratorio. A Francesco por mis primeros pasos en el estabulario. A Helena por ser tan jovial y dar buenos consejos estadísticos y logísticos. A Bastien por ser el mejor alumno de castellano que he tenido nunca, y las veladas probando gastronomía francesa.

Gracias al equipo de Jaime y Albert, por discusiones enriquecedoras, por hacer las preguntas adecuadas y darme la oportunidad de reflexionar de forma diferente. Gracias, Carles, por inspirarme a ser un poco más creativa. Y a Balma, por regalarme una sonrisa cada vez que hemos coincidido; me hubiera gustado trabajar más contigo.

Gracias en especial a mi corrillo, os quiero muchísimo. A Anna, por ser un apoyo incondicional durante todas las idas y venidas de la tesis y de mi vida. Gracias por tus abrazos sanadores cuando más se necesitan. Eskerrik asko Jon, por ofrecerme siempre una opinión sincera, tu criterio tanto científico como vital ha sido un regalo todos estos años. Gracias a Paula por infundirme fuerza con absoluta generosidad cuando tú también la necesitabas. A los tres os he echado tanto en falta estos últimos meses.

Gracias a Laura, Beatriz, Marina y Berta por haber puesto vuestra confianza en mí durante vuestros primeros pasos en el laboratorio. Me llevo mucho de vosotras para mis futuras experiencias como mentora. Gracias a Laura por tu torbellino de energía positiva contagioso, a Beatriz por alegrarme los días con tus masajes y frases en dudoso castellano, a Marina por ser tan atenta y cálida, y a Berta por la refrescante buena compañía estos últimos meses. Sois las cuatro brillantes y deseo que en el futuro veáis fruto de todo el esfuerzo y perseverancia que ponéis a vuestro trabajo.

Gracias a todos los que hacéis cada día que las cosas funcionen: a Maite, a Pep y al equipo técnico del estabulario.

Gracias al 3B, a Paqui y a Manel, y en especial a Marta por ser un refugio al otro lado del pasillo; siempre has estado ahí cuando te he necesitado. Gracias a Carlos por ser tan generoso, tienes un corazón enorme. Gracias a Águeda por ayudarme a valorar cada pequeño paso. A Bryan por tu forma de mejorar cualquier café, cerveza o plan.

Thank you to Laurent Groc for taking me in your lab and giving me the opportunity to learn from your great team. Thank you to all the people that made my short stay in Bordeaux one of the funniest, craziest, and most enjoyable periods of my Ph.D. To the office that took me as a part of them. Thank you, Juan and Ivo, for bringing so many laughs to every plan and making me feel so welcomed. Thank you, Domi, for being so warmhearted and empathetic. To Morgane for all the beautiful plans around Bordeaux and Biscarrosse. To Nathan for closing the door for the gossip. Merci beaucoup madame Zoë, for almost killing my liver and for a nice project together; it was a pleasure.

Thank you to the new friends that I know will be for a lifetime. To Dani for all the stories, anecdotes, and lab historical context that we discussed during our breaks. My experience in Bordeaux would have been very different without you. To Flavia, for being the greatest surprise; eu não esperava encontrar uma alma gêmea em Bordeaux, sharing these months with you has been a rollercoaster of beautiful emotions.

Gracias a Leyre y Tanya, porque a lo largo de los años hemos ido compartiendo las conquistas de cada una juntas. Os llevo en el corazón. A Unai por saber estar cerca estando lejos, por hacerme entrar en razón cuando voy sin freno y coger siempre la llamada cuando he querido desahogarme.

Gracias a los siete artífices que colateralmente tanto habéis contribuido a que llegara aquí. A Pujana y López por hacerme disfrutar tanto el primer año en Barcelona. A mis amigas porque habéis comprendido y sostenido esta locura que es hacer un doctorado. Gracias a Kixki por la complicidad, a Uxue por la valentía, a Itziar por la empatía y a Josune por la sinceridad. Gracias a Nerea por haber sido un refugio en el último tramo, siempre a un paso de distancia, física y emocionalmente. No tengo palabras, pero tampoco hacen falta; ya lo sabéis todo.

A mi familia adoptiva: a Carmen, Fraski, Tino y Loli por acogerme con amor infinito y cuidarme como una hija. A Carol, Jonathan, Miri y Rosalía por quererme como una hermana. A Noa y Martina, y próximamente a Jana, porque habéis sido una fuente de alegría constante; todo el tiempo que he compartido con vosotras me ha dado vida.

A mi hermano Héctor, por ser un ejemplo de que hay que soñar grande y perseverar por los objetivos. A Lavinia por cuidar de mi familia cuando yo no he podido estar cerca. Gracias a mi tía Edurne por ser la persona más auténtica que conozco y confiar siempre en que todo lo que hago es sumamente importante.

Gracias, Ama, por ser lo mejor que tengo. Eres la razón por la que estoy aquí, por enseñarme y transmitirme tu curiosidad por el mundo, por ayudarme a confiar en mí, por ser mi eterna confidente. Siempre vas a ser mi inspiración.

Gracias a Mizu por echarte unas siestas interminables mientras escribía, comerte mis libros y morder mi portátil. Sé que ha sido tu forma de contribuir a este libro.

Gracias a David, porque esta tesis también es tuya. Desde que viniste corriendo a buscarme al Clínic porque me habían concedido la beca, no has parado un día de estar en mi equipo. Has vivido conmigo cada experimento, cada conflicto, cada dificultad y cada triunfo. No hay nadie que me admire tanto, que crea en mis aptitudes, que me comprenda y me quiera como tú. Contigo soy una persona mejor.

Finalmente, gracias a los pacientes, y a sus familias, porque sin vuestra generosa contribución la ciencia no podría seguir adelante.

¡Gracias!

The Brain—is wider than the Sky—
For—put them side by side—
The one the other will contain
With ease—and you—beside—

The Brain is deeper than the sea—
For—hold them—Blue to Blue—
The one the other will absorb—
As sponges—Buckets—do—

The Brain is just the weight of God—
For—Heft them—Pound for Pound—
And they will differ—if they do—
As Syllable from Sound—

Emily Dickinson, c. 1862